# EXTRUSION FOAMING OF BIOPLASTICS FOR LIGHTWEIGHT STRUCTURE IN FOOD PACKAGING

A thesis submitted for the degree of Doctor of Philosophy

by

Sitthi Duangphet

School of Engineering and Design

Brunel University

December 2012

# Abstract

This thesis reports the systematic approaches to overcome the key drawbacks of the pure PHBV, namely low crystallisation rate, tensile strength, ductility, melt viscosity, thermal stability and high materials cost. The physical, mechanical, thermal, and rheological properties of the pure PHBV were studied systematically first to lay a solid foundation for formulation development. The influence of blending with other biopolymers, inclusion of filler, and chain extender additives in terms of mechanical properties, rheology, thermal decomposition and crystallization kinetics were then followed. Creating lightweight structures by foaming is considered to be one of the effective ways to reduce material consumption, hence the reduction of density and morphology of PHBV-based foams using extrusion foaming technique were studied comprehensively in terms of extrusion conditions (temperature profiles, screw speed and material feeding rate) and the blowing agent content.

The material cost reduction was achieved by adding low-cost filler (e.g. $CaCO_3$) and reduction of density by foaming. The thermal instability was enhanced by incorporation of chain extender (e.g. Joncryl) and blending with a high thermal stability biopolymer (e.g. PBAT). The polymer blend also improved the ductility. Adding nucleation agent enhanced the crystallization rate to reduce stickiness of extruded sheet. The final formulation (PHBV/PBAT/$CaCO_3$ composite) was successfully extruded into high quality sheet and thermoformed to produce prototype trays in an industrial scale trial.

The effect of the extrusion conditions (temperature profiles, screw speed and material feeding rate) and the blowing agent content are correlated to the density reduction of the foams. 61 and 47 % density reduction were achieved for the commercial PHBV and the PHBV/PBAT/$CaCO_3$ composite respectively and there exists further scope for more expansion if multiple variable optimisation of the conditions are carried out.

# Table of Contents

# List of Tables

# List of Figures

# List of Abbreviations

| | |
|---|---|
| AD | anaerobic digestion |
| aPLA | amorphous poly(lactic acid) |
| ASTM | the American Society for Testing and Materials |
| BC | bacterial cellulose |
| BN | boron nitride |
| CA | cellulose acetate |
| CBA | chemical blowing agent |
| $CO_2PC$ | carbon dioxide permeability coefficient |
| $CO_2TR$ | carbon dioxide transmission rate |
| CPD | critical point dried |
| cPLA | crystalline poly(lactic acid) |
| DS | degree of substitution |
| DSC | differential scanning calorimetry |
| DTG | derivative thermogravimetric |
| EVOH | ethylene-vinyl alcohol copolymer |
| GPC | gel permeation chromatography |
| GWP | global warming potential |
| HB | hydroxybutyrate |
| HDPE | high-density polyethylene |
| HV | hydroxyvalerate |
| iPP | isotactic polypropylene |
| ISO | International Organization for Standardization |
| LDPE | low-density polyethylene |
| MAP | modified atmosphere packaging |
| MMT | montmorillonite |
| ODP | ozone depletion potential |
| OMMT | organically modified montmorillonite |
| OPC | oxygen permeability coefficient |

| | |
|---|---|
| OTR | oxygen transmission rate |
| PECH-EO | poly(epichlorohydrin-*co*-ethylene oxide) |
| P(3HB-*co*-4HB) | poly(3-hydroxybutyrate-*co*-4-hydroxybutyrate) |
| P(3HB-*co*-3HHx) | poly(3-hydroxybutyrate-*co*-hydroxyhexanoate) |
| P(3HB-*co*-3HP) | poly(3-hydroxybutyrate-*co*-3-hydroxypropionate) |
| PBA | physical blowing agents |
| PBAT | poly(butylene adipate-*co*-terephthalate) |
| PBS | poly(butylene succinate) |
| PBSA | poly(butylene succinate-*co*-adipate) |
| PBST | poly(butylene succinate-*co*-terephthalate) |
| PBT | poly(butylene terephthalate) |
| PCL | polycaprolactone |
| PDLA | poly(D-lactide) |
| PE | polyethylene |
| PEA | poly(ester amide) |
| PET | poly(ethylene terephthalate) |
| PEO | poly(ethylene oxide) |
| PGA | poly(glycolic acid) |
| PHAs | poly(hydroxyalkanoates) |
| PHB | poly(3-hydroxybutyrate) |
| PHV | poly(3-hydroxyvalerate) |
| PHBV | poly(3-hydroxybutyrate-*co*-hydroxyvalerate) |
| PHEE | poly(hydroxy ester ether) |
| PHH | poly(hydroxyhexanoate) |
| PLA | poly(lactic acid) |
| PLLA | poly(L-lactide) |
| PP | polypropylene |
| PS | polystyrene |
| PTMAT | poly(tetramethylene adipate terephthalate) |
| PU | polyurethane |
| PVOH | poly(vinyl alcohol) |

| | |
|---|---|
| PVAC | poly(vinyl acetate) |
| PVC | polyvinyl chloride |
| PVDF | poly(vinylidene fluoride) |
| RIM | reactive injection molding |
| ROP | ring opening polymerization |
| rpm | revolution per minute |
| SCF | supercritical fluid |
| SEM | scanning electron microscope |
| TG | thermogravimetric |
| TGA | thermogravimetric analysis |
| TPS | thermoplastic starch |
| VOC | volatile organic compound |
| WVPC | water vapour permeability coefficient |
| WVTR | water vapour transmission rate |

# Acknowledgements

First of all, I would like to take this opportunity to express my deepest gratitude to my first supervisor Professor Jim Song and my second supervisor Dr. Karnik Tarverdi for their encouragement, guidance and help throughout this project. I must also thank Professor Song for his valuable comments in the completion of the thesis.

I would like to thank staff and technicians in the Wolfson Centre for Materials Processing and the School of Engineering and Design at Brunel University, in particular Dr. Damien Szegda for his constructive advice and technical support.

I would like to thank the support from all the participants in the project especially Bangor University, Nextek Ltd., Imperial College London, Sharp Interpack Ltd., Wells Plastic Ltd. and Imerys Ltd., for their provision of data, insight and valuable comments.

I am grateful to the UK Government Department of Trade & Industry (Technology Strategy Board), for financing my research as part of the project "Biobased Lightweight Sandwich Structures for Packaging Applications".

I owe my sincere gratitude to the Royal Thai Embassy for my financial support and all staff in Office of Educational Affairs for their kindly support and helpful.

Finally, my thanks go to my family and friends for their everlasting support and encouragement throughout this period of time.

# Chapter 1
# General Introduction

## 1.1 Background

Metals, paper and board, glass, oil-based plastics or their combinations are the most commonly used materials for packaging applications. Due to large volume and short service life, the large amount of waste generated from post-consumer packaging materials has attracted criticisms from media and general public. Increasingly stringent legislations require measures to enhance materials efficiency and reduce impact of packaging wastes to environment (e.g. The EU Packaging and Landfill Directives). In addition to efforts to reduce packaging from design stage, recycling, reuse of packaging materials, and recovery for energy production are increasingly adopted along the supply chains of packaging (Weber, 2000).

Although reuse and recycling are on top of waste management hierarchy, these methods are not completely suitable to deal with all packaging, especially food packaging materials because they frequently compost of many different materials to achieve optimal (e.g. mechanical or barrier) properties. This leads to complicated material compositions, causing problems in sorting as well as losing of physical performance after recycling (Davis & Song, 2006). Besides, contamination of foodstuffs on food packaging adds significant costs in clearing and decontamination. To date, there has been only limited success in recycling of plastic packaging from relatively purer sources such as water and milk bottles (WRAP, 2008).

In the last decades or two, Bio-based plastics of bioplastics have been rapidly developed as alternatives to petro-chemical plastics from renewable resources such as plants and microorganisms (Avella *et al.*, 2001). Most of them possess good biodegradability which also facilitates biological waste management so that food products and their packaging can be composted or generate fuel by anaerobic digestion and thus divert waste from landfill. The benefits have motivated researchers in both academic and industry to develop alternative bio-based sustainable plastic materials - bioplastics.

Bioplastics consist of *bio-based plastics* originated from renewable biological resources and/or *biodegradable plastics* which may also include those from petrochemical resources (Song *et al*., 2011). Biodegradation is the degradation resulted from the action of microorganisms, such as bacteria, fungi etc. which should be differeciated from other degradation such as photodegradation or chemical degradation (Petersen *et al*., 1999). Biodegradation can occur in anaerobic composting or aerobic digestion environment and result in compost or sludge or produce biogas (methane and hydrogen), respectively.

This work is a part of Technology Strategy Board (TSB) project "Biobased Lightweight Sandwich Structures for Packaging Applications" (BLT) and the aim of the project is to produce the novel lightweight, high barrier and home compostable food packaging container. The objectives of the project are:

i) Develop formulations for required properties;

ii) Understand processing windows in sheet extrusion, foaming and thermo forming;

iii) Evaluation of cost, manufacturing applications and home compostability.

The candidate bioplastic materials in this project consist of starch, poly(lactic acid) (PLA) and poly(hydroxyalkanoates) (PHAs). Starch is encouraging material because of its low cost and completely biodegradable however, its hydrophilicity that influences on its performance is the serious issue for using as food packaging (Davis & Song, 2006; Sorrentino *et al*., 2007). PLA is one promising material that is commercially available. It possess the better moisture barrier than starch (Petersen *et al*., 1999) but its medium gases and vapours barrier properties and its brittleness are the most important handicaps for the use for food packaging container (Siracusa *et al.*, 2008).

The other candidate matateriał is poly(3-hydroxybutyrate) (PHB), one of the well-known bacterial derived polyester in PHAs family. It has promising properties for food packaging applications, because it presents a good combination of mechanical strength, stiffness (Sato *et al*., 2004; Sudesh *et al*., 2007; Serafim, 2008) and excellent gas barrier properties (Parra *et al*., 2006) as well as biodegradability in a soil, sea water, activated

sludge, etc. (Sudesh *et al*., 2000). However, it is known to be brittle and prone to thermal degradation during processing, which restricts its widespread application.

Poly(3-hydroxybutyrate-*co*-hydroxyvalerate) (PHBV) is developed from PHB. The addition of 3-hydroxyvalerate (HV) monomers to the PHB results in reduction of melting point and crystallinity, and hence improved ductility. Although high HV ratio is known to improve ductility (Choi & Lee, 2000), it results in high cost of PHBV making it to be far more expensive than other conventional plastics and commercially less competitive. Consequently, PHBV has been identified as the key polymers for the project by partners because this polymer has the performance potential to deliver the final product for the project. To develop PHBV into an adequate bioplastic material for high barrier food packaging, there are several challenges to be overcome:

i) The high material cost which constrains its widespread employ in packaging market;

ii) The thermal instability and low melt strength which restrict its processibility;

iii) The brittleness problem which limits final product application.

As a result, the objectives of this study are to develop PHBV formulations and identify processing windows in solid sheet extrusion for thermoforming and extrusion foaming for lightweight container.

## 1.2 Scope of the research

The purpose of this study is to develop novel home compostable and lightweight, high barrier food packaging solutions based on PHBV.

Several approaches are to be undertaken to overcome the drawbacks described above (high cost, thermal instability, low melt strength and brittleness) which include:

a) Blending with more ductile bioplastics for improvement of ductility without sacrificing its biodegradability and gas barrier properties.
b) Inclusion of inorganic fillers for cost reduction and modifications of melt flow and barrier properties.

c) Use of food-safe processing additives e.g. chain extenders to improve resistance to thermal degradation and processibilities (such as higher melt strength required for foaming and thermoforming)
d) Foaming of PHBV for reduction in density and material usage.

The physical, mechanical, thermal, and rheological properties of the pure PHBV was studied systematically first to lay a solid foundation for formulation development.

The influence of blending with other biopolymer, inclusion of filler, and chain extender additives in terms of mechanical properties, rheology, thermal decomposition and crystallization kinetic were then followed.

Extrusion foaming behaviour of PHBV and modified formulations was then investigated using a food-safe chemical blowing agent to study the effects of processing conditions, blowing agents and filler contents, on foaming of PHBV based formulations are correlated to cell structural development and properties.

### 1.3 Layout of the thesis

This thesis of ten chapters outlined below:

- Chapter 1 provides general background of the work and identifies aims, objectives and the approaches of the work to achieve them.

- Chapter 2, the literature review, provides an overview of the useful information and related background in this study.

- Chapter 3 describes materials and treatments, if any and details of experiments in processing and characterization.

Results and discussions of the work are included in Chapter 4-9 including:

- Chapter 4 on general properties of PHBV and the effect of thermal treatment on its properties.

- Chapter 5 on effect of blending of PHBV with poly(butylene adipate-*co*-terephthalate) (PBAT) on properties of the blends at different polymer ratios.

- Chapter 6 on the effects of calcium carbonate ($CaCO_3$) filler on properties of PHBV.

- Chapter 7 on the effect of an epoxy-functionalized oligomer (Joncryl® ADR-4368 S) as a chain extender.

- Chapter 8 on the effect of extrusion foaming conditions on PHBV foam structure and properties and optimum foaming conditions.

- Chapter 9 on the extrusion foaming of the final formulation of the bioplastic blend developed.

- Chapter 10 presents general conclusions and suggests areas for further work.

# Chapter 2
# Literature Review

This work focuses on development of lightweight bioplastic materials for high performance of food packaging. In this chapter, literature on the backgrounds in food packaging, biodegradable plastic materials and plastic foams are reviewed.

## 2.1 Food packaging

Food packaging plays an important role in contemporary economy and daily life for food safety, preservation and protection. There are also many additional functions that the packaging producers should consider and be aware of, such as providing product information to consumers, handling and using easily, presenting brand communication, updating sale promotion, and sharing environmental responsibility (Coles, 2003).

The primary functionalities of food packaging are to contain and protect food products to maintain their qualities until consumption. Foodstuffs could be damaged from physical, chemical and microbiological spoilage (Cowell, 1993) that lead to loss of food qualities. Change in colour, flavour, masticatory properties can become a toxicological hazard (Brody, 1997).

Requirements for food packaging, food packaging design to meet requirements and plastics in food packaging are described in some details below.

### 2.1.1 Requirements for food packaging

The requirements of food packaging are very complicated because of dynamic nature of the food supply chain. Table 2.1 shows the general food packaging requirements categorized along the supply chain (Haugaard *et al*., 2000).

**Table 2.1:** Food packaging requirements (Haugaard *et al*., 2000)

| Area | Overall | Specific |
|---|---|---|
| Food Quality | Maintain or enhance sensory properties | Maintain taste;<br>Maintain smell;<br>Maintain colour;<br>Maintain texture. |
| | Maintain the necessary microbiological standards | Should not support the growth of unwanted microorganisms. If necessary, can be pasteurized or sterilized |
| Manufacturing | Offer simple, economic processes for package formation | Sheet, film, containers, pouches;<br>Adequate mechanical properties. |
| | Give compatibility in product filling | Dimension stability;<br>Good runability on filling lines;<br>Closeability;<br>Compatibility with existing machinery. |
| Logistic | Facilitate distribution | Conform to industry requirements (e.g. size, palletisation);<br>Carry the required codes (bar code, product and sell-by). |
| Marketing | Enhance point of sale appeal | Good graphics;<br>Aesthetically pleasing;<br>Culture-specific consumer preferences;<br>Deliver the required functionally (e.g. openability, dust-free). |
| Environment | Not endanger human safety | Safe food contact interactions;<br>Avoid physical harm. |

| | | |
|---|---|---|
| | Use resources responsibility | Have a positive LCA |
| | Facilitate waste management | Should be recoverable;<br>Ought to be recyclable, burnable or compostable. |
| Legislation | National laws | Meet labeling, hygiene and migration conditions. |
| Financial | Cost effectiveness | Acceptable price per food package;<br>Price of concomitant machinery. |

Protection of food to ensure food quality during the product's shelf-life is the highest priority in all requirements of food packaging. Therefore, the descriptions of fundamental requirements for food packaging will be focused on:

1) General properties of food packaging;
2) Safety of food packaging and
3) Their environmental compatibility.

#### 2.1.1.1 General properties of food packaging

During distribution of packed foods, the products might be damaged from three distribution environments: climatic, physical, and biological environments (Coles, 2003) and consequently affect spoilage of foods. Packaging must maintain the quality, freshness, and appearance of food until use. Extending shelf-life is meant to extend storage time and reduces spoilage of food products and reduces food wastage. To extend the shelf-life, the product characteristics, properties of individual package and storage as well as the product distribution have to be in consideration (Petersen *et al*., 1999). Among others, the key requirements in food packaging properties for general protection and extension of food storage time are barrier properties and mechanical properties.

**a) Barrier properties**

Barrier properties are crucial to maintain desirable atmospheric environments for conservation of food characteristics such as flavour, colour, taste and texture. Generally,

barriers to oxygen, water vapour and carbon dioxide may be required depending on the type of foods (Siracusa *et al*., 2008).

*Oxygen barrier*

Oxygen concentration is the main factor in preservation as use to control food degradation (Siracusa, 2012). The shelf-life of the product can be extended by reducing the oxygen concentration to the specific level where the oxidation is retarded. However, some products such as fresh meats require high amount of oxygen to maintain red oxymyoglobin colour (Petersen *et al.*, 1999).

The oxygen permeability coefficient (OPC) is used to quantify oxygen barrier property of a material. OPC is determined as the amount of oxygen permeation per unit of area and time through packaging materials ($mol \cdot m^{-1} \cdot s^{-1} \cdot Pa^{-1}$). The low OPC value therefore corresponds to high oxygen barrier property. Oxygen transmission rate, OTR ($mol \cdot m^{-2} \cdot s^{-1}$) is also used to specify the oxygen barrier property. The relationship between OPC and OTR is shown in Equation 2.1:

$$\mathrm{OPC} = \mathrm{OTR} \times l / \Delta P \qquad (2.1)$$

Where $l$ is the thickness of the film ($m$), $\Delta P = p_1 - p_2$, is the difference between oxygen partial pressures ($p_1$ and $p_2$) across the film ($Pa$).

*Water vapour barrier*

Moisture content is an important factor to a majority of foods. Dehydration of fresh vegetable leads to shrinkage, wilting and unfresh appearance, while, uptake of water in crackers and cookies result in lack of crispiness.

Water vapour barrier is quantified by water vapour permeability coefficient (WVPC) which indicates the amount of water vapour permeates per unit of area and time in packaging materials ($mol \cdot m^{-1} \cdot s^{-1} \cdot Pa^{-1}$). Low WPVC indicates high water vapour barrier of the material used. It can also be converted to water vapour transmission rate (WVTR) by using Equation 2.1.

*Carbon dioxide barrier*

$CO_2$ barrier is very important parameter in packaging of carbonated drinks and $O_2/CO_2$ ratio in the gas mixture can control the respiration rate of fresh foods (Siracusa, 2012). Same as oxygen and water vapour, carbon dioxide permeability coefficient ($CO_2PC$) presents the $CO_2$ barrier property and can be converted to carbon dioxide transmission rate ($CO_2TR$) using Equation 2.1. Again, lower $CO_2PC$ or $CO_2TR$ refer to higher $CO_2$ barrier.

**b) Mechanical properties**

During distribution storage and handling, packages may encounter many stress conditions, for example vibration during transport, compression loading when stacked and impacts when dropped. Hence, the mechanical properties must be adequate to sustain the loading situations to prevent from damage of the package (the products and packaging). The mechanical properties requirements depend on their applications.

Many standards and test methods relevant to specific materials are designed by various authorities to meet the necessary requirements. For example, in case of plastic, tensile test is generally used in order to determine the tensile strength (*MPa*), the elongation at yield (%) or at break (%) represent ductility of the material and the tensile modulus (*GPa*) is used to determine stiffness. As for the thin plastic sheet, the testing should follow ASTM D882-02 - Standard Test Method for Tensile Properties of Thin Plastic Sheet.

In addition, packed products are meant to keep at difference suitable environment. For instance many chilled or frozen foods and containers are stored at low temperature, thus mechanical performance at service conditions must be considered (Auras *et al*., 2005).

### 2.1.1.2 Safety of food packaging

Packaging is served as the protection against external hazards and contamination of the products from surroundings. Food packaging, especially primary packaging - the packaging that touch with goods and take away by consumers (Davis & Song, 2006), is normally in direct contact with food products, thus interaction between foodstuffs and packaging might occur and leading to problems. The common undesirable interactions

from direct contact between packaging and foods are migration and sorption (Tehrany *et. al*., 2006). When migration occurs, which is the transfer of contaminants from packaging into foods; it may compromise the food quality or even introduce hazards while sorption, the transfer of food substances to the packaging may result in loss of mechanical, physical or esthetic properties of the packaging.

Besides, gas permeation, through packages in either direction can lead to loss of food quality (Feigenbaum *et. al*., 1991). Council Directive 89/109/EEC, which covers all food contact materials, states that materials anticipated to be in contact with food must not transfer any of their elements to the food that might endanger human health, change the composition of the food, or cause a deterioration in its properties.

#### 2.1.1.3 Environmental compatibility

Endorsement of environment regulations has increased awareness of food packaging environmental compatibility along the supply chain from manufacturers to users and consumers resulting in strengthening of legislations.

In Europe for example, the Packaging and Packaging Waste Directive (94/62/EC) regulates responsibilities in packaging waste. This directive aims the reduction of creation of packaging and promoting recycling, reuse and energy recovery by incineration. In the 94/62/EC also points out that compostability can be managed under controlled condition only and not in landfills. The other sample is the Landfill Directive (99/31/EC) that aims to minimize the amount of waste sent to landfill and also plans to reduce the total amount of biodegradable municipal waste (BMW) going to landfill in three successive stages eventually to 35% of the 1995 total of BMW by 2020 (Song *et al.*, 2009).

According to the “Waste Hierarchy” - a sequential listing of waste management options based on their relative environmental benefits and order of sustainability, the most attractive waste management is reduction of material used following by reuse, recycling or compost, recovery of value in some other way and landfill as the least preferable (DEFRA, 2011; Song *et al*., 2011).

The best methods in solving the waste problem are reducing the packaging consumption and/or reuse them so that the amount of materials entering the waste stream would be decreasing, however, reducing material for creating packaging possible risk of hygiene and product damage issues whereas reuse of food packaging is limited by contamination from food (Song *et al*., 2011). Recycling is considered to be another preferred solution but still has limitations, which are emerged mainly from such factors as their collection, separation, and contamination (Davis & Song, 2006) and the excessive energy consumption during recycle is currently concerned (Scott, 2000). Consequently, the one of currently preferable managements for food packaging is compostable.

The increasing attention in sustainability including sustainable packaging is the concept to minimize the environment impact. The approach of sustainable packaging concept is various and complex such as reduce energy and material use, reduce carbon dioxide and green house gases (GHGs), using low carbon and renewable energy technologies for packaging production, and so on (Coles, 2011). In term of material, using of renewable source materials is one of the ideas on sustainable packaging. Moreover, economic consideration on limitation of crude oil and natural gas resources has been highlighted. Those issues are good driving force for using packaging from renewable resource to replace non-renewable resources. As a result, packaging is not only design for requirement functions but also environment compatibility. Using compostable packaging produced from renewable resource is the option in food packaging design.

### 2.1.2 Food packaging design to meet requirements

Modern food packaging is not only limited to the containment and protection of food stuffs also needs to meet a range of other requirements of marketing, production, legal, logistic and environmental compatibility. Corresponding to these demands, packaging designs should consider characteristics of the food products and the requirements during packing, transport and distribution selection of packaging materials and their manufacturing, preference of consumer, market needs and wants as well as the environment impact (Coles, 2003).

Packaged products might be damaged by climatic, physical, and biological contamination during packing, storage and distribution until they are consumed. As a

result, the designed packaging must essentially prevent such damages by careful selection of materials and design solutions with appropriate mechanical, physical and chemical/biological properties. This often requires use of a good solution may rely on a combination of two or more materials such as multilayer films or use of composites (Abreu *et al.*, 2007; Azeredo, 2009) in a packaging solution. Other considerations in providing necessary technical functionalities are also briefly discussed.

The food characteristics and storage condition are the essential factors concerning preservation of food quality in packaging design. Packed food can be classified into 3 main groups (Brody, 1997):

1) Fresh food products;
2) Partially processed food products and
3) Fully processed food products,

and thus require different designs. For instance, in order to reserve the red oxymyoglobin colour of meat, oxygen permeability is required. Unfortunately, high amount of oxygen results in short storage caused by microbial spoilage. Consequently, to solve this problem, using Modified Atmosphere Packaging (MAP) with 70-80% oxygen combined with 20-30% carbon dioxide using a high oxygen and carbon dioxide barrier film is designed (Petersen *et al.*, 1999). Many other techniques are proposed to obtain higher barrier properties for diverse food characteristics, such as plasma treatment (Bonizzoni & Vassallo, 2002) and nanocomposite systems (Abreu *et al*., 2007; Azeredo, 2009).

During food manufacturing and packing, packaging must be design to withstand the processing conditions in all processing steps. For example, in high pressure food processing for pathogen reduction, packaging must tolerate the high pressure condition (Belcher, 2006).

Convenience offered by food packaging is often the center of attention for most consumers where food packagings are designed to facilitate and match with lifestyle and behavior of the consumers in their daily life. Due to lack of cook skill among young generations, changing into urgent life style and disinclination to prepare meal of the

retired, the microwavable packaging for example, has emerged as one of popularly packaging developments (Eilert, 2005). For this particular food packaging type, the silicon dioxide barrier is used instead of aluminium so that it permits for microwave reheating.

### 2.1.3 Plastics in food packaging

Packaging is the single largest user of plastic materials (http://www.lotfi.net/recycle/plastic.html). Plastics have versatile properties that for various applications in food packaging. They have good mechanical properties, liquid and gas barrier properties and heat-sealable to prevent food from contaminations. Plastics are quite inert when in contact with foods (Kirwan & Strawbridge, 2003). Moreover, they are inexpensive, light weight, easy to process and available in different forms (e.g. film, sheet and foam) to suit the needs of a wide range of food packaging.

Different food products require different protections. Thus, selection of plastics is important to achieve appropriate packaging. Type of plastics is one of the main factors for functionality. For example, low-density polyethylene (LDPE), high-density poly ethylene (HDPE) and poly(ethylene terephtalate) (PET) are used for frozen foods because they can withstand sub-zero (often -18 °*C*) temperature, whereas polypropylene (PP), polystyrene (PS) and polyvinyl chloride (PVC) are used for chilled products (~5 °*C*) (Watts, 1990). PET is widely used for beverage bottles because its excellent impact resistance and clarity. To improve barrier properties for carbonated beverage, injection stretch blow molding can be employed (Kirwan & Strawbridge, 2003; Briston, 1994a). Sometimes, one type of plastic is not sufficient to meet the requirements. Plastics of different types can be blended, co-extruded, laminated or coated to provide the multi-functions required. For instance, introduction of ethylene-vinyl alcohol copolymer (EVOH) which posses low oxygen permeability in middle layer between PP layers by co-extrusion to produce PP/EVOH/PP multilayer films is used to improve oxygen barrier property of squeezable bottles, such as tomato ketchup bottles (Briston, 1994b).

There are many processes to convert plastics to various forms (Briston, 1994b and 1994c). Injection molding can produce e.g. from a miniature valve for aerosol to a big container. A small vial or large barrel or drum can be made by extrusion and injection

blow molding. Using blow molding, wide- and narrow-necked containers can be obtained. Moreover, sheet plastics, the primary materials to make cups, pots and trays, are produced by extrusion and thermoforming.

Because of these advantages, the demand for plastics is increasing every year (DEFRA, 2009). The intensive application of plastic packaging however, has raised serious concerns in their impact to sustainability of the materials and large amount of waste generated. As most of them are non-biodegradable, the problem of littering in particular attracts increasing criticism from the general public and media. Plastics, especially those for food packaging are difficulty to recycle and the recycling rate of plastics is the lowest of all packaging materials (WRAP, 2008). This is attributable to the facts that (Davis & Song, 2006; Song *et al.*, 2009):

- lack of a continuous and reliable supply of quality, sorted material,
- large number of different types of plastics, additives, colourants and plasticizers in use;
- difficulties and high financial cost in collection, separation and identification of plastics;
- high contamination and cleaning cost;
- degradation due to repeated processing and
- time consuming.

In the last two decade or so, bioplastics have emerged, and became commercially available, as alternatives to petrochemical-based or conventional plastics as described later.

#### 2.1.3.1 Bioplastics in food packaging

In the last decade or two, many efforts have been made so as to develop bioplastics as alternatives to the conventional oil-based plastics. Single-use, short service life or disposable items, as in many food packaging applications are increasingly produced from bio-based or bioplastics, particularly for high-value products such as organic foods.

The using of renewable resource and biodegradability are the key features of bioplastic to be attractive in food packaging. Biodegradability allows the bioplastics enable to go to biological waste treatments, such as composting and anaerobic digestion (AD) without having to separate packaging resulting in divert organic waste from landfill. Moreover, the production by using renewable resource is environmentally friendly sound and promotes sustainability.

Compared with conventional plastics, bioplastics are still in their early stage of development. The relatively higher materials costs and lack of certain technical performances are among the main challenges to overcome. Classifications and descriptions of some main bioplastics are given in some details in the section below.

## 2.2 Bioplastic materials and composites

Many bioplastics have become commercially obtainable and some of them are under development. The information below gives a brief overview of the main types of bioplastics and their blends.

### 2.2.1 Classification of bioplastics

There are many ways to categorize and classify bioplastics based on, for instance, their origins, chemical compositions, synthesis method, or applications. Generally, based on origins, bioplastics can be classified as from renewable or non-renewable resource. For renewables, they can be divided into plastics that a) natural polymer extracted from plant or animal sources, b) synthesized from renewable monomers, and c) produced by microorganisms or bacteria. For non-renewables, they can be categorized into bioplastics with a) hydrolysable backbone and b) carbon backbone. Classification of biodegradable plastics based on their origin is shown in Figure 2.1.

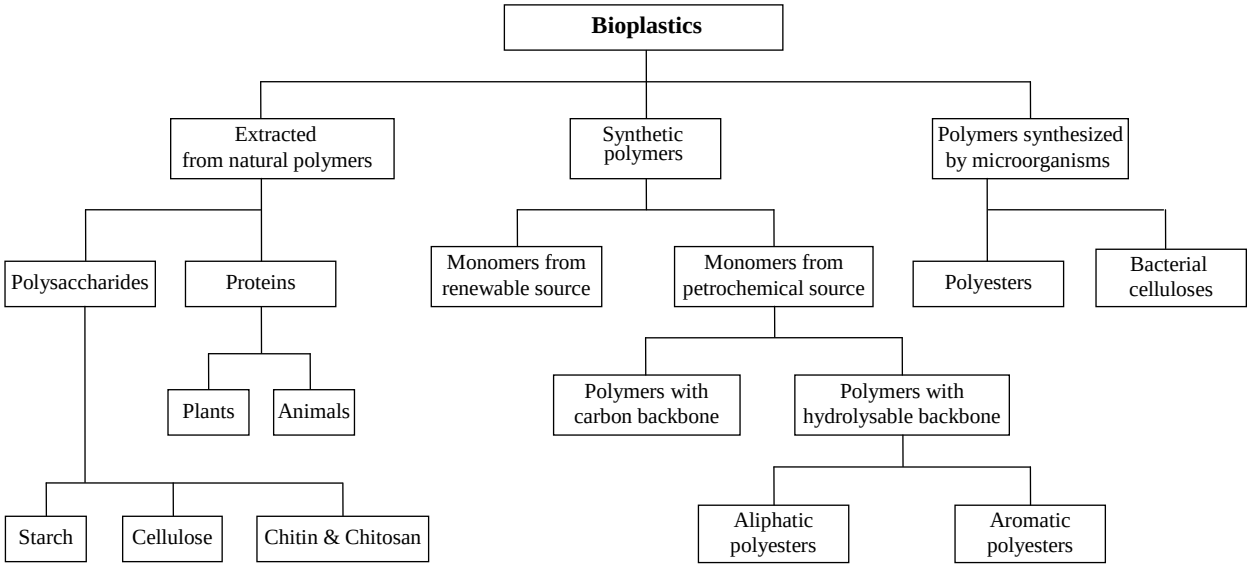


**Figure 2.1:** Classification of bioplastics based on their origin (adapted from Song *et al*., 2011)

Chitosan can be coated on paper-based packaging in order to enhance fat barrier properties; however, the coating cost is quite high compared to general treatment (Ham-Pichavant *et al.*, 2005). Moreover, chitosan-based film also shows the probability to be used as antimicrobial packaging for food preservation because it possesses high antimicrobial activity (Dutta *et al.*, 2009).

Poly(lactic acid) (PLA) is one of the popular biodegradable polymers, which is increasingly being used as packaging. The packages that applied PLA as its materials are containers, drinking cups, sundae and salad cups, overwrap and lamination films and blister packages (Auras *et al.*, 2004). Although PLA is also developed for antimicrobial food packaging, the combination of PLA and nisin can improve for higher antimicrobial efficiency of PLA (Jin & Zhang, 2008).

Poly(hydroxyalkanoates) (PHAs) have been mainly developed as films coating of the packaging. They can be produced as shopping bags, containers and paper coatings, disposable items such as razors, utensils, diapers, feminine hygiene products, cosmetic containers, and cups. Also, according to Proctor & Gamble, Biomers, Metabolix, and several other companies, PHAs turns to be packaging material for medical surgical garments, upholstery, carpet, compostable bags and lids, or tubs for thermoformed articles (Chen, 2010).

Bucci *et al*. (2005) compared the potential performance between poly(3-hydroxybutyrate) (PHB) and PP in term of food packaging and found that PHB could become the alternative option for using it as food packaging in the future. Though PHB shown the better performance than PP at high temperature, its application cannot replace PP under normal refrigeration and freezing condition.

Cava *et al*. (2006) reported the thermal and retorting resistance and oxygen, water vapour, aroma and solvent barrier properties of polycaprolactone (PCL), amorphous poly(lactic acid) (aPLA) and poly(3-hydroxybutyrate-*co*-hydroxyvalerate) (PHBV) and some of their nanocomposites compared with PET for food packaging applications. PHBV withstood retorting condition (120 °*C*) and presented water and aroma (limonene and linalool) barrier properties at same level of PET, however it was inferior on solvent resistance (toluene and ethanol) and oxygen barrier properties. PCL and aPLA melted below 120 °*C* and presented low oxygen barrier property. Although the incorporation of nanocomposites improved PCL and aPLA oxygen barrier property, they are not comparable with high-oxygen-barrier grades of PET films.

For the next part, the details of the bioplastic would be discussed.

#### 2.2.1.1 Extracted from natural polymers

**a) Polysaccharide**

***Starch***

Starch is a polymer which occurs widely in plants. It is the storage polysaccharide of cereals, legumes and tubers. In nature, starch is found as semi-crystalline granules.

Starch is a polymer of D-glucose structured in two major components: amylose (Figure 2.2) and amylopectin (Figure 2.3) (Clarimval & Halleux, 2005). Amylose is linear polymer of 1-4-linked α-D-glucopyranosyl units, while amylopectin is highly branched polymer composed of chains of α-D-glucopyranosyl units linked together mainly by 1-4-linkages but with 1-6-linkages at the branching points. The ratio of the two components varies according to starch types (Petersen *et al*., 1999). Both fractions are readily hydrolysable at the acetal link by enzymes (Chandra & Rustgi, 1998). The α-

1,4-link in both constituents of starch is attacked by amylases and the α-1,6-link in amylopectin is attacked by glucosidase.

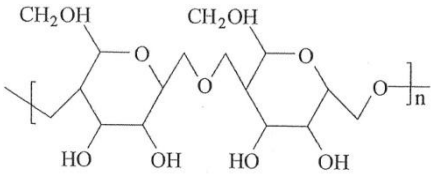


**Figure 2.2:** Structure of amylose (Clarimval & Halleux, 2005)

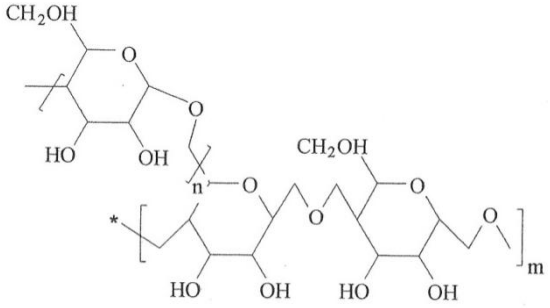


**Figure 2.3:** Structure of amylopectin (Clarimval & Halleux, 2005)

The high biodegradability and low cost of starch makes it attractive for production of biodegradable packaging materials. However, starch alone does not possess melt processibility and adequate mechanical properties for packaging applications (Davis & Song, 2006) and it is very hydrophilic. Therefore, destructurisation of the native semi-crystalline structure is necessary to allow further processing and physical or chemical modifications. Dry starch is not a thermoplastic but by adding plasticizer such as water, starch becomes thermally processable (Petersen *et al*., 1999). Thermoplastic starch or TPS is an amorphous thermoplastic starch after destructurization of the crystalline structure and plasticization (Clarimval & Halleux, 2005).

The most significant limitation of starch is possibly its hydrophilic nature. Chemical modification of starch by acetylation adjusts the hydrophilic character of starch and improves its physical properties (Copinet *et al.*, 2001; Guan *et al*., 2005). The hydroxyl groups in starch are substituted by bigger and less polar acetyl groups. The degree of substitution (DS) presents the average number of hydroxyl groups substituted by acetyl groups. Source of starch, amylase and amylopectin ratio, the amount of reagents and

reaction time all affects DS value and water resistance. The modification is expensive and decrease biodegradability (Xu *et al*., 2005).

Thermoplastic starch (TPS) is one of interesting modified starch and already launched in the market. The plasticizers are used to reduce glass transition and improve brittleness of starch and the most employed plasticizer used to process starch to TPS is glycerol due to its high boiling point, availability and low cost (Kaseem *et al*., 2012). Other plasticizers can be water, urea formamide, ethylenebisformamide, sorbitol, citric acid, N-(2-hydroxyethyl)formamide and amino acids. More recently, thermoplastic starch has been blended with synthetic polymers to improve its brittleness and hydrophilicity or reduce cost and enhance the biodegradability of conventional plastics such as LDPE (Mazinos *et al.*, 2001) and PP (Zuchowska *et al.*, 1998). Mater-Bi® is a family of such TPS manufactured by Novamont spa, Italy.

***Cellulose***

Cellulose is an abundant natural polymer commonly found in plant fibres and is a low cost material. It is a fully biodegradable renewable resource. Cellulose (Figure 2.4) is almost a linear polymer of andhydroglucose (Tull *et al*., 2000). This chemical structure permits the chains to form strong hydrogen bonding and high crystallinity. The main uses of cellulose are for paper, membranes, dietary fibres, explosives and textile (Clarimval & Halleux, 2005). A well-know product is the transparent packaging film called "Cellophane", produced by dissolving cellulose in "Xanthation" mixture and recast in sulphuric acid. It has good mechanical properties and good oxygen barrier at low relative humidity but at high relative humidities, the gas barrier properties are poor (Peterson *et al*., 1999; Nayak, 1999).

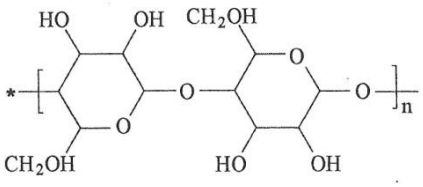


**Figure 2.4:** Structure of cellulose (Clarimval & Halleux, 2005)

Besides, cellulose may be modified by chemicals reaction such as esterification or etherification of individual hydroxyl groups on the polysaccharide backbone so as to improve its thermoplastic behaviour (Clarimval & Halleux, 2005). A number of derivatives are commercially obtainable, including cellulose acetate, ethyl cellulose, hydroxyl ethyl cellulose, hydroxyl propyl cellulose, hydroxyl alkyl cellulose, carboxyl methyl cellulose and fatty acid esters of cellulose. The thermoplasticity of cellulose derivatives increases with rising degree of substitution (DS). But higher DS gives rise to reduction in biodegradability (Simon *et al*., 1998). The most popular cellulose derivative is cellulose acetate (CA). Commercially CA is available with a DS between 1.7 and 3.0 (Moore & Saunders, 1997; Nayak, 1999). CA with low DS values can be said to be readily biodegradable but those with DS above 2.5 are slowly biodegradable. Applications of cellulose ester are including coating, film and membrane and controlled releasing in pharmaceutical applications (Edgar *et al*., 2001).

***Chitin and chitosan***

Chitin is one of the most abundant polysaccharide found in the exoskeletons of crustacean such as crabs, lobsters, shrimps, insect cuticles and many fungal species (Clarimval & Halleux, 2005). Most chitins and derivatives are extracted in concentrated sodium hydroxide (NaOH) solutions. Chitosan is a deacetylated derivative of chitin and can be dissolved in weak acids such as acetic acid, which is usually a test criterion to differentiate chitin and chitosan. Chitin and chitosan are repeating units of glucosamine and *N*-acetylated glucosamine (2-acetylamino-2-deoxy-d-glucopyranose) units link by (β1→4) glycosidic linkage. The structure of chitin and chitosan are presented in Figure 2.5 and 2.6 respectively. Chitin is in an acetylated form, while chitosan is in a deacetylated form (Koide, 1998). Chitin and chitosan show biodegradability, bio-functionality and biocompatibility and are nontoxic. They usually are employed in food contact applications, edible films and food additives. They are found to have high antimicrobial activity and studied for antimicrobial packaging to improve the quality and safety and to extend the shelf-life of perishable foods. (Ham-Pichavant *et al*., 2005; No *et al*., 2007; Dutta *et al*., 2009; Tripathi *et al*., 2009).

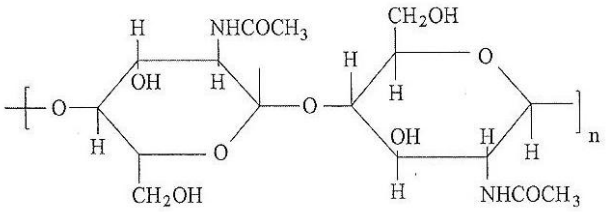

**Figure 2.5:** Structure of chitin (Clarimval & Halleux, 2005)

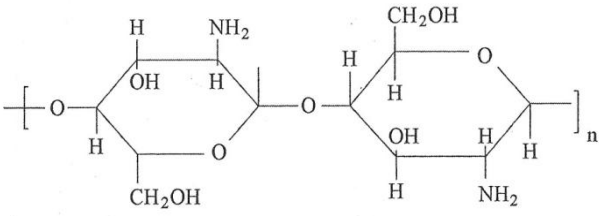

**Figure 2.6:** Structure of chitosan (Clarimval & Halleux, 2005)

**b) Protein**

Proteins are random copolymers of amino acids and the side chains obtainable from either plant or animal origins. Proteins are traditionally applied in adhesives and as edible films/coating. As a class of natural biodegradable polymers, they are gaining more attention in wider food packaging applications (Petersen *et al*., 1999).

***Plant-based proteins***

Zein proteins are corn proteins that are soluble in alcohol and the cast films possess excellent grease resistance (Nayak, 1999; Tull, 2000). The films are brittle and therefore need to be plasticized. Films and coatings based on zein are used in preserving fresh food, producing edible films, and used in bio-based packaging.

Gluten films show high gloss like PP and are flexible, transparent, completely biodegradable (Tull, 2000; Clarinval & Halleux, 2005). They are insoluble in water but adsorb water during immersion. They are moderate $O_2$ and $CO_2$ barriers and thus used to preserve fresh vegetables (Nayak, 1999). The films are also used to improve the quality of cereal products, and retain antimicrobial or antioxidant additives on food surface.

Soy beans consist of about 38% protein among other components (Clarinval & Halleux, 2005). Soy proteins are commercially obtained with different protein content from the lowest as soy flour, then, soy concentrate and the highest as soy isolate (Tull, 2000). Its mechanical properties are similar to gluten. Soy proteins have been successfully used in adhesive, inks and paper coatings.

***Animal-based proteins***

The main proteins from animal origins are collagen, gelatin, casein and whey. Collagen is a fibrous, structural protein found in animal tissue (skin, bone and tendons) (Tull, 2000). Gelatin is a derivative of collagen obtained by degradation via acid or alkaline hydrolysis. Collagen and gelatin are usually used in film applications (Nayak, 1999). Collagen has been used in edible coating in meat industry while gelatin has been used in producing transparent, flexible, water resistance and oxygen barrier films.

Casein is protein derived from milk (Tull, 2000). Although casein materials do not dissolve directly in water, after 24 hour immersion, they gain weight approximately by 50%. Because it shows favorable adhesive properties, it is used for binder or adhesive, and they are also extensively studied for edible films (Chambi & Grosso, 2006).

Similar to casein, whey is also milk protein, capable of forming transparent flexible, colourless, and odourless films.

#### 2.2.1.2 Synthetic bioplastics

Synthetic bioplastics are man-made plastics produced from monomers either from renewable or petrochemical origins by polymerization technologies.

**a) Monomers from renewable source**

Poly(lactic acid) (PLA) shown in Figure 2.7 is one of the most commercially exploited biopolymers, which is produced from renewable resource, e.g. lactic acid monomer, by fermentation of sugar feedstock such as corn, other cereals as well as sugar cane etc. (Cabedo *et al.*, 2006). PLA can be synthesized by two pathways: direct condensation of lactic acid and ring opening polymerization (ROP) of the cyclic lactide (Imam *et al.*, 2008). The direct condensation is a difficult method to obtain high molecular weight

PLA because of the reversible reaction with water that is produced during polymerization. Most work has focused on the ROP method.

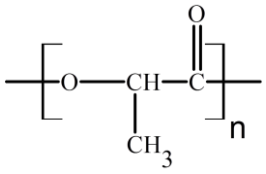


**Figure 2.7:** Structure of PLA (adapted from Auras *et al.*, 2004)

PLA is readily biodegradable by industrial composting but not by lower temperature home composting (Song *et al.*, 2009). It is transparent and has good mechanical properties. The properties of the PLA material are highly related to the ratio between L-lactide and D-lactide enantiomers. Modifying this ratio can vary PLA from semi-crystalline to amorphous form and thus control the properties. PLA with L-lactide content more than 93 % is semi-crystalline polymer while PLA with L-lactide between 50-93% is amorphous (Auras *et al.*, 2004). Naturework$^{TM}$ is a well-known PLA resin produced by Cargill Dow LLC, USA.

Composting of commercial PLA products, such as water bottles, trays and deli containers, is studied by Kale *et al*. (2006). Gel permeation chromatography (GPC), differential scanning calorimetry (DSC), thermal gravimetric analysis (TGA) and visual assessment were used to investigate the degradability of the PLA products under controlled composting conditions (T > 55 °*C*, > 65% RH, pH~7.5). It was shown that, under the composting conditions, PLA trays and deli containers degraded completely within 30 days.

PLA also offers safety for food contact applications. The amount of lactic acid and its derivatives that migrate to the food stimulant solution is lower than any of the current average dietary lactic acid intake values (Auras *et al.*, 2004).

At room and lower temperatures, PLA packaging performs as well as PET, PS containers (Siracusa *et al.*, 2008). The heat distortion, gas permeability, impact strength and processability, are often relatively poor. The most important limitations on the use of PLA for food packaging applications are the moderate oxygen and carbon dioxide

permeability, poor water vapour barrier (Auras *et al.*, 2004 & 2005) and its brittleness. The latter can be improved e.g. by blending with other polymer such as polycarprolactone (PCL) (Cabedo *et al.*, 2006).

**b) Monomer from petrochemical sources**

The bioplastics in this section are divided in two main groups: polymers with hydrolysable backbones and those with carbon backbones.

***Polymers with hydrolysable backbones***

Polyesters are the main family of hydrolysable polymers which can be further divided into aliphatic and aromatic polyester. A selection of polyesters and their derivatives are shown in Table 2.2.

Generally, aliphatic polyesters are more susceptive to hydrolysis and biodegradation than aromatic (Gross & Bhanu, 2002) as the presence of aromatic rings in the latter leads to more resistance to chemical attack and hydrolysis.

**Table 2.2:** Biodegradable polyesters (adapted from Clarimval & Halleux, 2005)

| Group | | Type | Derivates | Origin | Production |
|---|---|---|---|---|---|
| Polyesters | Aliphatic | PHA | PHB | Natural | Natural |
| | | | PHV | Natural | Natural |
| | | | PHH | Natural | Natural |
| | | PGA | | Double | Synthetic |
| | | PLA | | Double | Synthetic |
| | | PBS | PBSA | Mineral | Synthetic |
| | | PCL | | Mineral | Synthetic |
| | Aromatic | PBT | PBAT | Mineral | Synthetic |

| | | | | | |
|---|---|---|---|---|---|
| | | | PBST | Mineral | Synthetic |
| | | | PTMAT | Mineral | Synthetic |

*Alipahatic Polyesters*

Aliphatic polyester is synthesized via the polycondensation reaction of aliphatic diols and aliphatic dicarboxylic acids. Among the aliphatic polyester family, polycaprolactone (PCL), poly(lactic acid) (PLA) and poly(glycolic acid) (PGA) are commercially produced in large volumes (Gunatillake & Adhikari, 2003).

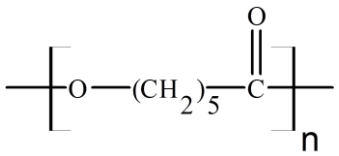


**Figure 2.8:** Structure of PCL (adapted from Nayak, 1999)

PCL is a semi-crystalline (~50% crystallinity) polymer as shown in Figure 2.8, can be obtained by the ring opening polymerization of ε-caprolactone. PCL shows good resistance to water, oil, solvent and chlorine, low viscosity and easy to process (Siracusa *et al.*, 2008) with a low melting point (55-60 °*C*) and glass transition temperature (-60 °*C*) (Ray & Bousmina, 2005; Nair & Laurencin, 2007).

PCL can slowly be degraded by microorganisms (Pandey *et al.*, 2005). Their degradation rate decrease with increase of molecular weight and crystallinity (Moore & Saunders, 1997). Because it is high permeability to many drugs, nontoxic and slow biodegradation, it has found applications in time-dependant release mechanisms such as drug/vaccine delivery (Nair & Laurencin, 2007). General applications of PCL also include orthopedic casts, mould release agents and pigment dispersant (Nayak, 1999). It is often used to compound with other biodegradable materials, such as starch to produce biodegradable polymer blends.

*Aromatic Polyesters*

Aromatic polyesters are synthesized by polycondensation of aromatic dicarboxylic acids. The outstanding representative polyesters from this group are poly(ethylene

terephthalate) (PET) and poly(butylene terephthalate) (PBT). Since the aromatic ring induces resistance to chemical attack and hydrolysis, addition of hydrolysis-sensitive monomers is applied to increase their biodegradability. For example, modification of PBT with succinic acid results in poly(butylene succinate-*co*-terephthalate) (PBST) or introducing adipic acid to form poly(butylene adipate-*co*-terephthalate) (PBAT). Combination of tetramethylene glycol, adipic and terephthalic acids produces poly(tetramethylene adipate terephthalate) (PTMAT) (Clarimval & Halleux, 2005).

***Polymers with carbon backbones***

Poly(vinyl alcohol) (PVOH) is the most recognized example in this group. It is a water-soluble polymer shown in Figure 2.9. According to Sakai *et al*. (1986), the mechanisms of biodegradation consist of two steps. The first step is the oxidation of secondary alcohol, then, degradation with β-diketone hydrolase. It is difficult to prepare PVOH via general polymerization so it is usually manufactured by the hydrolysis of poly(vinyl acetate) (PVAC). The degree of water solubility and the physical characteristics of PVOH are dependent on molecular weight and degree of hydrolysis of PVAC to PVOH (Moore & Saunders, 1997). The melting point of a fully hydrolyzed grade PVOH is around 230 °*C*. Rapid thermal decomposition takes place at temperature above 200 °*C* which causes difficulties in processing. For partially hydrolyzed grades, the melting temperature falls into 180-190 °*C* region (Nayak, 1999).

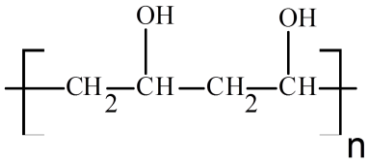


**Figure 2.9:** Structure of PVOH (adapted from Nayak, 1999)

**2.2.1.3 Polymers synthesized by microorganisms**

**a) Poly(hydroxyalkanoate) (PHA)**

Poly(hydroxyalkanoate) (PHA) is a family of microbial polymers. The most renowned member among them is poly(3-hydroxybutyrate) (PHB) produced in nature by bacterial fermentation of glucose and acetic acid (Savenkova *et al.*, 2000). PHB has physical and

mechanical properties that are similar to those of low- density polyethylene (LDPE) and isotactic polypropylene (iPP) (Sato *et al*., 2004; Sudesh *et al*., 2007; Serafim, 2008). It provides strong barrier properties with better oxygen barrier than polypropylene (PP) and poly(ethylene terephthalate) (PET) and good resistance to water (Parra *et al*., 2006). This polymer also possesses biocompatibility and biodegradability. These characteristics of PHB make it suitable as a packaging material, especially for advanced food packaging (Bucci *et al.*, 2005; Bucci *et al*., 2007; Sanchez-Garcia *et al.*, 2008). However, its inherent physical properties such as brittleness (Koning & Lemstra, 1993) and thermal instability (Hablot *et al*., 2008) restricted its processing and application.

Many methods were proposed to overcome these disadvantages, such as blending (Chee *et al*., 2002; Kaito, 2006) and grafting (Liu *et al*., 2009; Zhijiang *et a*l., 2011). Copolymerization of PHB with other monomers becomes one of the current effective approaches. Copolymerization of PHB with hydroxyvalerate (HV) to produce poly(3-hydroxybutyrate-*co*-hydroxyvalerate) (PHBV) for instance results in a lower melting point and better flexibility (Liu *et al*., 2002; Vroman & Tighzert, 2009). Other bacterial materials in the PHA family include poly(3-hydroxybutyrate-*co*-4-hydroxybutyrate) or P(3HB-*co*-4HB), poly(3-hydroxybutyrate-*co*-hydroxyhexanoate) or P(3HB-*co*-3HHx), and poly(3-hydroxybutyrate-*co*-3-hydroxypropionate) or P(3HB-*co*-3HP) (Lee *et al.*, 2008). Figure 2.10-2.12 present structures of some polymers and copolymers in the PHA family.

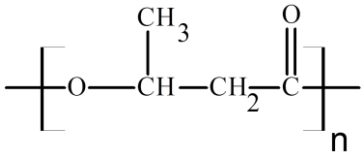

**Figure 2.10:** Structure of PHB (adapted from Imam *et al.*, 2008)

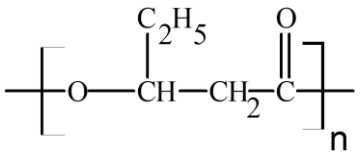

**Figure 2.11:** Structure of PHV (adapted from Imam *et al.*, 2008)

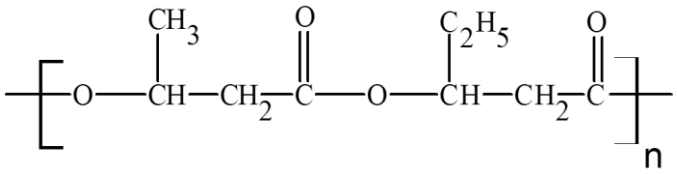

**Figure 2.12:** Structure of PHBV copolymer (adapted from Imam *et al.*, 2008)

PHAs can be biodegraded by a number of aerobic and anaerobic microorganisms in various environments, e.g. soil, activated or anaerobic sludge, seawater and fresh water (Shah *et al.*, 2008). In composting trials at 55% moisture level and 60 °*C*, PHBV was composted up to 85% within 7 weeks, and PHA-coated paper was degraded and incorporated into the compost (Nayak, 1999).

The most significant obstacle to overcome to achieve more widespread application in packaging, as for many other bio-plastics, is its competitiveness in cost. To overcome this problem and improve properties, blending of PHB and PHBV (Avella *et al.*, 2000), the use of waste as a food source to the microorganisms (Khardenavis *et al.*, 2007), use of transgenic plants instead of bacteria (Snell & Peoples, 2002) are recently being explored.

***Properties of PHB and PHBV***

The mechanical properties of PHB are similar to LDPE and iPP but more brittle. Incorporation of HV produces a copolymer PHBV and leads to lower stiffness but higher toughness (Tull, 2000; Siracusa *et al*., 2008). The properties of the PHBV materials can be controlled by adjusting HV and hydroxybutyrate (HB) ratio via management of the growth medium (Petersen *et al*., 1999; Pijuan *et al*., 2009). Generally, the higher the HB/HV ratio is the stronger and stiffer but more brittle the materials become. Increasing amount of HV in PHBV leads to an improvement on toughness by decreasing in tensile strength, tensile modulus and flexural modulus but increasing in elongation at yield and elongation at break as shown in Table 2.3 (Asrar & Hill, 2002). The increasing of 3HV unit in PHBV copolymer also presents the improvement on izod impact strength and decreasing in Young's modulus (Lee, 1996). The Young's Modulus decreased from 3.5 *GPa* for PHB to 0.7 *GPa* for 25 *mol%* HV whereas the izod impact strength increased from 50 to 400 *J/m*.

**Table 2.3:** Mechanical properties of PHB and its copolymer with HV

| Polymer | Tensile Strength (*MPa*) | Tensile Modulus (*MPa*) | Flexural Modulus (*MPa*) | Elongation at Yield (%) | Elongation at Break (%) |
|---|---|---|---|---|---|
| PHB | 36 | 2500 | 2850 | 2.2 | 2.5 |
| PHB7HV | 24 | 1400 | 1600 | 2.3 | 2.8 |
| PHB11HV | 20 | 1100 | 1300 | 5.5 | 17 |
| PHB22HV | 16 | 620 | 750 | 8.5 | 36 |

Data adapted from Asrar & Hill (2002).

The brittleness of PHB is generally attributed to its high degree of crystallinity (Chen *et al*., 2002). The increasing amount of HV decreases the crystallinity of PHBV (Holmes, 1985; Bauer & Owen, 1988). The results from NMR study confirm that the addition of HV boost the molecular mobility (Chen *et al*., 2002) and increase the ratio of amorphous region (Zhang *et al*., 2007). However, increase materials cost of the copolymer polymer, making it uneconomical for packaging applications. Table 2.4 presents the effect of HV content on rate of crystallization. The results show the significant drop of maximum crystallization rate, crystallization temperature ($T_c$) and melting temperature ($T_m$) with increasing HV content (Asrar & Hill, 2002).

**Table 2.4:** Effect of HV content on the maximum crystallization rate of PHBV

| Polymer | Maximum Crystallization Rate (microns, s) | $T_c$ (°*C*) | $T_m$ (°*C*) |
|---|---|---|---|
| PHB | 4.5 | 88 | 197 |
| PHB6HV | 1.4 | 80 | 186 |
| PHB12HV | 0.43 | 78 | 173 |
| PHB16HV | 0.23 | 70 | 167 |

Data adapted from Asrar & Hill (2002).

The melting point of PHB homopolymer is around 175 °*C* but its decomposition temperature is around 185 °*C* (Poirier *et al.*, 1995) leading to degradation during thermal processing. However, it has been reported that the melting point of PHB can be

controlled by adjusting the 3-hydroxyvalerate (HV) content in the copolymerization (Bluhm *et al.*, 1986; Kunioka *et al*., 1989; Scandola *et al.*, 1992; Poirier *et al.*, 1995; Asrar & Hill, 2002). Melting point can be reduced from 178 *°C* to 70*°C*, the lowest achievable melting point when the ratio of HB/HV is 60/40. This behaviour consents the processing with less thermal degradation.

PHB offers stronger oxygen barrier than PP and PET (Parra *et al.*, 2006) where as the oxygen barrier of 8 *mol%* PHBV is poorer than PET, but better than PP (Cava *et al*., 2006) and comparable water vapour permeability to PET (Shogren, 1997). The study of HV content on WVTR shows that the WVTR is increase when the HV content increases corresponding to the reduction of crystallinity.

**b) Bacterial cellulose (BC)**

Bacterial cellulose (BC) which is synthesized by bacteria such as *Acetobacter*, *Rhizobium*, *Agrobacterium*, and *Sarcina* (Jonas & Farah, 1998) is another class of polymers synthesized by microorganisms. It's the most efficient producers are gram-negative, acetic acid bacteria *Gluconacetobacter xylinus* (previously as *Acetobacter xylinum*) (Krystynowicz *et al.*, 2005). One of the most important features of BC is its chemical purity, unlike cellulose from plants that is usually associated with hemicelluloses, pectin and lignin and thus requires harsh chemical treatments to be extracted and purified.

### 2.2.2 Bioplastic blends and composites

A single bioplastic may not be able to provide sufficient properties on its own and this can be improved by physical and/or reactive compounding with other polymers. In some case, such compounding can also reduce material costs.

PLA is one of the most popular biodegradable polyesters. Blending of poly(L-lactide) (PLLA) and poly(D-lactide) (PDLA) to change the ratio between L-lactide and D-lactide, as discussed in the previous section. PLA can also mix with other bioplastics. For example, it was mixed with PCL to reduce its rigidity (Cabedo *et al.*, 2006). Suyatma *et al*. (2004) studied improvement in water vapour barrier property of chitosan

by addition of PLA. PLA was able improve the water vapour barrier and hydrophobicity of the blends but increasing of PLA content leads to drop of mechanical properties.

PHA, consisting of over 90 different types, is considered one of most promising bioplastics for the near future and blends based on the PHA family was reviewed by Yu *et al*. (2006). PHB for instance was blended with other polymers so as to improve the properties, especially brittleness, and reduce material cost. For instance, blends with cellulose derivatives, which are highly compatible with PHB and thus able to be incorporated at high concentrations, have been studied extensively (Zhang *et al.*, 1997; Maekawa *et al.*, 1999; El-Shafee *et al*., 2001; Wang *et al.*, 2003).

One type of relatively low cost bioplastics is based on blends of starch and other polymers such as PLA, PHEE, PHB and PHBV. Ke and Sun (2001) investigated properties of starch/PLA system as a function of water contents. Foaming of blends of starch and bioplastics (PLA, PHEE and PHBV) using twin-screw extruders was reported by Willet and Shogren (2002). The addition of the bioplastics had considerably reduced foam density and increased radial expansion.

Natural fibres, in place of glass and carbon fibres, are increasingly studied in bioplastic composites to improve their mechanical properties. Avérous *et al*. (2001) showed improvements in modulus, strength and temperature stability by addition of small amount of cellulose fibres in wheat starch-based films. The results corresponded to Shogren *et al*. (2002) who incorporated softwood fibres compatiblied with magnesium stearate, in PVOH and starch using baking method to produce clamshell containers for hot sandwiches.

Currently more focuses are placed on nano-scale bioplastic composites. Addition of nono particles especially nanoclay, have been studied e.g. by Bordes *et al.* (2009), in agro- and petroleum-based biodegradable polyesters and achieved significant improvement in reinforcing effect by using small amounts (<5 *wt*%) of nanoclay. Yu *et al.* (2006) reviewed the nanoclay composites in starch, protein and PLA systems and found the improvement on mechanical properties especially modulus.

### 2.2.3 Test methods for biodegradability of bioplastics

There are many methods to measure the rate of biodegradability and compostability of materials. For example, Chandra and Rustgi (1998) described modified strum test, closed bottle test, petri dish screen, environmental chamber method, and soil burial test. Shah *et al*. (2008) suggested that the rate of biodegradability can be assessed by several methods or a combination of them including visual observations, weight loss measurements, change in mechanical properties or molecular weight, $CO_2$ evolution or $O_2$ consumption, radiolabeling, clear-zone formation, enzymatic degradation (the action of intracellular and extracellular of depolymerases in bacteria and fungi), and controlled composting test.

To harmonize the methods, many of national and international organizations launched standards of testing for biodegradability and/or compostability. The details of some standard tests are reviewed by Narayan (1994) and Narayan & Pettigrew (1999). For example, ASTM committee D20.96 issued "Standard Specification for Compostable Plastics" D6400-99, which corresponds to the European standard EN 13432 "Requirements for Packaging Recoverable through Composting and Biodegradation—Test Scheme and Evaluation Criteria for the Final Acceptance of Packaging" and German Standard DIN 54900. The International Organization for Standardization has also developed ISO 17088, "Specification for Compostable Plastics" which is in similar to the above standards.

The intrinsic biodegradation test measures the conversion of materials to $CO_2$, water and biomass through microbial assimilation. The most important condition is the requirement of >90% conversion of carbon to $CO_2$ for blends, copolymers etc., as measured by ISO 14855 (controlled composting) test method. The pass/fail specification is one significant difference between the standards. D6400 requires 180 days measurement, while EN 13432 and DIN 54900 require 90 days. As well as passing the biodegradation tests, a material must also meet disintegration and safety tests. In terms of disintegration, ISO 16929 and ISO 20200 require more than 90% of its original dry weight to pass through a 2.0 *mm* sieve. The end product of composting must pass the plant growth test for ecotoxicity and its heavy metals level should below certain limit e.g. 50% of the EPA (USA, Canada) prescribed thresholds.

### 2.2.4 Growth of bioplastic market

In 2010, the global plastics production is about 265 million tons a year, with an approximately 6% growth from 2009 (PlasticEurope, 2011). 46.4 million tons was used in Europe and packaging presents the largest segment as 39% of overall European demand. Fossil-based plastics are still the dominant plastic packaging materials. They are of low cost and possess good mechanical, physical and chemical properties.

Development of bioplastics is in its earlier state in comparison with the well developed petro-chemical industry. Current share is approximately 50,000 tons or 5–10% in the total annual plastic consumption in Europe (Siracusa *et al*., 2008).

With the intention to develop bioplastics from renewable resources as alternatives the petrochemical counterparts so as to establish more sustainable economy, greater efforts are to be made in enhancement of their properties, increase in production scales and hence reduce unit cost and persistent marketing.

The most important factor for development of bioplastics is the enhancement of their properties. Certain properties of bioplastics packaging materials, especially the moisture sensitivity, are relatively poor than those of conventional plastics. In order to obtain the desired barrier and mechanical properties demanded by the industry, bioplastics can be blended, coated and laminated with appropriate materials; physical and chemical modifications of bioplastic materials can also be employed to broaden their versatility in conjunction with emerging of new bioplastics from novel bio-refinement and synthesis.

Cost is one of the main barriers to the widespread embracing of bioplastic packaging materials. The current high material costs are attributable largely to the high development costs and low scale of production. In the long term however, the utilization of bioplastics is necessary because the crude oil and natural gas are limited resources. The reduction of production cost can also be assisted by using cheaper raw materials. For example, in PHA production, the production costs can be reduced by use of waste materials as substrates such as agro-industrial wastes (e.g., whey, molasses and palm oil mill effluents) (Salehizadeh & Van Loosdrecht, 2004).

Another important issue from a commercial viewpoint is consumer opinion to bioplastic packaging. With increase of consumer perception and awareness of environmental responsibility, it is expected that consumers will actively support and adopt more widespread use of bioplastic packaging and bulks of consumers are more willing to pay more for a more environmentally friendly product. A study in Kassel, Germany is an example. The packaging made from bioplastics were introduced to the market and the consumers were informed the way to identify, separate and collect them. 82 percent of Kassel's population knew the symbol that indicates compostable packaging (Klauss & Bidlingmaier, 2003). Then, the packagings were collected, mixed with the organic waste and send to a full-scale composting site. The compost quality from bio-waste with and without bioplastics did not show the difference and can be applicable for agricultural purpose (Klauss & Bidlingmaier, 2004).

The consumers' attitude to the new packaging and the method of recycling were also analyzed (Klauss & Bidlingmaier, 2003). 87 percent tended to buy them again and almost 90 percent accepted the replacement of conventional plastic packaging by compostable plastic packaging whereas 75 percent agreed on additional costs for compostable packaging.

The above issues are some examples showing that bioplastics need to be improved in order to compete with the conventional plastics in the world market. It is clear that numerous factors influence the development and success of bioplastic packaging materials. However, the exploitation of bioplastic materials for food packaging will undoubtedly increase because the improvement on their properties, competition price with petro-based plastic and their environmental friendly profiles (Robertson, 2008). Currently they are used in many niche markets, but in the long run bioplastic materials are likely to capture a significant share of the market with improvements in performance, availability and costs.

## 2.3 Bioplastic foams

### 2.3.1 Introduction to foams

Cellular materials are found practically everywhere in our modern life and used in a wide range of applications. According to Gibson and Ashby (1997), cellular materials are generally divided into honey-comb and foam categories. Regular shaped cells of honey-comb are in two-dimensional array while that of foams are less regular and arranged in three dimensions. In Banhart's study (1999), the term "Foam" was defined as the dispersion of gases phase in either liquid or solid phase as depicted in Figure 2.13. In this work, only solid foam or cellular solid is considered and it will be referred as simply "foam". Besides, foam materials can also be subdivided into those with open and closed-cell structures.

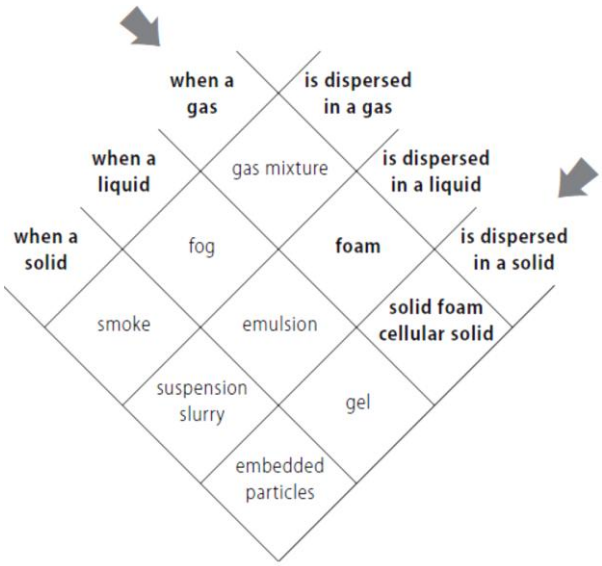


**Figure 2.13:** Definition of foam in terms of dispersion of one phase into a second one. Each phase can be in one of three states of matter (Banhart, 1999)

Foams are extremely attractive materials. For example, they present good stiffness with very low density or high gas permeability with high ability to absorb and damp sound.

The properties and applications of foams materials depend primarily on the solid materials and the cell structure created in foaming processes. The general characterizations of foams may consist of foam density, cell size, fraction of open cells,

anisotropy, and cell shape (Eaves, 2004). Some properties of polymer cellular solids compared with other foams and solid materials are shown in Figure 2.14 (Gibson & Ashby, 1997).

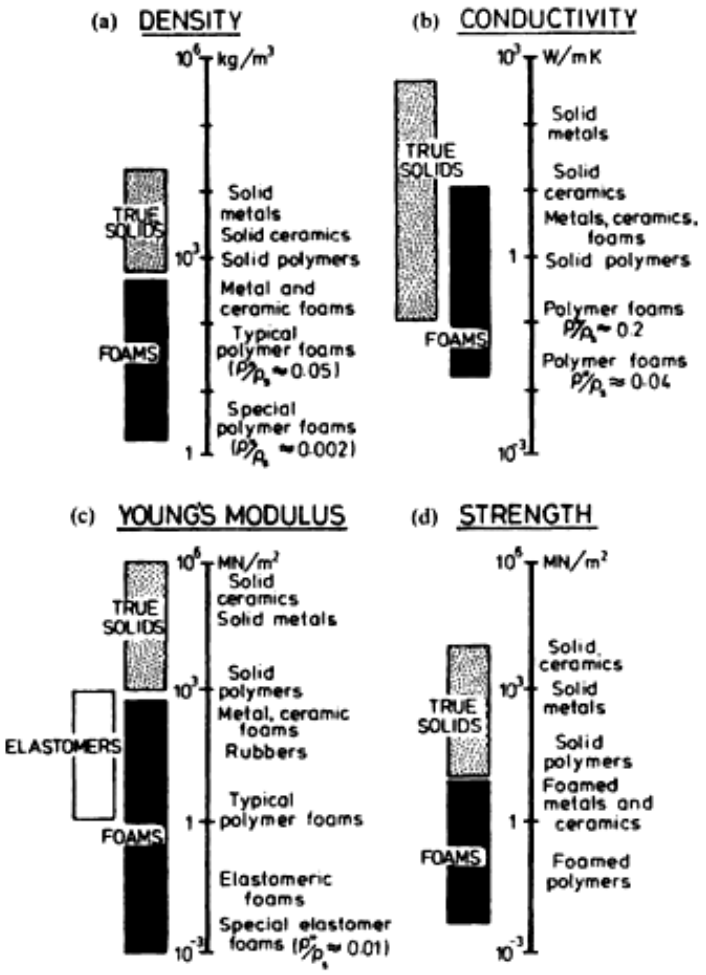


**Figure 2.14:** The range of properties available to engineers through foaming: (a) density; (b) thermal conductivity; (c) Young's modulus; (d) compressive strength (Gibson & Ashby, 1997)

The properties of foamed materials can fulfill applications difficult for true solid materials. The low density of foams allow the materials to be appropriate for light weight or buoyancy applications, such as aircraft, space vehicles, skis, racing yachts and portable buildings. A broad range of cushion materials can be produced by foaming soft materials into low density for energy absorption applications. Foams for thermal insulations can be obtained with materials with low thermal conductivity.

Polymers and elastomers, metals and ceramics are three main groups of materials that are generally used for producing foams (Gibson & Ashby, 1997). Polymers and elastomers foams are probably the most widespread used in various applications varying from common applications, such as acoustic and thermal insulations and cushioning (Frisch & Klempner, 1991) to advanced applications such as engineered scaffold tissues (Mikos & Temenoff, 2000) and hydrogen storage for vehicles (Banyay *et al*., 2007). The properties of these foams vary a great deal because of the variation of polymer structures and cell structures produced (Gibson & Ashby, 1997). Polymers may be amorphous or semicrystalline; linear, branched or cross-linked chains. The molecular weight distributions may also vary considerably. The service temperature is another factor determining polymer properties as they normally act rubber-like at high temperature, whereas glass-like at low temperature. In terms of cell structure, structural parameters (cell density, expansion ratio, cell size distribution, open-cell content, and cell integrity) influence on characteristics of polymeric foams (Lee *et al*., 2007a). These parameters are dominated by foam processing which generally depends on the type of polymer. More details in the correlation between cell structures and foam properties will be informed in section 2.3.2.2.c later.

Polymer foams are produced in a number of different ways. They can be foamed via continuous process such as extrusion foaming or batch process such as injection mould foaming. As this work focus on foaming of bioplastics, foaming technologies for plastic foams are described below in some details.

### 2.3.2 Polymer foaming technologies

#### 2.3.2.1 Principles of foaming

Foams are usually formed by two basic methods (Saunders & Hansen, 1972). The gas phase in the first method is directly introduced in the liquid phase by dispersing an initially continuous gas phase into a continuous liquid phase. In the other method, the gas phase is generated within the liquid phase and letting it to be appears as separate bubbles. The foaming process involves 3 general steps (Saunders, 1991): formation of bubbles in the liquid system, growth of the bubbles and stabilization of the bubbles as discussed in more details below.

**a) Bubble initiation**

Bubble initiation within a liquid including molten polymer is generally known as *nucleation*.

When bubbles are formed within an initially truly homogeneous liquid, which is a rare situation in practice, the process is called *self-nucleation*. Whereas, presence of heterogeneity such as in suspensions with solid particles, nuclei of bubbles tend to form more easily at the liquid-solid interfaces. These solid particles are often referred to as *nucleating agents*. In absence of solid nucleating agents, the liquid phase may actually contain many microbubbles of air which may serve as sites for bubble to grow. As a result, the formation of new bubbles may not be necessary. Even in homogeneous liquid material sites such as the hot spots during exothermic reaction, may serve as nucleating sites. Moreover, mechanical agitation of the liquid may be used to aid in bubble formation, as in the frothing of latex systems.

The formation of bubbles in a liquid will result in new interfaces and thus an increase in the free energy of the system, $\Delta F$ (Saunders, 1991):

$$\Delta F = \gamma \times A \qquad (2.2)$$

Where $\gamma$ is the surface tension of the liquid and $A$ is the total interfacial area. Thus, lowering the surface tension e.g. by adding surfactant will make it easier for the bubbles to form. Besides, the presence of effective nucleating agents may provide significantly reduced surface tension of the liquid-solid interface by forming voids at these interfaces. The presence of voids or dispersed microbubbles of air reduces the requirement for the foaming gas in the process of separating itself from the liquid to form bubbles.

As seen in Figure 2.15, the gas molecules try to form a bubble resulting in positive free energy. If the radius of nucleated cells reaches critical radius ($R_{cr}$), the bubble will grow spontaneously whereas if the radius is smaller than $R_{cr}$, the bubble will collapse.

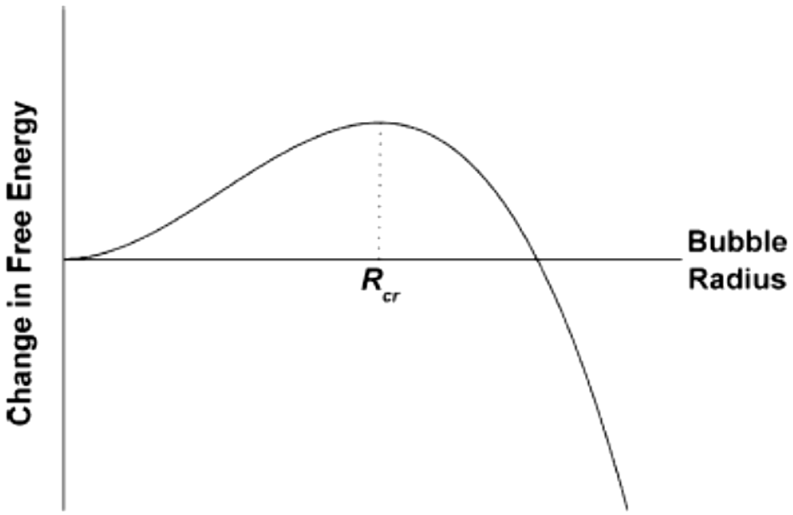


**Figure 2.15:** Change in free energy vs. bubble radius (Leung *et al.*, 2009)

Saunders and Hansen (1972) have described in detail foaming of polymers utilizing blowing agents. The formation of new bubbles in gas-liquid phase takes place in several stages.

i) The gas generated is dissolved into the solution until it exceeds the equilibrium saturation concentration and becomes supersaturated.

ii) When the gas concentration reaches the concentration where self-nucleation begins, then gas comes out of the solution and forms bubbles.

iii) When sufficient bubbles have been formed to reduce the gas concentration in solution under the self-nucleation level, no more bubbles will be formed, and the concentration of gas in solution is further reduced by diffusion from solution into the existing bubbles, causing them to grow in size.

**b) Bubble growth**

As mentioned earlier, the size of the foam cells changes with time because of diffusion of gas from the solution into the cells (Saunders & Hansen, 1972) and diffusion of gas from smaller bubbles to larger ones (Saunders, 1991). Equation 2.2 implies that a greater increase of free energy of the system is required in order to produce fine cells thus the presence of few larger cells is more thermodynamically stable than many smaller cells. This induces the combination or coalescence of cells.

At equilibrium the gas pressure in a spherical bubble is larger than the pressure by $\Delta p$ in the surrounding fluid, the radius ($r$) of the bubble at equilibrium is related to surface tension , $\gamma$ and $\Delta p$ is given in Equation 2.3 (Saunders, 1991),

$$\Delta p = 2\gamma/r \qquad (2.3)$$

Gas pressure in a small bubble is greater than that in a large bubble. To equalize the pressures, smaller bubbles tend to growing, breaking the wall separating the cells, or diffusion of gas from the smaller bubbles into larger ones as indicate by the Equation 2.4 (Saunders, 1991),

$$\Delta p_{1,2} = 2\gamma(1/r_1 - 1/r_2) \qquad (2.4)$$

When $\Delta p_{1,2}$ is the difference in pressure between the two bubbles having radii of $r_1$ and $r_2$.

Given sufficient time, this will lead to the disappearance of the small bubbles and the increase in size of larger bubbles.

**c) Bubble stabilization**

When foaming is completed, the polymer is in the unstable state and needs to stabilize the structure into a solid state for applications. A rapid increase in viscosity of polymeric foams is the major stabilizing mechanism. Reducing the temperature is the common method to enhance material strength to maintain the foamed product structure. In addition the increase of viscosity by polymerization or curing is another option.

In thermoset foams, polymerization and foaming take place at the same time and viscosity rises with degree of polymerization. For molten thermoplastics, they are foamed and then cooled immediately after foaming to obtain the necessary increase in viscosity. In this context, bubble stability is influenced by temperature. An increase in temperature reduces both viscosity and surface tension in a thermoplastic, consequently resulting in the thinning of membranes and leading to rupture of membranes. Conversely, a rise in temperature may also increase polymerization rates in a thermoset system, which can be favourable to stabilize the foam, where ultimate stabilization depends on further polymerization.

For foamed latexes, they are expanded as a fluid polymer-in-water emulsion and stabilized by phase inversion, usually with additional curing.

In liquid foams, bubble walls may be thinned by drainage of the liquid in the bubble walls due to gravity and capillary action. The theory of LaPlace and Young claimed that capillary pressure at the junction of two or more ribs in a cell is lower than that in the membrane and thus promote flow from the membranes into the ribs (Saunders & Hansen, 1972). This effect can also lead to excessive thinning of cell walls and rupture.

**d) General methods for gas generation in foaming**

Production of plastics foams generally utilizes one of the seven methods for gas bubble generation or blowing (Landrock, 1995):

1. Decomposition of a chemical blowing agent (CBA) in the polymer melt at an elevated temperature generate gas(es).

2. Injecting a gas, usually nitrogen, into molten or partially cured resin. The gas may be injected into the resin, either in the barrel of an extruder or injection press, or into a large plastic mass in an autoclave. Subsequent decrease in pressure on the resin leads to the gas expansion and formation of cellular structure.

3. Combination of a bi-functional material, such as an isocyanate, with polyester or other liquid polymer to produce a gas during the polymerization. This technique is usually used for producing polyurethane foams.

4. Evaporation of low-boiling point liquid, either by the heat released by an exothermic reaction or by externally applied heat.

5. Introduce air into a colloidal-resin suspension by frothing and then cure to stabilize the bubbles. This is the principle for foaming latex rubbers.

6. Mixing a nonchemical gas liberating agent, e.g. a gas adsorbed on to the surface of finely divided carbon, into a resin. The mix will release the gas when heated.

7. Heating a pregnant blowing agent, such as pentane, to expand small beads of thermoplastic resin, such as polystyrene.

**e) Blowing agents**

The gas or a gas generating agent that is employed in foaming process is called a blowing agent. The blowing agent plays an important role in controlling density, cellular microstructure, and morphology of polymer foams. All of these affect foam properties and usage. Many blowing agents may be employed in foaming technologies. These agents have been categorized into 2 main groups (Singh, 2004), either physical or chemical blowing agents.

Physical blowing agents (PBA) exploit a change of physical state of the substances, i.e. volatilization, boiling or releasing of compressed gas to expand the materials. Boiling point, molecular weight, vapour pressure in the temperature range used, heat of vaporization, solubility in the materials and finished foams are the general parameters that must be considered (Singh, 2004) alongside with toxicity, flammability and compatibility with the materials in order to choose suitable blowing agents for a safe and economic manufacturing process. Environment compatibility is also one of the important factors. Ozone depletion potential (ODP), global warming potential (GWP), and volatile organic compound (VOC) have also to be considered before using blowing

agents. Finally, the performance, price and competitiveness of the final products are economical considerations in choosing blowing agents.

Chemical blowing agents (CBA) are made of a solid or liquid compounds that release gas(es) by thermal decomposition or chemical reactions under the foaming condition. Moreover, they can be used without any modification of the existing equipment (Vachon, 2005). Generally, the decomposition of CBA results in one or more gases, e.g. $N_2$ and $CO_2$ for expansion process, and solid decomposition products may also remain in the foamed materials. When choosing a CBA, the first and foremost factor is that the polymer processing temperature and the gas liberating temperature should closely matched (Singh, 2004). The reaction products and residue of CBA are the other considerations for CBA selection. There should be no negative effect on either properties or colour of the foamed products. For food contact applications, the toxicity of both the CBA themselves and their decomposition products must be considered.

CBA can be divided into two groups: exothermic and endothermic compounds (Vachon, 2005). Exothermic compounds release energy during decomposition leading to a rapid and efficient decomposition of the chemical agent. On the other hand, endothermic compounds absorb energy during decomposition, which imparts some kind of auto-cooling to the process and be more favorable for a heat-sensitive polymer than exothermic compounds (Vachon, 2005; Lee *et al.*, 2007b). A blend of citric acid and sodium bicarbonate is an example for food-approved endothermic blowing agent and its reaction is shown below (Lee *et al.*, 2007b):

$$C_6H_8O_7 + 3NaHCO_3 \longrightarrow (C_6H_5Na_3O_7)2H_2O + 3CO_2 + H_2O \qquad (2.5)$$

The decomposition temperature can be designed to match polymer processing temperature by changing ratio of citric acid and sodium bicarbonate (Singh, 2004).

### 2.3.2.2 Foam structure and properties

Properties of foamed plastics are influenced by composition of the original polymer, including additives they may contain and geometry of the foam cell structure, which are often referred to as structural variables.

Wide ranges of properties in rigid and flexible plastics foams are shown in Table 2.5 and 2.6, respectively (Suh & Tusim, 1997) and brief descriptions are given below.

**a) Foam structure**

Foam cell structure contains three main elements (Mills, 2007): faces, edges, and, vertices as shown in Figure 2.16. In undeformed polymer foams, faces are usually planar, because there is no pressure difference between the cells. When the faces meet one another, they form edge or ribs. Theoretically, under equilibrium of surface tension, three faces will meet at each edge with interface angle of 120 *°C*. In unloaded foams, cell edges are normally straight. Vertices are the points where, ideally, four cells and four edges meet. In some cases, polymer foams contain some higher order vertices. Two fourfold vertices may merge along one edge, leading to vertices connecting six edges.

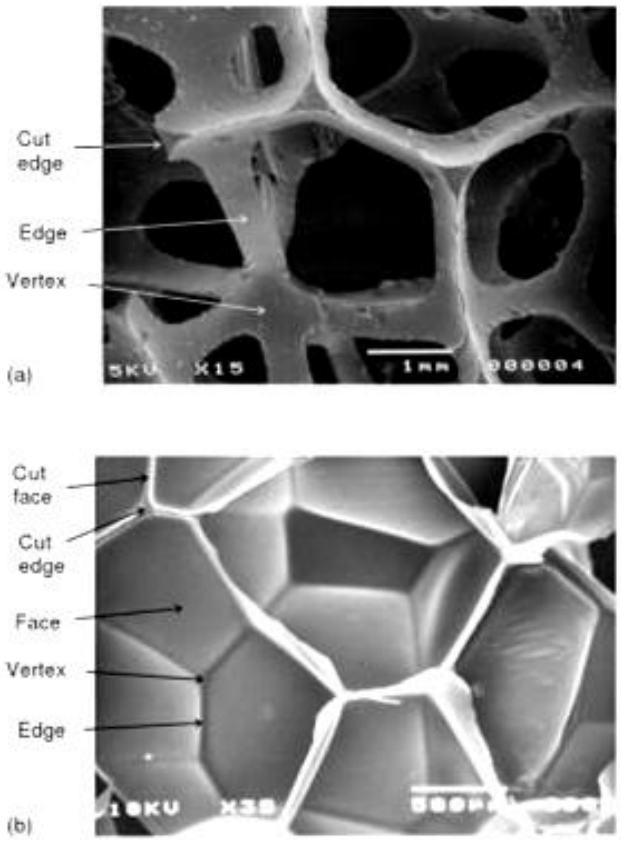


**Figure 2.16:** SEM photographs of (a) open-cell PU foam and (b) closed-cell LDPE foam (Mills, 2007)

Because of the thermodynamic requirement for minimum values of interfacial area and capillary pressure, spherical bubble is the most stable configuration (Shutov, 1991). Nevertheless, idealized closed-pack monodisperse spheres can be in contact with no more than 12 neighbours and the gas-filling ratio cannot exceed 74% (Shutov, 1991). Practically, the shape of foamed cell, however, is almost never spherical. Increasing of gas-filling ratio leads to deformation of the spheres to form dodecahedrons with pentagonal faces. Kelvin's tetrakaidecahedral (14-hedron) presented in Figure 2.17b (Shutov, 1991) is a preferable shape close to the geometry of regularly packed spheres. However, the 12-hedron, which consist of regular pentagons as shown in Fig 2.17c, is a more probable structure, because its equiangular of angles whereas 14-hedron produces a foam structure that is sensitive to coalescence since there is an imbalance in capillary pressure.

**Table 2.5:** Physical properties of commercial rigid foamed plastics (Suh & Tusim, 1997)

| | | | | | Polystyrene | | | | | | | | | Polyurethane | | | | |
|---|---|---|---|---|---|---|---|---|---|---|---|---|---|---|---|---|---|---|
| | | | | | | | | | | | | | | | | Isocyanurate | | |
| Property | ASTM test | Cellulose Acetate | Epoxy | Phenolic | Extruded Plank | | Expanded Plank | | | Extruded Sheet | | PVC | | Polyether | | Bun | Laminate | Urea-formal dehyde |
| Density, kg/m$^{3a}$ | | 96-128 | 32-48 | 32-64 | 35 | 53 | 16 | 32 | 80 | 96 | 160 | 32 | 64 | 32-48 | 64-128 | 32 | 32 | 13-19 |
| Mechanical properties, compressive strength, kPa$^{b}$ at 10% | D1621 | 862 | 138-172 | 138-620 | 310 | 862 | 90-124 | 207-276 | 586-896 | 290 | 469 | 345 | 1,035 | 138-344 | 482-1896 | 210 | 117-206 | 34 |
| Tensile strength, kPa$^{b}$ | D1623 | 1,172 | | 138-379 | 517 | | 145-193 | 310-379 | 1020-1186 | 2070-3450 | 4137-6900 | 551 | 1,207 | 138-482 | 620-2000 | 250 | 248-290 | |
| Flexural strength, kPa$^{b}$ | D790 | 1104 | | 172-448 | 1138 | | 193-241 | 379-517 | | | | 586 | 1,620 | 413-689 | 1380-2400 | | | |
| Shear strength, kPa$^{b}$ | C273 | 965 | | 103-207 | 241 | | | 241 | | | | 241 | 793 | 138-207 | 413-896 | 180 | 117 | |
| Compression modulus, MPa$^{b}$ | D1621 | 38-90 | 3.9 | | 10.3 | | | 3.4-14 | | | | 13.1 | 35 | 2.0-4.1 | 10.3-31 | | | |
| Flexural modulus, MPa$^{b}$ | D790 | 38 | | | 41 | | | 9.0-26 | | | | 10.3 | 36 | 5.5-6.2 | 5.5-10.3 | | | |
| Shear modulus, MPa$^{b}$ | C273 | | | 2.8-4.8 | 10.3 | | | 7.6-11.0 | | | | 6.2 | 21 | 1.2-1.4 | 3.4-10.3 | | 1.7 | |
| Thermal properties, thermal conductivity W/(m×K) | C177 | 0.045-0.046 | 0.016-0.022 | 0.029-0.032 | 0.030 | | 0.037 | 0.035 | 0.035 | 0.035 | 0.035 | 0.023 | | 0.016-0.025 | 0.022-0.030 | 0.054 | 0.019 | 0.026 |
| Coefficient of linear expansion, $10^{-5}$/°C | D696 | | 1.5 | 0.9 | 6.3 | 6.3 | 5.4-7.2 | 5.4-7.2 | | | | | | 5.4-7.2 | 7.2 | 7.2 | | |
| Maximum service temperature, °C | | 177 | 205-260 | 132 | 74 | | 74-80 | 74-80 | 74-80 | 77-80 | 80 | | | 93-121 | 121-149 | 149 | 149 | |
| Specific heat, kJ/(kg×K)$^{c}$ | C351 | | | | 1.1 | | | | | | | | | ~0.9 | ~0.9 | ~0.9 | | |
| Electrical properties | | | | | 1.19-1.20 | <1.05 | <1.05 | 1.02 | 1.02 | 1.02 | 1.27 | 1.28 | | | 1.05 | 1.1 | 1.4 | |
| Dieclectric constant | D1673 | 1.12 | | | 0.028-0.031 | <0.0004 | <0.0004 | 0.0007 | 0.0007 | 0.0007 | 0.00011 | 0.00014 | | | 13 | 18 | | |
| Dissipation factor | | 20 | | | | | | | | | | | | | | | | |
| Moisture-resistance water absorption, vol% | C272 | 4.5 | | 13-51 | 0.02 | 0.05 | 1-4 | 1-4 | 1-4 | | | | | | | | | |
| Moisture-vapour transmission, g/(m×s×GPa)$^{b}$ | E96 | | 58 | | 35 | | <120 | 35-120 | 23-35 | 86 | 56 | 15 | | 35-230 | 50-120 | | 230 | 1610-2000 |

[a] To convert kg/m$^3$ to lb/ft$^3$, multiply by 0.0624

[b] To convert kPa to psi, multiply by 0.145

[c] To convert kJ/(kg×K) to Btu/(lb×°F), divide by 4.184

**Table 2.6:** Physical properties of commercial flexible foamed plastics (Suh & Tusim, 1997)

| | | | | | | | Polyethylene | | | Ploypropylene | | Polyurethane | | | | Silicone | |
|---|---|---|---|---|---|---|---|---|---|---|---|---|---|---|---|---|---|
| Property | ASTM test | Expanded Natural Rubber | | Expanded SBR | Latex Foam Rubber | | Extruded Plank | Extruded Sheet | Crosslinked Sheet | Modified | Sheet | Standard Cushioning | High-Resilience Type | Poly(vinyl chloride) | | Liquid | Sheet |
| Density, kg/m$^{3a}$ | | 56 | 320 | 72 | 80 | 130 | 35 | 43 | 26-28 | 64-96 | 10 | 24 | 40 | 56 | 112 | 272 | 160 |
| Cell structure | | Closed | Closed | Closed | Open | Open | Closed | Closed | Closed | Closed | | Open | Open | Closed | Closed | Open | Open |
| Compression strength 25%, deflection, kPa$^{b}$ | D33574 D3575 | | | | | | 48 | | | 206 | 4.8 | 5.7 | 4.6 | | | | |
| Tensile strength, kPa$^{b}$ | D33574 | | 206 | 551 | 103 | | 138 | 41 | | 344 | | 118 | 103 | 10.3 | 24 | 36 at 20% | |
| Tensile elongation, % | D33574 | | | | 310 | | 60 | 276 | 276-480 | 1380 | 138-275 | 205 | 160 | | | 227 | 310 |
| Rebound resilience, % | D3574 | | | | 73 | | | 50 | | 75 | | 40 | 62 | | | | |
| Tear strength, (N/m)$^{c}$ x10$^2$ | D3574 | | | | | | 10.5 | 26 | | | | 4.4 | 2.4 | | | | |
| Maximum service temperature, °C | | 70 | 70 | 70 | | | 82 | 82 | 79-93 | 135 | 121 | | | | | 350 | 260 |
| Thermal conductivity W/(m×K) | C177 | 0.036 | 0.043 | 0.030 | | 0.050 | 0.053 | 0.040-0.049 | 0.036-0.040 | 0.039 | 0.039 | | | 0.035 | 0.040 | 0.078 | 0.086 |

[a] To convert kg/m$^3$ to lb/ft$^3$, multiply by 0.0624

[b] To convert kPa to psi, multiply by 0.145

[c] To convert kJ/(kg×K) to Btu/(lb×°F), divide by 4.184

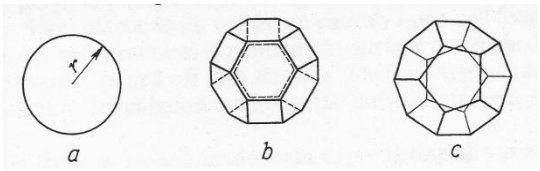


**Figure 2.17:** Several ideal cell geometries (Shutov, 1991)

a. Sphere

b. 14-hedron, with a surface composed of 6 squares and 8 hexagons

c. 12-hedron, with a surface composed of regular pentagons only

Figure 2.18 depicts potential geometries of ribs formed by three contacting bubbles in equal size to produce three-dimensional cell edge (Harding, 1973). The first model (Figure 2.18a) presents the spherical closed-packing. The second (Figure 2.18b) is a structure consisting of absolutely regular dodecahedrons which is unstable because infinity capillary pressure in the liquid phase. The third model (Figure 2.18c) expected to be found in closed-cell foam where gas/solid ratio is more than 74%. Draining of liquid phase results in face deformation and bending of ribs. The actual distribution of liquid between faces and ribs depend on force balances of polymer viscosity, capillary pressure, and surface tension. In the cases that the gas phase increases further, the cell walls become thinner and more liquid phase drains to the ribs. When the walls collapse, the open-cell foam occurs and that presents in Figure 2.18d. Figure 2.18e illustrates the impractical structure that all faces completely drain to the ribs produced minimum-surface dodecahedron.

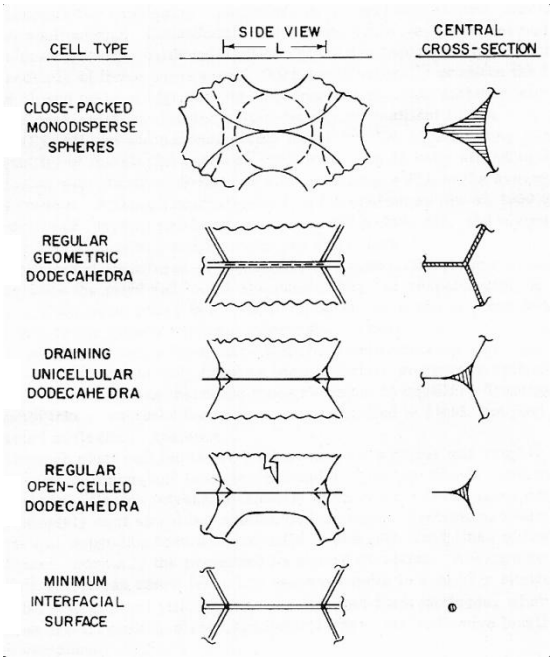


**Figure 2.18:** Potential geometries of the ribs between adjacent cells (Harding, 1973)

**b) Foam properties**

*Mechanical properties*

The mechanical properties are one of the general properties to evaluate foam performance. Compression property is the most popular mechanical property for foams. The stress-strain curve of foams shown in Figure 2.19 may be divided into three regions. In region 1, the linear or 'Hookian' behavior, the cell wall linear elastic bending and stretching determine their behavior. In region 2 the "collapse plateau", significant energy can be absorbed by cell wall buckling, plastic yielding or brittle crushing. Finally, densification of the foam is presented in region 3 where the foam cells completely collapse leading to sharp increase of the compressive stress.

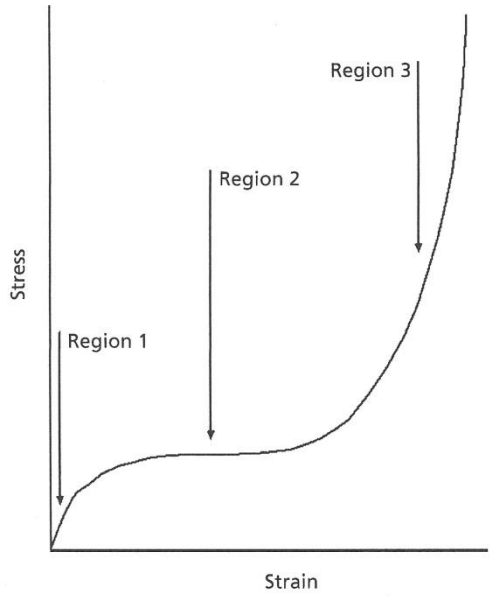


**Figure 2.19:** Schematic compression stress-strain curve for a foam (Eaves, 2004)

The other general foam mechanical characterizations include, for example, flexural, falling dart impact and dynamic shock cushioning (Bureau, 2005). Flexural tests characterize flexural modulus and the flexural strength of foam and also give tensile stress, which is very difficult to achieve for polymeric foams in tensile testing due to stress concentration effects at the grips used to hold the tensile specimens. The impact tests such as falling dart impact informs the ability of foam to resist high velocity puncture while dynamic shock cushioning reports the ability to absorb dynamic compressive shocks and retain its properties.

*Thermal properties*

Thermal conductivity ($k$) of foams is dependent on four factors as follows (Shutov, 1991):

$$k = k_r + k_s + k_g + k_{c,} \qquad (2.6)$$

where $k_r$, $k_s$, $k_g$, and $k_c$ represent heat conductivities from radiation, solid conduction, gases conduction, and convection, respectively. Thermal conductivity of most materials decreases when temperature is lowered (Eaves, 2004) as a result of reduction in thermal conductivity of the solid, gas and radiation.

Specific heat of foamed materials can be established from the sum of the specific heats of the solid components neglecting that of gas as the contribution of it is small.

The thermal expansion coefficients of foamed polymers are basically higher than that of the solid polymer because gas thermal expansion coefficients is higher than those of most rigid materials at ambient. Higher expansion coefficient tends to appear in closed-cell foams, which is attributed to the expansion of the contained gas at high temperature.

*Environment aging*

The effects of environment on foamed plastics are the function of composition of the polymer phase. The large surface area of the materials when expanded into cellular state results in faster reactions of the foam with vapours and liquids when compared with unexpansion materials. All cellular polymers are affected under the combined effect of light, heat and oxygen although additives may control the deterioration rate.

*Energy Absorption Properties*

Foam structure allows deformation of the polymers to absorb more energy compared with their solid state (Eaves, 2004). The plateau region in the stress-strain curve is where the most of energy is absorbed by cell deformation. The cell deformation in elastomer foams respond by elastic buckling of the cell resulting in energy absorption during impact and releasing after impact. However, the hysteresis by polymer deformation and flowing of the air in open cell foams can be driven away some of energy without recovery. In plastic foam, the energy is absorbed by plastic flow of cells while the cell fracture and crushing is the way to absorb energy in brittle foams.

*Other properties*

Although polymers by themselves are poor materials for reducing sound transmission, the foamed materials with open cells on the surface are effective in absorbing sound waves of certain frequencies by less constrained vibration of the cell structure.

Open cells in foam however induce higher permeation rates of gases or vapour as they can permeate through the cell structure by diffusion and convection. Such permeation is

much reduced in closed-cell foams to a degree depending on, polymer and gas compositions, foam density, and cellular structure. Absorption of moisture is correlated to rot, mildew, and fungus resistance of foams and therefore closed-cell foams generally resist microbial attack better than open-cell foams.

**c) Correlation between cell structure and properties of foams**

The properties of plastic foams depend on many parameters. The primary factors are the polymer used to produce the foam and the cell morphology (Shutov, 1991; Suh & Tusim, 1997). Geometry of cells is primarily controlled by the finishing foam density, orientation of cells known as cell anisotropy, the average cell size and ratio of open/close cells.

Since gas is relatively compressible, lower density foams with reduced solid phase will in general be less strong and rigid as demonstrated by Bureau & Gendron (2003) in polystyrene foams.

Cell size also affects mechanical properties. Foams of similar densities but different cell size present the different mechanical properties. Bureau & Gendron (2003) assessed the compressive and impact test of PS foam in term of density to cell diameter ratio ($\rho/d$) and found the enhancement of compressive and impact strength in similar densities PS foams by decreasing in cell size. This result indicated that the mechanical performance of foam might be possible to maintain while density decrease with refinement of cell size. In addition, thermal properties of plastic foams are also influenced by the cell size. As the cell size increases, heat radiation and convection are also increase, leading to rise of thermal conductivity (Shutov, 1991).

Cell anisotropy affects mechanical strengths and stiffness in different directions. Strength and stiffness of anisotropic foam along the elongated cell direction are better than in the perpendicular ones (Ramsteiner *et al*., 2001). For instance, longitudinal compressive strength of polystyrene, polyurethane and phenolic foams were found to increase with the degree of cell elongation (Harding, 1973)

Ratio of open/closed cells also has some effects on the mechanical properties of the foams. Foams with closed cells are more stiff and strong than those of the open cells

(Ramsteiner *et al*., 2001). Blair (1967) (cited by Shutov, 1991) compared compressive strength between nonreticulated and reticulated polyurethane foams. The compressive strength comes from stretching of walls and bending of ribs for the nonreticulated foams while only ribs respond to compressive strength in reticulated foams. Moreover, the gas pressures contained in closed cells also enhance compressive strength (Eaves, 2004) while this is absent in open celled foams where strength rely only on bending resistant of the cell ribs and hence more deformable. Because gas phase plays an important role in thermal conductivity of foams, open and closed cells will have different effects. While open cell foams allow air to penetrate, closed cell foams encapsulate gas inside. Using gases that have low thermal conductivities is an effective way to produce thermal insulating foams reducing overall the conductivity. As thermal conductivity of gas increase with molecular weight, using heavy gas is desirable for thermal insulation. Choosing blowing agents that have desirable gas compositions can assist control of foam thermal conductivities.

#### 2.3.2.3 Foaming Processes

**a) General plastic foaming processes**

*Extrusion foaming* is a general technology combining plastics with blowing agent to produce foams in a continuous process (Lee *et al*., 2007c). The extruder is used to homogenize the polymer and blowing agents under suitable pressure and temperature to produce a gas-polymer solution and when pressure is dropped at the exit, cellular structure will be produced. Figure 2.20 shows the key steps and mechanisms in extrusion foaming.

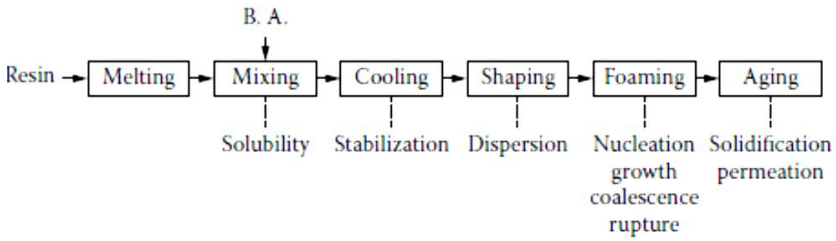


**Figure 2.20:** Foam extrusion steps and the mechanisms involved (Lee *et al*., 2007c)

The important elements consist of melting, mixing, cooling and shaping. First of all, the polymeric solid (resin) is converted into molten stage in the melting stage. Gaseous component is introduced and mixed into the polymer melt in the mixing stage. The solution is then transferred to cooling stage to reduce the bulk heat and adjust the viscosity and is then discharged through a die exit in the shaping stage and to expand in the foaming stage. This is followed by a post-extrusion procedure (the aging stage) where the foam is solidified and stabilized to obtain certain dimensions. This may them be followed directly by a post-extrusion process such as lamination or thermoforming.

In *reactive foaming* of thermoset plastics, generation of gas and polymerization of the resins to trap the gas take places at the same time (Lee *et al*., 2007c). The most common examples are foaming of polyurethane (PU), polyisocyanate, pheniolics and epoxy. In the case of PU, polyols, isocyante, amine catalyst and other additives are mixed and foamed in a continuous, semi-continuous or a batch process. The foaming process can either be of free expansion, as shown in Figure 2.21, or restricted expansion, such as in reactive injection foam molding discussed below.

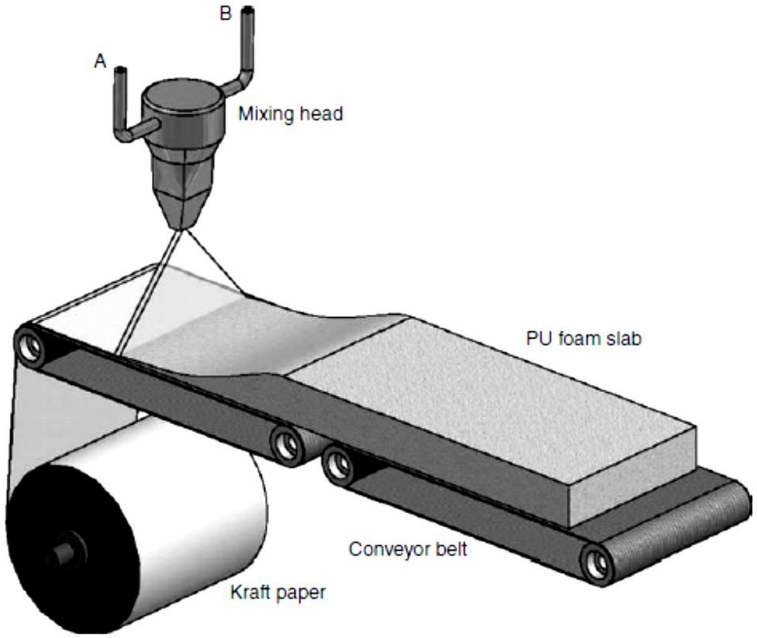


**Figure 2.21:** Continuous free foaming of polyurethane (Lee, 2009)

To manufacture irregular-shaped foam products, *injection mold foaming* can be employed. It is a batch process, but it may also enable several molds to be filled the same injection to increase productivity. Injection mold foaming can be subdivided to five main processes of foaming (Lee *et al*., 2007c):

1. Reactive injection Molding (RIM);
2. Low-Pressure Structural Molding;
3. Co-injection Structural Molding;
4. Gas-Assisted Injection Molding and
5. Microcellular Injection Molding.

*Reactive injection molding* (RIM) is a popular process which generates gas during condensation polymerization of, for example, polyurethane (Lee *et al*., 2007c). The schematics of PU reactive injection foam molding is depicted in Figure 2.22. All components in the PU foam formulation is pumped into a mixing head for preliminary reaction. The mixture is then injected into a mold. The foaming, cooling and setting process take place in the mold and the product is ejected when curing is complete.

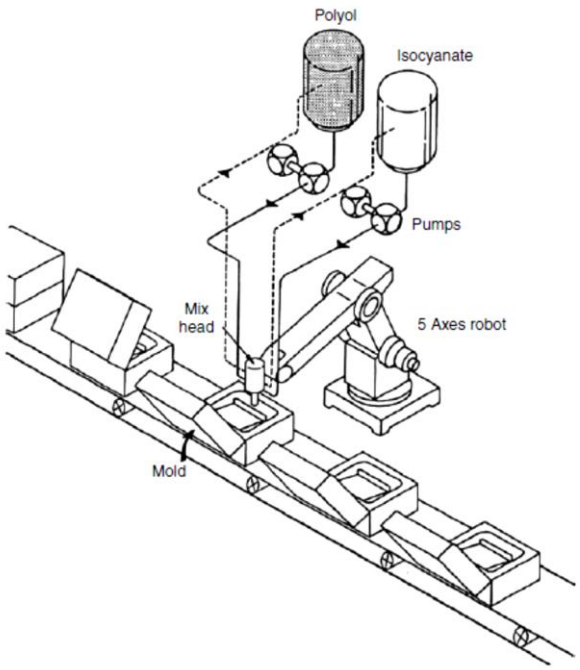


**Figure 2.22:** A set-up of reactive injection foam molding process (Lee *et al*., 2007c)

Typical injection foam molding with an extruder for preparing foamable composition is illustrated in Figure 2.23. The polymer is melted and mixed with either chemical or physical blowing agent in the extruder, or in the case of *gas-assisted injection molding*, with gas introduced by gas nozzle at given pressures and different processing stages (Lee *et al*., 2007c). After homogenization, the molten mixture is injected to a clamed and thermo-controlled mold by the ram. Foaming, forming, cooling and curing take place in the mold followed by ejection.

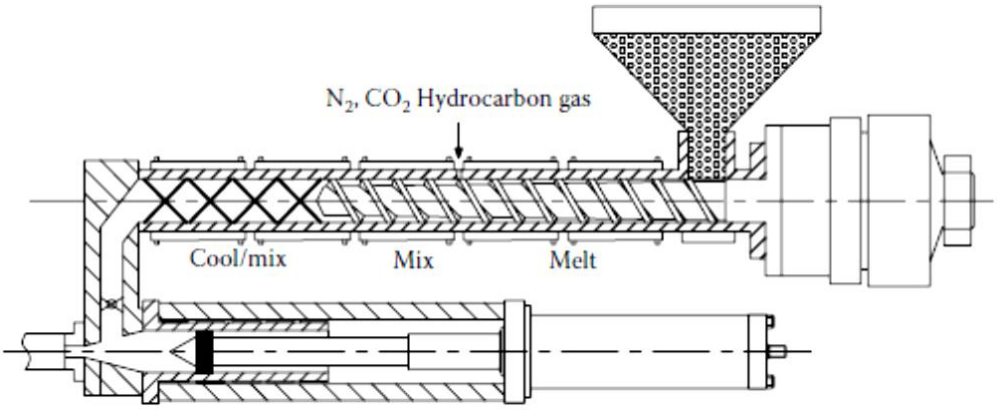


**Figure 2.23:** A typical injection mold foaming process (Lee *et al*., 2007c)

In *microcellular injection molding* as presented in Figure 2.24, the technique takes advantage of supercritical fluid (SCF) - generally inorganic PBA such as $CO_2$ or $N_2$ (Okamoto, 2003). The SCF is injected into the mixing section during the screw recovery step and homogenized with molten polymer creating single-phase solution. Then, it is introduced to a low pressure mold. This method allows the cell size in the magnitude of 10 microns (Lee *et al*., 2007c).

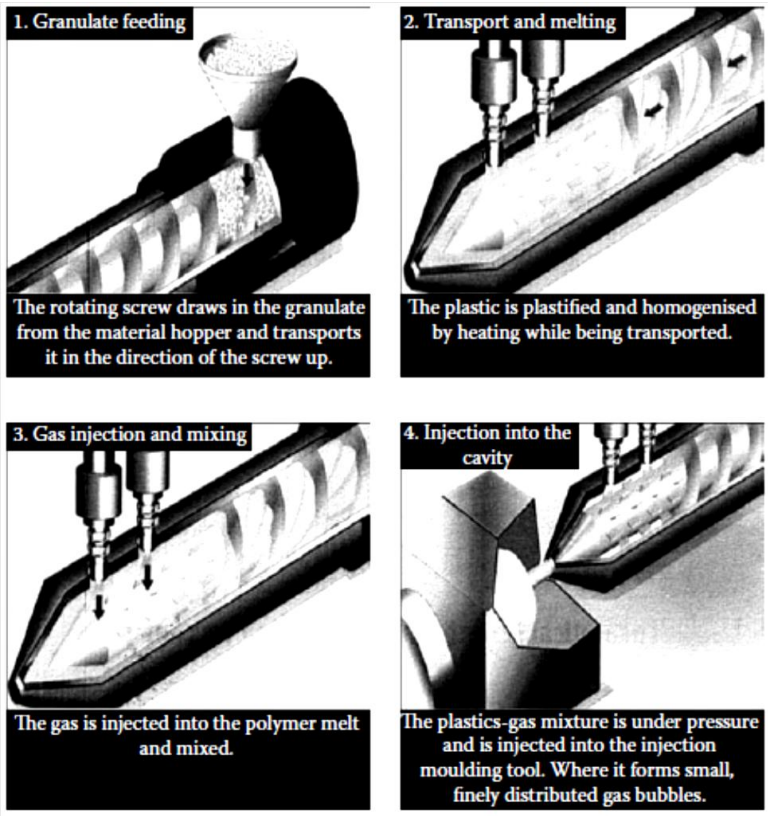


**Figure 2.24:** Microcellular injection molding (Lee *et al*., 2007c)

*Cross-linking* of semi-crystalline polymer is often used for enhancement of melt strength and cell stabilization during foaming (Lee, 2009). The general cross-linking process used for polyethylene is depicted in Figure 2.25.

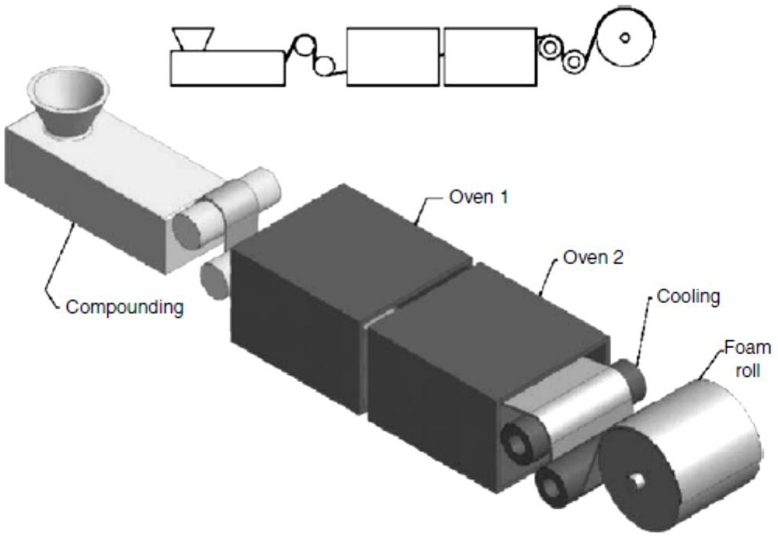


**Figure 2.25:** Cross-linking process for foaming of PE (Lee, 2009)

The chemical blowing agent, cross-linking agent and polymer is compounded via extrusion or roll mils. The material than pass through a lower temperature zone (Oven 1) to activate the cross-linking reaction and followed by a higher heating zone (Oven 2) to decompose the CBA for foaming. The fine cell structure produced results in good resiliency and thermal strength.

In *bead foam molding* as shown in Figure 2.26, the resin is saturated with a physical blowing agent and exposed to a super-saturated condition by lowering pressure or increasing temperature or both. The controlled expansion results in fine and isotropic cell structure. As a batch process however, the productivity is relatively lower compared with the continuous extrusion process. Common applications of this process, for example, are polystyrene bead foams for cushion packaging and protecting helmet (Moosa & Mills, 1998).

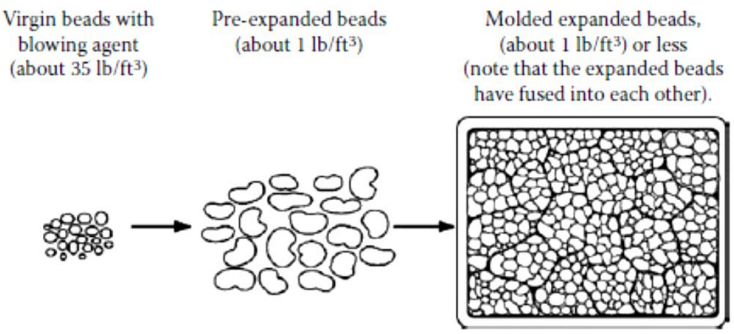


**Figure 2.26:** Schematic diagram of bead foam molding (Lee *et al*., 2007c)

**b) Bioplastic foam processing**

Because of the environment awareness, the increasing amount of wastes and price of petroleum products, there has been increasing demands for bioplastics and foams.

One of the most studied bioplastic foams is starch loose-fill foams for cushion packaging (Lacourse & Altieri, 1989; Sachetto *et al*., 1991; Bastioli *et al*., 1991; Neumann & Seib, 1993). Some researchers have studied the mechanical properties of the starch-based foams including Hayter *et al*. (1986) and Hutchinson *et al*. (1987) on the impact, compression, tension and flexural behavior of starch foams. A power law was found generally applicable to correlate these mechanical properties and the bulk

density. Besides, amylase content, moisture levels and extrusion temperature were found to affect properties of starch foams (Lourdin *et al*., 1995; Cha *et al*., 2001). Potente *et al*. (2006) studied flow and nucleation behavior of the extruded starch foam using a transparent slit die. Use of high pressure gradient and low shear rate led to delay in cell nucleation followed by a high expansion ratio.

Foaming of PLA for disposable food trays, cups, thermal insulators, and cushioning materials was explored by Ajioka *et al*. (1995). The system used were mixture of PLLA, PDLA and 0.5 *wt*% talc in an extruder at 200 °*C* with 140 °*C* at the die. Either dichlorodifluoromethane or butane was used as the blowing agent and injected under pressure into the extruder. Azodicarbonamides powder (a food additive) was also used as a chemical blowing agent in extrusion foaming of PLA. In addition, Sterzel (1995) also described injection mold foaming PLA using a range of physical blowing agents (methyl formate, ethyl formate, methyl acetate, propyl acetate, dioxane and methyl ethyl ketone) at 15–25 *wt*% levels.

As low-cost bioplastics, starch blends with other bioplastics were also investigated. The incorporation of PLA, PHEE and PHBV considerably promoted higher expansion ratio and resulted in lower density foams (Willett & Shogren, 2002). The foams were also more water resistant than starch foams. Extrusion foaming of PLA and acetylated starches blend with 5 *wt*% talc and various amounts of ethanol were studied by Guan *et al*. (2005). Increasing PLA concentration led to more foam expansion while ethanol acted not only as a blowing agent but also a solubilizing agent to homogenize PLA and starch. Preechawong *et al*. (2005) used baking method to produce starch/PLLA foams. They baked the mixtures in a hot mold at 220 °*C* for 2 *min*. The result showed that the addition of PLA increased the foam resistance to water uptake. Moreover, the foams gave rise to superior tensile strength and elongation at break compared with the starch foam. Ganjyal *et al*. (2007) studied the composting of extruded foams from starch acetate and its blend with PLA and confirmed that the starch acetate foam took longer to degrade than the pure starch foam. Addition of PLA can control the degradation rate of the starch acetate foams. The sample containing higher amount of PLA degraded faster.

PHA is a family of promising bioplastics to produce food packaging because it possesses high gas barrier properties (Shogren, 1997; Cava *et al*., 2006) and

compostability (Wang *et al.*, 2005) but there have only been limited studies. Two patents of PHA moldable bead foams were claimed by Kaneka Corporation. In first patent, Fuminobu *et al*. (2007) described method for producing moldable bead foams. Dimethyl ether, diethyl ether or methyl ethyl ether were incorporated under pressure into solid beads of poly(3-hydroxyalkanoate) as blowing agent and expanded by heating. The second patent followed the previous patent but improved the quality of foams by adding an isocyanate as chain extender (Toshio *et al*., 2008). The latter patent also claimed the additional blowing agents including isobutene and pentane.

However, the PHA foams for food packaging have not been well studied. This work focused on extrusion foaming of PHBV using food-approved chemical blowing agent to wider the processing method in bioplastic foam in packaging market.

# Chapter 3
# Materials and Experimental Details

## 3.1 Raw materials and additives

### 3.1.1 PHBV

The two grades of PHBV (Figure 3.1) used in this study were ENMAT™ Y1000P and ENMAT™ Y1010 manufactured by Tianan Biologic Material Co. (Ningbo, P. R. China). ENMAT™ Y1000P is PHBV containing antioxidant and nucleating agent and supplied in yellowish-white pellet form with a solid density of 1.24 *g/cm*$^3$ and 3 *mol%* hydroxyvalerate (HV) content. ENMAT™ Y1010 is PHBV with 3 *mol%* of hydroxyvalerate (HV) content without any additive substances and supplied in white powder form.

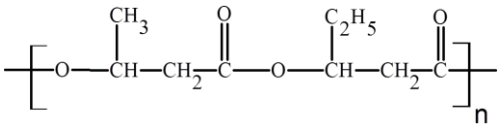

**Figure 3.1:** Structure of PHBV copolymer (adapted from Imam *et al.*, 2008)

### 3.1.2 PBAT

The PBAT (Figure 3.2) used in this study were obtained from two suppliers: Biolice® RFX11 by Limagrain (Ennezat, France) and Ecoflex® F BX7011 by BASF Corporation (Ludwigshafen, Germany) in pellet form. Both PBATs have a solid density of 1.25-127 *g/cm*$^3$ and melting point between 110-120 *°C*.

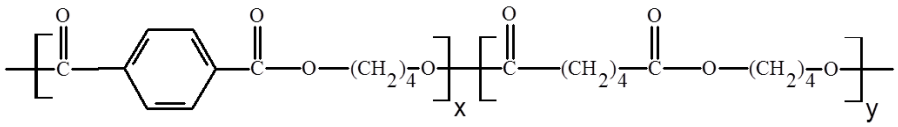

**Figure 3.2:** Structure of PBAT copolymer (adapted from Al-Itry *et al.*, 2012)

### 3.1.3 Chain extender

Joncryl® ADR-4368 S, supplied by BASF Germany in powder form is an epoxy-functionalized chain extender with high number average functionality ($f_n$ >4) and epoxy equivalent rate = 285 *g/mol*. General structure of the epoxy-functionalized chain extender is presented in Figure 3.3.

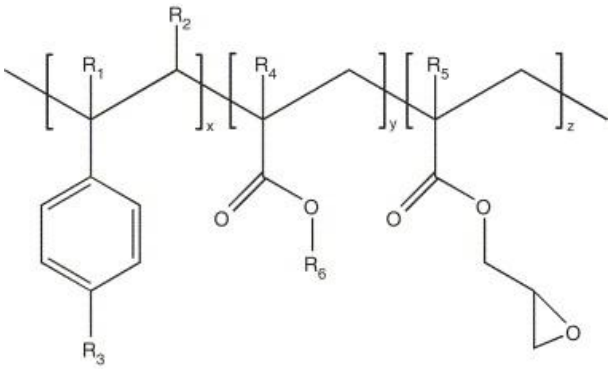


**Figure 3.3:** General structure of the epoxy-functionalized chain extenders. Where R1–R5 are H, $CH_3$, a higher alkyl group, or combinations of them; R6 is an alkyl group, and x, y and z are each between 1 and 20 (Villalobos *et al.*, 2006)

### 3.1.4 Blowing agent

BA.F4.E MG is a blowing agent (BA) masterbatch in a LDPE carrier which contains 40 *wt%* active agents (a mixture of sodium bicarbonate and citric acid). This was supplied in white pellet form by Adeka-Palmarole (Saint Louis, France). It has a solid density of 0.74 $g/cm^3$ and the onset decomposition temperature is 150 °*C*.

### 3.1.5 Calcium carbonate

The calcium carbonate RLO 7999 with density of 2.71 $g/cm^3$ was supplied by Imerys Minerals Ltd. (Par, UK) and its particle size distribution is shown in Figure 3.4.

### 3.1.6 Other additives

Antioxidant 1010, (Pentaerythrite Tetra-[β-(3,5-di-tert-butyl-4-hydroxyphenyl)-propionate]) and BN 1010, a boron nitride nucleating agent, were also supplied by Tianan in powder form. Crodamide ER powder from Croda Europe Ltd. (East

Yorkshire, UK) was used as a slip aid in extruded sheet for thermoforming of food containers.

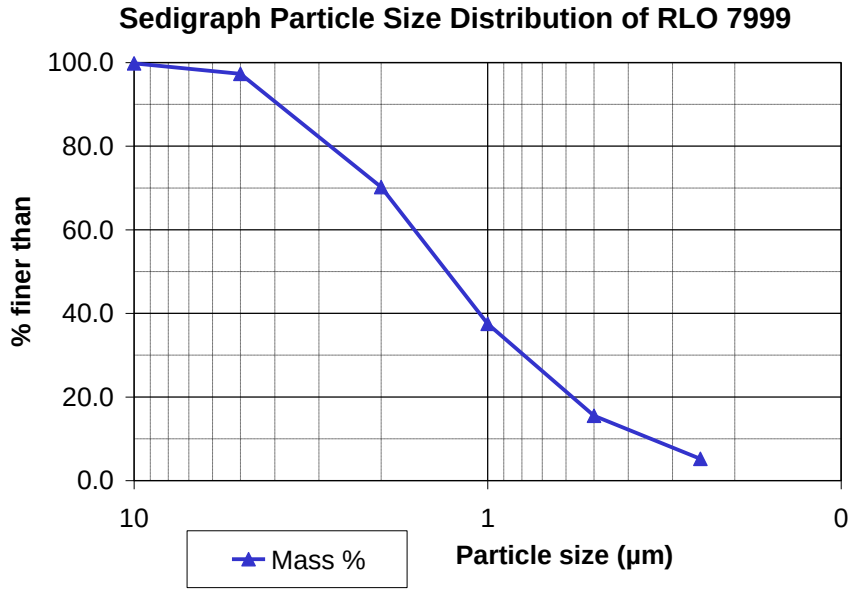


**Figure 3.4:** Particle size distribution of calcium carbonate RLO 7999

### 3.2 Extrusion

Extrusion was employed throughout this work for compounding of the PHBV with other additives and preparing both solid and foamed samples. Details of the extrusion facilities and procedures for different formulation systems are described in this section.

#### 3.2.1 The extrusion facilities

Two twin-screw extruders were employed in the project. One was a Betol (BTS30) co-rotating twin-screw extruder fitted with a single screw feeder. The screw diameter was 30 mm and its length to diameter ratio (L/D) was 30 with gentle screw profile for feeding the bulk polymer with inclusions of mixing discs (Figure 3.5a). The extruder consisted of five barrel sections and each section was equipped with independently controllable electric heating and water cooling system. All extrusion variables, including barrel and die temperatures, screw speed and percentage torque were monitored on the control panel. Two types of die with built-in heating elements were

used: a) a sheet die with 150 *mm* width and adjustable nip and b) a circular strand die with inserts of diameters 5 or 7 *mm*.

The other was a HAKKE Polylab co-rotating twin-screw extruder (Mess-Technic GmbH, Germany) fitted with a twin-screw feeder (K-Tron, K·2 modular, Switzerland). The screw diameter was 24 *mm* and the L/D ratio was 40 with feeding screws to carry forward the polymer granules followed by pockets of mixing elements for homogenisation of the bulk polymer (Figure 3.5b). The extruder consisted of ten heating zones and each zone was equipped with independently controllable electric heating and water cooling system. All extrusion variables, including barrel and die temperatures, die pressure, screw speed and percentage torque were monitored with a computer interface. Two types of dies with heating elements were used: a) a "coat hanger" sheet die with 150 *mm* width and adjustable nip and b) a circular strand die with diameter of 6 *mm*.

Both feeders were calibrated for each material formulation to acquire the linear relationships between the screw speed and the actual material feed rate.

(a)

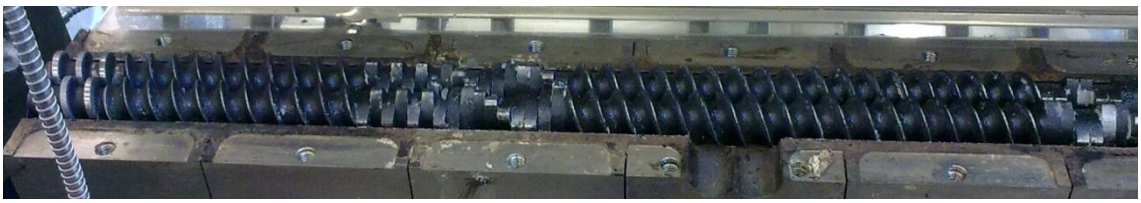

(b)

**Figure 3.5:** Screw profile for (a) Betol (BTS30) and (b) HAKKE Polylab

### 3.2.2 Extrusion compounding

To study the effect of additives or blends on PHBV behaviour, the PHBV-based compounds were prepared using extrusion compounding. This section will give details of formulations and processing conditions of all the compounding systems as follows:

- PHBV with antioxidant and nucleating agents;
- PHBV with PBAT;
- PHBV with chain extender and
- PHBV with calcium carbonate.

#### 3.2.2.1 Pure PHBV with antioxidant and nucleation agents

To incorporate additives into pure PHBV the as-received ENMAT$^{TM}$ Y1010 was extrusion compounded with the Antioxidant 1010 at 0.5 *wt%* and the nucleating agent BN 1010 at 1.0 *wt%*. The additive powders were manually tumble mixed with the PHBV powder in a plastic bag and compounded in the HAKKE Polylab twin screw extruder. The extrusion was conducted using a temperature profile shown in Table 3.1. The samples were extruded under screw speed 100 *rpm* through the sheet die with 150 *mm* width and 2 *mm* nip, and collected on a metal plate at room temperature. The extrudate was used for investigation of the effect of boron nitride nucleation agent on crystallisation of the PHBV.

**Table 3.1:** Temperature profile for extrusion of the PHBV (ENMAT$^{TM}$ Y1010)

| **Zone** | **1** | **2** | **3** | **4** | **5** | **6** | **7** | **8** | **9** | **10** | **Die** |
|---|---|---|---|---|---|---|---|---|---|---|---|
| Temperature (°*C*) | 100 | 130 | 160 | 160 | 160 | 160 | 160 | 160 | 160 | 160 | 160 |

To study the effect of the thermal history on thermal degradation of PHBV during extrusion, the as-received ENMAT$^{TM}$ Y1000P was given an additional extrusion thermal treatment so as to compare the change in its rheology. Pellets of ENMAT$^{TM}$ Y1000P was pre-dried in a vacuum oven for 120 *min* at 100 °*C* and extruded in the HAKKE Polylab twin screw extruder. The extrusion was performed under the negative temperature profile shown in Table 3.2. The samples were extruded under screw speed

90 *rpm* through the 150 *mm* width sheet die with a nip of 2 *mm*, and collected onto a water cooled roller calendering unit.

**Table 3.2:** Temperature profile for extrusion of the PHBV (ENMAT$^{TM}$ Y1000P)

| **Zone** | **1** | **2** | **3** | **4** | **5** | **6** | **7** | **8** | **9** | **10** | **Die** |
|---|---|---|---|---|---|---|---|---|---|---|---|
| Temperature (°*C*) | 120 | 175 | 175 | 170 | 165 | 160 | 155 | 150 | 145 | 140 | 135 |

### 3.2.2.2 PHBV and PBAT compounds

The PHBV (ENMAT$^{TM}$ Y1000P) was pre-dried in a vacuum oven for 120 *min* at 100 °*C*, while the PBAT (Biolice® RFX11) was pre-died in vacuum oven for 30 *min* at 70 °*C* recommended by the suppliers. Pellets of PHBV and PBAT were then manually tumble mixed with composition ratio as PHBV/PBAT = 100/0, 85/15, 70/30 and 50/50 *wt%*. Then the materials were compounded in the HAKKE Polylab twin screw extruder. The negative temperature profile in Table 3.2 was used to blend PHBV/PBAT compound. The samples were extruded under screw speed 90 *rpm* through 150 *mm* width sheet die with nip of 2 *mm*, and collected on to the water cooled rollers calendering unit.

### 3.2.2.3 PHBV with chain extender

The PHBV (ENMAT$^{TM}$ Y1000P) was pre-dried in a vacuum oven for 120 *min* at 100 °*C* while the chain extender was used as-received. Pellets of the PHBV were manually tumble mixed with the chain extender at varying concentrations: 0.00, 0.25, 0.50 and 1.00 *wt%* and then compounded in the HAKKE Polylab twin screw extruder. The extruder was fitted with a rod die with diameter of 6 *mm*. Temperature profile was flat 180 °*C* across all zones and screw speed was 100 *rpm*. The extrudates were collected on a metal plate at room temperature.

### 3.2.2.4 PHBV with calcium carbonate

The extrusion compounding was conducted by collaborators at the Biocomposite Centre, Bangor University. The PHBV (ENMAT$^{TM}$ Y1000P) was compounded with 5, 12 and 20 *wt%* $CaCO_3$ using the temperature profile in Table 3.3.

**Table 3.3:** Temperature profile for the extrusion compounding at Biocomposite Centre

| Zone | 1 | 2 | 3 | 4 | 5 | 6 | 7 | 8 | 9 | Die |
|---|---|---|---|---|---|---|---|---|---|---|
| Temperature (°*C*) | 100 | 185 | 185 | 185 | 185 | 185 | 170 | 170 | 170 | 175 |

Pellets of the PHBV compounds were dried in a vacuum oven for 120 *min* at 100 °*C* and extruded in the HAKKE Polylab twin screw extruder. Table 3.4 presents the temperature profile used to extrude PHBV compounds. The samples were extruded under screw speed 90 *rpm* through 150 *mm* width sheet die with a nip of 2 *mm* and collected with a water cooled roller calendering unit. For comparison, The PHBV without $CaCO_3$ was also extruded using the temperature profile in Table 3.2.

**Table 3.4:** Temperature profile for extrusion of the PHBV/$CaCO_3$ compounds

| Zone | 1 | 2 | 3 | 4 | 5 | 6 | 7 | 8 | 9 | 10 | Die |
|---|---|---|---|---|---|---|---|---|---|---|---|
| Temperature (°*C*) | 130 | 185 | 185 | 170 | 165 | 160 | 155 | 150 | 145 | 140 | 155 |

### 3.2.3 Extrusion foaming

#### 3.2.3.1 Foaming of PHBV (ENMAT™ Y1000P)

Pellets of the PHBV (ENMAT™ Y1000P) were dried in an air-circulating oven at temperature of 100 °*C* for three hours. The dried material was then manually tumble-mixed with the blowing agent masterbatch BA.F4.E MG at active contents from 0.50 – 3.00 *wt%* and extruded with the Betol co-rotating twin screw extruder described in section 3.2.1. The negative temperature profile was used as shown in Table 3.5 so that the polymer would melt in the early zones of the extruder and enters a super-cool state towards the exit. This temperature profile was designed to minimise thermal degradation and to achieve desirable high melt viscosity at the die exit for foam stabilisation. Die temperature was also chosen to match the decomposition temperature of the blowing agent. The screw speed was varied between 20 to 50 *rpm* and material flow rate from 2.2 to 5.6 *kg/h*, respectively. Two die configurations were used: a sheet die with 150 *mm* width and variable nip and a circular strand die with diameter of 5 or 7 *mm*.

**Table 3.5:** Temperature profile for foaming of the PHBV

| **Zones** | **1** | **2** | **3** | **4** | **5** | **Die** |
|---|---|---|---|---|---|---|
| Temperature (°*C*) | 100 | 180 | 170 | 160 | 150 | 150 |

### 3.2.3.2 Foaming of PHBV composites

Two PHBV composites supplied by Bangor University and Wells Plastics (Staffordshire, UK) were used in this extrusion foaming study. Both compounds had the same composition as shown in Table 3.6 but slight difference extrusion conditions due to differences in the equipment set up.

**Table 3.6:** Compounding formulation

| **Name** | **Amount (*wt%*)** | **Notes** |
|---|---|---|
| ENMAT$^{TM}$ Y1010 | 38.8 | PHBV |
| BN 1010 | 0.4 | Nucleating agent |
| Antioxidant 1010 | 0.2 | Antioxidant |
| Ecoflex® F BX7011 | 39.4 | PBAT |
| RLO 7999 | 20.0 | $CaCO_3$ |
| Joncryl® ADR-4386 S | 0.7 | Chain extender |
| Crodamide ER | 0.5 | Slip aid |

The PHBV compounds had a solid density of 1.36 $g/cm^3$ and the melting and crystallisation temperature of the blends was determined from DSC (model 2000, TA Insturments) using a heating rate of 10 °*C/min* in nitrogen atmosphere.

Pellets of the PHBV compound were preheated in vacuum oven for 120 *min* at 100 °*C*. The compounded pellets were then manually tumble mixed with the as-received blowing agent masterbatch BA.F4.E MG at active contents from 1.00 – 3.00 *wt%* and extruded using the HAKKE Polylab twin screw extruder. The screw speed was varied between 60 and 100 *rpm* and material flow rate from 5.18 to 9.15 *kg/h* respectively. Two die configurations were used: a "coat hanger" sheet die with 150 *mm* width and variable nip and the other a circular strand die with diameter of 6 *mm*. Three

temperature profiles (I, II and III) as shown in Table 3.7 were employed to study the effect of temperature profile on foaming.

**Table 3.7:** Temperature profiles (set as *ºC* for each barrel) for foaming of the PHBV composites

| | Zone | | | | | | | | | | |
|---|---|---|---|---|---|---|---|---|---|---|---|
| **Profile** | **1** | **2** | **3** | **4** | **5** | **6** | **7** | **8** | **9** | **10** | **Die** |
| I | 100 | 120 | 165 | 170 | 172 | 170 | 165 | 160 | 160 | 160 | 160 |
| II | 100 | 120 | 165 | 170 | 172 | 165 | 160 | 160 | 160 | 155 | 155 |
| III | 100 | 120 | 165 | 170 | 172 | 160 | 160 | 155 | 155 | 155 | 155 |

## 3.3 Characterisations

### 3.3.1 Differential scanning calorimetry (DSC)

Differential scanning calorimetry (DSC) measurements of the PHBV or its compounds were conducted using a Q2000 DSC (TA Instrument, USA) within nitrogen atmosphere with a flow rate of 50 *mL/min*. Samples with a mass of 9.5±0.5 *mg* were first heated from -40 to 190 *ºC* and annealed for 3 *min* at 190 *ºC* to eliminate thermal history. Then the samples were cooled down to -40 *ºC* and kept in isothermally at this temperature for 3 *min*. The non-isothermal thermograms from first cooling scan were used for assessment of crystallization. Then, the same heating process was repeated for the second cycle. The rates of heating and cooling were maintained at 10 *ºC/min*. The second cycle non-isothermal thermograms were used to derive melting point.

For isothermal thermograms in study of crystallization, the sample was initially heated to 190 *ºC* and held for 3 *min* to eliminate thermal history. Then, the samples were cooled down at a cooling rate of 50 *ºC/min* to the predetermined temperatures varying from 110 to 150 *ºC* and held at these constant temperatures until the crystallization process complete.

### 3.3.2 Thermal gravimetric analysis (TGA)

The thermal decomposition behaviour of the blends was investigated with a Q500 TGA (TA Instruments, USA) in nitrogen with a flow rate of 10 *mL/min*. The temperature ranged from 40 to 600 °*C* at various heating rates (5, 10, 20, and 40 °*C/min*) using approximately 10 *mg* of samples.

### 3.3.3 Rheological characterisation

#### 3.3.3.1 Sample preparation

The samples of PHBV or compounds were first ground using a Retsch SM2000 cutting mill fitted with a sieve with 1.50 *mm* trapezoid apertures. The ground samples were dried for 2 hours at temperature of 100 °*C* in a vacuum oven prior to the measurements.

#### 3.3.3.2 Complex viscosity measurement

Viscosity measurements were performed by using ARES Φ25 *mm* parallel plate rotational rheometer (TA Instruments, USA) and conducted at a range of temperatures from 145 to 180 °*C*. To maintain similar thermal history, each sample was kept for 4 *min* at temperature of 180 °*C* in the rheometer prior to the testing. Heating time was increase to 6 *min* for extruded foams in order to decompose any residual blowing agent. Once the polymer was molten, the gap between the parallel plates was set to 1.8 *mm* and after reaching equilibrium at prescribed temperature, the measurement was commenced. To minimise the effect of thermal degradation at temperatures above the melting point, the angular speed sweep was conducted in the range from 1 to 512 *rad/s* for all tests, since the use of angular speeds lower than 1 *rad/s* could result in much longer measurement times per point and potentially leads to considerable thermal degradation and decrease in viscosity. The commanded strain was set to 1% for all tests.

### 3.3.4 Mechanical testing

The extruded PHBV sheet was cut into dumbbell specimens according to BS EN ISO 527-3 type 5. The specimens were then tested using a H10KT universal testing machine (Tinius Olsen, UK) fitted with 1 *kN* load cell and mechanical extensometer (100SC). Crosshead speed was set to be 5 *mm/min* and testing temperature was maintained at 21 *°C*.

### 3.3.5 Characterisation of the foamed samples

#### 3.3.5.1 Scanning electron microscopy (SEM)

A Zeiss Supra 35VP field emission scanning electron microscope (SEM) was used to observe the foam morphology. Extruded foams were quenched in liquid nitrogen and fractured. The fracture surfaces perpendicular to the direction of extrusion were then sputter-coated with gold prior to the examination. The average cell size and cell population density (*N*) were analysed from SEM images. The cell population density was calculated using Equation (Mihai *et al.*, 2010):

$$N = \left(\frac{n}{A}\right)^{3/2} \times \frac{\rho_S}{\rho_f} \qquad (3.1)$$

where $n$ is the number of cells in the defined area $A$, $\rho_s$ is the density of unfoamed material and $\rho_f$ is the density of the foam.

#### 3.3.5.2 Density measurement

Foam density was measured using a density determination device AB204-S from Mettler Toledo Ltd. (Beaumont Leys Leicester, UK). Density reduction was calculated from Equation:

$$\Delta\rho = 100\% \times \frac{\rho_s - \rho_f}{\rho_s} \qquad (3.2)$$

# Chapter 4

# General Properties of PHBV

## 4.1 Crystallization behaviour

### 4.1.1 Effect of boron nitride on crystallization behaviour of PHBV

The thermal properties of filled (1.0 *wt%* BN and 0.5 *wt%* antioxidant) and unfilled PHBV were investigated using DSC as shown in Figure 4.1. Figure 4.1(a) presents the first cooling scan at a cooling rate of 10 *°C/min* whereas Figure 4.1(b) presents the second heating scan for the PHBVs test so as to avoid the effect of previous thermal history. The melting temperature ($T_m$), the enthalpies of melting ($\Delta H_{Tm}$), the melt crystallization temperatures ($T_{mc}$) and the melt crystallization enthalpies ($\Delta H_{Tmc}$) are summarized in Table 4.1.

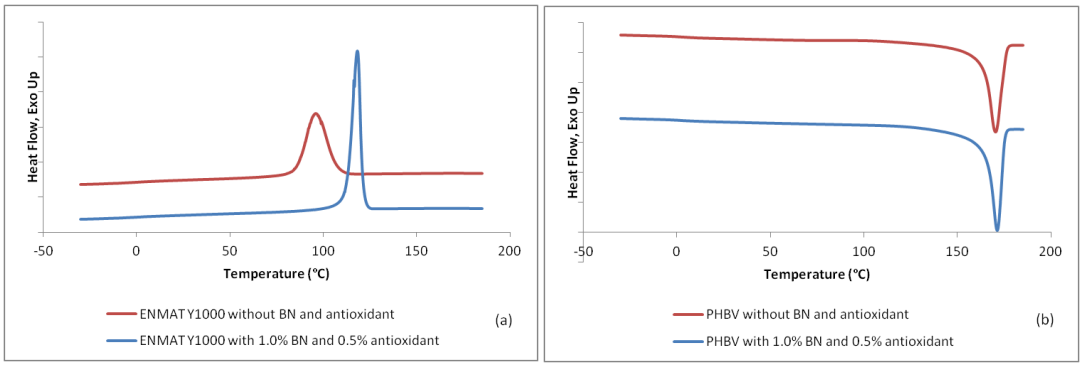


**Figure 4.1:** DSC curves of unfilled (red) and filled PHBV (blue) at a cooling/heating rate of 10 *ºC/min*: a) first cooling scan and b) second heating scan

There was only a single melting peak and crystallization peak found in each sample during the DSC run. The melt crystallization temperature, $T_{mc,}$ could be considered as indirect measurements of crystallization rate (Kai *et al*., 2005) and generally, a lower $T_{mc}$ indicates a slower crystallization. From Figure 4.1(a), it could therefore be said that the melt crystallization temperatures of the filled PHBV has been considerably increased and thus addition of the BN significantly improved the crystallization rate of the PHBV. The antioxidant is believed no involving in the crystallization as it has melted during extrusion and solubilised in the polymer matrix.

From Table 4.1, there is no noticeable difference in $T_m$ and $\Delta H_{Tm}$ were found between the filled and unfilled PHBVs. The similar $\Delta H_{Tm}$ values imply that the difference in crystallinity of both samples is insignificant. There exhibits a considerable difference however in $\Delta H_{Tmc}$ between the filled and unfiled PHBV. The different value of $\Delta H_{Tmc}$ might be due to the slow and incomplete crystallization of pure PHBV at the given cooling rate.

**Table 4.1:** DSC thermal characteristics of the unfilled and filled PHBV (1.0 *wt%* BN and 0.5 *wt%* antioxidant)

| Sample | $T_m$ (°C) | $\Delta H_{Tm}$ (J/g) | $T_{mc}$ (°C) | $\Delta H_{Tmc}$ (J/g) |
|---|---|---|---|---|
| Unfilled PHBV | 170.3 | 96.5 | 98.8 | 77.4 |
| Filled PHBV | 171.2 | 98.3 | 118.2 | 87.9 |

The PHBV crystallization was further studied under isothermal condition at various crystallization temperatures ($T_c$s). Figure 4.2 shows the DSC heating curves of unfilled and filled PHBV which isothermally crystallized at four different crystallization temperatures. By increasing the crystallization temperature, the crystallization rate decreased, judged from the flatter curves and delay of the crystallization exothermic peak with increase in temperature. At 140 °*C*, for instance, the unfilled PHBV (Figure 4.2a) can hardly crystallize within 120 minutes.

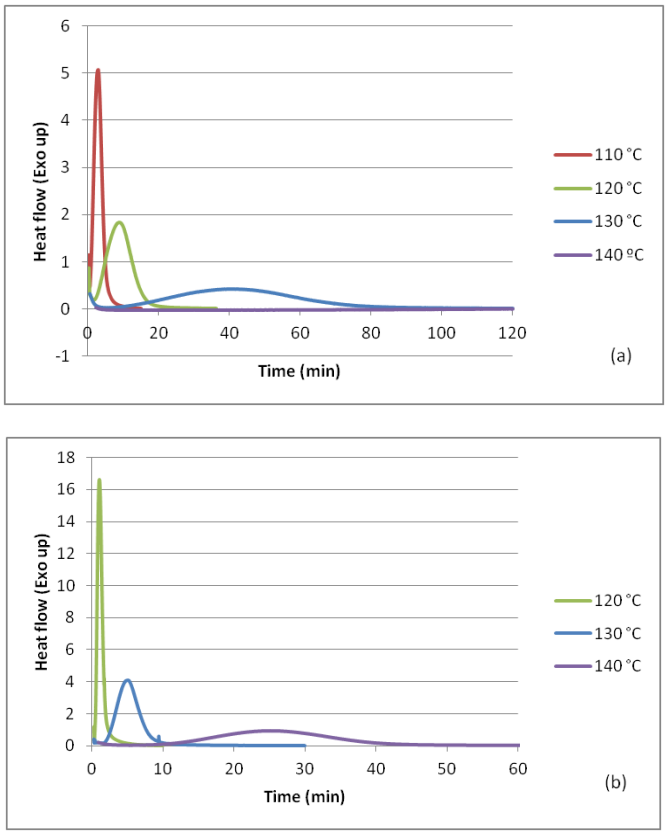


**Figure 4.2:** DSC isothermal crystallization thermograms at different temperatures for:

a) the unfilled;
b) the filled PHBV.

The kinetics of crystallization could be determined from the isothermal DSC thermograms which were integrated in order to determine the degree of crystallinity as a function of time.

The well-know Avrami equation (4.1) has been used for analysing the isothermal crystallization kinetics (Avrami, 1939, 1940 & 1941):

$$X_{rel} = 1 - \exp(-k.t^n), \qquad (4.1)$$

where $X_{rel}$ refers to the relative crystallinity at time ($t$), $k$ is the crystallization rate constant, and $n$ is the Avrami exponent which is dependent on the nucleation mechanism and the dimension of crystal growth.

$X_{rel}$ could be determined from DSC thermograms using Equation 4.2:

$$X_{rel} = \frac{X_c(t)}{X_c(\infty)} = \int_0^t \frac{dH(t)}{dt} dt / \int_0^\infty \frac{dH(t)}{dt} dt \qquad (4.2)$$

where $X_c(t)$ and $X_c(\infty)$ refer to the degree of crystallinity at given time $t$ and at the end of crystallization process, respectively. Equation 4.1 may be rewritten into the double-logarithmic form as in Equation 4.3:

$$\log[-ln(1 - X_{rel})] = \log(k) + n\log(t) \qquad (4.3)$$

Plotting $\log[-ln(1 - X_{rel})]$ against $\log(t)$ gives a straight line and the two parameters ($\log k$ and $n$) can be determined from the intercepts and slopes, respectively.

The crystallization half time $t_{1/2}$, which is the time when half of the crystallization has been completed, $X_{rel} = 0.5$, can be obtained from Equation 4.4:

$$t_{1/2} = \left(\frac{ln2}{k}\right)^{\frac{1}{n}} \qquad (4.4)$$

Figure 4.3(a) presents the relative crystallinity versus time of the unfilled PHBV at three different crystallization temperatures and Figure 4.3(b) shows the Avrami plots of unfilled PHBV at the same temperatures.

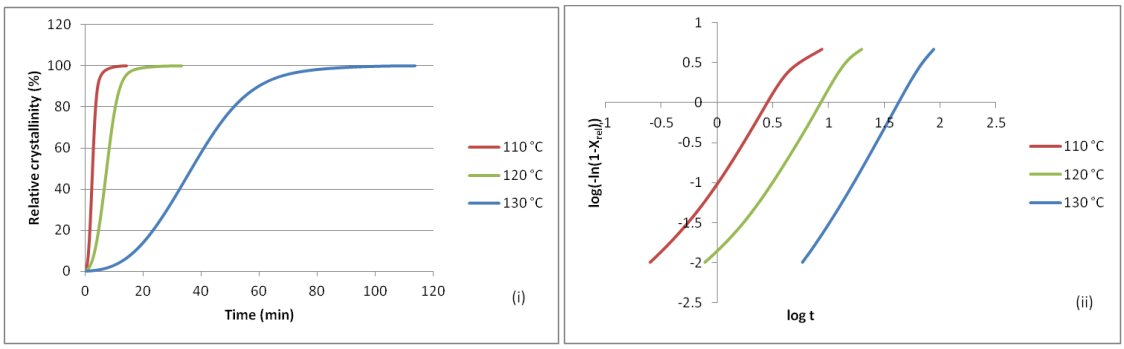


**Figure 4.3a:** (i) Relative crystallinity as function of time and (ii) the related Avrami plots at various isothermal crystallization temperatures for the unfilled PHBV

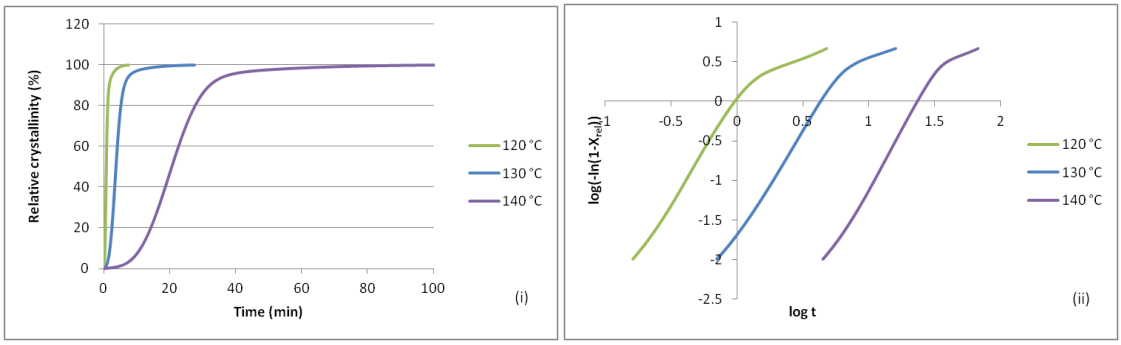


**Figure 4.3b:** (i) Relative crystallinity as function of time and (ii) the related Avrami plots at various isothermal crystallization temperatures for the filled PHBV

Figure 4.3a (i) and Figure 4.3b (i) indicates that the degree of crystallization as function of time is dependent on the temperature and crystallization rate decreases with the increase in the crystallization temperature.

Regarding to the Avrami plots (Figure 4.3a (ii) and Figure 4.3b (ii)), each curve shows a linear segment during the initial stage of crystallization and bending to level off due to the existence of secondary crystallization at a later stage (Wunderlich, 1977). As a result, each line exhibits approximately two linear regions. In pure PHB and PHBV, the form of crystal growth transformed from the primary to secondary crystallization following spherulite impingement (An *et al*., 1999). However, when comparing the 3 crystallization temperatures of PHBV, the higher temperature, the lines become straighter and the later crystallization areas become smaller.

Since the basic Avrami equation (Equation 4.1) relies on many assumptions such as linear crystal growth, primary nucleation, constant volume, and so forth, it is usually valid at low conversions as long as the impingement is not serious (Wunderlich, 1976). Therefore, the *n* and *k* should be calculated from the early linear segment of the Avrami plot (Liu *et al*., 2002; Kai *et al*., 2004 & 2005; Lorenzo *et al*., 2007). The *n* and *k* values of the unfilled and filled PHBV calculated from linear segment of the plots in Figure 4.3a (ii) and Figure 4.3b (ii) are listed in Table 4.2.

**Table 4.2:** The Avrami's parameters for the unfilled and filled PHBV

| Sample | $T_c$ (ºC) | $n$ | $k$ ($min^{-1}$) | $t_{1/2}$ (min) |
|---|---|---|---|---|
| Unfilled PHBV | 110 | 2.34 | $8.85 \times 10^{-2}$ | 2.41 |
| | 120 | 2.37 | $6.18 \times 10^{-3}$ | 7.32 |
| | 130 | 2.52 | $7.98 \times 10^{-5}$ | 36.59 |
| Filled PHBV | 120 | 2.62 | 1.125 | 0.83 |
| | 130 | 2.81 | $1.66 \times 10^{-2}$ | 3.76 |
| | 140 | 3.06 | $6.56 \times 10^{-5}$ | 20.69 |

In Table 4.2, the highest crystallization rate constant ($k$) for both the unfilled and filled PHBVs was achieved at the lowest temperature corresponding to the shortest half time ($t_{1/2}$). This reflects the fact that the melt crystallization is a temperature dependent process. This process is considered to be the characteristic of nucleation controlled crystallization and the rate is dependent on the gap between the crystallization temperature ($T_c$) and the melting temperature ($T_m$) (Kai *et al*., 2005).

The $n$ values for the unfilled and filled PHBV are between 2 and 3 and these values changed very little with the temperature. The depression of the $n$ value at lower crystallization temperature is probably due to the occurrence of athermal crystallization during the crystallization process (Kai *et al*., 2005) and thus the $n$ value decreases when there is a bigger gap between the crystallization and melting temperature. In the ideal state of crystallization, the $n$ value for spherical growth should be exactly at 4 whereas the $n$ value for spherical growth with the presence of heterogeneous phase should be exactly at 3 (Avrami, 1940). Because the derivation of the Avrami equation contains a number of simplifications, which do not necessarily apply to the real crystallization of macromolecules (Wunderlich, 1976), the practical circumstances cannot satisfy the ideal state that the Avrami equation is supposed to have. Hence, the $n$ values from the experiment have the deviation from the theoretical value (Liu *et al*., 2002; Kai *et al*., 2004 & 2005). However, the $n$ values of filled PHBV are higher than the unfilled PHBV in every selected temperature resulted from heterogeneous nucleation by the addition of the BN nucleating agent.

The effect of the nucleating agent on the rate of crystallization of the pure PHBV is shown by the comparisons of the isothermal crystallization thermograms (Figure 4.4)

and the relative crystallinity with time (Figure 4.5) between the unfilled and the filled PHBVs at two different temperatures.

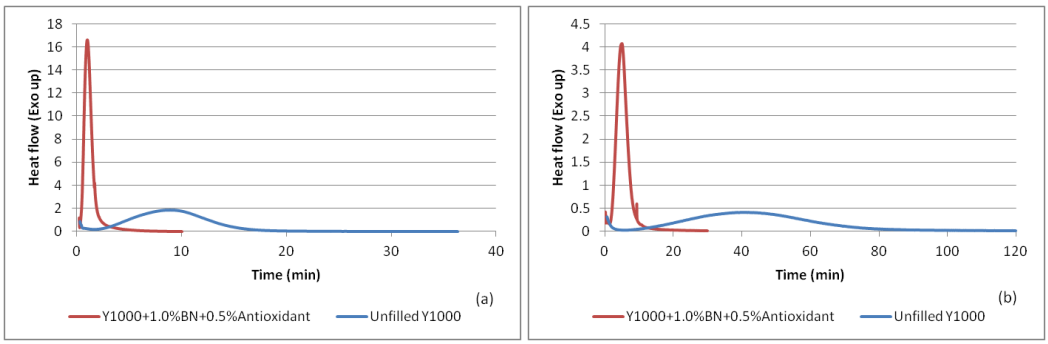


**Figure 4.4:** Comparison of DSC isothermal crystallization thermograms of unfilled (blue) and filled (red) PHBVs at (a) 120 and (b) 130 *ºC*

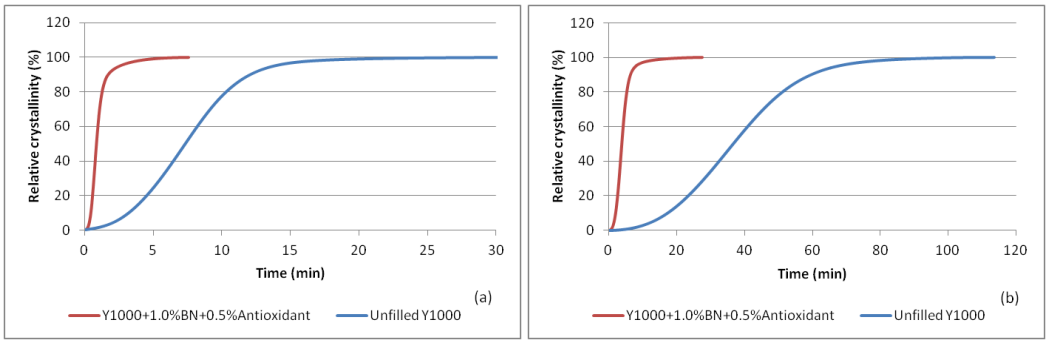


**Figure 4.5:** Comparison of relative crystallinity with time of the unfilled (blue) and filled (red) PHBVs at (a) 120 and (b) 130 *ºC*

The results confirmed that the addition of the BN nucleation agent enabled faster crystallization rate at all selected crystallization temperatures. This phenomenon can be attributed to the effect of the nucleating agent. The BN particles act as heterogeneous nucleation sites which decrease activation energy for nuclei formation and increase the rate of nucleation in the high temperature state (Kai *et al.*, 2005). As a result, the presence of heterogeneous particles increases the nucleation density and decreased the spherulite size. It pushes $T_{mc}$ to higher temperature and lead to reduction in crystallization time.

### 4.1.2 Effect of thermal treatment on crystallization behaviour

It has been reported that thermal treatment induced thermal degradation of PHB (Janigová *et al.*, 2002; Erceg *et al.*, 2005; Wang *et al.*, 2008), shifting the melting peak

to a lower temperature. To investigate the effect of thermal history on change in properties of PHBV, the received ENMAT$^{TM}$ Y1000P pellets and that after an additional extrusion run (as described in section 3.2.2.1, page 65) were compared. Figure 4.6 compares the first cooling and the second heating DSC curves between the as-received pellets and the extruded PHBV and their thermal characteristics are summarized in Table 4.3.

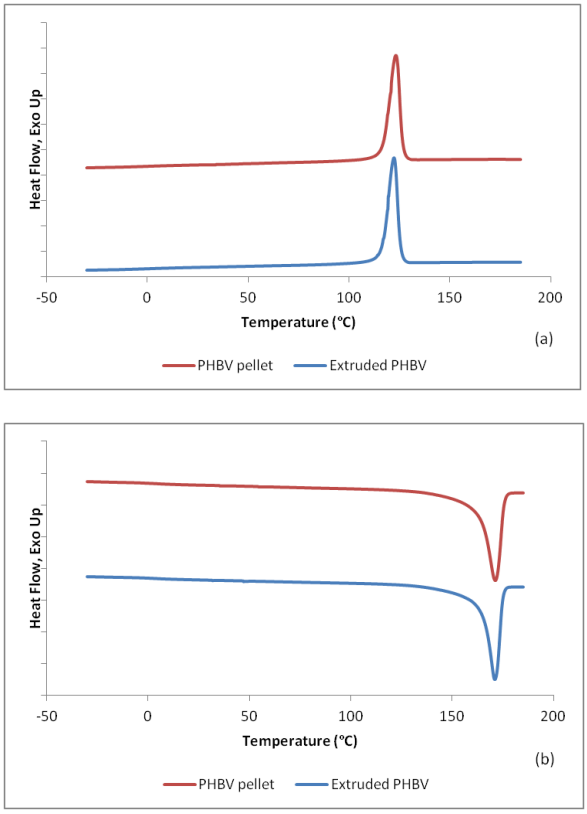


**Figure 4.6:** DSC thermograms for the as-received pellets (red) and the extruded PHBV (blue) during a) first cooling scan and b) second heating scan at a cooling/heating rate of 10 *ºC/min*

It can be observed from the Figure 4.6 that there is hardly noticeable change in melting temperature between the pellet and extruded PHBV. Data in Table 4.3 show that the melt crystallization temperature, $T_{mc,}$ of PHBV pellet is slightly higher than the extruded PHBV. This suggests a slight degradation had taken place during the extrusion. The reduction in enthalpies of melting and crystallization indicate a reduction of crystallinity by the extra thermal treatment and mechanical shearing, based on Kai *et al*. (2005), and the reduction in $T_{mc}$ also lowered the crystallization rate.

**Table 4.3:** DSC thermal characteristics of the PHBV pellet and the extruded PHBV

| Sample | $T_m$ (ºC) | $\Delta H_{Tm}$ (J/g) | $T_{mc}$ (ºC) | $\Delta H_{Tmc}$ (J/g) |
|---|---|---|---|---|
| PHBV pellet | 171.2 | 91.7 | 123.2 | 84.6 |
| Extruded PHBV | 170.9 | 88.3 | 122.0 | 82.6 |

Isothermal crystallization was employed for further confirmation. Figure 4.7 shows the comparison between isothermal crystallization thermograms of the pellet and extruded PHBVs at (a) 130, (b) 140 and (c) 150 *ºC*. The relative crystallinity with time at the same temperatures are presented in Figure 4.8. The *n*, *k*, and $t_{1/2}$ values of the pellet and extruded PHBVs are also summarized in Table 4.4.

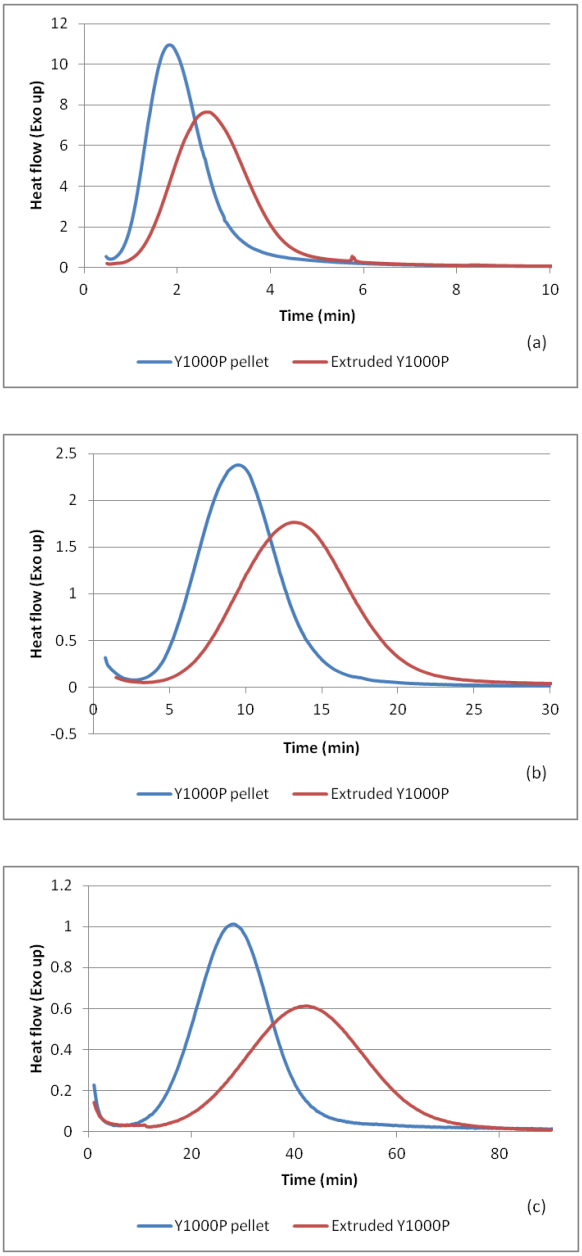


**Figure 4.7:** Comparison of DSC isothermal crystallization thermograms of the as-received PHBV pellets (blue) and extruded PHBV (red) at (a) 130, (b) 140 and (c) 150 *°C*

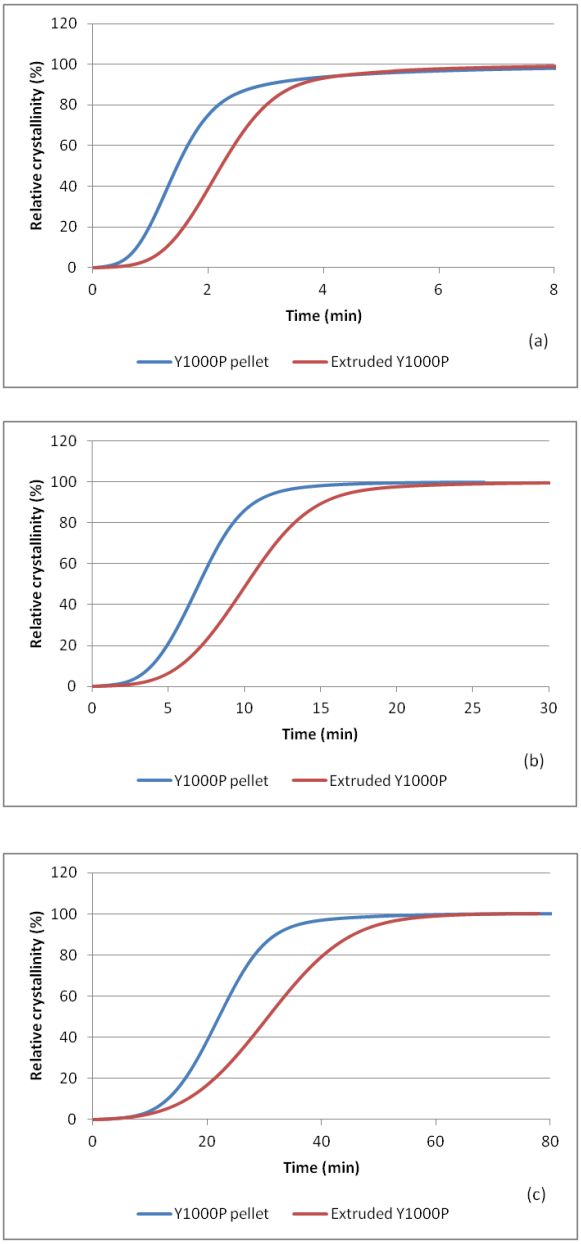


**Figure 4.8:** Comparison of relative crystallinity with time of the as-received PHBV pellets (blue) and extruded PHBV (red) at (a) 130, (b) 140 and (c) 150 *ºC*

**Table 4.4:** The Avrami's parameters for the PHBV pellet and the extruded PHBV

| Sample | $T_c$ (ºC) | $n$ | $k$ ($min^{-1}$) | $t_{1/2}$ (min) |
|---|---|---|---|---|
| PHBV pellet | 130 | 2.71 | $2.47 \times 10^{-1}$ | 1.46 |
| | 140 | 3.17 | $1.47 \times 10^{-3}$ | 6.98 |
| | 150 | 3.61 | $9.77 \times 10^{-6}$ | 22.07 |
| Extruded PHBV | 130 | 3.22 | $5.29 \times 10^{-2}$ | 2.23 |
| | 140 | 3.28 | $3.52 \times 10^{-4}$ | 10.11 |
| | 150 | 3.11 | $1.65 \times 10^{-5}$ | 30.68 |

The Avrami exponents ($n$) for the PHBVs were mostly between 3 and 4 (except for the PHBV pellet crystallized at 130 °*C*). This indicates that the crystallisation is effectively intermediate between spherical growth and with the presence of heterogeneous phase (Avrami, 1940).

Unlike the insensitivity in melting temperature (in Table 4.3), there is a marked effect of the additional extrusion thermal history on crystallization rate at isothermal crystallization temperatures and significant increase in half-time of the crystallization process (Table 4.4). The extruded PHBV that experienced extra thermal and mechanical shearing history shows slower crystallization rate at all crystallization temperatures. The crystallization half times, $t_{1/2}$s, increase 52.74, 44.84 and 39.01% at 130, 140 and 150 °*C*, respectively. This may be attributed to the drop of nucleation density due to the reduction of molecular weight in crystalline polymers (El-Hadi *et. al*., 2002).

### 4.2 Rheological behaviour

Complex viscosity was evaluated on the as-received PHBV and that received an extra extrusion (as in section 3.2.2.1, page 65) to identify if the additional thermal history affect the rheological behaviour of the PHBV. The plate-plate rotational rheological tests are as described in section 3.3.3.2 (page 70). The shear rate (directly related to the angular speed, $\omega$) and temperature effects on rheological behaviour of the as-received PHBV are shown in Figure 4.9. The result reveals that the as-received PHBV exhibits shear-thinning behaviour when subject to increasing shear rate. The complex viscosity

at 180 *°C* and 1 *rad/s* was about 1300 *Pa·s* which nearly 4 times lower compared with cPLA which has a viscosity of about 5000 *Pa·s* at the same condition (Mihai *et al*., 2010). Lowering the temperature led to considerable increased in viscosity and at 145 *°C* the viscosity at 1 *rad/s* increased to about 3000 *Pa·s*. This provides the basis to control viscosity via processing temperature.

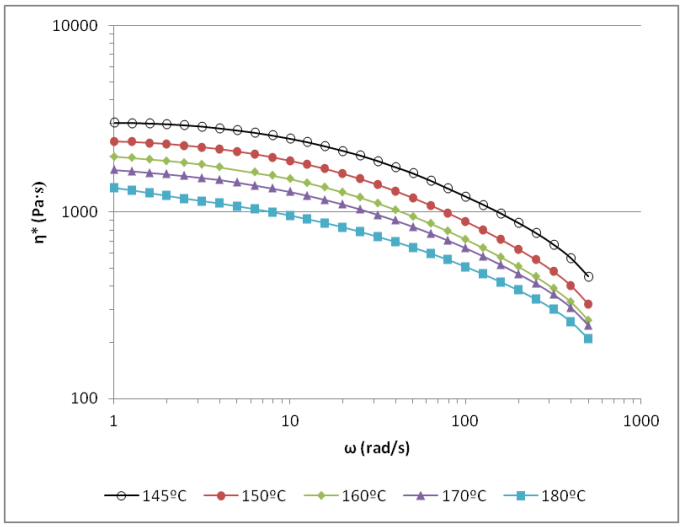


**Figure 4.9:** Complex viscosity of the as-received PHBV measured as a function of angular speed at different temperatures

When tested at a fixed angular speed (at 1 *rad/s*) at different temperatures, the complex viscosity of the PHBV melt changed over time as shown in Figure 4.10. At temperatures above melting point (170 and 180 *°C*), viscosity was continuously decreasing, indicating that the polymer was undergoing chain scission. At temperatures below melting point however, viscosity could be seen to increase over time. This can be attributed to crystallisation of the super-cooled PHBV melt. Such increase in viscosity is strongly dependant on the degree of super cooling. The lower the temperature, the faster the viscosity increase and eventually leads to solidification and slippage at the surfaces of the plates, resulting in a plateau.

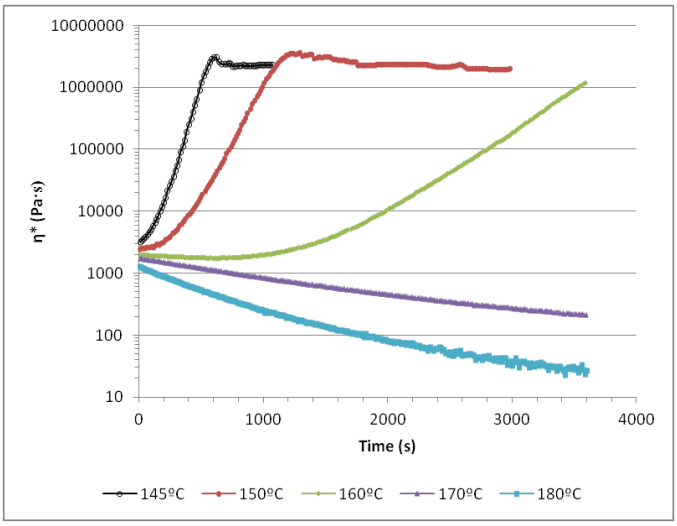


**Figure 4.10:** Complex viscosity of the as-received PHBV as a function of time at fixed angular speed of 1 *rad/s* and different temperatures

Figure 4.11 presents time at *G'/G"* crossover for the super-cooled PHBV, where *G'* is storage modulus and *G"* is loss modulus. The crossover point is when *G'=G"*. Prior to the crossover point, the molten polymer is predominantly viscous and after the crossover, the melted polymer becomes more elastic. Increase in melt elasticity over time is indicative of crystallisation which eventually results in solidification. This phenomenon was observed during extrusion foaming of PHBV and will be discussed later.

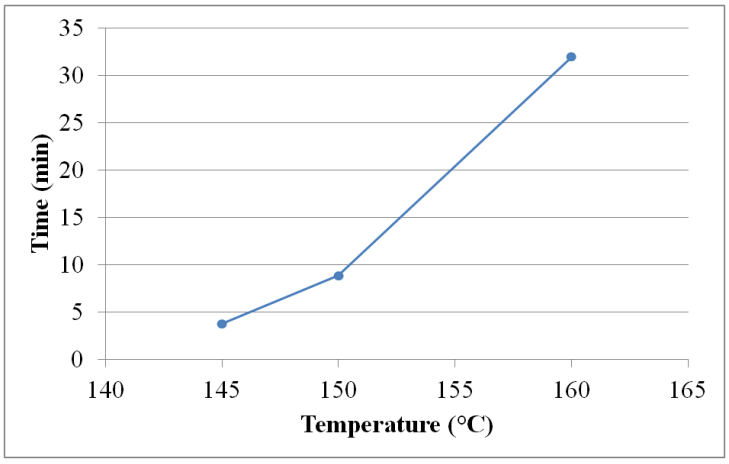


**Figure 4.11:** *G'/G"* crossover times for the super-cooled PHBV (as-received) melt at different temperatures

The effect of extra extrusion thermal history treatment on PHBV viscosity was evaluated by comparing complex viscosity, as a function of angular speed, of the as-received PHBV pellet and the extruded PHBV at temperature of 180 °*C*, the peak extrusion temperature. Figure 4.12 shows clear reduction of viscosity post the extra extrusion indicating considerable thermal degradation of the PHBV.

The viscosity at 1 *rad/s* of the PHBV pellet at 180 °*C* was about 1380 *Pa·s* while that of the extruded PHBV at the same condition reduced to 590 *Pa·s*, representing a 57.3% reduction. This is clearly attributable to the reduction of molecular weight from random chain scission reaction of the PHBV (Grassie *et al*., 1984a-c).

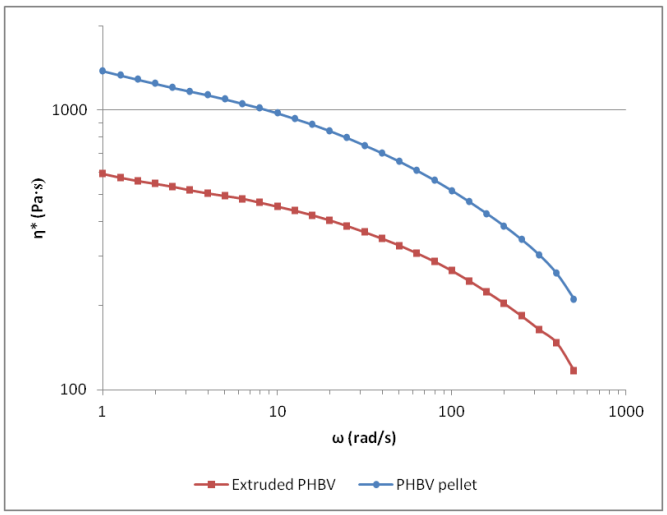


**Figure 4.12:** Comparison of complex viscosity measured at 180 °*C* between the as-received PHBV pellet (blue) and the extruded PHBV (red) showing the effect of thermal degradation from the extra thermal history

## 4.3 Thermal degradation behaviour

### 4.3.1 Effect of thermal treatment on thermal degradation behaviour

The effect of extra extrusion thermal treatment on thermal degradation behaviour was investigated using TGA. The TG and the derivative thermogravimetric (DTG) curves of the PHBV pellet measured at temperatures ranging from 40 to 600 °*C* at different heating rate (5-40 °*C/min*) are shown in Figure 4.13. Result for extruded PHBV has similar feature and thus not shown here.

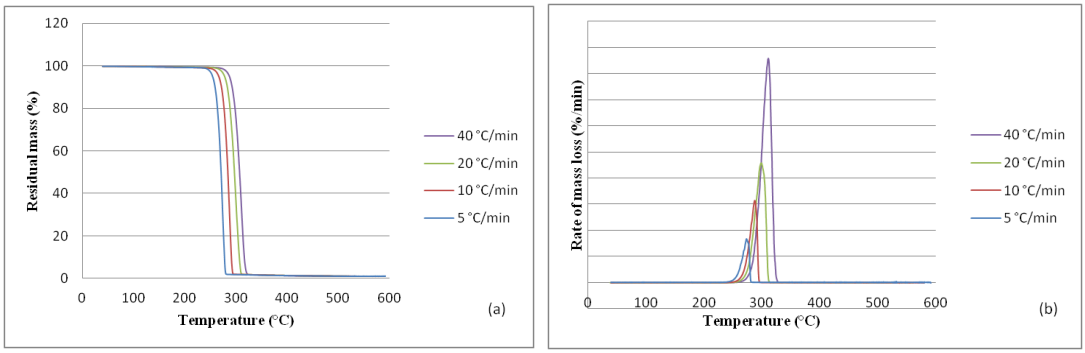


**Figure 4.13:** TG (a) and DTG (b) of the as-received PHBV pellet at different heating rates

From these figures, it becomes evident that the weight loss of PHBV occurs in a one-step process between 250 and 320 °*C* and the maximum decomposition rate of material are shown by the peaks for each heating rate. When the heating rate increases, the decomposition signal of the PHBV starts at higher temperature and the temperature of the maximum decomposition rate shifts to higher temperatures. Moreover, the maximum rate of decomposition also increases with higher heating rate. This proves that the heating rate effects on the decomposition of PHBV. At the end of decomposition, a trace of residues remains.

Figure 4.14 presents comparison of TG and DTG curves between the as-received PHBV and the extruded PHBV in the temperature range of 40–600 °*C* at a heating rate of 10 °*C/min*. It shows that the signal of weight loss of the extruded PHBV emerges earlier. The DTG curve of the extruded PHBV is broader but the maximum decomposition rate is lower than the as-received PHBV pellet. This means that the extra thermal history has considerable affected on thermal decomposition behaviour of the PHBV.

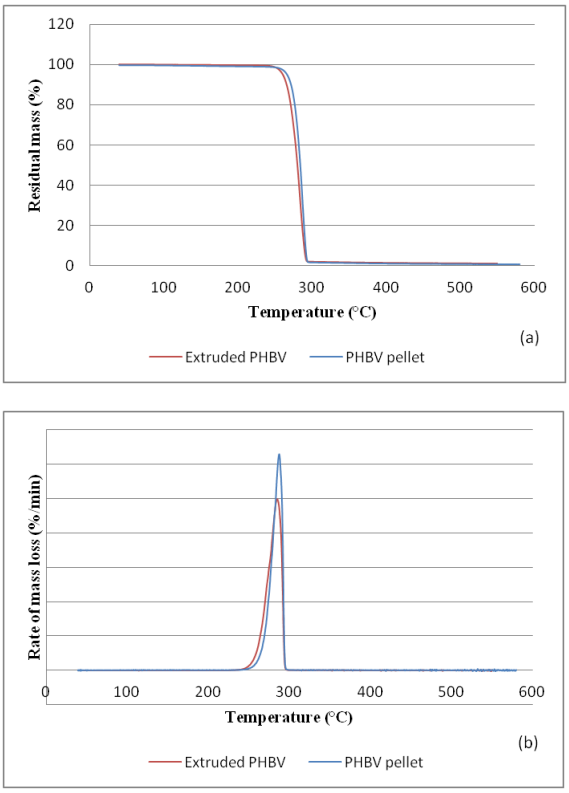


**Figure 4.14:** Comparison of TG (a) and DTG (b) curves of the as received PHBV pellet (blue) and the extruded PHBV (red) at 10 *°C/min* showing effect of the thermal history on thermal degradation of the PHBV

For the purpose of further explanation of the thermal decomposition behaviour, the kinetic parameter-activation energy was calculated.

The thermal decomposition activation energy of PHBV is determined using one of the isoconversional method after Flynn, Wall and Ozawa (FWO) (Flynn & Wall, 1966; Ozawa, 1965) which is featured by its high reliability (Schneider, 1985) and applicability to polymers which are degraded via random chain scission (Schneider, 1985; Wendlandt, 1986).

The FWO method can be derived from an ordinary fundamental kinetic equation for heterogeneous chemical reactions. It determines activation energy directly from data between weight loss and temperature, using several different heating rates. The term of activation energy with the FWO method is defined in Equation 4.5 (Flynn & Wall, 1966; Ozawa, 1965):

$$E_a = -\frac{R}{b}\left(\frac{d(\log\beta)}{d\left(\frac{1}{T}\right)}\right) \quad (4.5)$$

where $E_a$ is the activation energy (*J/mol*); $R$ is the gas constant (8.314 *J/mol·K*); $T$ is the temperature at a given degree of conversion (*K*); $\beta$ is the heating rate (*K/min*); $b$ is the constant value ($\approx$0.457 ± 0.03 for $20 < E_a/RT < 60$).

The reliance of log$\beta$ on 1/$T$ for each constant conversion corresponds to a straight line, known as isoconversional line. For every selected conversion, activation energy can be calculated from the slope of these lines. Because the activation energy from this method is the sum of activation energies of chemical reactions and physical processes in thermal decomposition, it is referred as apparent activation energy.

The values from TG curves of PHBV at different heating rates were used to calculate the activation energy of thermal decomposition process by the FWO method. Typical plots obtained by the FWO method at various heating rate of both PHBVs are shown in Figure 4.15.

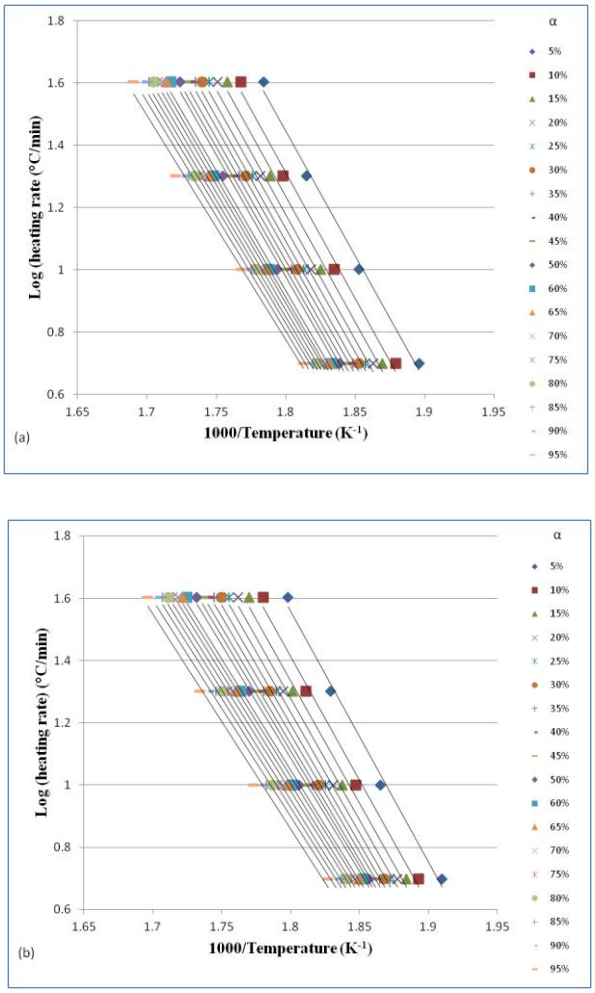


**Figure 4.15:** Plots used in the FWO method to calculate activation energy of thermal decomposition for: (a) the PHBV pellet and (b) the extruded PHBV

The individual lines correspond to differently degree of conversion (from 5 to 95%). The slopes of the lines in Figure 4.15 can be determined as value of the derivative, d(log$\beta$)/d(1/$T$), in Equation (4.5) and then $E_a$ can be calculated. In Table 4.5, the activation energy values of non-isothermal decomposition of both PHBVs were evaluated using the data from Figure 4.15 in the conversion range $\alpha$ = 10-90% and also plotted as Figure 4.16 for easier exploration.

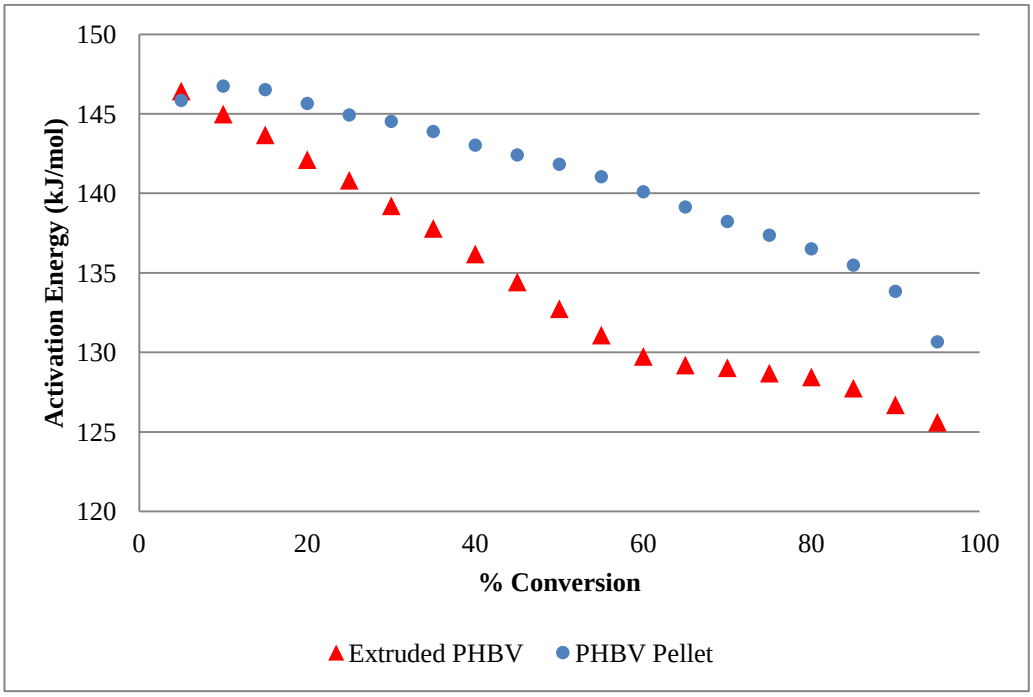


**Figure 4.16:** Comparison of activation energy of the PHBV pellet and the extruded PHBV using the FWO method showing the effect of the extra extrusion on thermal degradation of the PHBV

From Figure 4.16, $E_a$ of both PHBVs gradually declined with the increase in degree of conversion. This decline can be described by similar autocatalytic reaction in PHB thermal decomposition (Kopinke *et al.*, 1996). The thermal decomposition products, e.g. crotonic acid, decrease the activation energy by behaving like a catalyst in the reaction. In comparison with the PHBV pallet, $E_a$ for the extruded PHBV is lower and hence the extra thermal treatment made the PHBV less thermally stable.

**Table 4.5:** Activation energies by the FWO method for the PHBV pellet and extruded PHBV

| Sample | | Conversion, $\alpha$ (%) | | | | | | | | |
|---|---|---|---|---|---|---|---|---|---|---|
| | | 10 | 20 | 30 | 40 | 50 | 60 | 70 | 80 | 90 |
| PHBV Pellet | $E_a$(*kJ/mol*) | 146.74 | 145.65 | 144.52 | 143.02 | 141.82 | 140.09 | 138.22 | 136.50 | 133.83 |
| | $R^2$ | 0.993 | 0.993 | 0.994 | 0.993 | 0.994 | 0.993 | 0.993 | 0.991 | 0.990 |
| Extruded PHBV | $E_a$(*kJ/mol*) | 144.98 | 142.11 | 139.21 | 136.18 | 132.74 | 129.74 | 129.03 | 128.45 | 126.69 |
| | $R^2$ | 0.993 | 0.993 | 0.994 | 0.994 | 0.994 | 0.994 | 0.994 | 0.992 | 0.992 |

$R^2$ = the coefficient of determination

## 4.4 Summary

The slow crystallization behaviour of PHBV can be improved by adding BN as the nucleating agent. The DSC results on both non-isothermal and isothermal crystallization show enhancement of crystallization rate with small amount of BN. The crystallization rate of PHBV can also be enhanced by reduce the isothermal crystallization temperature. These are two ways to improve the solidification and reduce the stickiness of PHBV melt in processing. Conversely, adding further thermal treatment leads to retardation of crystallization and repeated heating should be avoided.

The thermal sensitivity of PHBV was also shown by the rheological study and TGA. The extra thermal treatment leads to degradation and results in dropping of the complex viscosity.

The thermal degradation behaviour confirms the thermal sensitivity of PHBV as the thermal decomposition of the extruded PHBV starts earlier and the $E_a$ is lower than the as-received PHBV.

These results demonstrated the benefit of nucleation agent to speed the crystallization process in PHBV and the importance to avoid repeated exposure to heat.

# Chapter 5

# The Blending of PHBV/PBAT

## 5.1 Crystallization behaviour

The DSC curves, obtained from the neat PHBV, PBAT and various PHBV/PBAT blends, as described in 3.2.2.2 (page 66) on the first cooling scans and the second heating scans at a cooling rate of 10 *°C/min* are presented in Figure 5.1(a) and (b). Table 5.1 summarizes obtained data in the melting temperature ($T_m$), the enthalpy of melting ($\Delta H_{Tm}$), the melt crystallization temperatures ($T_{mc}$) and the melt crystallization enthalpy ($\Delta H_{Tmc}$).

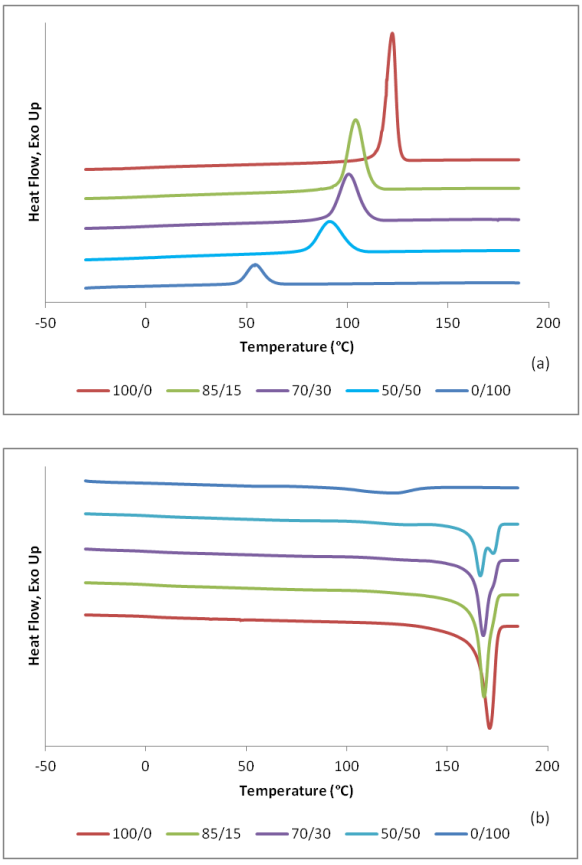


**Figure 5.1:** DSC curves of the neat PHBV, PBAT and the PHBV/PBAT blends at a cooling/heating rate of 10 *ºC/min*: (a) first cooling scans and (b) second heating scans

For all blend ratios, only a single melt crystallization peak can be observed from each sample (Figure 5.1a and Table 5.1). Comparing with $T_{mc}$ of the neat PHBV, $T_{mc}$ of the

blends considerably decreased with the increase of PBAT content. This indicates slower crystallization at higher PBAT contents. This suggests that crystallization of PHBV was hindered by the presence of the bulky polyvinyl ester (Buzarovska *et al*., 2001; Buzarovska & Grozdanov, 2009).

Similar phenomena were also reported elsewhere. Decrease in $T_{mc}$ was also observed in a miscible PHB/poly(butylene succinate) (PBS) blends (Qiu *et al*., 2003), where $T_{mc}$ of PHB moved to lower temperature with increasing PBS content. The lowest $T_{mc}$ (55 °*C*) was observed at PHB/PBS ratio of 40/60. It was also found in immiscible blends like PHB/poly(methylene oxide) (POM), where $T_{mc}$ of the blends dropped from 95 °*C* for the neat PHB to 44 °*C* at PHB/POM ratio of 20/80 (Avella *et al*., 1997).

Figure 5.1(b) shows that when the PBAT content increases, the separation of melting peaks of PHBV and PBAT becomes more distinguishable indicating that the blend system is immiscible. At blend ratio 50/50 (Figure 51b and Table 5.1), three melting peaks became identifiable. The melting peak at 133.2 °*C* corresponds to melting of PBAT and other two peaks at 166.3 and 172.7 °*C* corresponds to the splitted melting peaks of PHBV, which is attributable to the melting of existing crystals (the lower temperature peak) and the restructure of crystals formed during the DSC heating run (the higher temperature peak) (Organ & Barham, 1991; Zhang *et al*., 2000).

**Table 5.1:** Thermal characteristics of the neat PHBV, PBAT and the PHBV/PBAT blends

| Sample ID | PHBV (*wt%*) | PBAT (*wt%*) | $T_m$ (*ºC*) | $\Delta H_{Tm}$ (*J/g*) | $T_{mc}$ (*ºC*) | $\Delta H_{Tmc}$ (*J/g*) |
|---|---|---|---|---|---|---|
| PHBV/PBAT (100/0) | 100.0 | 0.0 | 170.9 | 88.3 | 122.0 | 82.6 |
| PHBV/PBAT (85/15) | 85.0 | 15.0 | 168.2 | 76.1 | 105.8 | 70.3 |
| PHBV/PBAT (70/30) | 70.0 | 30.0 | 167.8 | 61.8 | 102.1 | 57.3 |
| PHBV/PBAT (50/50) | 50.0 | 50.0 | 131.2, 166.3, 172.7 | 42.3 | 92.2 | 43.9 |
| PHBV/PBAT (0/100) | 0 | 100 | 121.3 | 15.8 | 54.0 | 20.7 |

Table 5.1 also shows that the melting point, $T_m$, the melting enthalpies, $\Delta H_{Tm,}$, and melt crystallization enthalpies, $\Delta H_{Tmc}$ decreased with higher PBAT contents in the blend. It is expected as the result of dilution of PHBV content with increasing PBAT with low melting point, melting enthalpy and melt crystallization enthalpy.

The isothermal crystallization was also employed to further study the crystallization behaviour of the neat PHBV and their blends are shown in Figure 5.2 and 5.3. Figure 5.2 represented (a) the DSC isothermal crystallization thermogram, (b) relative crystallinity and (c) the Avrami's plot of the neat PHBV while the results for PHBV/PBAT (85/15) are shown in Figure 5.3. Results for those with PHBV/PBAT ratios of 70/30 and 50/50 have similar features and thus not shown here.

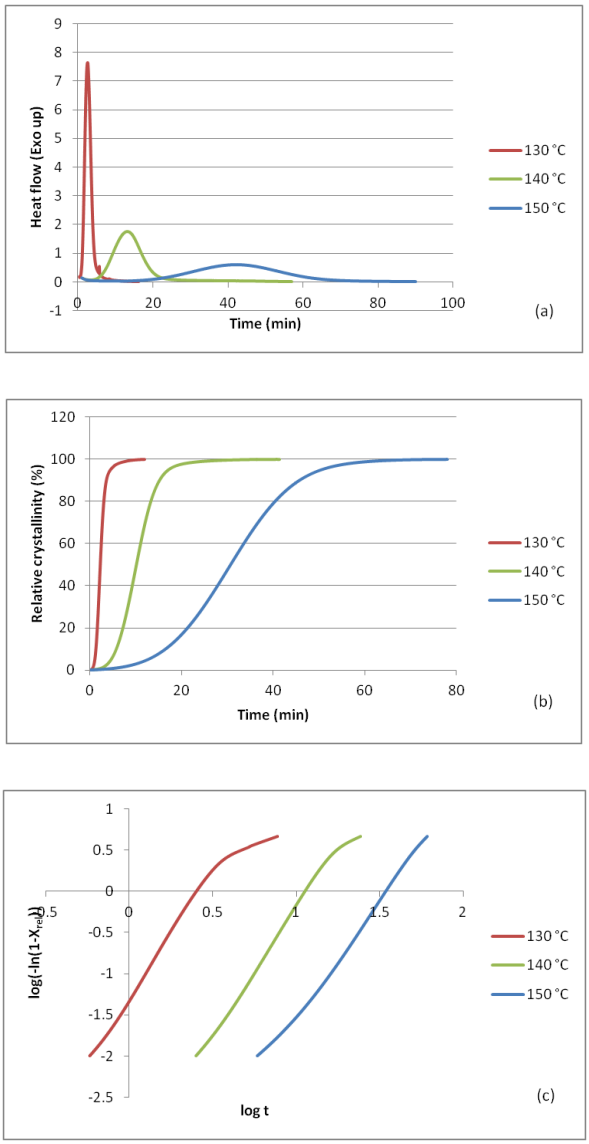


**Figure 5.2:** (a) DSC isothermal crystallization thermograms of the neat PHBV at different temperatures; (b) development of the relative crystallinity in the neat PHBV with time and (c) the Avrami's plots (as described in 4.1.1) of the neat PHBV at various isothermal crystallization temperatures

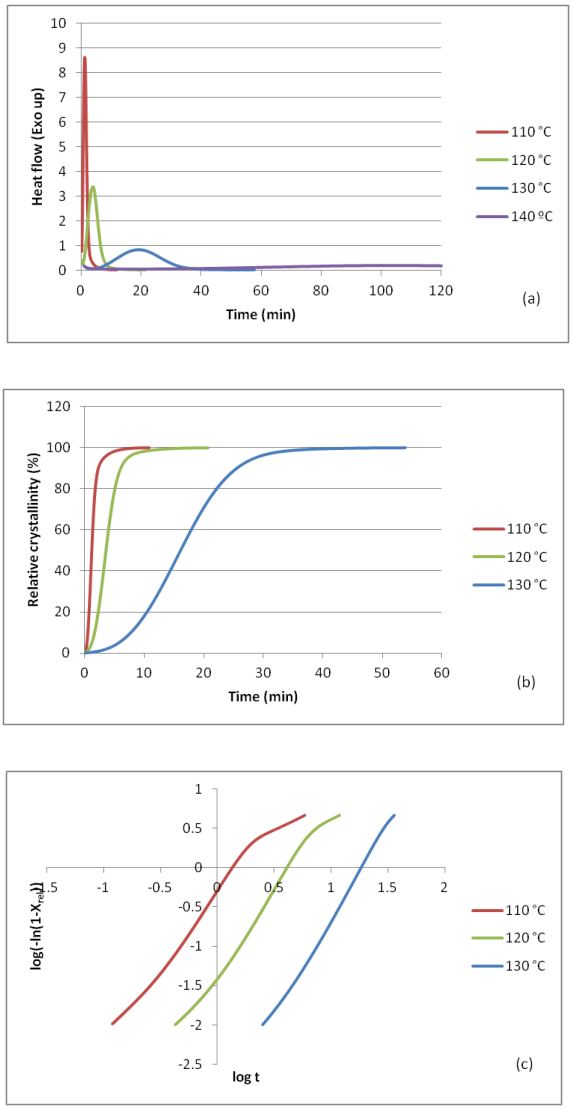


**Figure 5.3:** (a) DSC isothermal crystallization thermograms of the PHBV/PBAT (85/15) at different temperatures; (b) development of the relative crystallinity in the PHBV/PBAT (85/15) with time and (c) the Avrami's plots of the PHBV/PBAT (85/15) at various isothermal crystallization temperatures

Comparison between Figures 5.2(a) and 5.3(a) shows that there are some restrictions on the kinetic study of the isothermal crystallization of PHBV/PBAT blends. Firstly, the isothermal crystallization of the neat PHBV (Figure 5.2a) below 130 °*C* was inadequate due to too rapid crystallization. In contrast, introducing PBAT in to PHBV at ratio 85/15 hindered isothermal crystallization so that isothermal crystallization was pushed to lower temperature (below 130 °*C* shown in Figure 5.3a and b) while above this temperature e.g. at 140 °*C*, the isothermal crystallization of the PHBV/PBAT 85/15

blend could not be completed even after 2 hours. At even high PBAT contents (e.g. at PHBV/PBAT ratios of 70/30 and 50/50) no isothermal crystallization could be observed at 140 °*C*.

Figure 5.4 and 5.5 compares the isothermal crystallization thermograms and relative crystallinity of the PHBV/PBAT blends at ratios 85/15, 70/30 and 50/50 as a functions of time at 110, 120 and 130 °*C*. That for the neat PHBV is also included (Figure 5.4c and 5.5c) as a reference. Noting the time scale differences in Figure 5.4(a-c) and 5.5(a-c), increases in PBAT content or isothermal crystallization temperature results in marked delay in crystallization.

The values of *n*, *k* and $t_{1/2}$ in the Avrami's equation (see 4.1.1, page 74, for details) are summarized in Table 5.2. It gives more quantitative confirmed that the crystallization rate (*k*) decreases and half-time ($t_{1/2}$) increases with the rising of PBAT content at each temperature. The Avrami exponent (*n*) for the blends varies between 2 and 3 depending on the temperatures. There were only small changes in the *n* value with the presence of PBAT at the same temperature. The depression of the *n* value was probably due to the existence of athermal crystallization during the crystallization process (Kai *et al*., 2005).

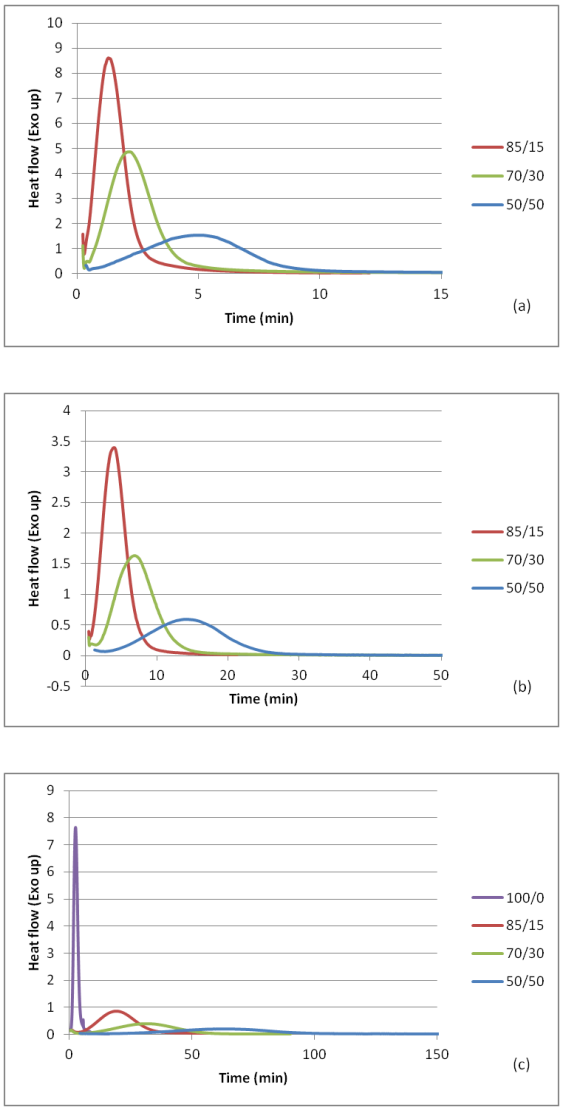


**Figure 5.4:** Comparison of the DSC isotherms crystallization thermograms of PHBV/PBAT blends as function of time at (a) 110, (b) 120 and (c) 130 *ºC* showing delay of crystallization with increasing PBAT content and temperature

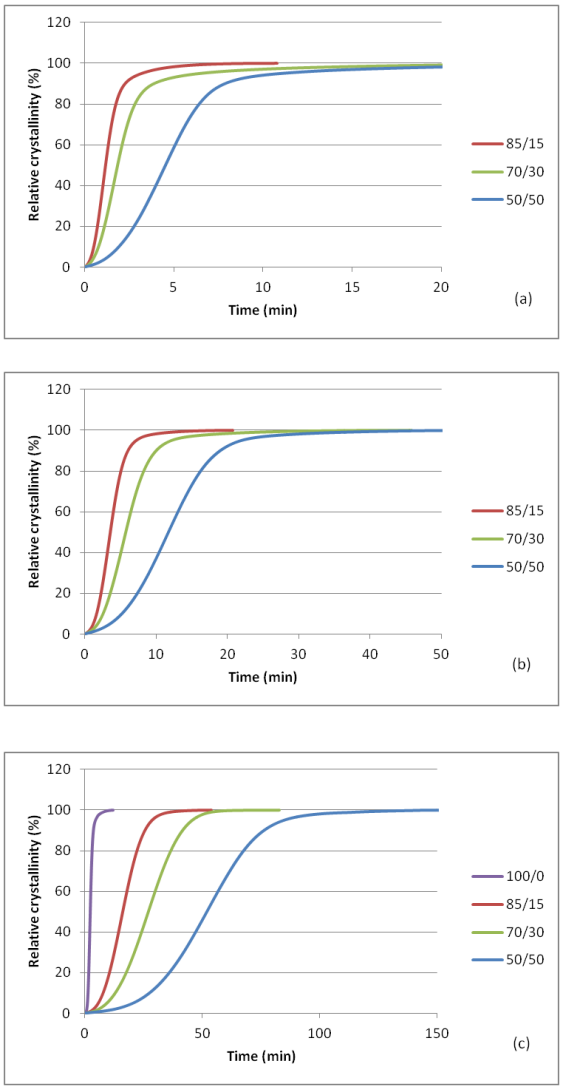


**Figure 5.5:** The relative crystallinity of PHBV/PBAT blends as function of time at (a) 110, (b) 120 and (c) 130 *ºC* showing delay of crystallization with increasing PBAT content and temperature

The reduction in crystallization rate in the PHBV/PBAT blends is believed to result from the physical restriction by the PBAT domains in crystal growth of the PHBV similar to that in poly(ethylene terephthalate)/polycarbonate (PET/PC) system (Kong & Hay, 2002) in which the crystallization of PET was constrained by PC.

**Table 5.2:** Avrami's parameters of PHBV/PBAT blends

| Sample ID | $T_c$ (ºC) | $n$ | $k$ ($min^{-1}$) | $t_{1/2}$ (min) |
|---|---|---|---|---|
| PHBV/PBAT (100/0) | 130 | 3.22 | $5.29 \times 10^{-2}$ | 2.23 |
| | 140 | 3.28 | $3.52 \times 10^{-4}$ | 10.11 |
| | 150 | 3.11 | $1.65 \times 10^{-5}$ | 30.68 |
| PHBV/PBAT (85/15) | 110 | 2.25 | $5.03 \times 10^{-1}$ | 1.15 |
| | 120 | 2.48 | $2.99 \times 10^{-2}$ | 3.55 |
| | 130 | 2.63 | $4.69 \times 10^{-4}$ | 16.06 |
| PHBV/PBAT (70/30) | 110 | 2.20 | $1.84 \times 10^{-1}$ | 1.83 |
| | 120 | 2.38 | $1.10 \times 10^{-2}$ | 5.72 |
| | 130 | 2.67 | $1.05 \times 10^{-4}$ | 27.03 |
| PHBV/PBAT (50/50) | 110 | 2.34 | $2.04 \times 10^{-2}$ | 4.51 |
| | 120 | 2.48 | $1.56 \times 10^{-3}$ | 11.70 |
| | 130 | 3.12 | $3.13 \times 10^{-6}$ | 51.85 |

## 5.2 Rheological behaviour

In this section, the effect of PHBV/PBAT ratio on complex viscosity of the blends was evaluated. Figure 5.6 presents the complex viscosity as a function of angular speed for the PHBV/PBAT blends at different ratios measured at 180 °*C*.

The neat PHBV used as reference shows the lowest complex viscosity. Its complex viscosity at 1 *rad/s* was about 590 *Pa·s* which is much lower than that of the neat PBAT at 2890 *Pa·s* at the same condition. As expected, the complex viscosities of the blends lie in between that of the neat PHBV and PBAT and increases considerably with increase of the PBAT and thus improvement in melt viscosity for better process control in sheet extrusion and foaming.

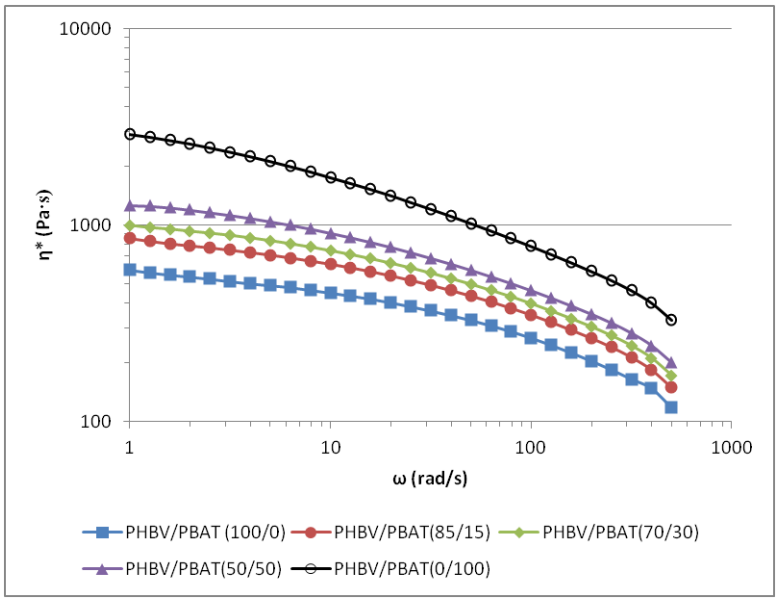


**Figure 5.6:** Complex viscosity of neat PHBV, PBAT and the PHBV/PBAT blends as a function of shear angular speed measured at180 °*C* with 1% strain

### 5.3 Mechanical properties

Tensile tests were performed using extruded sheet from the neat PHBV and PHBV/PBAT blends as described in 3.2.2.2 (page 66). Figure 5.7 shows comparison in of (a) elastic modulus, (b) tensile strength and (c) elongation at break of the neat PHBV and the blends. It can be seen that the elastic modulus of the PHBV/PBAT blends decreased when the softer and tougher PBAT is increased in content. Figure 5.7(a) shows that the PHBV/PBAT 50/50 blend had the lowest elastic modulus at 1.51 *GPa* compared with 2.84 *GPa* for the neat PHBV.

Additionally, the addition of PBAT considerably improved the tensile strength compared with the neat PHBV as shown in Figure 5.7(b). The tensile strength of the neat PHBV was around 17 *MPa* and was increased to around 20, 21 and 20.5 *MPa* at 15, 30 and 50 *wt%* PBAT contents representing increases of 17-23%.

Furthermore, the elongation at break also increased by the addition of PBAT as shown in Figure 5.7(c). The elongation at break extended from 2.4% for the neat PHBV to 3.7% in the 50 *wt%* PBAT blend.

These results demonstrate the benefits of the PHBV/PBAT blending approach to produce a stronger, less rigid and more ductile bioplastic blend system.

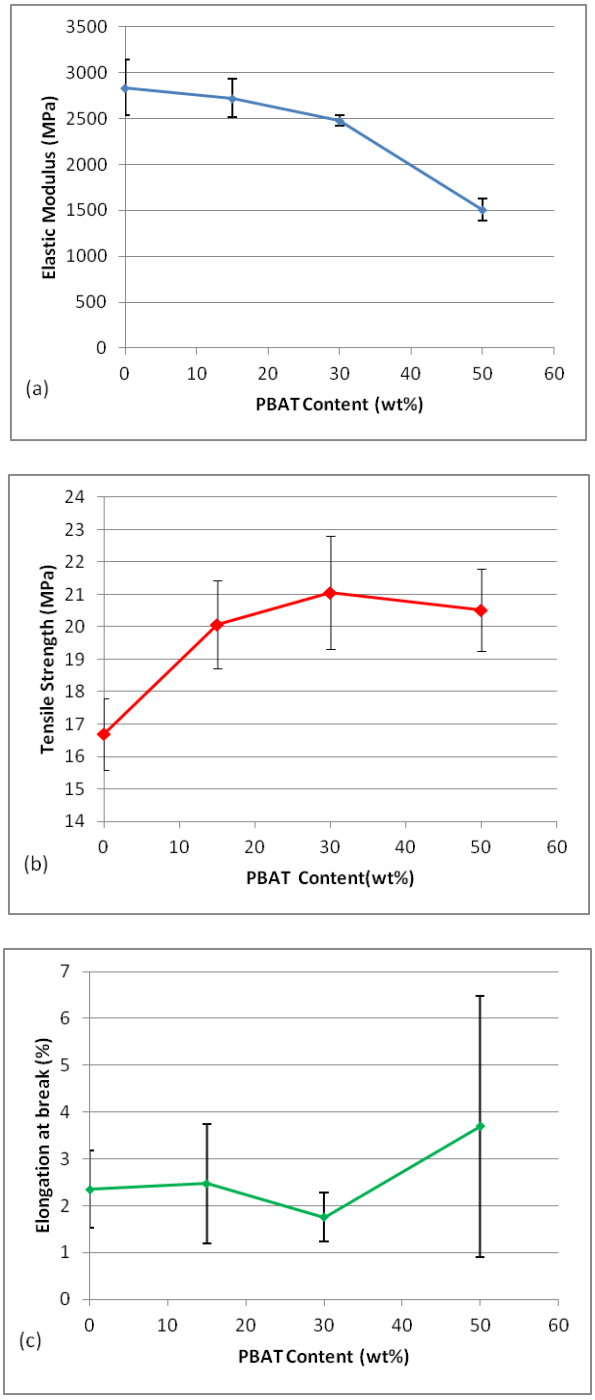


**Figure 5.7:** Mechanical properties of the PHBV/PBAT blends: (a) elastic modulus, (b) tensile strength and (c) elongation at break

## 5.4 Thermal degradation behaviour

The effect of PBAT content on thermal degradation behaviour of the PHBV/PBAT blends was investigated using TGA. Figure 5.8 presents (a) the non-isothermal thermogravimetric (TG) and (b) the corresponding derivative thermogravimatric (DTG) curves of the neat PHBV measured in the temperature range 40-600 *°C* at heating rate of 5, 10, 20, and 40 *°C/min* in nitrogen atmosphere.

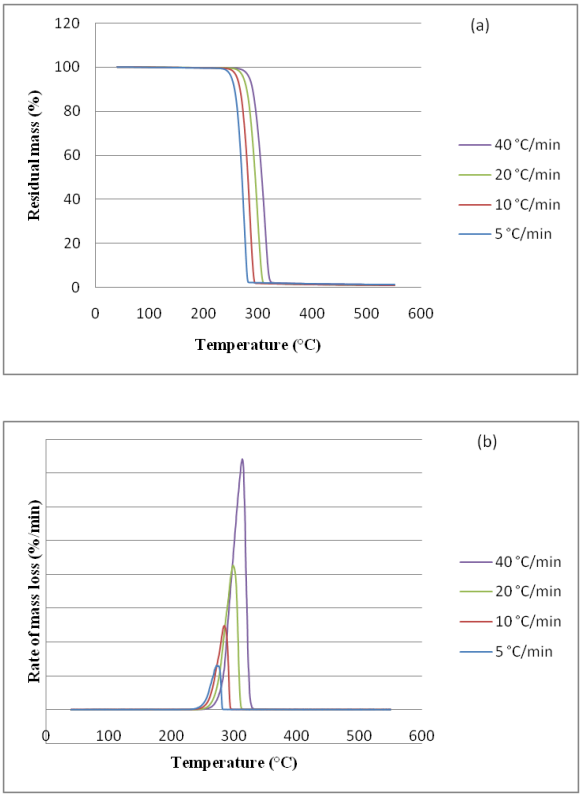


**Figure 5.8:** TG curves (a) and DTG curves (b) of the neat PHBV at different heating rates

From these Figures, it proved that the mass loss of the neat PHBV occurred in a one-step process between 240 and 325 *°C* (Figure 5.8a) corresponding to DTG curves (Figure 5.8b) with a single peak representing the maximum decomposition rate and the temperature. The DTG peak postpones with the increase in heating rate accompanied with increase in the maximum rate of decomposition. It is evident that heating rate affects on the rate of PHBV decomposition. At the end of the decomposition, only trace of residues remains.

Figure 5.9(a) and (b) present the non-isothermal TG and the corresponding DTG curves of the neat PBAT measured in the temperature range 40-600 °*C* at heating rate of 5, 10, 20 and 40 °*C/min* in nitrogen atmosphere.

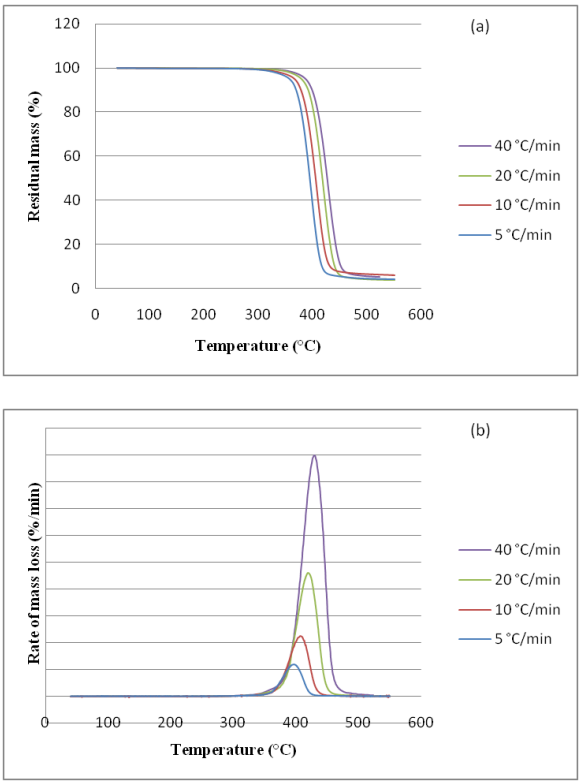


**Figure 5.9:** TG curves (a) and DTG curves (b) of the neat PBAT at different heating rates

Similarly to PHBV, one-step thermal decomposition of the PBAT occurred as between 340 and 475 °*C*, depending on heating rate. The rate of PBAT decomposition was also dependant on heating rate. However, the PHBV is less thermally stable than PBAT as the thermal decomposition of PHBV kicked off earlier and the temperature range was narrower.

Figure 5.10 presents comparison of (a) TG and (b) DTG curves of the blends obtained during temperature range 40–600 °*C* at heating rate of 10 °*C/min*.

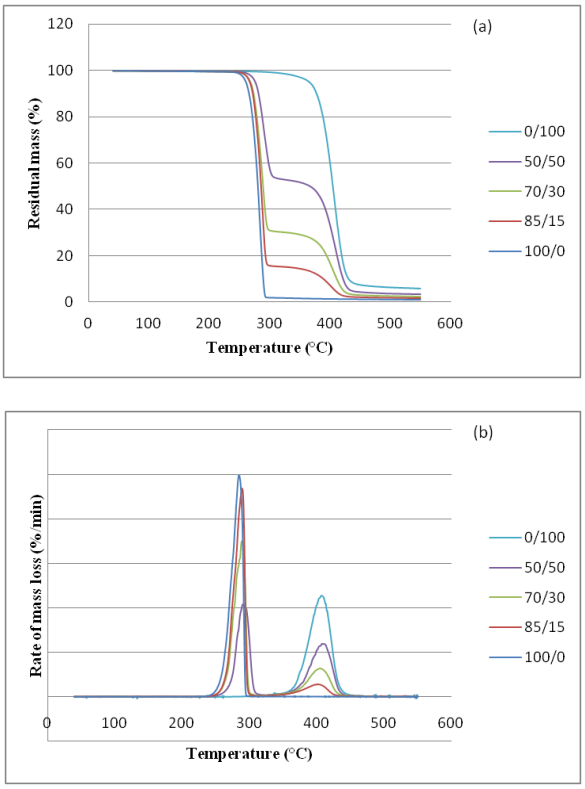


**Figure 5.10:** Comparison of TG (a) and DTG (b) curves of the neat PHBV, PBAT and the PHBV/PBAT blends at a heating rate of 10 *°C/min*

From Figure 5.10, the thermal decomposition of the PHBV/PBAT blends consisted of two separate decomposition steps (Figure 5.10a) and accompanied by two separate peaks of decomposition rate (Figure 5.10b). The lower temperature region curves correspond to the thermal decomposition of the PHBV and that in the higher temperature region correspond to that of the PBAT. This confirms the immiscible nature of the blends between PHBV and PBAT. Relative to the neat PHBV and PBAT, the heating rate affects on thermal decomposition of the polymer blends in similar way as described earlier.

From the TG curves in Figure 5.10(a), it can be seen that mass loss of the neat PHBV emerged the earliest, while that of the PHBV/PBAT blends appeared later owing to increasing contents of the more heat resistant PBAT.

As shown in Figure 5.10(b), the inclusion of PBAT reduced the peak thermal decomposition of the blends at lower temperature (from PHBV) in expense of a delayed

peak of thermal decomposition at higher temperature (from PBAT). Overall, the PHBV/PBAT blends are more thermally stable than the neat PHBV.

Some characteristic temperatures associated with degradation of PHBV in the blends from the TG and DTG curves at different heating rates are plotted in Figure 5.11. These are (a) the onset temperatures of the PHBV degradation, $T_{onset}$ in Figure 5.10(a), (b) the transition temperature from decomposition of PHBV to PBAT, $T_{trans}$, in Figure 5.10(a) and (c) the temperatures of the peak of decomposition rate of PHBV, $T_{max}$ that at the lower temperature peak in Figure 5.10(b). They were obtained using from the Universal Analysis programme in the TA Instruments software.

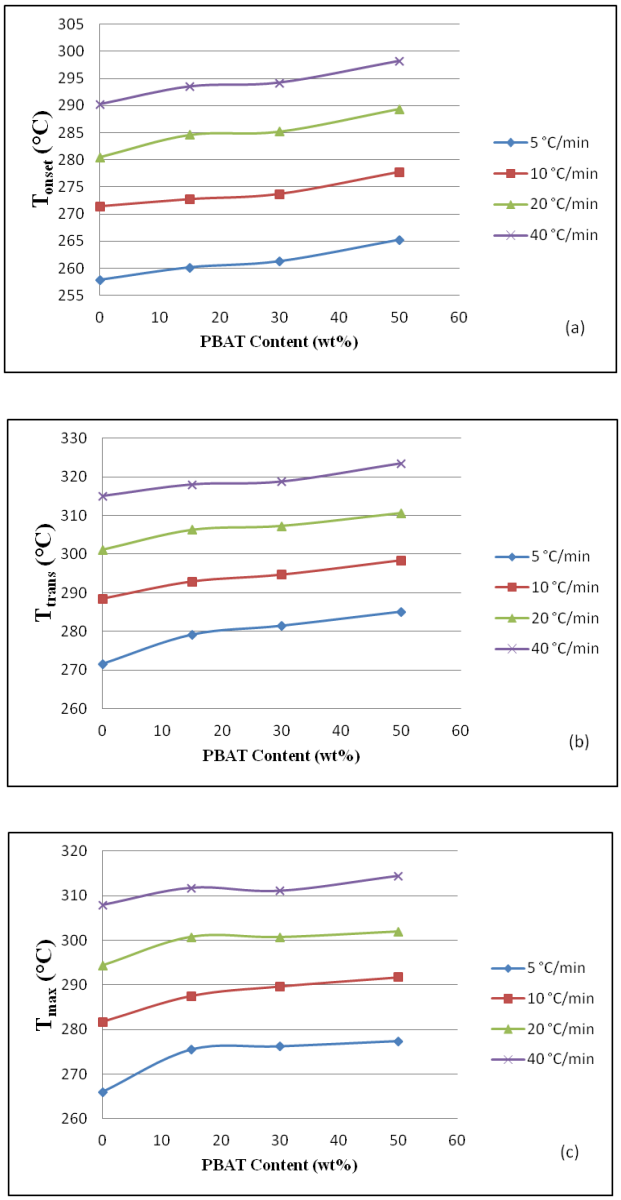


**Figure 5.11:** Effect of PBAT content in the blends and heating rate on
(a) the onset temperatures of the PHBV degradation, $T_{onset}$
(b) the transition temperature from decomposition of PHBV to PBAT, $T_{trans}$ and
(c) the temperatures at the peak decomposition rate of PHBV, $T_{max}$

It is apparent from Figure 5.11 that both the PBAT content in the blends and the heating rate affect on these characteristic temperatures. They increase with increase of heating rate and the PBAT content and thus the addition of PBAT retarded the thermal decomposition of PHBV.

## 5.5 Summary

The complex viscosity of PHBV/PBAT blends investigated by rotational rheometer shows the improvement with increasing PBAT content. By adding higher PBAT content, the complex viscosity raises toward PBAT region. This enhances the ability of PHBV in melt processing such as sheet extrusion or foaming.

PBAT also improves ductility of PHBV. Generally, it makes PHBV more flexible by increase elongation at break and tensile strength but reduce elastic modulus which would benefit final product to be less brittleness.

From TGA results, PBAT is better thermal stability than PHBV and the blending between PHBV and PBAT develops the thermal stability of PHBV. Increase PHBV/PBAT ratio raises onset and final decomposition temperatures and the temperature of the peak of decomposition rate of PHBV. This behaviour proves to be beneficial on processing with less thermal degradation and widening of processing window.

However, addition of the PBAT significantly retards the crystallization rate of the PHBV and also reduces in crystallinity. The kinetic study by Avrami's equation confirms the retardation effect of PBAT content on crystallization rate. As a result, the sagging might be present during processing, so the solidification of the polymer melt must be taken carefully.

These results suggest blending PHBV with PBAT in order to improve processibility of PHBV and produce flexible product.

# Chapter 6

# The Blending of PHBV and $CaCO_3$

In this work, an engineered $CaCO_3$ powder was incorporated in to PHBV primarily as filler to reduce PHBV material cost. The effect of the $CaCO_3$ on crystallization, mechanical, rheological and thermal behaviours of the PHBV/$CaCO_3$ system was studied.

## 6.1 Crystallization behaviour

Figure 6.1(a) shows the DSC thermograms of non-isothermal melt crystallization of the "neat" PHBV (ENMAT$^{TM}$ Y1000P containing BN nucleation agent and an antioxidant) and $CaCO_3$ at different concentrations whereas the melting behaviour of the composites is presented in Figure 6.1(b).

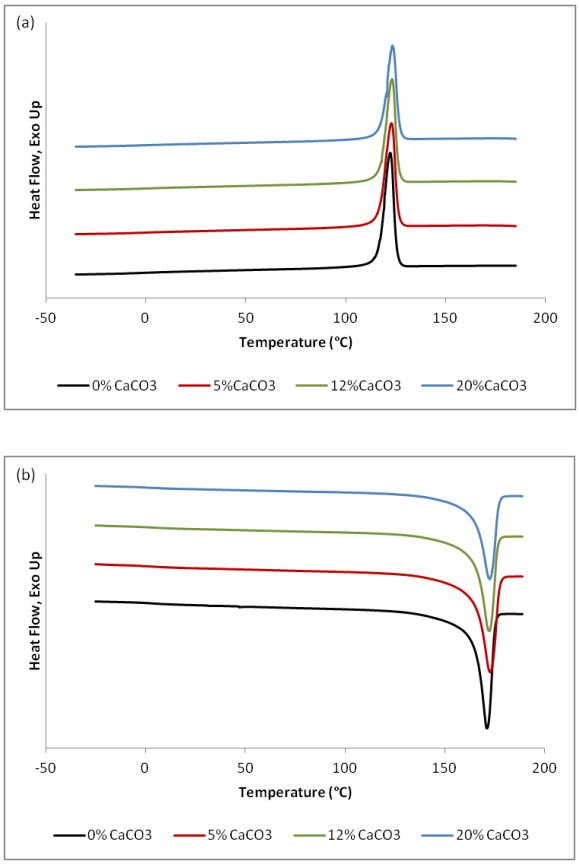


**Figure 6.1:** DSC thermograms of PHBV/$CaCO_3$ composites at a cooling/heating rate of 10 *°C min*$^{-1}$: a) the first cooling scans and b) the second heating scans

The compounded PHBV/$CaCO_3$ composites were compared with the extruded "neat" PHBV as a reference, which underwent slightly different thermal history resulted from the difference in extrusion equipment used at Bangor University and Brunel University as described in 3.2.2.4 (page 66).

The "neat" PHBV and PHBV/$CaCO_3$ composites showed only a single crystallization peak (Figure 6.1a) and a single melting peak (Figure 6.1b). The melt crystallization temperatures ($T_{mc}$), melt crystallization enthalpy ($\Delta H_{Tmc}$), melting temperatures ($T_m$) and melting enthalpy ($\Delta H_{Tm}$) are summarized in Table 6.1.

**Table 6.1:** Thermal characteristics of the neat PHBV and the PHBV/$CaCO_3$ blends

| Sample ID | PHBV (*wt%*) | $CaCO_3$ (*wt%*) | $T_m$ (*°C*) | $\Delta H_{Tm}$ (*J/g*) | $T_{mc}$ (*°C*) | $\Delta H_{Tmc}$ (*J/g*) |
|---|---|---|---|---|---|---|
| PHBV0C | 100.0 | 0.0 | 170.9 | 85.2 | 122.2 | 83.1 |
| PHBV5C | 95.0 | 5.0 | 172.6 | 81.2 | 122.8 | 74.4 |
| PHBV12C | 88.0 | 12.0 | 172.0 | 77.2 | 123.0 | 72.4 |
| PHBV20C | 80.0 | 20.0 | 172.4 | 69.9 | 123.4 | 65.0 |

The results in Table 6.1 do not show major change of thermal behaviour. There are only slight shifts in $T_m$ and $T_{mc}$ to higher temperatures with $CaCO_3$ inclusions whereas $\Delta H_{Tm}$ and $\Delta H_{Tmc}$ are reduced slightly due to dilution of the PHBV content.

It should be noted that the "neat" PHBV had already included boron nitride (BN) as a nucleating agent, so the additional effect of $CaCO_3$ on crystallization of the PHBV should be studied further. The isothermal crystallization of the PHBV/$CaCO_3$ composites was conducted using the Avrami's method described earlier (see 4.1.1, page 74, for details). Figures 6.2 represented (a) the DSC isothermal crystallization thermograms, (b) relative crystallinity as function of time and (c) the Avrami's plot of composite containing 5 *wt%* $CaCO_3$. Results for those with addition of $CaCO_3$ at 12 and 20 *wt%* levels have similar feature and thus not shown here. The results show that the crystallization rate of the PHBV/$CaCO_3$ blends depended on temperature (Figure 6.2a and 6.2b) and it decreases with the rising of crystallization temperature.

In comparison with the "neat" PHBV (already containing BN nucleating agent), the crystallization peaks are narrower and emerged earlier than the "neat" PHBV with increasing $CaCO_3$ contents and the dependence of crystallization on the isothermal crystallisation temperatures (Figure 6.3a, b and c, noting the time scale difference). Figure 6.4 also confirms that the PHBV crystallization takes less time to complete at higher $CaCO_3$ contents, noting the differences in time scale. These results demonstrate that the $CaCO_3$ filler has acted as an additional nucleation agent and enhanced crystallization of the PHBV.

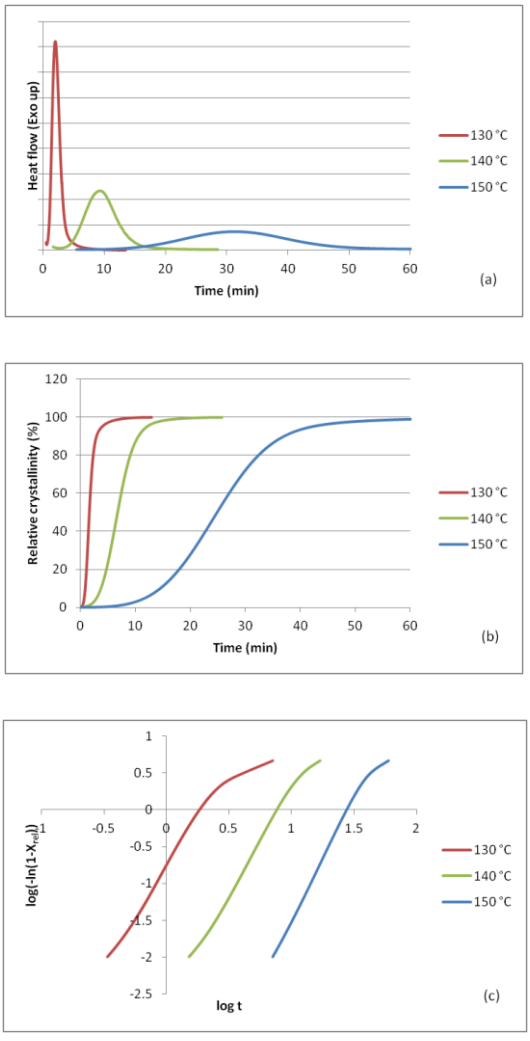


**Figure 6.2:** Characterisation of isothermal crystallization of the PHBV with 5 *wt%* $CaCO_3$: (a) DSC isotherms crystallization thermograms at different temperatures, (b) relative crystallinity with crystallization time and (c) the related Avrami plots at various isothermal crystallization temperatures

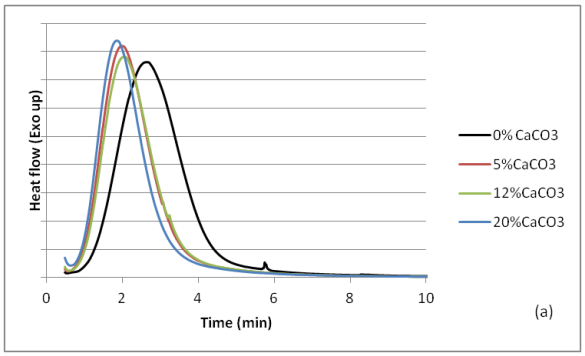


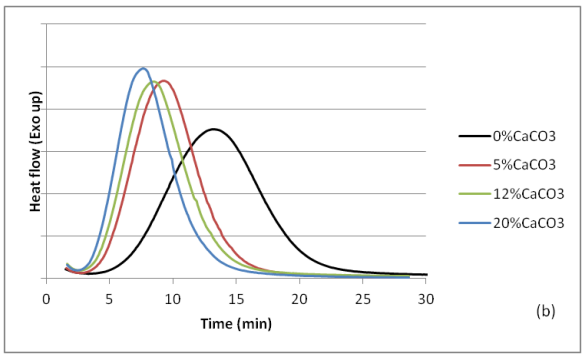


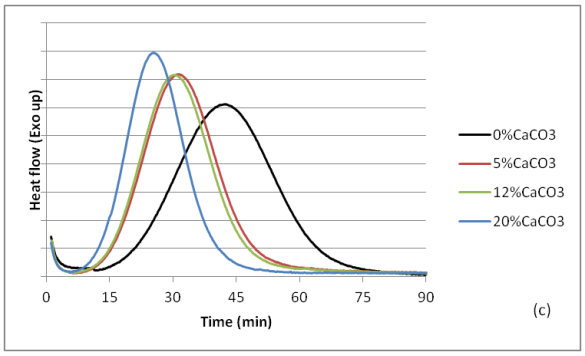


**Figure 6.3:** Comparison of DSC isothermal crystallization thermograms of the "neat" PHBV and PHBV at different $CaCO_3$ concentrations at: (a) 130, (b) 140 and (c) 150 *ºC*

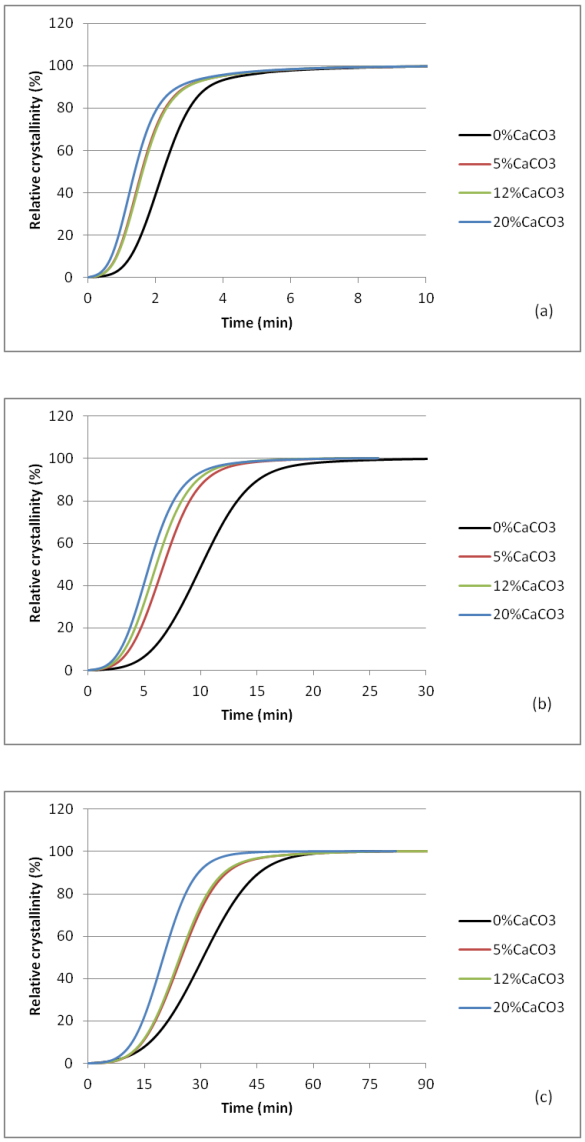


**Figure 6.4:** The relative crystallinity with crystallization time of the "neat" PHBV and PHBV at different $CaCO_3$ concentrations obtained at: (a) 130, (b) 140 and (c) 150 *ºC*

Analysis of the isothermal crystallization kinetics of the "neat" PHBV and PHBV/$CaCO_3$ composites is presented in Table 6.2 using the Avrami method.

**Table 6.2:** The Avrami's parameters of the "neat" PHBV and the PHBV/$CaCO_3$ composites

| $CaCO_3$ content (*wt%*) | $T_c$ (*°C*) | *n* | *k* ($min^{-1}$) | $t_{1/2}$ (*min*) |
|---|---|---|---|---|
| 0.00 | 130 | 3.22 | $5.29 \times 10^{-2}$ | 2.23 |
| | 140 | 3.28 | $3.52 \times 10^{-4}$ | 10.11 |
| | 150 | 3.11 | $1.65 \times 10^{-5}$ | 30.68 |
| 5.00 | 130 | 2.83 | $1.87 \times 10^{-1}$ | 1.59 |
| | 140 | 3.12 | $1.80 \times 10^{-3}$ | 6.74 |
| | 150 | 3.45 | $1.07 \times 10^{-5}$ | 24.85 |
| 12.00 | 130 | 2.85 | $1.77 \times 10^{-1}$ | 1.61 |
| | 140 | 2.99 | $3.11 \times 10^{-3}$ | 6.09 |
| | 150 | 3.49 | $9.91 \times 10^{-6}$ | 24.42 |
| 20.00 | 130 | 2.65 | $2.93 \times 10^{-1}$ | 1.38 |
| | 140 | 2.92 | $4.82 \times 10^{-3}$ | 5.47 |
| | 150 | 3.51 | $1.83 \times 10^{-5}$ | 20.06 |

Comparing the rate constant (*k*) and half time ($t_{1/2}$) at a given temperature, addition of higher concentration of $CaCO_3$ clearly increase crystallisation rate or reduce crystallisation time. This tendency can be explained in terms of $CaCO_3$ as nucleating agent in addition to the BN already included (Qian *et al*., 2007).

At a given temperature, the *n* values of the PHBV with different $CaCO_3$ concentrations showed little change. This implies that the crystallization mechanism was not affected by the presence of $CaCO_3$.

## 6.2 Rheological behaviour

Rotational rheometry was conducted in order to see the effect of the filler on complex viscosity of the PHBV/$CaCO_3$ blends. Complex viscosity as a function of shear angular speed was measured at temperature of 180 °*C* and shown in Figure 6.5. Both the "neat" PHBV and the PHBV/$CaCO_3$ blends show shear thinning behaviour and addition of the $CaCO_3$ filler exhibits a considerable increase in the melt viscosity. The complex viscosity of the "neat" PHBV at 1 *rad/s* was about 590 *Pa·s* and increased to 717 *Pa·s*

or by 21.5% by adding 20 *wt%* $CaCO_3$. This is expected as the filler particles restrict movement of the polymer chains (Luengo *et al*., 1997).

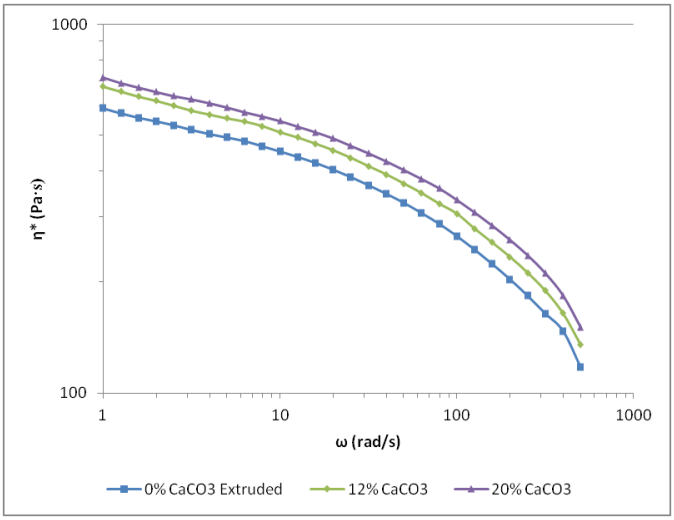


**Figure 6.5:** Complex viscosity of the "neat" PHBV and two PHBV/$CaCO_3$ composites as a function of angular speed measured at180 °*C* with 1% strain

### 6.3 Mechanical properties

The tensile experiments were performed to investigate the effect of $CaCO_3$ content on mechanical properties of the PHBV/ $CaCO_3$ blends. Comparison of (a) elastic modulus, (b) tensile strength and (c) elongation at break of the "neat" PHBV and the PHBV/$CaCO_3$ composites are presented in Figure 6.6.

It can be seen in Figure 6.6(a) that the elastic modulus increased from 2.84 *GPa* for the "neat" PHBV to 3.05 *GPa* at 5 *wt%* $CaCO_3$. However, adding 20 *wt%* of $CaCO_3$ reversed the elastic modulus to 2.86 *GPa*. The same trend was also observed in the tensile strength as shown in Figure 6.6(b) where 5 *wt%* $CaCO_3$ increased tensile strength from 17 *MPa* to 20 *MPa* whereas at 20 *wt%* $CaCO_3$ it declined to18 *MPa*. The improvement of elastic modulus and tensile strength at the lower filler concentration can be explained by law of mixing and the decreasing of both values at higher $CaCO_3$ concentration is rather unexpected but may be attributable to less effective dispersion of the filler (Azeredo, 2009; Bordes *et al*., 2009). Addition of the $CaCO_3$ filler did not enhance elongation at break as shown in Figure 6.6(c). The elongation at break of the "neat" PHBV and the PHBV with 5 *wt%* $CaCO_3$ was at similar level around 2.4% and

reduced to 1.7% when the amount of $CaCO_3$ was increased to 20 *wt%*. This phenomenon is normally seen in polymer/filler systems because poor interfacial adhesion between polymer and filler results in cavity creation and lower ductility (Azeredo, 2009; Bordes *et al*., 2009).

It can be concluded that addition of $CaCO_3$ at lower concentration (e.g. 5 *wt%*) improved mechanical properties of the blend. At higher filler concentrations, the benefit is less significant but still worth considering as it give raise other benefit such as cost reduction of the materials.

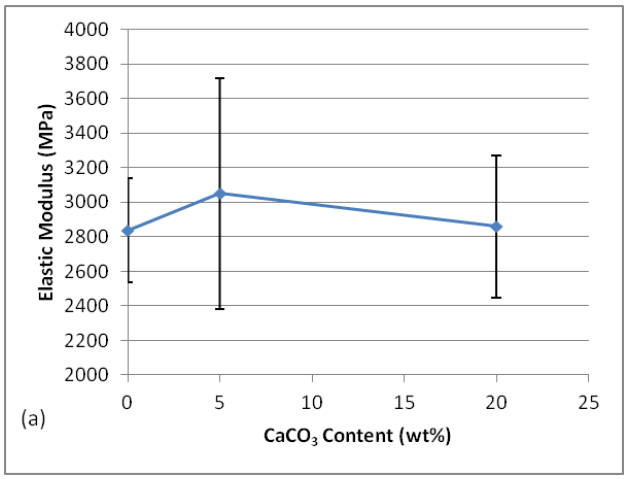


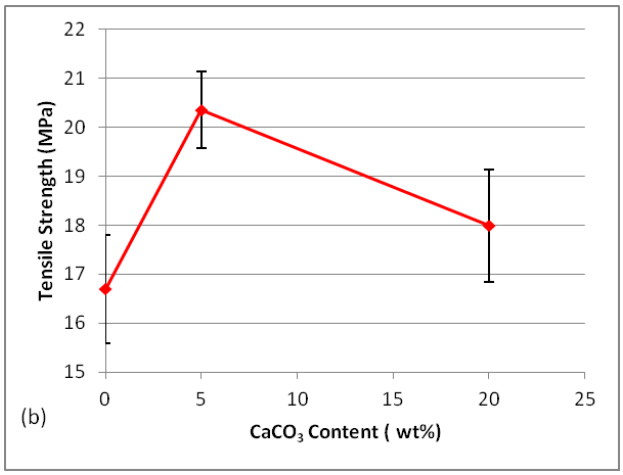


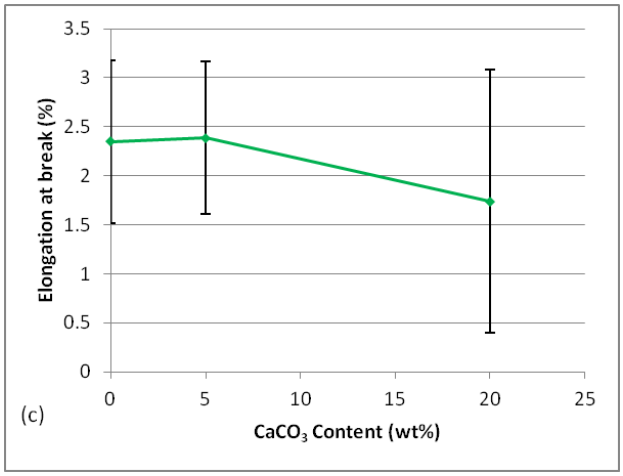


**Figure 6.6:** Mechanical properties of the "neat" PHBV and the PHBV/$CaCO_3$ composites: (a) elastic modulus, (b) tensile strength and (c) elongation at break

## 6.4 Thermal degradation behaviour

The thermal stability of the PHBV and its composites were study using TGA. Figure 6.7 compares the TG and DTG curves of the "neat" PHBV and the PHBV/$CaCO_3$ composites obtained in the temperature range 40–600 °*C* at a heating rate 20 °*C/min*. Results for those at heating rate of 5, 10 and 40 °*C/min* are similar to that at 20 °*C/min* and thus not presented.

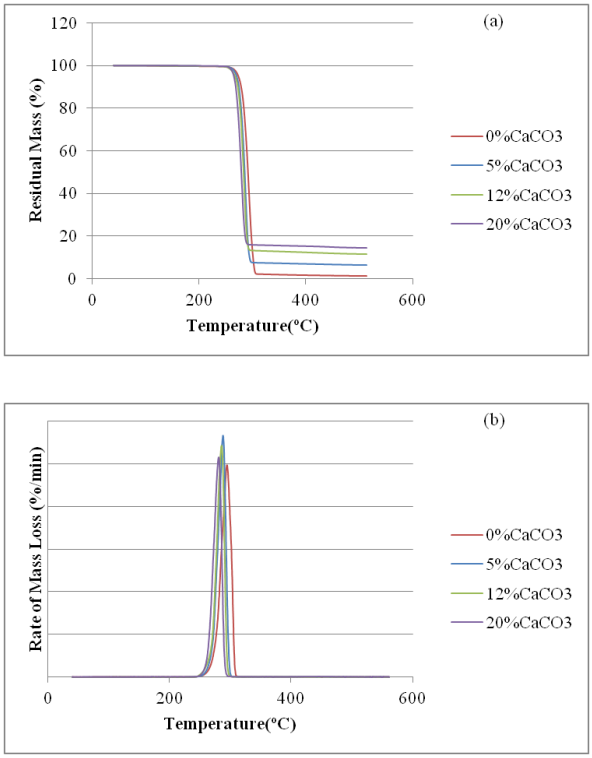


**Figure 6.7:** TG (a) and DTG (b) of the neat PHBV and the PHBV/$CaCO_3$ blends at different $CaCO_3$ concentrations

The single major mass loss for every PHBV/$CaCO_3$ composition corresponds to the loss of PHBV. The residual levels at the end of the degradation are attributable to the $CaCO_3$ contents. The addition of the $CaCO_3$ has resulted onset of mass loss at lower temperature with the increase of $CaCO_3$ concentration (Figure 6.7a) corresponding to a slight shift of the decomposition peaks to lower temperatures (Figure 6.7d).

This is confirmed by the characteristic temperatures of PHBV decomposition i.e. the onset of decomposition, $T_{onset}$, the finish of decomposition, $T_{final}$ and the temperature at the peak rate of decomposition, $T_{max}$, as shown in Figure 6.8.

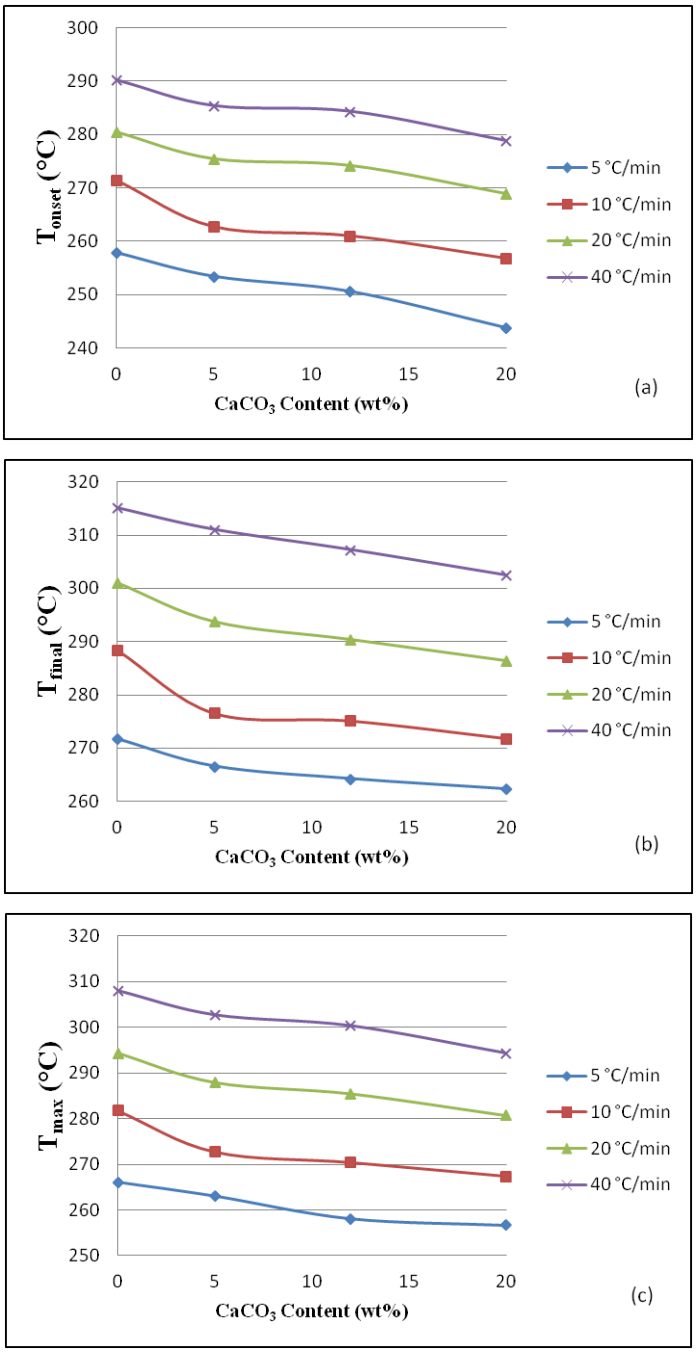


**Figure 6.8:** Effect of $CaCO_3$ content in the PHBV/$CaCO_3$ blends and the heating rate on the characteristic decomposition temperatures of PHBV (a) the onset of the degradation, $T_{onset}$ (b) the finish of decomposition, $T_{final}$ and (c) the temperature at the peak rate of decomposition, $T_{max}$

All these temperatures decrease with the increase in $CaCO_3$ concentration and lower heating rates. The above results confirmed that addition of the $CaCO_3$ filler to the PHBV reduces its thermal stability. This may have arisen from attrition of the polymer chains between the filler particle or potentially some catalytic effect from the filler.

## 6.5 Summary

The effect of $CaCO_3$ on PHBV's properties was evaluated. The introduction of $CaCO_3$ improves the crystallization rate of PHBV. The kinetic study by Avrami's method shows the shorter crystallization half time ($t_{12}$) and higher crystallization rate constant ($k$) with higher $CaCO_3$ content. This advantage can be helpful in solidification during extrusion and reduce the stickiness of the polymer melt.

Moreover, the $CaCO_3$ also considerably improves rheological behaviour by increasing the complex viscosity which would be useful for extrusion foaming.

The mechanical properties present the significant improvement by adding small amount of $CaCO_3$. Although, the mechanical properties does not further develop at higher $CaCO_3$ content, its other advantage such as cost reduction of the materials is worth to considered.

The TGA results, unfortunately, suggests the dropping of thermal stability. The increasing amount of $CaCO_3$, results in the decreasing of onset and final decomposition temperatures and temperature at the peak rate of decomposition rate of PHBV. Thus, the extrusion of the composite requires the processing temperature as low as possible.

Calcium carbonate is not only reducing material consumption but also decrease crystallization time as additional nucleation agent. The improvements of mechanical and rheological properties are also benefits. Although, it induces thermal instability of PHBV, it is still worth considered adding in the final product.

# Chapter 7
# The Effect of Chain Extender on PHBV

In this study, an epoxy-functionalized chain extender (BASF Joncryl® ADR-4368) was employed. The reactive processing was carried out in a co-rotating twin screw extruder to investigate the effect of chain extender on crystallization, rheological and thermal degradation behaviours of PHBV.

## 7.1 Crystallization behaviour

The dynamic thermal properties were investigated in order to obtain useful information in melting and crystallization characteristics in relation to processing and product application. The DSC curves, obtained from PHBV/Joncryl blends on the first cooling scans are presented in Figure 7.1(a) while Figure 7.1(b) shows the non-isothermal DSC thermograms on the second heating scans at heating rate of 10 *°C/min*. The melt crystallization temperatures ($T_{mc}$), melt crystallization enthalpies ($\Delta H_{Tmc}$), the melting temperature ($T_m$) and the enthalpies of melting ($\Delta H_{Tm}$) are summarized in Table 7.1.

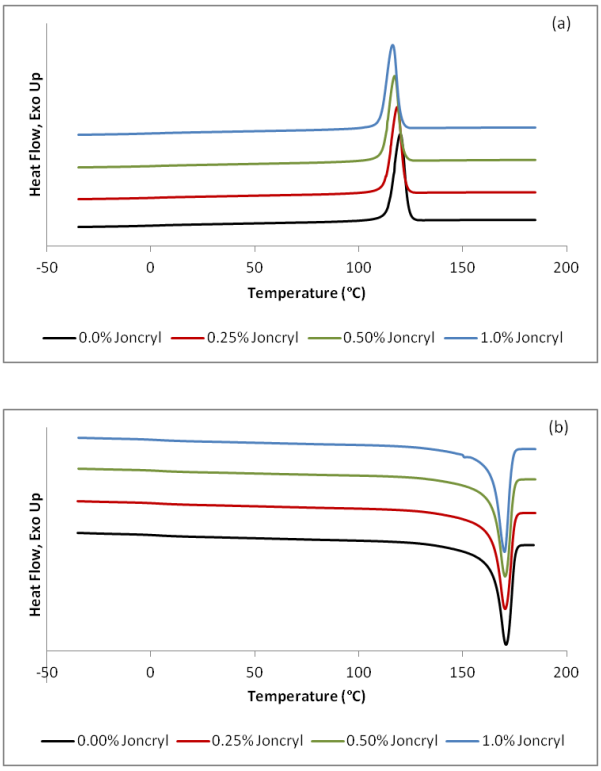


**Figure 7.1:** DSC curves of PHBV/Joncryl blends at a cooling/heating rate of 10 *°C/min*: (a) first cooling cycles and (b) second heating cycles

For all PHBV/Joncryl blends at different Joncryl concentrations, only a single crystallization peak can be observed. The melt crystallization temperature, $T_{mc}$, is an indirect indication of the crystallization rate and generally, a lower $T_{mc}$ indicates slower crystallization (Kai *et al.*, 2005). Figure 7.1(a) and Table 7.1 show that with increasing Joncryl content, $T_{mc}$ shifted to a lower temperature and the enthalpies of crystallization ($\Delta H_{Tmc}$) also slightly decreased. This indicated that the chain extender resulted in a lower crystallization rate and lower percentage of crystallinity.

Only a single melting peak is observed for each sample as seen in Figure 7.1(b). The results did not show much change in the melting temperature but there is a decrease in enthalpies of melting with increase in the chain extender which can be attributed to the decrease in crystallinity mentioned earlier. Chain extenders are used to increase molecular weight by branching or cross-linking. This would lead to more complex molecular configuration and reduction in mobility of the polymer chains and thus to lower crystallinity and crystallinity perfection (Rao & Dweltz, 1986). Addition of

diepoxide as a chain extender to PET (Bikiaris & Karayannidis, 1998) has also shown similar effect in the decrease of crystallinity of PET.

**Table 7.1:** Thermal characteristics of the PHBV/Joncryl blends

| Joncryl concentration (*wt%*) | $T_m$ (*°C*) | $\Delta H_{Tm}$ (*J/g*) | $T_{mc}$ (*°C*) | $\Delta H_{Tmc}$ (*J/g*) |
|---|---|---|---|---|
| 0.00 | 170.6 | 94.8 | 120.2 | 88.0 |
| 0.25 | 170.4 | 91.8 | 118.6 | 84.5 |
| 0.50 | 170.4 | 91.2 | 117.5 | 83.8 |
| 1.00 | 170.2 | 90.6 | 116.3 | 83.4 |

The crystallization of PHBV and PHBV/Joncryl blends from molten state was also studied under isothermal conditions at various crystallization temperatures ($T_c$). Figures 7.2 represented (a) the DSC isothermal crystallization thermograms, (b) relative crystallinity as function of time and (c) the Avrami's plot of composite containing 0.25 *wt%* Joncryl. Results for those with addition of Joncryl at 0.50 and 1.00 *wt%* levels have similar feature and thus not shown here.

In Figure 7.2a, with rising crystallization temperature, the crystallization rate decreases as shown by a shift of the onset of crystallization and the exothermic peak to longer time and the curves became flatter and Figure 7.2(b) shows that the completion time of crystallization increases with temperature, or the crystallization rate decreases with the increase of crystallization temperature.

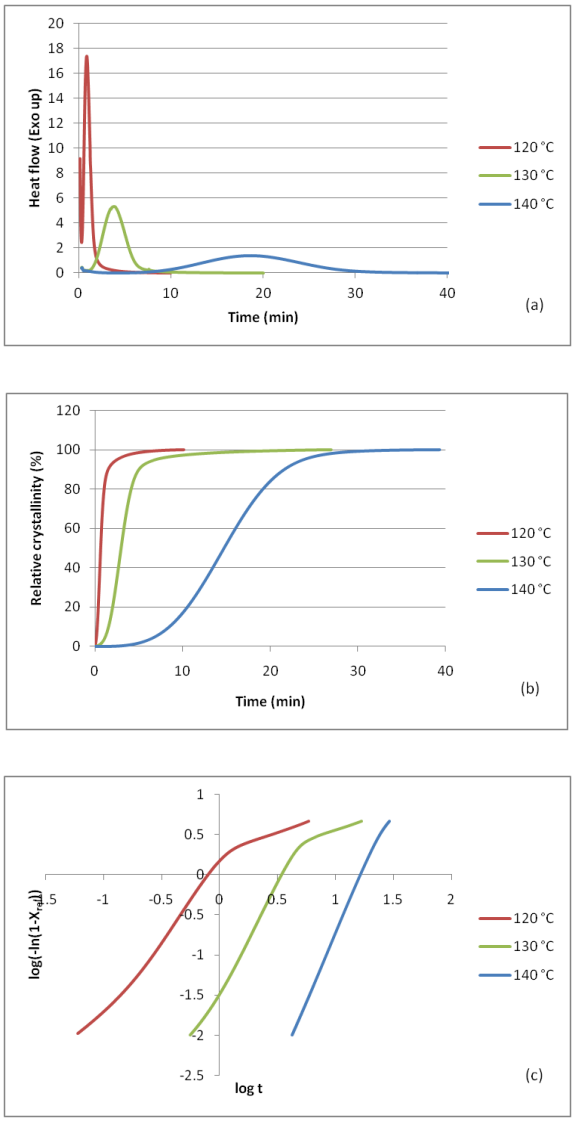


**Figure 7.2:** Characterisation of isothermal crystallization of the PHBV with 0.25 *wt%* Joncryl: (a) DSC isotherms crystallization thermograms at different temperatures, (b) relative crystallinity with crystallization time and (c) the related Avrami plots at various isothermal crystallization temperatures

Effect of the chain extender Joncryl addition on isothermal crystallization of PHBV was studied using the Avrami's method described earlier (see 4.1.1, page 74, for details). The comparison of the DSC thermogram and the relative crystallization at different temperatures were shown in Figure 7.3 and 7.4, respectively. Clearly, addition of the chain extender to PHBV reduced crystallization rate and prolonged the crystallization time.

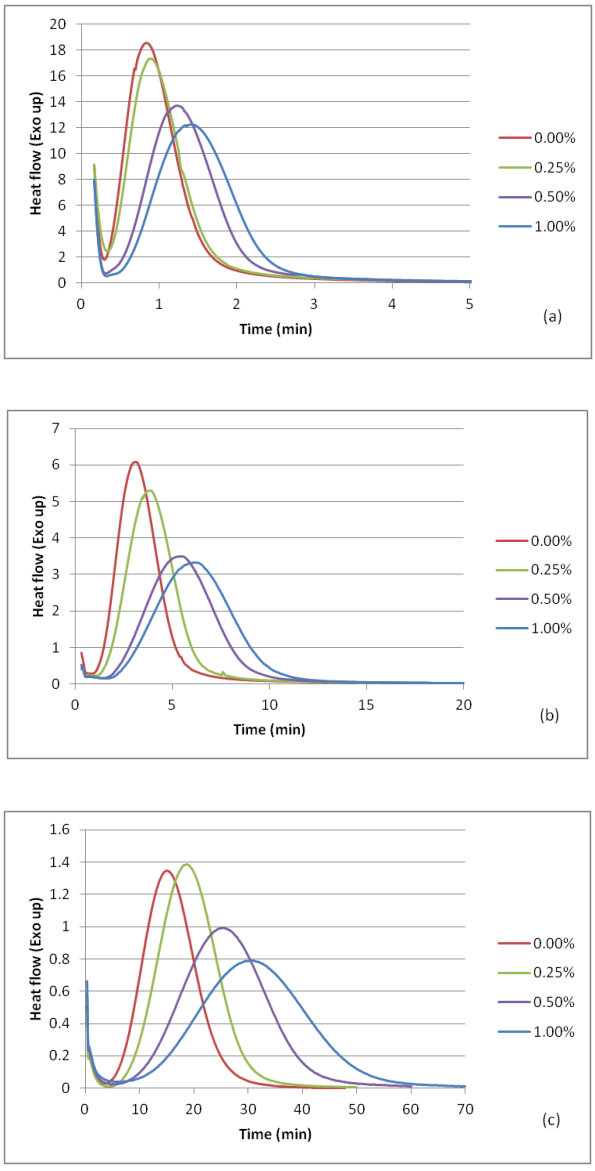


**Figure 7.3:** The comparison of DSC isothermal crystallization thermograms of PHBV/Joncryl blends at (a) 120, (b) 130 and (c) 140 *ºC*

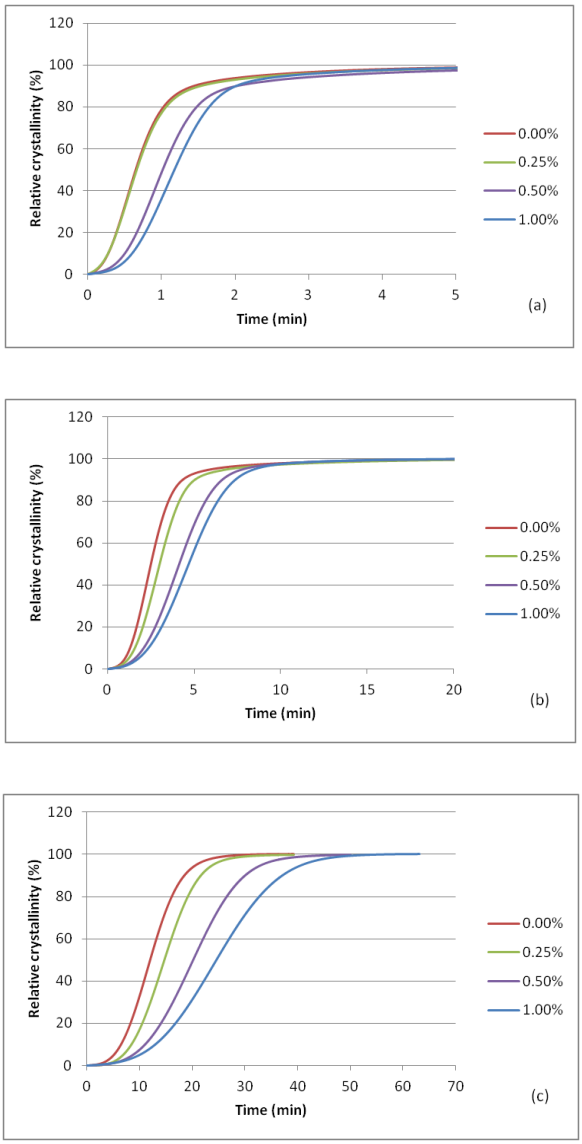


**Figure 7.4:** The comparison of development of relative crystallinity with crystallization time of PHBV/Joncryl blends at (a) 120, (b) 130 and (c) 140 *ºC*

The values of *n*, *k*, and $t_{1/2}$ are obtained as described earlier and summarized in Table 7.2. The *n* value for the PHBV in this experiment ranged from 2 to 3 depending on temperature. Change in *n* value is predominated by the crystallization temperature (degree of super cooling) and insensitive to the Joncryl concentration. This suggests that the addition of the chain extender has not changed the mechanism of nucleation. Change in crystallization rate is clearly demonstrated by the decrease in *k* value and increase in $t_{1/2}$ with increase in temperature and content of Joncryl. While temperature remained the dominating factor for *k* and $t_{1/2}$, addition of the chain extender can also be significant.

For instance, addition of 1.0 *wt%* Joncryl cans double the crystallization half time at 140 *°C*.

This phenomenon of crystallization retardancy from chain extender might be explained by change in tacticity of the molecules. Zhong *et al*. (1999) described the effect of chain extender on crystallization behaviour of PLA as a function of tacticity. PLA chains were branched after the chain-extending reaction and lowered the tacticity of the PLA molecule. Only the unbranched chains could crystallize at earlier stage while the branched chains could crystallize at a later period. This is consistent with the result shown here.

**Table 7.2:** Avrami's parameters of the PHBV/Joncryl blends

| Joncryl concentration (*wt*%) | $T_c$ (*°C*) | *n* | *k* ($min^{-1}$) | $t_{1/2}$ (*min*) |
|---|---|---|---|---|
| 0.00 | 120 | 2.17 | 1.75 | 0.65 |
| | 130 | 2.77 | $5.48 \times 10^{-2}$ | 2.50 |
| | 140 | 3.03 | $3.64 \times 10^{-4}$ | 12.05 |
| 0.25 | 120 | 2.14 | 1.66 | 0.66 |
| | 130 | 2.87 | $2.97 \times 10^{-2}$ | 3.00 |
| | 140 | 3.36 | $8.12 \times 10^{-5}$ | 14.74 |
| 0.50 | 120 | 2.64 | $6.61 \times 10^{-1}$ | 1.02 |
| | 130 | 2.76 | $1.37 \times 10^{-2}$ | 4.13 |
| | 140 | 3.14 | $5.54 \times 10^{-5}$ | 20.16 |
| 1.00 | 120 | 2.75 | $4.43 \times 10^{-1}$ | 1.18 |
| | 130 | 2.77 | $9.59 \times 10^{-3}$ | 4.68 |
| | 140 | 2.99 | $4.84 \times 10^{-5}$ | 24.60 |

## 7.2 Rheological behaviour

The effect of chain extender on melt viscosity of the PHBV/Joncryl blends was evaluated by change in complex viscosity as a function of frequency at 180 °*C*. As shown in Figure 7.5, the blends exhibit typical shear thinning characteristic, i.e. decrease of viscosity with increase of frequency or shear rate. The PHBV blend without Joncryl used as reference showed the lowest viscosity (about 525 *Pa·s* at 1 *rad/s*). Increasing content of the chain extender resulted in consistent increase in viscosity and at 1.00 *wt*% level led to considerable increase to 630 *Pa·s*. This enhancement in shear viscosity indicated that macromolecular chain-extension had occurred during the extrusion compounding process (Mihai *et al*., 2010). Corre *et al*. (2011) showed that by adding similar level of Joncryl (0.9 *wt*% using a 3 *wt*% masterbatch) to PLA resulted in a 30 times increase in the complex shear viscosity (measured at 180 °*C* using an angular frequency of 0.1 *rad/s*). PLA is known to be much more resistant to thermal degradation than PHBV and it is possible that the relatively low efficiency in viscosity enhancement in the PHBV/Joncryl blends has resulted from competition of chain extension against thermal degradation of PHBV.

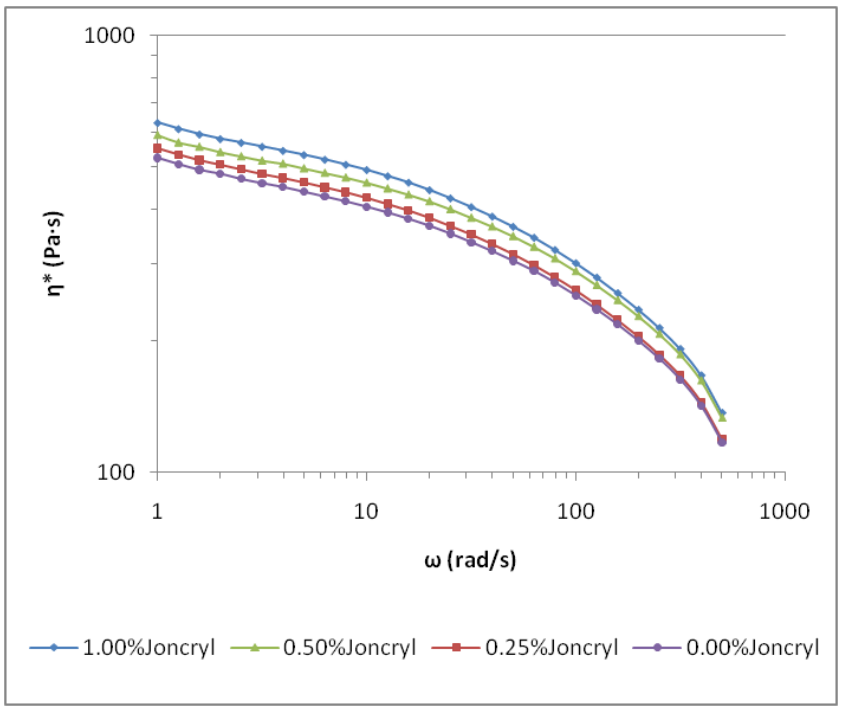


**Figure 7.5:** Complex viscosity of PHBV/Joncryl blends as a function of angular speed measured at180 °*C* with 1% strain

## 7.3 Thermal Degradation Behaviour

The effect of Joncryl on thermal degradation behaviour of PHBV was investigated using TGA. Figure 7.6 shows the TG and DTG curves for PHBV containing 0.25 *wt%* Joncryl. Results for those with Joncryl additions up to 1.0 *wt%* level have similar feature and thus not shown here.

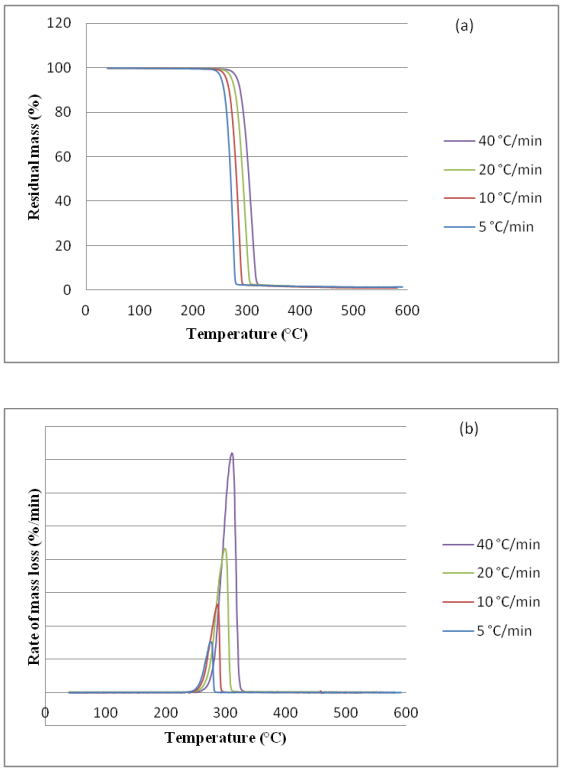


**Figure 7.6:** TG (a) and DTG (b) of PHBV containing 0.25 *wt%* Joncryl at different heating rates

It is noted that weight loss of PHBV and its blend with Joncryl occurs in a one-step process between 250 and 320 °*C* and the maximum rate of mass loss is identifiable by the single peak in DTG. Both TG and DTG are heating rate dependant: when heating rate is increased, the decomposition peak is delayed to higher temperature and the maximum decomposition rate is intensified.

The effect of chain extender to thermal stability of PHBV is studied by comparison of activation energy of thermal decomposition using the Flynn-Wall-Ozawa (FWO) method (see 4.3.1, page 88, for details). Typical plots obtained by the FWO method at

various heating rate of PHBV containing 0.00 and 1.00 *wt%* Joncryl are shown in Figure 7.7.

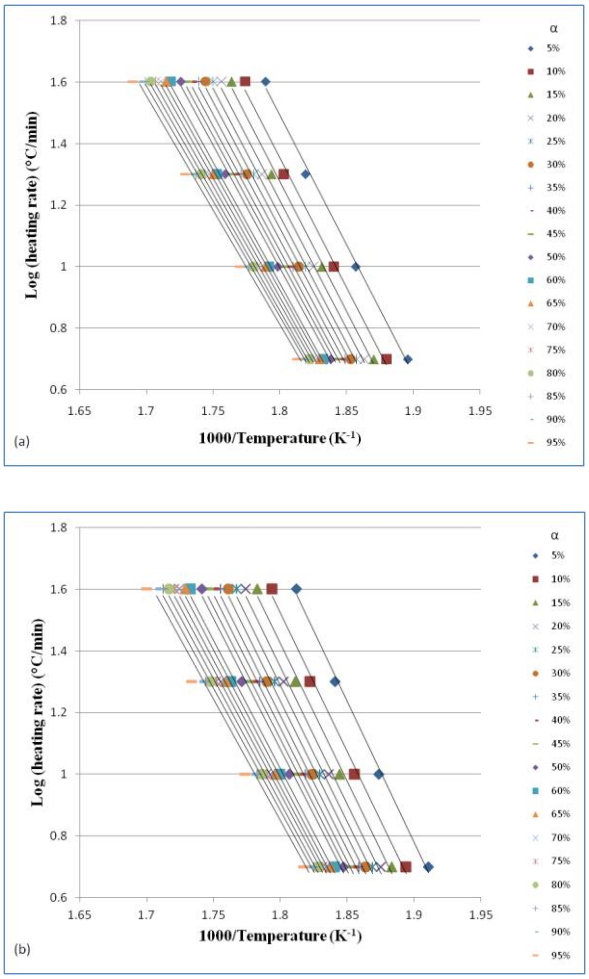


**Figure 7.7:** The application of Flynn-Wall-Ozawa method to calculate activation energy of thermal decomposition for PHBV/Joncryl blends at: (a) 0.00 *wt%* and (b) 1.00 *wt%* Joncryl

The activation energy values of all samples of non-isothermal decomposition for each PHBV/chain extender blend which evaluated by using the data from Figure 7.7 in the conversion range α = 10-90% are shown in Table 7.3 and plotted in Figure 7.8. The unmodified PHBV has lowest $E_a$. By introduction of Joncryl to PHBV, $E_a$ values of the blends increased with the Joncryl content at any given conversion level.

This result leads to conclusion that the introduction of Joncryl increases the apparent activation energy ($E_a$) of PHBV. Use of blends with higher $E_a$ means that they are more thermally stable during processing and thus widen the processing windows in terms of

processing temperature or residence time without rapid loss of melt viscosity. The reason behind the higher thermal stability might be attributable to increasing molecular weight and chain rigidity.

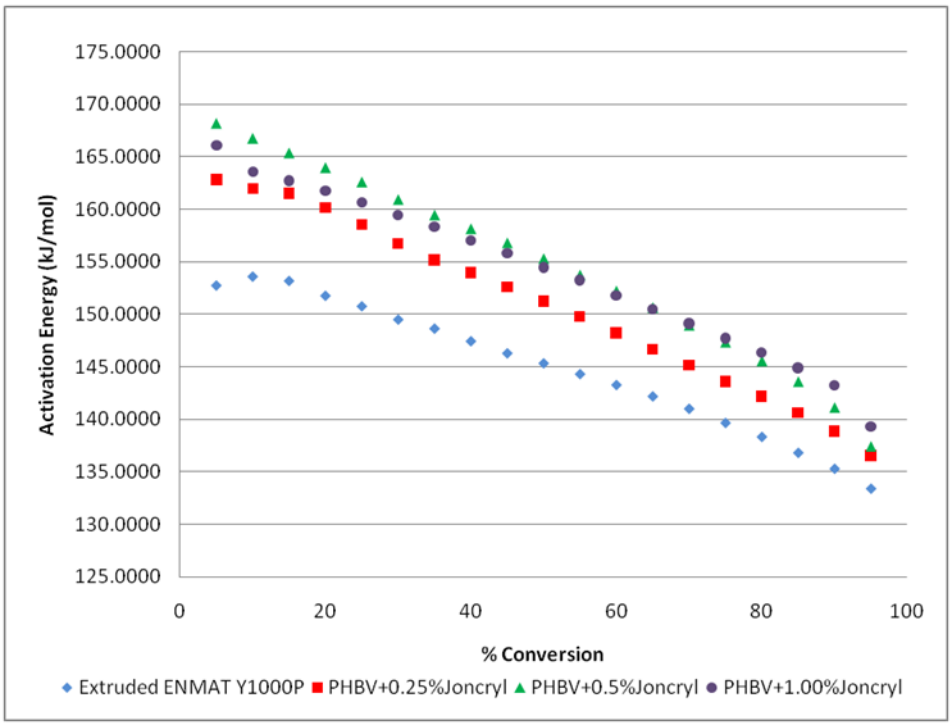


**Figure 7.8:** Activation energy of PHBV/Joncryl blends determined by FWO method

**Table 7.3:** Activation energies by Flynn-Wall-Ozawa method for PHBV/Joncryl blends

| Joncryl (*wt*%) | | Conversion, $\alpha$ (%) | | | | | | | | |
|---|---|---|---|---|---|---|---|---|---|---|
| | | 10 | 20 | 30 | 40 | 50 | 60 | 70 | 80 | 90 |
| 0.00 | $E_a$(*kJ/mol*) | 153.62 | 151.80 | 149.53 | 147.46 | 145.36 | 143.29 | 141.03 | 138.35 | 135.32 |
| | $R^2$ | 0.995 | 0.997 | 0.997 | 0.998 | 0.998 | 0.999 | 0.999 | 0.999 | 1.000 |
| 0.25 | $E_a$(*kJ/mol*) | 161.95 | 160.17 | 156.73 | 153.95 | 151.24 | 148.21 | 145.13 | 142.19 | 138.87 |
| | $R^2$ | 0.999 | 0.998 | 0.998 | 0.999 | 0.999 | 0.999 | 0.999 | 0.998 | 0.998 |
| 0.50 | $E_a$(*kJ/mol*) | 166.79 | 163.99 | 160.96 | 158.18 | 155.32 | 152.25 | 148.98 | 145.59 | 141.15 |
| | $R^2$ | 1.000 | 1.000 | 1.000 | 1.000 | 1.000 | 1.000 | 1.000 | 1.000 | 0.999 |
| 1.00 | $E_a$(*kJ/mol*) | 163.56 | 161.75 | 159.48 | 157.06 | 154.45 | 151.83 | 149.14 | 146.35 | 143.25 |
| | $R^2$ | 0.995 | 0.995 | 0.995 | 0.995 | 0.996 | 0.996 | 0.996 | 0.996 | 0.996 |

## 7.4 Summary

The effect of Joncryl chain extender on thermal degradation, crystallization and rheological behaviours of PHBV was investigated. The introduction of Joncryl improves thermal stability shown by increase in activation energy of thermal decomposition with increase in Joncryl content. This allows widening of processing window such as residence time.

The chain extender also improves rheological behaviour by increasing the complex viscosity which would benefit melt processing such as sheet extrusion or foaming of the high-crystallinity polymer.

The addition of Joncryl however showed marked retardancy to crystallization and hence care must be taken in solidification of the melt to avoid sagging.

The addition of Joncryl in this study was kept at low levels up to 1.0 *wt%* for food regulation considerations and thus may be significantly increased if not restricted by such condition to enhance the benefits.

# Chapter 8
# Extrusion Foaming of PHBV

In this work, the extrusion foaming using food-approved chemical blowing agent is reported. This includes effect of material formulations and extrusion conditions on the foaming behaviour of PHBV and the resulting foam structures.

## 8.1 Rheological behaviour of post-foaming PHBV

The complex viscosity of melts from the foamed PHBV with different amounts of blowing agent masterbatch is shown in Figure 8.1. The viscosity is noticeably lower than that of the as-received PHBV (when compared with that at 180 ℃ in Figure 4.9, page 84), which indicates that the polymer has undergone some thermal degradation during the extrusion foaming process. Moreover, with the increase of the BA masterbatch from 2.5 to 7.5 *wt%*, further decrease in viscosity was observed. This can be attributed to the hydrolytic degradation caused by water released from the decomposed sodium bicarbonate. Since PHBV is a polyester copolymer, it is susceptible to thermal and hydrolytic degradation by water at high temperatures and pressures (Verhoogt *et al*., 1996; Cabedo *et al*., 2009). In this regard, the use of negative temperature profile (Table 3.5, page 68) can reduce the high temperature exposure time and minimise the thermal and hydrolytic degradation.

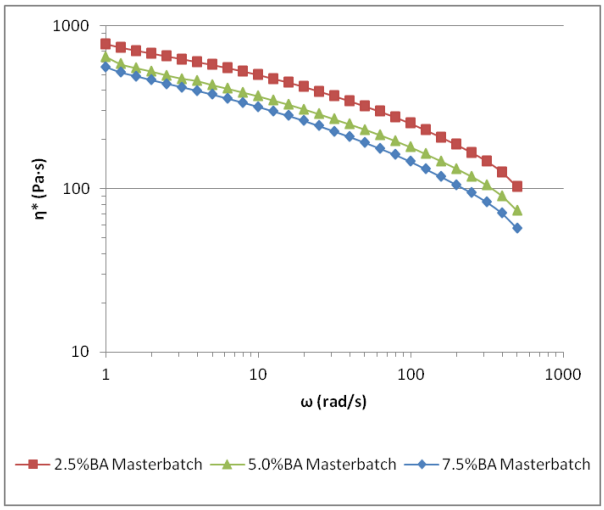


**Figure 8.1:** Complex viscosity the foamed PHBV measured at 180 °*C* showing reduction in the viscosity with increasing level of the $H_2O$ and $CO_2$ generating blowing agent

## 8.2 The PHBV foaming process

Figure 8.2 presents the morphologies of extruded foams using the sheet die at the blowing agent masterbatch levels of 1.25, 2.50 and 3.75 *wt%*, which correspond to 0.5, 1.0 and 1.5 *wt%* active contents, respectively. The sheets were extruded with temperature profile given in Table 3.5 (page 68) at 30 *rpm* screw speed and flow rate of 3.3 *kg/h*. The analysis in density reduction, cell size and cell population density determined from these foams are also presented in Figure 8.3. Sparse cell population of cells averaging 140 *μm* was observed for foams extruded with low blowing agent concentration (at 1.25 *wt%* masterbatch) and resulted in a small density reduction (14%). Increasing the masterbatch content to a medium level (2.50 *wt%*) gave rise to a high density reduction (of 32%) owing largely to the increased cell size to about 190 *μm* whereas the cell population hardly changed. At higher blowing agent concentration (3.75 *wt%*), density reduction reached 40% from considerable increasing in cell population while the cell size remained similar to that at 1.25 *wt%*. Clearly, this is attributable to more gas generated at higher blowing agent contents. One would expect the trend to continue to produce lighter foam by using higher concentrations of blowing agent. This was proved to be the case as will be discussed later.

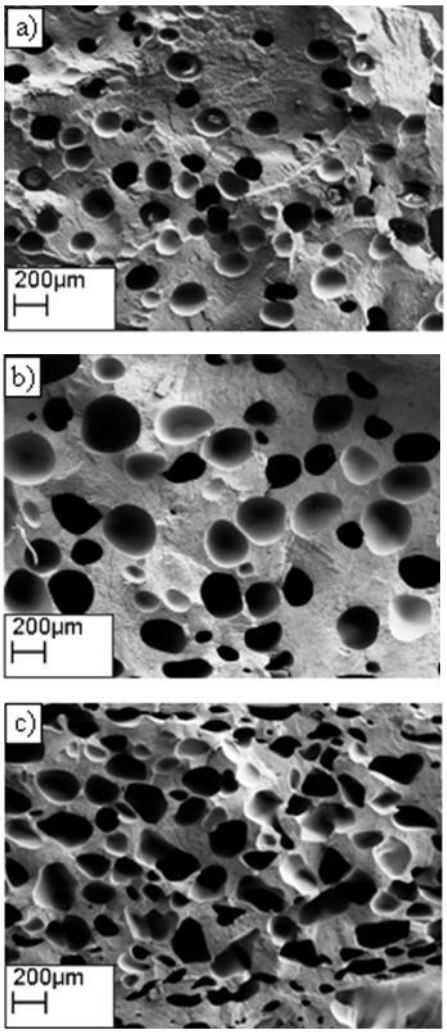


**Figure 8.2:** SEM images of PHBV foams extruded with the sheet die and BA masterbatch contents (*wt%*) of: (a) 1.25, (b) 2.50 and (c) 3.75

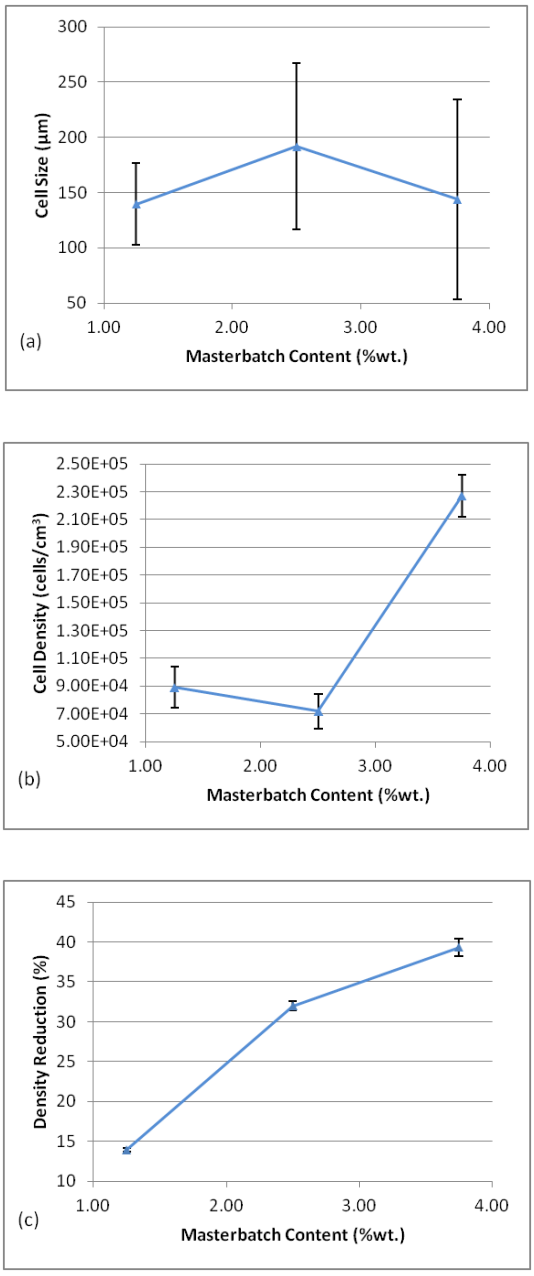


**Figure 8.3:** Effect of the amount of blowing agent on PHBV foam extruded with the sheet die: (a) cell size, (b) cell density population and (c) density reduction

Figure 8.4 shows the influence of screw speed increase from 30 to 50 *rpm* (with corresponding feeding rate from 3.3 to 5.6 *kg/h*) without changing the other parameters. The higher screw speed resulted in lower density reductions. Higher screw speed generates higher pressure drop at the die exit which should normally enhance cell nucleation and expansion. It also reduces the residence time of the material in the barrels, particularly when use a low L/D ratio extruder. Sodium bicarbonate is an

endothermic blowing agent with slow decomposition rate over wide range of temperatures (Padareva *et al*., 1998); therefore, this result can be attributed to the shorter residence time that affected the decomposition of the blowing agent. In addition, the shear thinning at high screw speed also reduced the melt viscosity, leading to cell rupture which was observed during the sheet foaming.

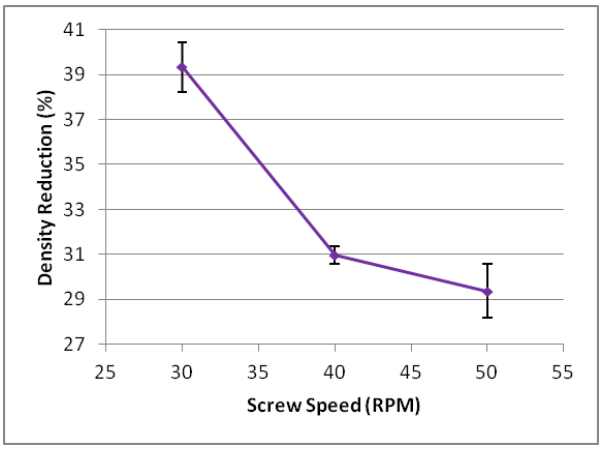


**Figure 8.4:** Density reduction as a function of screw speed in sheet foam extrusion at BA masterbatch content of 3.75 *wt%*

The blowing agent masterbatch content was extended further up to 7.50 *wt%* in the extrusion process performed using the 7 *mm* circular die. The foams were extruded with screw speed of 30 *rpm* and flow rate of 3.3 *kg/h*. The morphologies of extruded foams are shown in Figure 8.5 whereas Figure 8.6 presents analysis of cell size, cell density population and density reduction of the foams. The result shows that the maximum density reduction about 57% was achieved at 5.00 *wt%* addition of the masterbatch (corresponding to 2 *wt%* active content). Use of the strand die could result in the improved pressure profile over the sheet die, where premature foaming inside the sheet die was observed. This led to significantly higher cell density population and thinner cell walls as shown in Figure 8.5. At 5 *wt%* masterbatch addition, a fine tuning of processing parameters by reduction of the screw speed to 20 *rpm* with feeding rate to 2.2 *kg/h* and reduction of temperate in the last zone of the extruder and the die to 140 °*C* had shown further density reduction to 61.3%.

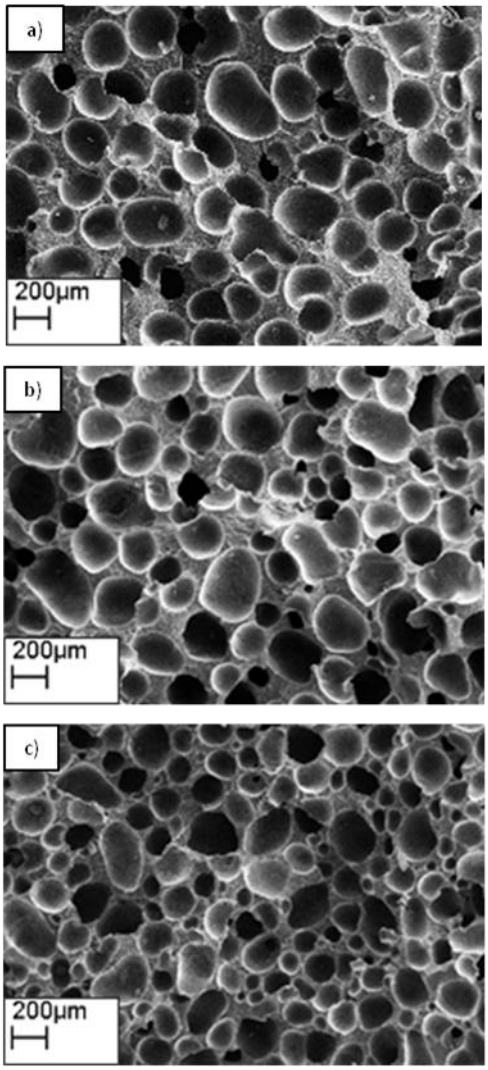


**Figure 8.5:** SEM images of foams extruded with the 7 *mm* strand die at BA masterbatch contents of (a) 2.5, (b) 5 and (c) 7.5 *wt%*, respectively

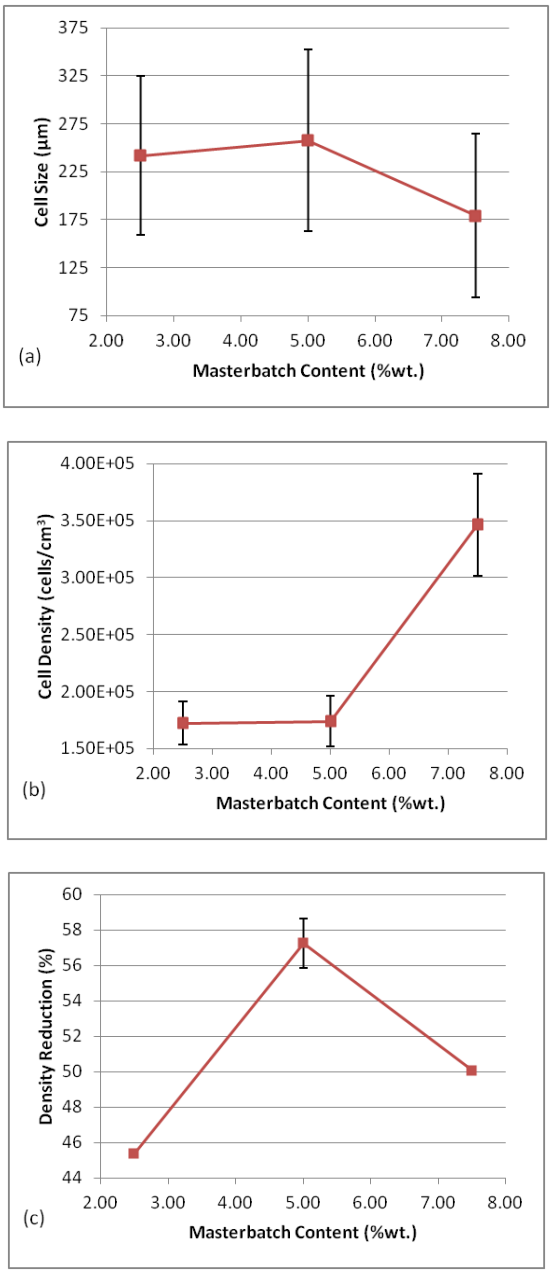


**Figure 8.6:** Effect of the amount of blowing agent on (a) cell size, (b) cell density population and (c) density reduction for foams extruded with the 7 *mm* strand die

Calcium carbonate particles were expected to act as nucleation sites and also enhance viscosity of the material for cell stabilisation. Figure 8.7 shows the foam morphologies corresponding to 5, 12 and 20 *wt%* calcium carbonate loading and Figure 8.8 presents cell size, cell density population and density reduction, respectively.

Increase in the calcium carbonate loading from 5 to 12 *wt%* reduced average cell size from 150 to about 100 *µm* (Figure 8.7a & b and Figure 8.8a) but no further change is

observed when the loading is increased to 20 *wt%* (Figure 8.7b & c and Figure 8.8a). In contrast, the cell density population increased with the loading of the calcium carbonate and reached the maximum at about 12 *wt%* and then dropped at 20 *wt%* as shown in Figure 8.8(b). The density reductions achieved (based on densities of the $CaCO_3$ filled PHBV) similar level to the unfilled PHBV (Figure 8.8c) for the range of $CaCO_3$ loadings but achieved much finer cell structure (comparing Figure 8.7 with Figure 8.5 or Figure 8.8a with Figure 8.6a). The decrease of cell size and increase of cell density population could be explained by the enhancement of heterogeneous nucleation by the $CaCO_3$ particles whereas the reduction of cell density population at high loading may be attributed to insufficient dispersion of $CaCO_3$ agglomerates.

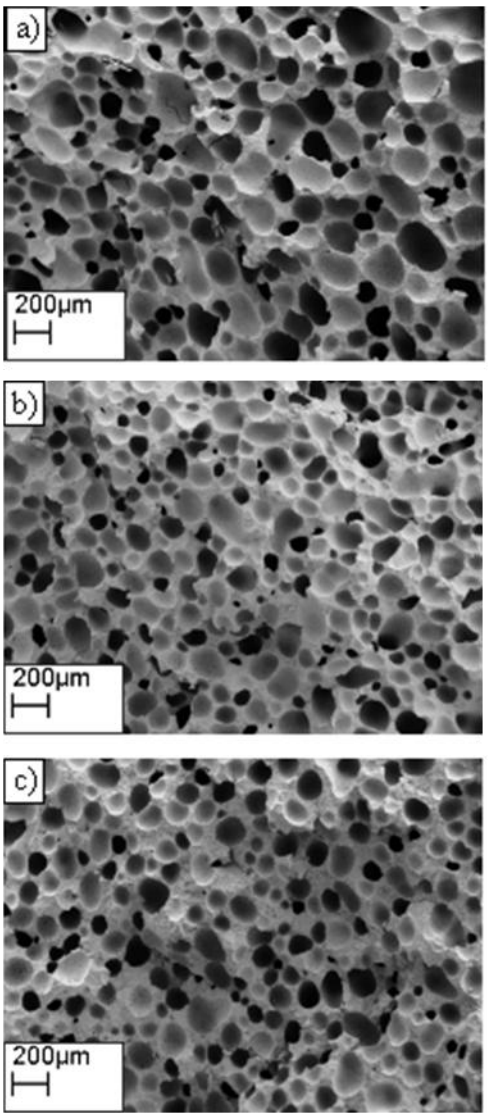


**Figure 8.7:** SEM images of foams extruded with the 5 *mm* strand die using 5 *wt%* BA masterbatch and filled with (a) 5, (b) 12 and (c) 20 *wt%* of the calcium carbonate

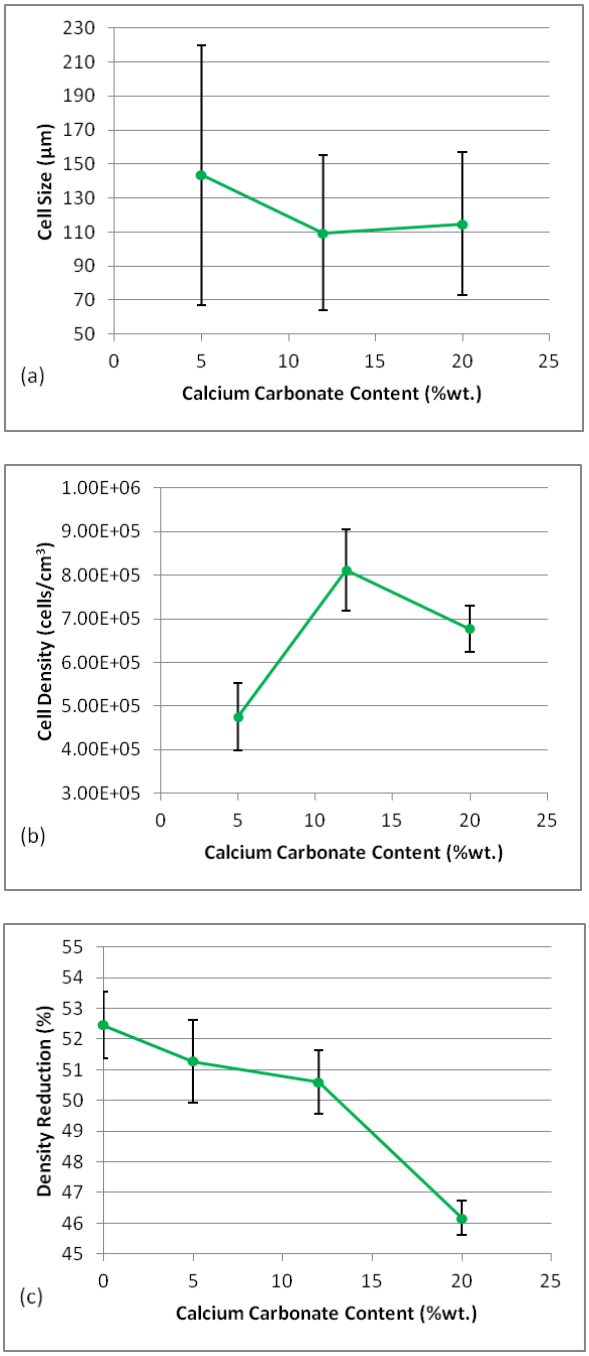


**Figure 8.8:** Effect of the amount of the calcium carbonate on (a) cell size, (b) cell density population and (c) density reduction for foams extruded with the 5 *mm* strand die

Further attempts were made to increase viscosity of the PHBV in order to increase the pressure drop at the die exit and enhanced melt strength to minimise cell rapture. This was achieved using higher degree of super cooling by reduction of temperature in the last zone of the extruder and the die to 140 °*C* (below the melting point of 168 °*C*). This

led to further expansion of the foams and achieved 57% density reduction using 5 *wt%* blow agent master batch and 20 *wt%* $CaCO_3$ loading. High level of super-cooling however can result in build-up of the material in the die as shown in Figure 8.9. This can be correlated to solidification of the melt under super-cooling conditions as shown earlier in Figure 4.10 (page 85). Rate of crystallization under super-cooling conditions is dependant on temperature. Temperature drop sharply across the narrow die channel and rapid crystallization could take place at the die surface, resulting in the build-up of a solidified polymer layer. The polymer was slowly accumulating from the wall to the centre and the rate of accumulation depended on temperature (degree of the super-cooling) and time under the super cooling conditions. The accumulation of the solid layer in the die can led to some changes in processing conditions (e.g. die pressure and flow characteristics) which led to the deterioration of foam quality and if not controlled, it was only possible to extrude quality foams for a limited time. Because this phenomenon took place at the narrow passages of the die, it seems to suggest that the stress induced crystallization may have also played a part (Mackley *et al*., 2000). Further work is thus necessary to identify the extent of the limitation and optimise the processing conditions.

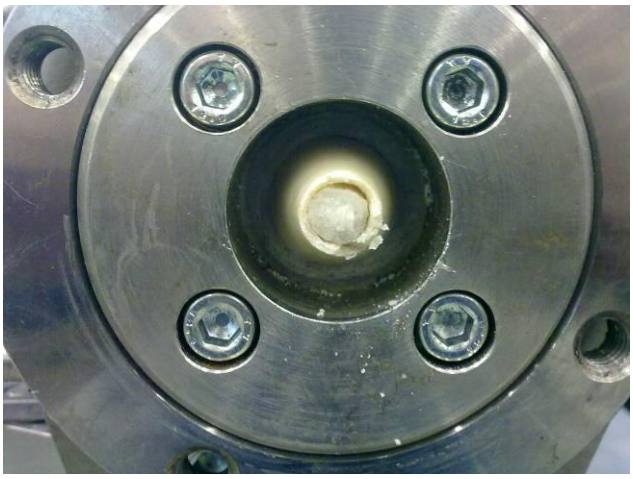

**Figure 8.9:** Die build-up associated with extrusion of the PHBV under super-cooled conditions. The outer layer is crystallized PHBV and the core is a purge polymer

## 8.3 Summary

Rheological behaviour of PHBV is sensitive to its thermal history and during extrusion foaming, it can experience both thermal degradation and hydrolytic degradations from a water-generating blowing agent.

PHBV foams with density reduction up to about 60% were extruded using negative temperature profile to super-cooling the polymer melt using a chemical blowing agent based on a sodium bicarbonate and citric acid. The temperature profile was chosen based on rheological characteristics of PHBV and experimental observations during extrusion foaming. The highest density reduction was obtained for extrusion with 5 *wt%* blowing agent masterbatch. Extruded foams were characterised by predominantly closed cell structure with cell sizes between about 100 to 250 $\mu m$.

For the selected blowing agent and relatively low L/D ratio extruder, it was shown that lower screw speed gave necessary residence time for the decomposition of the blowing agent and resulted higher expansion of the foams.

Moreover, the addition of calcium carbonate, while increasing overall density of the foams, resulted in much finer cell structure and decreased material costs. Super-cooling proved to be beneficial on two sides, viscosity increase and reduction of thermal degradation.

A drawback of such processing conditions was potential build-up of solidified polymer due to the crystallized material in the narrow channel of the die. Further refinement of processing conditions is necessary so as to remove premature crystallization and improve quality of the foams.

# Chapter 9

## Foaming of the PHBV/PBAT/$CaCO_3$ Composite in Final Formulation

Following work described in previous chapters, the final formulation of the PHBV based material is developed. This has resulted from systematic approaches to overcome the key drawbacks of the pure PHBV, namely slow crystallization rate, tensile strength, ductility, melt viscosity, thermal stability and high materials cost, by a combination of processing additives (nucleation agent, $CaCO_3$ filler, antioxidant agent and chain extender); and compounding with a biodegradable polymer as described earlier. The final formulation presented in Table 3.6 (page 68) has been chosen to achieve a balance of properties and procesibilities taking account of food safety regulations and cost of the final material.

The DSC thermogram of this compound presented the two peaks of the melting point at 124 (associated with that of the PBAT Ecoflex® F BX7011) and 172 *°C* (associated with that of the ENMAT$^{TM}$ Y1010) and the melt crystallization peak at 83 *°C*. The tensile test showed tensile strength of PHBV/PBAT/$CaCO_3$ composite at around 16 *MPa*, elongation at break at 18.1% and elastic modulus at 1.2 *GPa* (Project report M5).

The final formulation has been successfully extruded into high quality sheet as shown in Figure 9.1 on pilot scale extrusion lines at Brunel and Bangor Universities and thermoformed on laboratorial and industrial scale to produce a range of trays, as shown in Figure 9.2, for evaluation by the industrial partners.

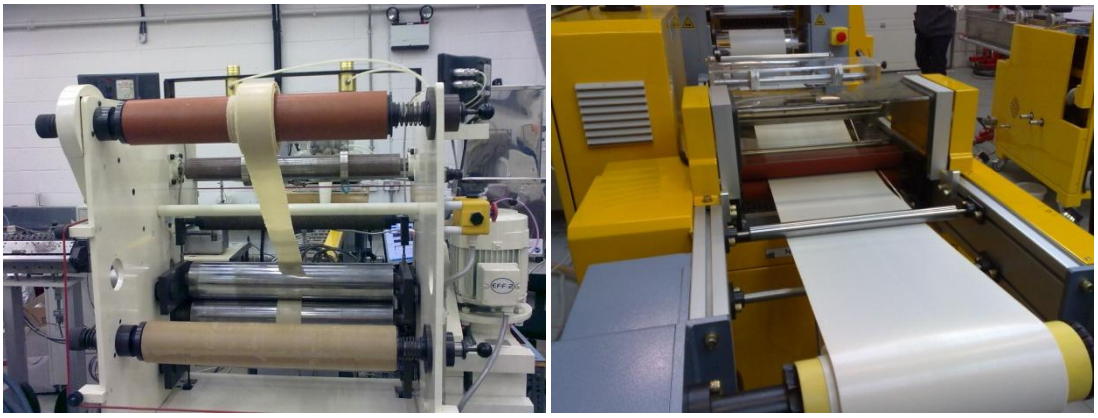

(a) (b)

**Figure 9.1:** Sheet extrusion (equipment + sheet) in (a) Brunel and (b) Bangor

(a) (b)

**Figure 9.2:** Examples of the thermal formed trays by (a) Brunel and (b) Sharp Interpack

In this chapter, foaming behaviour of the PHBV/PBAT/$CaCO_3$ composite is reported. Some key factors affecting extrusion foaming were studied individually but no attempt has been made to identify an optimised combination of them to achieve maximum density reduction for the PHBV/PBAT/$CaCO_3$ composite. The foaming behaviour of the PHBV/PBAT/$CaCO_3$ composite is compared with a commercial PHBV grade under identical foaming conditions to demonstrate potential of the material for sheet extrusion foaming.

Figure 9.3 shows the comparison of the density reduction between ENMAT$^{TM}$ Y1000P (the commercial PHBV grade) and the PHBV/PBAT/$CaCO_3$ composite (extrusion compounded at Wells Plastics). The comparison is made using a sheet die of 150 *mm* width and nip of 2 *mm*, 1.50 *wt%* active content of the Palmarole BA.F4.E. blowing

agent, screw speed of 80 *rpm* and feeding rate of 7.16 *kg/h* and temperature profile I in Table 3.7 (page 69). Details of other extrusion conditions are as described in 3.2.3.2 (page 68).

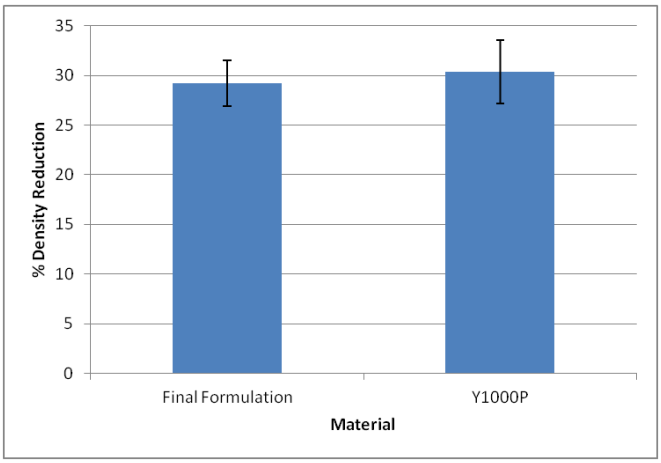


**Figure 9.3:** Comparison of density reduction of foams made from ENMAT$^{TM}$ Y1000P and the PHBV/PBAT/$CaCO_3$ composite under identical extrusion conditions

The result shows that the expandability of PHBV/PBAT/$CaCO_3$ composite is comparable to the commercial PHBV grade under the same extrusion foaming condition and, once optimum conditions are identified, can potentially be foamed to achieve similar low-density foams.

## 9.1 Effect of extrusion temperature on extrusion foaming

Effect of extrusion temperature on the PHBV/PBAT/$CaCO_3$ composite (compounded at Bangor University) was investigated using 1.50 *wt%* active content of the blowing agent (Palmarole BA.F4.E.), a sheet die as described earlier at screw speed of 80 *rpm* and feeding rate of 7.16 *kg/h*. Three temperature profiles were studied as shown in Table 3.7 (page 69). Foam morphologies at temperature profile (a) I, (b) II and (c) III are represented in Figure 9.4 while Figure 9.5 demonstrates the effect of extrusion temperature profiles on (a) cell size, (b) cell population density, (c) density reduction and (d) die pressure.

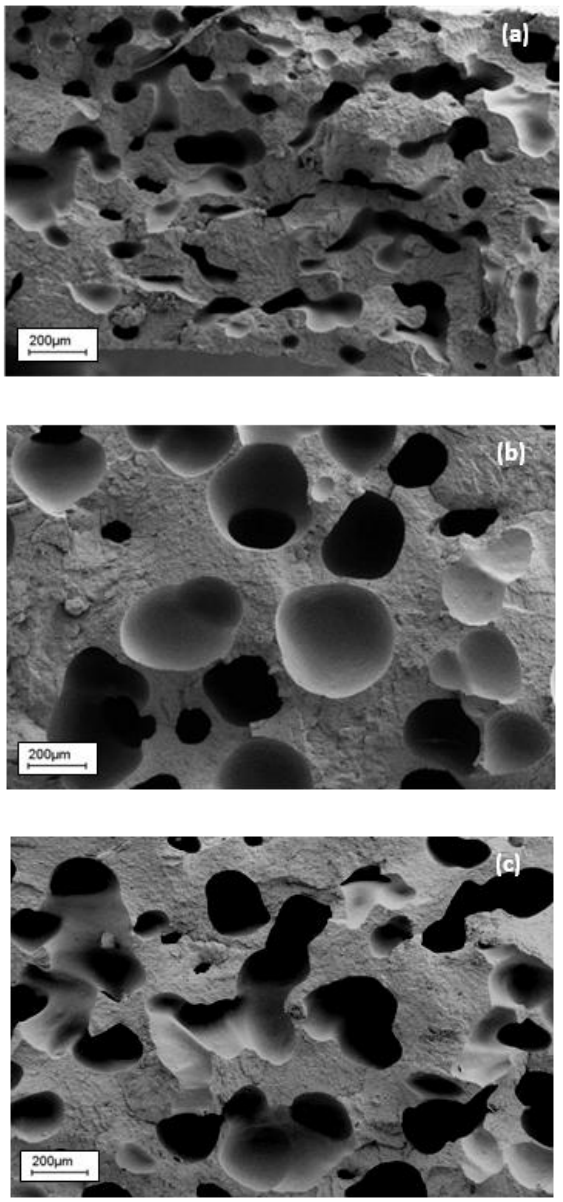


**Figure 9.4:** SEM images of foam extruded using temperature profiles (a) I, (b) II and (c) III (see Table 3.7, page 69, for details)

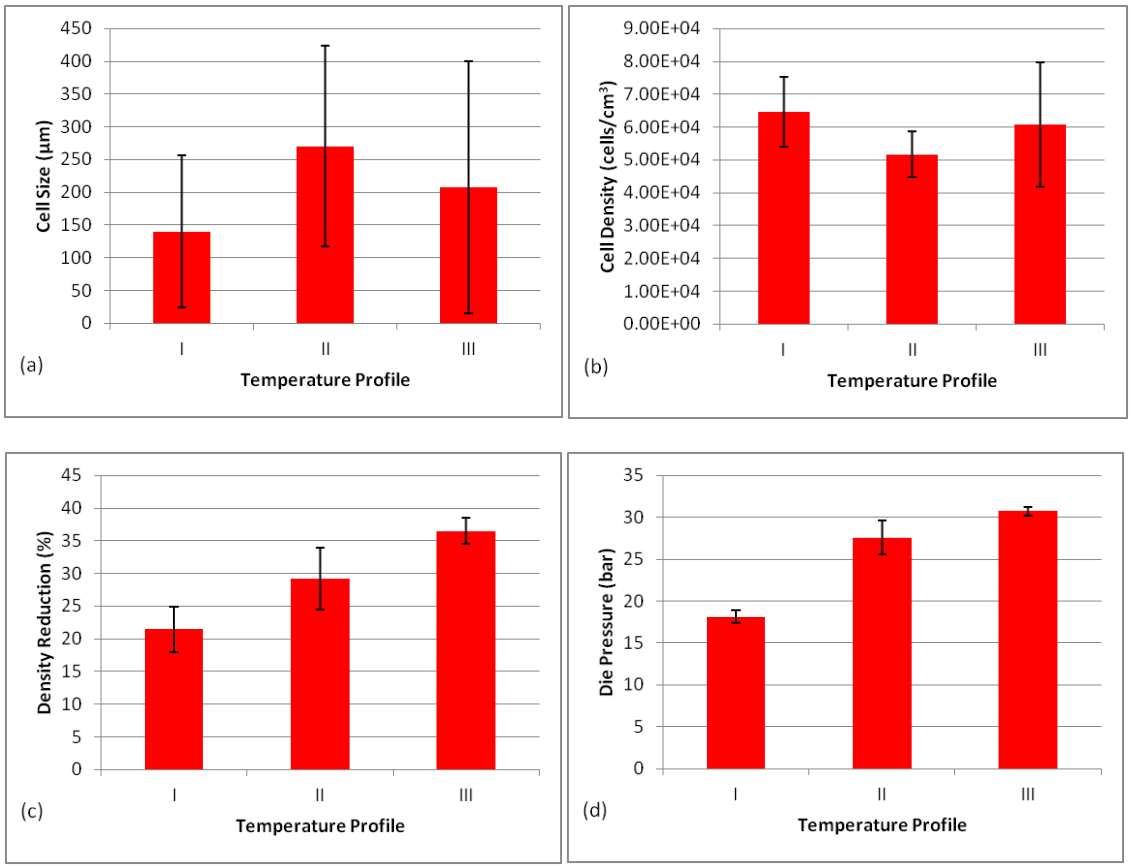


**Figure 9.5:** Effect of the extrusion temperature profiles (I, II and III in Table 3.7, page 69) on (a) cell size, (b) cell population density, (c) density reduction and (d) die pressure

From Figure 9.5c, the density reduction of the foamed PHBV/PBAT/$CaCO_3$ composite increased with gradient of the negative temperature profile. The temperature dropped more sharply in III, leading to higher melt viscosity (and melt strength) which helps to retain gas generated in the cells and prevent cell rupture (Lee *et al*., 2007d). Similarly, the rate of solidification of the polymer melt also affects stability of foam structure and its density reduction. The relatively higher melt temperature (and thus low melt strength) in profile I seem to have resulted in cell rupture (Figure 9.4a). The intermediate temperature profile II generated relatively larger cells (Figure 9.5a) and lower cell population density (Figure 9.5b). This may be attributed to cell coalescence to reduce the free energy as larger number of fine cells is thermodynamically less stable than smaller number of big cells (Saunders, 1991). The relatively lower melt temperature in profile III led to higher melt strength to prevent cell coalescence or rupture (and thus smaller cells and higher cell population density as shown in Figure 9.5

a & b) and more rapid solidification of the melt to stabilise the cell structure (Figure 9.4c), resulting in relatively higher density reduction.

Temperature profiles also affect the die pressure as shown in 9.5(d). The die pressure increased considerably with the reduction in melt temperature. Sharper pressure drop across the die is generally associated with finer cell structure as it favours higher cell population density (Park & Suh, 1996).

## 9.2 Effect of blowing agent concentration on extrusion foaming

Effect of the concentration of the blowing agent on extrusion foaming of the PHBV/PBAT/$CaCO_3$ composite (compounded at Bangor University) was investigated under temperature profile III (Table 3.7, page 69) using the sheet die described earlier at screw speed of 100 *rpm* and feeding rate of 7.16 *kg/h*. Four concentrations of the Palmarole BA.F4.E blowing agent were employed. The morphologies of the foams are presented in Figure 9.6 for active contents of the blow agent at (a) 1.00, (b) 1.50, (c) 2.00 and (d) 3.00 *wt%*. Figure 9.7 also shows the (a) cell size, (b) cell population density, (c) density reduction and (d) die pressure as functions of blowing agent content.

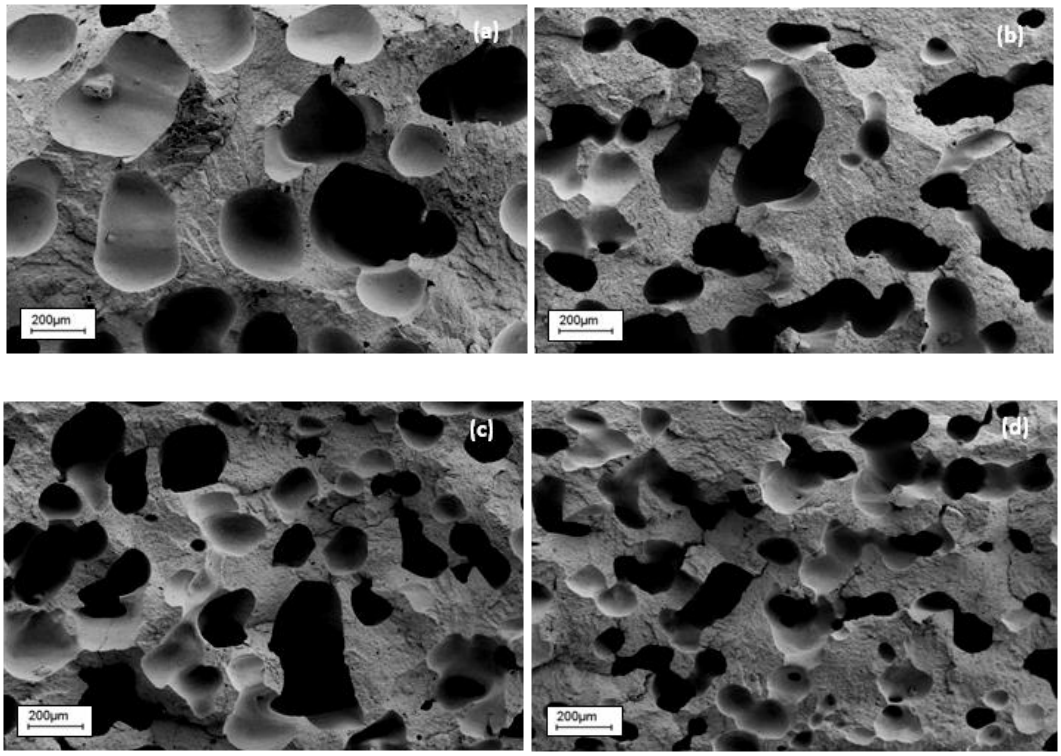


**Figure 9.6:** SEM images of foams extruded from the PHBV/PBAT/$CaCO_3$ composite at temperature profile III (Table 3.7, page 69) with screw speed of 100 *rpm*, feeding rate of 7.16 *kg/h* and various active contents of the blowing agent at: (a) 1.00, (b) 1.50, (c) 2.00 and (d) 3.00 *wt%*

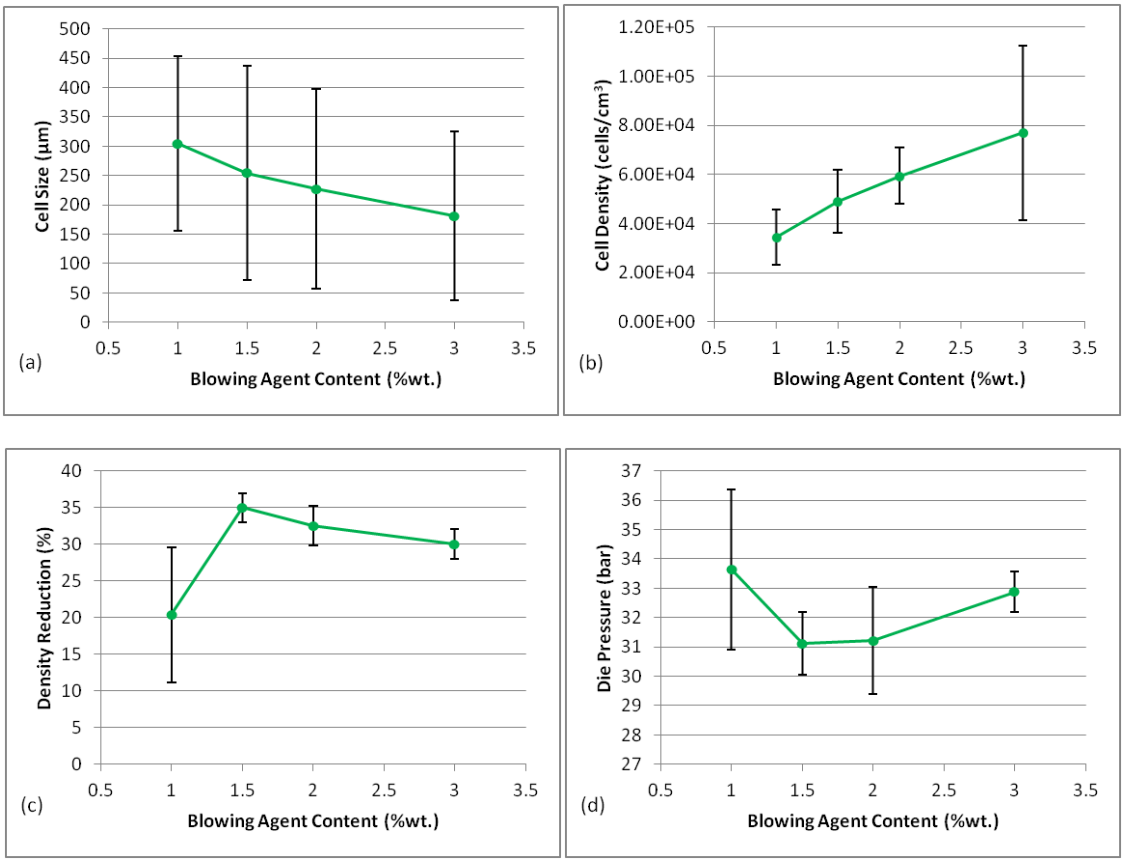


**Figure 9.7:** Effect of the blowing agent content on the foams extruded from the PHBV/PBAT/$CaCO_3$ composite: (a) cell size, (b) cell population density, (c) density reduction and (d) die pressure

The average cell size decreased (Figure 9.7a), and the cell population density increased (Figure 9.7b), with the increase in the blowing agent content, i.e., larger population density of finer cells were generated at higher blowing agent contents. This is because higher blowing agent concentration gave rise to greater driving force for bubble generation (Park & Cheung, 1997). When a polymer/gas mixture went through the die exit, the solubility of gas in the polymer dropped sharply as a result of drop in pressure and temperature, and the cell nucleation kicked off. With increasing concentration of gas dissolved in the polymer melt, it elevated thermodynamic instability and as a result, higher nucleating sites were generated. With the increased cell population density however, there would be less amount of gas per cell for the growth state (Pilla *et al.*, 2007). These two different trends in combination resulted in an initial increase in density reduction with increasing blowing agent content as shown in Figure 9.7c to reach a maximum at blowing agent content of about 1.50 *wt %*. This is then followed by

a plateau and no further gain in density reduction is achieved by increasing the blowing agent content.

Closer examination of Figure 9.6 reveals that there appear to be increasing level of cell merge or coalescence at higher blowing agent content. This may be related to plasticizing effect of the dissolved gas in the melt that reduces melt viscosity and strength (Naguib *et al*., 2002). Furthermore, PHBV is also known to be sensitive to hydrolytic degradation (Verhoogt *et al*., 1996; Cabedo *et al*., 2009) in presence of the water generated as a co-product of $CO_2$ by the blowing agent, which may also contribute to lowering melt viscosity and strength and thus the cell coalescence.

Unexpectedly, the die pressure at different blowing agent contents maintained at an almost constant level as shown in Figure 9.7d. This outcome may have resulted from the competition of pressure increase by higher gas generation from the higher blowing agent contents and pressure decrease due to the melt viscosity reduction mechanisms (plasticizing effect and hydrolytic degradation) mentioned above.

The further study was performed using rod die described in 3.2.3.2 (page 68) to investigate the effect of die configuration on foaming behavior. The PHBV/PBAT/$CaCO_3$ composite was extruded under identical condition using the temperatures III (Table 3.7, page 69), screw speed of 80 *rpm* and feeding rate of 7.16 *kg/h* and the active blowing agent content in the range of 1.0 to 3.0 *wt%*. The results are presented in Figure 9.8. It shows that density reduction continue to increase with increase of the blowing agent content and at the active blowing agent content of 3 *wt%*, a 47% density reduction is achieved. In contrast, the density reduction using the sheet die, as shown in Figure 9.7c declined after reaching a maximum and at the same blowing agent content only achieved at a 30%. This result suggested that there is scope to achieve further foam density reduction by design of die configuration.

Xu *et al*. (2003) studied the effects of die geometry on cell nucleation of polystyrene foams blown with $CO_2$. The pressure drop rate and the die pressure were shown to vary with different die geometry (diameter and length). However, the die pressure did not affect cell density but the pressure drop rate played an important role in cell density. The role of pressure drop rate in cell density was explained from point of view of

thermodynamic instability of the polymer/gas solution. The result suggested that the proper die design was required to achieve low density and fine cell foams.

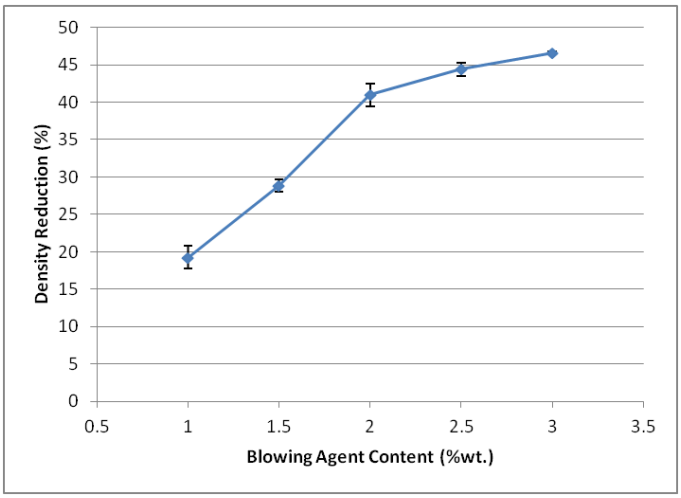


**Figure 9.8:** Effect of the blowing agent content on density reduction of the foams extruded with the rod die

### 9.3 Effect of screw speed on extrusion foaming

Effect of screw speed on extrusion foaming of the PHBV/PBAT/$CaCO_3$ composite (compounded at Bangor University) was investigated under temperature profile III (Table 3.7, page 69) with 1.50 *wt%* active content of the Palmarole BA.F4.E using the sheet die described earlier at feeding rate of 7.16 *kg/h*. The screw speed was varied from 60-100 *rpm* as screw speed below 60 *rpm* was found insufficient to generate foam. Foam morphologies produced at screw speed of (a) 60, (b) 80 and (c) 100 *rpm* are shown in Figure 9.9 and Figure 9.10 depicts the effect of screw speed on the (a) cell size, (b) cell population density, (c) density reduction and (d) die pressure.

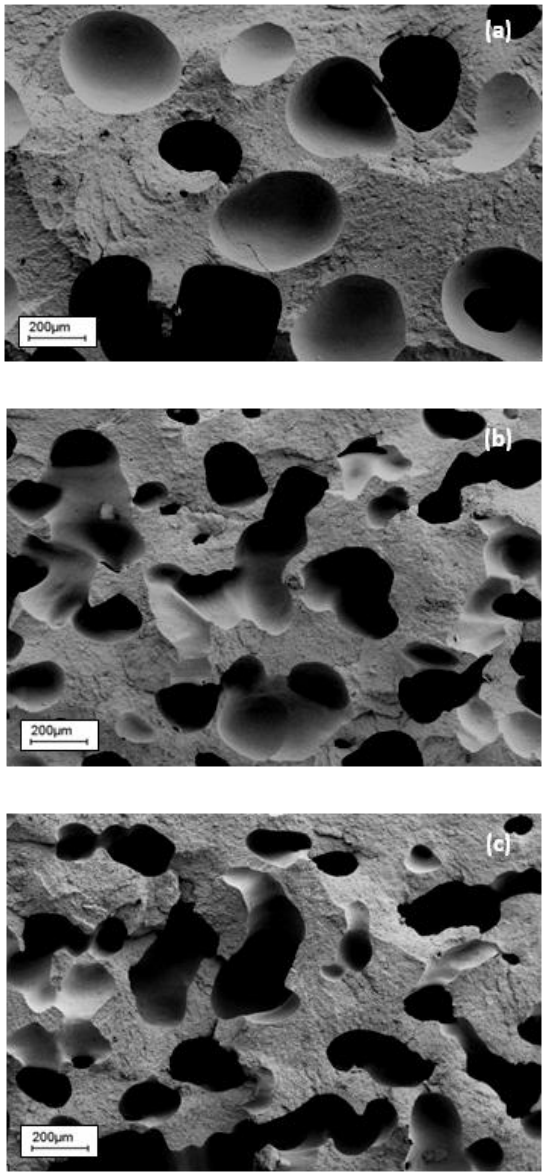


**Figure 9.9:** SEM images of foams extruded from the PHBV/PBAT/$CaCO_3$ composite at temperature profile III (Table 3.7, page 69) with 1.50 *wt%* active content of the Palmarole BA.F4.E., at feeding rate of 7.16 *kg/h* and various screw speeds: (a) 60, (b) 80, and (c) 100 *rpm*

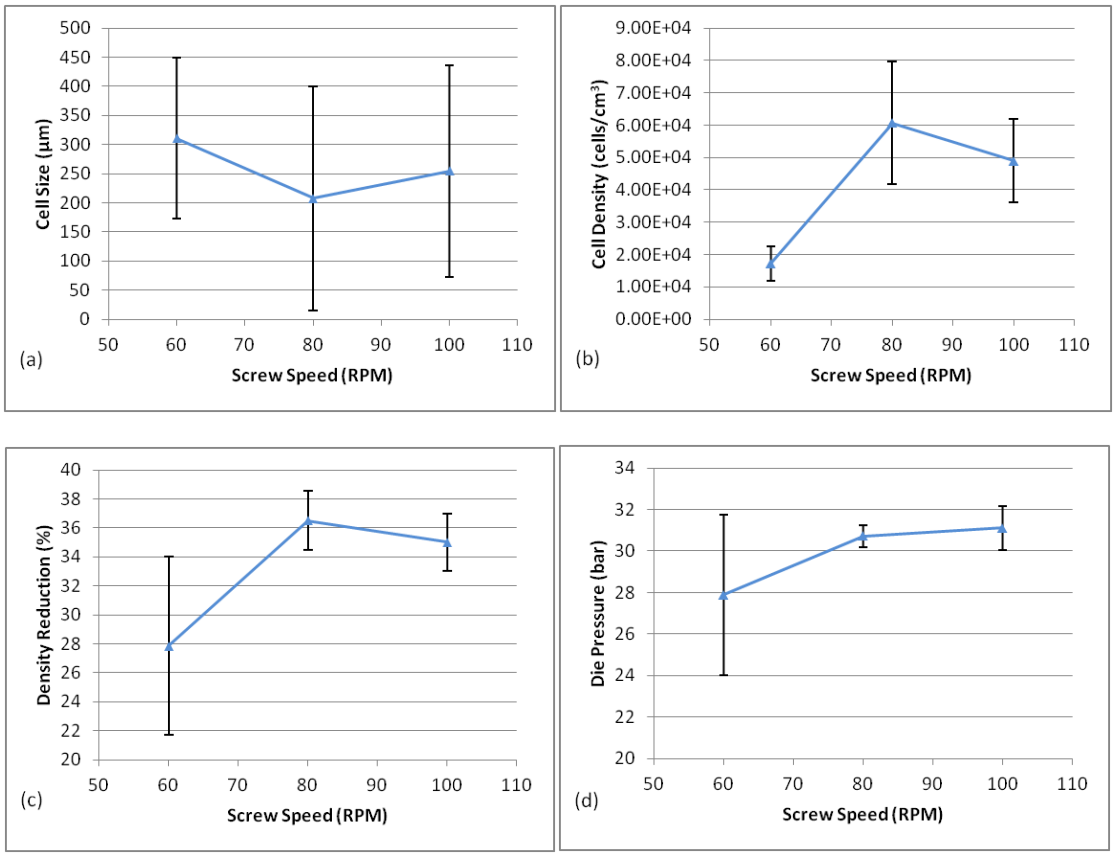


**Figure 9.10:** Effect of screw speed on the foams extruded from the PHBV/PBAT/$CaCO_3$ composite: (a) cell size, (b) cell population density, (c) density reduction and (d) die pressure

Figure 9.10c reveals that, under the other chosen conditions, there is an optimum screw speed at about 80 *rpm* to achieve a maximum in density reduction accompanied by fine cell size (Figure 9.10a) and a peak cell population density (Figure 9.10b). The die pressure increases, as expected, with increase in screw speed (Figure 9.10d).

At low screw speed and a constant feeding rate, the material may not be able to fill the extruder barrel properly giving chance for the gas to escape through the hopper. This leads to low amount of gas in the melt and thus bigger cell size with lower cell density population (Figure 9.9a). Also, the low material output generates less pressure drop at the die exit leading to lower expansion. On the other hand, high screw speed may give rise to insufficient residence time for effective decomposition of the blowing agent, leading to lower gas yield. The other possible reason is the decrease in melt viscosity of PHBV owning to the increase of shear rate, giving rise to the lower melt strength. This

in turn increases cell coalescence or rapture as evident from larger cell size and lower cell density population (Figure 9.9c) relative to that at the intermediate screw speed (Figure 9.9b).

### 9.4 Effect of material feeding rate on extrusion foaming

Effect of material feeding rate was investigated using the sheet die described earlier at fixed screw speed of 80 *rpm* under temperature profile III (Table 3.7, page 69) and 1.50 *wt%* active content of the Palmarole BA.F4.E. The use of feeding speed below 250 *rpm* was found insufficient for foaming and thus the higher feeding rates than this were studied. Figured 9.11 represents the morphologies of the foams using feeding rate (a) 5.18 *kg/h* (corresponding to feeding speed of 250 *rpm*), (b) 7.16 *kg/h* (feeding speed of 350 *rpm*), and (c) 9.16 *kg/h* (feed speed of 450 *rpm*). Figure 9.12 also presents the effect of the feeding rate on (a) cell size, (b) cell population density, (c) density reduction and (d) die pressure.

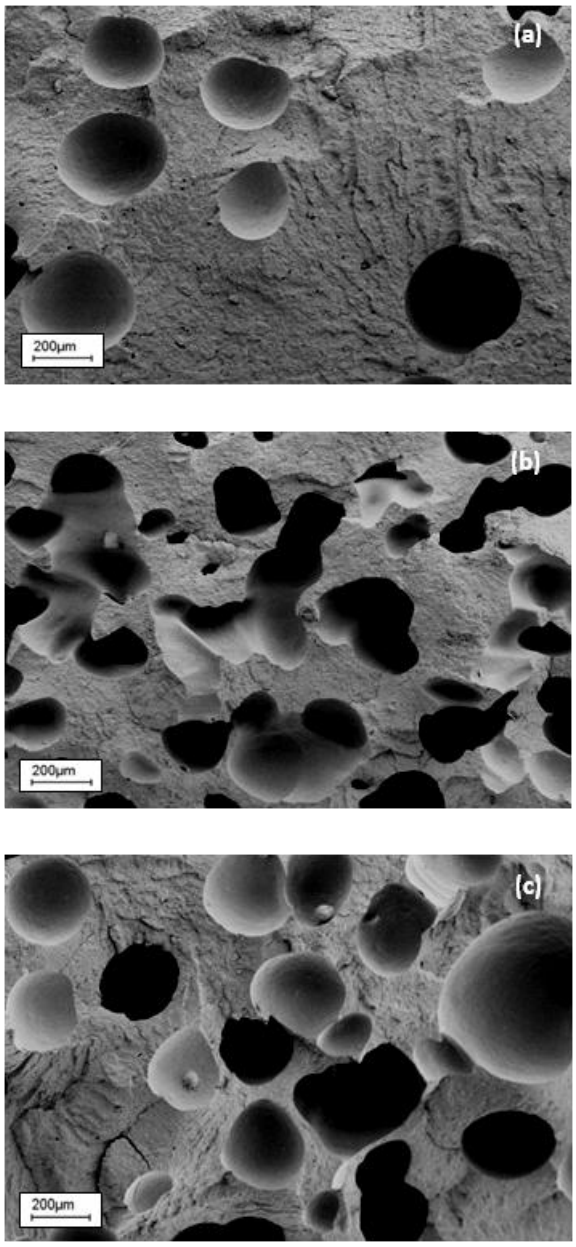


**Figure 9.11:** SEM images of foams extruded from the PHBV/PBAT/$CaCO_3$ composite at temperature profile III (Table 3.7, page 69) with 1.50 *wt%* active content of the blowing agent at screw speed of 80 *rpm* and various feeding rate: (a) 5.18, (b) 7.16, and (c) 9.15 *kg/h*

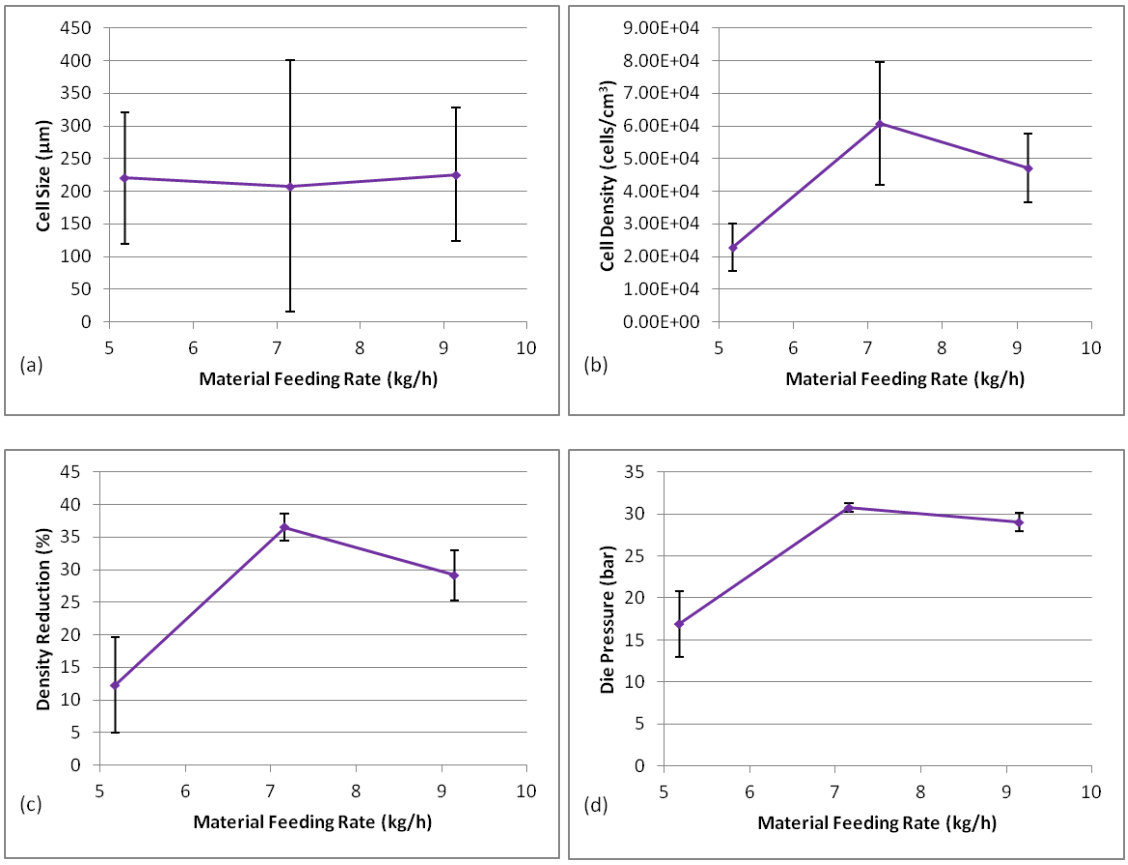


**Figure 9.12:** Effect of the material feeding rate on the foams extruded from the PHBV/PBAT/$CaCO_3$ composite: (a) cell size, (b) cell population density, (c) density reduction and (d) die pressure

The average cell size of PHBV compound foams does not show noticeable change at different feeding rates (Figure 9.12a) but cell density population increases with the feeding rate (Figure 9.12b) and gives rise to improved density reduction (Figure 9.12c). The intermediate feeding rate 7.16 *kg/h* (or feeding speed 350 rpm) results a maximum in cell density population and density reduction corresponding to a peak die pressure (Figure 9.12d).

It should be noted that the effect of material feeding rate should be considered in conjunction with that of the extrusion screw speed as together, they affect the degree of starve-feeding, the residence time and the pressure build-up which in turn affect the gas retention in the melt, the degree of blowing agent decomposition, and pressure drop at the die. When material was starve-fed, it was unable to seal the channels of the barrel which would allow gas to escape through the feeding hopper, leading to low amount of

bubbles (Figure 9.11a). The lack material conveyed to the die exit is reflected by the low die pressure (Figure 9.12d). In contrast, at high feeding rate, the material was excessive and could not go through the extruder at the fixed screw speed. Gas from blowing agent activated in the front barrel(s) could not be sealed off by the melt and would escape from the hopper, leading to lack of gas in the melt for foaming, as supported by the reduction of the cell density population and die pressure in Figure 9.12b and 9.12d.

## 9.5 Summary

The foaming behaviours of final formulation PHBV blend were reported. The variation in extrusion temperature, screw speed, feeding rate and blowing agent content affected on foaming behaviours and foam morphologies. The density reduction was the most important result in this study due to industrial purpose.

The density reduction was affected by the extrusion temperature. The increase of gradient of the negative temperature profile resulted in higher density reduction due to higher melt viscosity and faster solidification which prevented cell rupture and helped to stabilized foam structure.

The optimum screw speed in the chosen condition was found at *80 rpm*. The lower screw speed leads to improperly conveyed materials and resulted in unsealed system that allows gas to escape. However, the higher screw speed meant the blowing agent could not be efficiently activated because too short of residence time. The feeding rate which fitted to this screw speed was 7.16 *kg/h*.

The highest density reduction was obtained for extrusion with 1.50 *wt%* active content of the Palmarole BA.F4.E. The hydrolytic degradation followed by cell collapse restricted the further expansion at higher concentration.

The extrusion with sheet die achieved the maximum density reduction of 36.5% under selected extrusion foaming condition i.e. Temperature profile III (Table 3.7, page 69), 1.50 *wt%* active content of the Palmarole BA.F4.E., screw speed 80 *rpm* and material feeding rate 7.16 *kg/h*.

In addition, the study on die geometry demonstrated the possible way to improve quality of the foams. Changing die geometry from sheet to rod die with 3 *wt%* active content of blowing agent led to further expansion of the foams and resulted in the maximum density reduction at 46.6%.

To optimize quality of the foams, fine tuning of processing conditions (i.e. screw speed, die temperature, barrel temperature, kind and amount of blowing agent) and design of die configuration are necessary.

# Chapter 10
# Conclusions and Suggestions for Future Work

## 10.1 Conclusions

As part of a collaborative research project funded by Department of Environment, Food and Rural Affairs (DEFRA) of the UK Government, this project aimed at development of novel biodegradable and lightweight materials for high performance food packaging. Specific objectives of this work were:

i) Develop formulation of biodegradable materials for required properties and processibilities;

ii) Understand effects of processing additives and conditions on the materials and identify processing windows in sheet extrusion & thermal forming, and extrusion foaming;

iii) Evaluation of the materials in manufacturing and applications.

PHBV was identified as the key candidate and the basis for the material development following a screening study based on its outstanding gas barrier and overall good mechanical properties and biodegradability in aerobic composting, anaerobic digestion and marine environments as well as commercial availability. Sheet extrusion and thermoforming were identified as the main processing routes as required by the industrial manufacturer and end user and extrusion foaming using chemical blowing agent and low-cost inorganic fillers was chosen based on adaptability to the current production facilities as measures to minimise the material costs. The material development was then focused on methods to overcome the key drawbacks of PHBV (low crystallisation rate, low melt viscosity and melt strength and low thermal stability) in order to develop a PHBV based material system with a good balance of performances and processibilities without compromising cost or food safety. These include 1) inclusion of nucleation additive and antioxidant; 2) compounding with other biopolymers; 3) addition of inorganic fillers; 4) use of chain extender and 5) extrusion foaming of the PHBV based systems.

The material cost reduction was achieved by adding low-cost filler and reduction of density by foaming. The thermal instability was enhanced by incorporation of chain extender and blending with a high thermal stability biopolymer. The polymer blend also improved the ductility. Adding nucleation agent enhanced the crystallization rate to reduce stickiness of extruded sheet. The final formulation was successfully extruded into high quality sheet and thermoformed to produce prototype trays in an industrial scale trial.

The main outcomes of the investigations are summarized below:

1. PHBV is very sensitive to thermal history and repeated exposure to heat results in significant thermal degradation. This leads to lower crystallization rate, melt viscosity reduction and poorer thermal stability and in some cases, render the material unprocessible or unusable. Therefore the minimum thermal exposure of PHBV should be avoided by combining the various steps (additive compounding sheet extrusion and thermal forming) whenever possible.

2. The properties of PHBV (mechanical, crystallization rate and thermal stabilities) can be modified by adding processing additives (BN nucleation agent and antioxidant), blending with bioplastics with good ductility and thermal stability (e.g. PBAT), inorganic fillers (e.g. $CaCO_3$) and incorporating chain extenders (e.g. Joncryl).

    - Addition of BN significantly improved the crystallization rate of PHBV whereas additional thermal exposure in extrusion retarded the crystallization and also reduces melt strength and thermal stability. Use of nucleation agent such as BN and the avoidance of repeated thermal exposure are important in control of solidification and minimise thermal degradation of PHBV.

    - Introducing PBAT in to PHBV significantly reduces brittleness and improves complex viscosity and thermal stability of PHBV. However, PBAT was also found to delay crystallization of PHBV and thus appropriate concentration of PBAT should be chosen. 40-50 *wt%* was found acceptable.

    - The addition of $CaCO_3$ results in lower thermal stability of PHBV. However it speeds up the crystallization rate, increases complex viscosity and improves

mechanical properties. It also plays an important role in cost reduction of the materials and thus the inclusion at about 20 *wt%* is overall beneficial.

- Inclusion of the chain extender, Joncryl improves thermal stability and complex viscosity of PHBV and hence enhances the ability of PHBV in melt processing (sheet extrusion, thermoforming or extrusion foaming). But it results in slower crystallization of PHBV and hence care should be taken during the solidification of the melt to avoid sagging. The addition of Joncryl in this study was kept at low levels up to 1.0 *wt%* for food regulation considerations.

3. The commercial PHBV and the PHBV/PBAT/$CaCO_3$ composites developed in this work were successfully foamed using conventional twin-screw extrusion equipment and a sodium carbonate based blowing agent suitable for food contact packaging applications. The density reduction of the foams is dependent on the material formulations (additives), extrusion conditions (temperature profiles, screw speed and material feeding rate) and the blowing agent content. 61 and 47 % density reduction were achieved for the commercial PHBV and the modified PHBV respectively and there exist further scope for more expansion if multiple variable optimisation of the conditions are carried out.

    - The density reduction is affected by extrusion temperature profiles. The use of higher temperature gradient and negative temperature profiles results in highest density reduction owning mainly to lower thermal degradation and maintaining higher melt strength. Foaming of the materials under super cooling conditions can enhance melt strength and produce further expansion of the PHBV but care must be taken to avoid premature solidification at the die.

    - The screw speed affects the quality of the PHBV foam. The appropriate lower screw speed is necessary to allow sufficient activation of the blowing agent and enhance its efficiency to produce higher expansion. However, starve feed may occur when the speed is too low leading to unsealed material plug and escape of the gas.

- The material feeding rate should be considered together with the screw speed. it should be chosen so as to activate the blow agent, to avoid escape of gas and to generate sufficient pressure drop rate for maximum expansion.
- The blowing agent content plays an important role in density reduction of the foams. Generally, more gas is generated from higher blowing agent contents and higher driving forces for foaming. However water released from the blowing agent give rise in hydrolytic degradation of PHBV and leads to low melt strength and higher tendency of cell coalescence and/or collapse. As a result, there exists an optimum blowing agent content where density reduction peaks. This use found to be approximately 1.50 – 2.00 *wt%* active content under the foaming conditions studied.
- The addition of calcium carbonate, while increasing overall density of the material, was found beneficial to assist nucleation of cells and give rise to much finer cells in the foams and overall beneficial in foam structure control and reduction in material costs.
- The maximum (not optimized) density achieved for PHBV foams is 61.3% using 2.00 *wt%* active content of the Palmarole BA.F4.E, a 7 *mm* circular die, screw speed to 20 *rpm* with material feeding rate to 2.2 *kg/h* and a negative temperature profile with the materials super cooled to 140 *°C* at the die.
- The maximum (not optimized) density reduction of the PHBV/PBAT/$CaCO_3$ foams was 46.6% extrusion foamed using a high temperature gradient profile, 1.50 *wt%* active content of the blowing agent at screw speed of 80 rpm and material feeding rate of 7.16 *kg/h*.

## 10.2 Suggestions for future work

Some suggestions and remarks for further researches in the future are made as follows:

1. The commercial PHBV which contains low content of 3HV content is brittle, sensitive to thermal degradation resulting in low melt strength and thus difficult to be extrusion foamed. It is believed that PHBV with higher 3HV content which provides less crystallinity, high ductility and allows lower processing temperature

will give better control in foaming. The other medium-chain-length PHAs such as polyhydroxyhexanoate (PHH) or polyhydroxyoctanoate (PHO) are also possible to foam by extrusion process because they were claimed as thermoplastic elastomer with better elongation.

2. Modification of tooling, especially the die geometry is required optimize the pressure drop rate so as to achieve higher expansion and refined cells in extrusion foaming. Unlike for solid sheet extrusion, the pressure drop rate is vital to cell structure evolution and can be optimized by design of dimensions and shape of die cavity and the connection channel from extruder (Xu *et al*., 2003; Choudhary & Kilkami, 2008).

3. In this study, materials including the blowing agent are pre-mixed before feeding into the extruder. Gas may be generated prematurely and escaped from the hopper. This can be improved by sequential feeding using the downstream feeding ports.

4. This study did not attempt to optimize the multivariable extrusion foaming conditions for maximum density reduction but focused on understanding of the effect of individual variables under a chosen condition. It is believed that multivariable optimization of these conditions is desirable to achieve further density reduction beyond what have been achieved here.

# References

## A

**Abreu, D.A.P. de, Losada, P.P., Angulo, I. and Cruz, J.M.** (2007) Development of new polyolefin films with nanoclays for application in food packaging. Eur. Polym. J. **43**, 2229-2243.

**Ajioka, M., Enomoto, K., Yamaguchi, A., Suzuki, K., Watanabe, T. and Kitahara, Y.** (1995) Degradable foam and use of same. US Patent 5,447,962.

**Al-Itry, R., Lamnawar, K. and Maazouz, A.** (2012) Improvement of thermal stability, rheological and mechanical properties of PLA, PBAT and their blends by reactive extrusion with functionalized epoxy. Polym. Degrad. Stab. **97**, 1898-1914.

**An, Y., Li, L., Dong, L., Mo, Z. and Feng, Z.** (1999) Nonisothermal crystallization and melting behavior of poly(β-hydroxybutyrate)–Poly(vinyl-acetate) blends. J. Polym. Sci. Polym. Phys. Ed. **37**, 443-450.

**Asrar, J. and Hill, J.C.** (2002) Biosynthesic processes for linear polymers. J. App. Polym. Sci. **83**, 457-483.

**Auras, R., Harte, B. and Selke, S.** (2004) An overview of polylactides as packaging materials. Macromol. Biosci. **4**, 835–864.

**Auras, R.A., Singh, S.P. and Singh, J.J.** (2005) Evaluation of oriented poly(lactide) polymers vs existing PET and oriented PS for fresh food service containers. Packag. Technol. Sci. **18**, 207-216.

**Avella, M., Martuscelli, E., Orsello, G., Raimo, M. and Pascucci, B.** (1997) Poly(3-hydroxybutyrate)/poly(methyleneoxide) blends: thermal, crystallization and mechanical behaviour. Polymer. **38**, 6135-6143.

**Avella, M., Martuscelli, E. and Raimo, M.** (2000) Properties of blends and composites based on poly(3-hydroxy)butyrate (PHB) and poly(3-hydroxybutyrate-hydroxyvalerate) (PHBV) copolymers. J. Mater. Sci. **35**, 523-545.

**Avella, M., Bonadies, E., Martuscelli, E. and Rimedio, R.** (2001) European current standardization for plastic packaging recoverable through composting and biodegradation. Polym. Test. **20**, 517-521.

**Avérous, L., Fringrant, C. and Moro, L.** (2001) Starch-based biodegradable materials suitable for thermoforming packaging. Starch/Stärke. **53**, 368-371.

**Avrami, M.** (1939) Kinetics of phase change. I general theory. J. Chem. Phys. **7**, 1103-1112.

**Avrami, M.** (1940) Kinetics of phase change. II transformation-time relations for random distribution of nuclei. J. Chem. Phys. **8**, 212-224.

**Avrami, M.** (1941) Granulation, phase change and microstructure kinetics of phase change. III. J. Chem. Phys. **9**, 177-184.

**Azeredo, H.M.C. de** (2009) Nanocomposites for food packaging applications. Food res. Int. **42(9)**, 1240-1253.

**B**

**Banhart, J.** (1999) Foam metal: the recipe. Europhys. News. **30**, 17-20.

**Banyay, G.A., Shaltout, M.M., Tiwari, H. and Mehta, B.V.** (2007) Polymer and composite foam for hydrogen storage application. J. Mater. Proc. Technol. **191**, 102-105.

**Bastioli, C., Bellotti, V., Del Giudice, L., Lombi, R. and Rallis, A.** (1991) Expanded articles of biodegradable plastic materials and a method of their production. PCT Int. Appl. WO 91 02023.

**Bauer, H. and Owen, A.J.** (1988) Some structural and mechanical properties of bacterially produced poly-β-hydroxybutyrate-co-β-hydroxyvalerate. Colloid. Polym. Sci. **266**, 241-247.

**Belcher, J.N.** (2006) Industrial packaging developments for the global meat market. Meat Science. **74**, 143-148.

**Bikiaris, D.N. and Karayannidis, G.P.** (1998) Calorimetric study of diepoxide chain-extended poly(ethylene terephthalate). J. Therm. Anal. **54**, 721-729.

**Bluhm, T.L., Hamer, G.K., Marchessault, R.H., Fyfe, C.A. and Veregin, R.P.** (1986) Isodimorphism in bacterial poly(β-hydroxybutyrate-co-β-hydroxyvalerate). Macromolecules. **19**, 2871-2876.

**Bonizzoni, G. and Vassallo, E.** (2002) Plasma physics and technology: industrial applications. Vacuum. **64**, 327-336.

**Bordes, P., Pollet, E. and Avérous, L.** (2009) Nano-biocomposites: biodegradable polyester/nanoclay systems. Prog. Polym. Sci. **34**, 125-155.

**Briston, J.H.** (1994a) Blow moulding. In "Rigid and Semi-Rigid Plastic Containers", Longman scientific & technical, pp 61-72.

**Briston, J.H.** (1994b) Extrusion. In "Rigid and Semi-Rigid Plastic Containers", Longman scientific & technical, pp 43-46.

**Briston, J.H.** (1994c) Injection moulding. In "Rigid and Semi-Rigid Plastic Containers", Longman scientific & technical, pp 47-60.

**Brody, A.L.** (1997) Packaging of food. In "The Wiley Encyclopedia of Packaging Technology" (2nd ed.), John Wiley & Sons, pp 699-704.

**Bucci, D.Z., Tavares, L.B.B. and Sell, I.** (2005) PHB packaging for the storage of food products. Polym. Test. **24**, 564-571.

**Bucci, D.Z., Tavares, L.B.B. and Sell, I.** (2007) Biodegradation and physical evaluation of PHB packaging. Polym. Test. **26**, 908-915.

**Bureau, M.N.** (2005) The relationship between morphology and mechanical properties in thermoplastic foams. In "Thermoplastic Foam Processing: Principles and Development" (Gendron, R., ed.), CRC press, pp 235-281.

**Bureau, M.N. and Gendron, R.** (2003) Mechanical-morphology relationship of PS foams. J. Cell. Plas. **39**, 353-367.

**Buzarovska, A., Koseva, S., Cvetkovska, M. and Nedkov, E.** (2001) Poly(ethylene oxide) blends with poly(ethylene oxide)/poly(dicyclohexyl itaconate) block copolymers Eur. Polym. J. **37**, 141-149.

**Buzarovska, A. and Grozdanov, A.** (2009) Crystallization kinetics of poly(hydroxybutyrate-*co*-hydroxyvalerate) and poly(dicyclohexylitaconate) PHBV/PDCHI blends: thermal properties and hydrolytic degradation. J. Mater. Sci. **44**, 1844-1850.

**C**

**Cabedo, L., Feijoo, J.L., Villanueva, M.P., Lagarón, J.M. and Giménez, E.** (2006) Optimization of biodegradable nanocomposites based application on a PLA/PCL blends for food packaging application. Macromol. Symp. **233**, 191–197.

**Cabedo, L., Plackett, D., Gime´nez, E. and Lagaro J.M.** (2009) Studying the degradation of polyhydroxybutyrate-covalerate during processing with clay-based nanofillers. J. App. Polym. Sci. **112**, 3669–3676.

**Cava, D., Gimenez, E., Gavara, R. and Lagaron, J.M.** (2006) Comparative performance and barrier properties of biodegradable thermoplastics and nanobiocomposites versus PET for food packaging applications. J. Plast. Film. Sheet. **22**, 265-274.

**Cha, J.Y., Chung, D.S., Seib, P.A., Flores, R.A. and Hanna, M.A.** (2001) Physical properties of starch-based foams as affected by extrusion temperature and moisture content. Ind. Crop. Prod. **14**, 23-30.

**Chambi, H. and Grosso, C.** (2006) Edible films produced with gelatine and casein cross-linked with transglutaminase. Food Res. Int. **39**, 458-466.

**Chandra, A. and Rustgi, R.** (1998) Biodegradable polymer. Prp. Polym. Sci. **23**, 1273-1335.

**Chee, M.J.K., Ismail, J., Kummerlöwe, C. and Kammer, H.W.** (2002) Study on miscibility of PEO and PCL in blends with PHB by solution viscometry. Polymer. **43**, 1235-1239.

**Chen, G.Q.** (2010) Plastics completely synthesized by bacteria: polyhydroxyalkanoates. In "Plastics from Bacteria: Natural Functions and Applications, Microbiology Monographs" (Chen, G.Q. ed.), Vol. 14, Springer-Verlag Berlin Heidelberg, pp 17-37.

**Chen, Y., Yang, G. and Chen, Q.** (2002) Solid-state NMR study on the structure and mobility of the noncrystalline region of poly(3-hydroxybutyrate) and poly(3-hydroxy butyrate-co-3-hydroxyvalerate). Polymer. **43**, 2095-2099.

**Choi, J. and Lee, S.Y.** (2000) Economic considerations in the production of poly(3-hydroxybutyrate-co-3-hydroxyvalerate) by bacterial fermentation. Appl. Microbiol. Biotechnol. **53**, 646-649.

**Choudhary, M.K. and Kilkami, J.A.** (2008) Modeling of three-dimensional flow and heat transfer in polystyrene foam extrusion dies. Polym. Eng. Sci. **48**, 1177-1182.

**Clarimval, A.M. and Halleux, J.** (2005) Classification of biodegradable polymers. In "Biodegradable Polymers for Industrial Applications" (Smith, R., ed.), Woodhead Publishing, pp 3-31.

**Coles, R.** (2003) Introduction, in "Food Packaging Technology" (Coles, R., McDowell, D. and Kirwan, M.J., ed.), Blackwell Plublishing, pp 1-31.

**Coles, R.** (2011) Introduction, in "Food and Beverage Packaging Technology, Second Edition" (Coles, R. and Kirwan, M., ed.), Wiley-Blackwell, pp 1-29.

**Copinet, A., Bliard, C., Onteniente, J.P. and Couturier, Y.** (2001) Enzymatic degradation and deacetylation of native and acetylated starch-based extruded blends. Polym. Degrad. Stab. **71**, 203-212.

**Corre, Y. M., Duchet, J., Reignier, J. and Maazouz, A.** (2011) Melt strengthening of poly (lactic acid) through reactive extrusion with epoxy-functionalized chains. Rheol. Acta. **50**, 613-629.

**Cowell, N.D.** (1993) Storage, handling and packaging. In "Food Industries Manual 23rd Edition" (Ranken, M.D. and Kill, R.C., ed.), Chapman & Hall, pp 482-536.

**D**

**Davis, G. and Song, J.H.** (2006) Biodegradable packaging based on raw materials from crops and their impact on waste management. Ind. Crop. Prod. **23**, 147-161.

**DEFRA** (2009) Making the most of packaging - a strategy for a low-carbon economy. PB13189. London, UK: Department for Environment, Food and Rural Affairs.

**DEFRA** (2011) Applying the waste hierarchy: evidence summary. PB13529. London, UK: Department for Environment, Food and Rural Affairs.

**Dutta, P.K., Tripathi, S., Mehrotra, G.K. and Dutta, J.** (2009) Perspectives for chitosan based antimicrobial films in food applications. Food Chem. **114**, 1173-1182.

**E**

**Eaves, D.** (2004) Foam fundamentals. In "Handbook of Polymer Foams" (Eaves, D., ed.), Rapra Technology, pp 1-8.

**Edgar, K.J., Buchanan, C.M., Debenham, J.S., Rundquist, P.A., Brian, D.S., Shelton, M.C. and Tindall, D.** (2001) Advances in cellulose ester performance and application. Prog. Polym. Sci. **26**, 1605-1688.

**Eilert, S.J.** (2005) New packaging technologies for the 21st century. Meat Science. **71**, 122-127.

**El-Hadi, A., Schnabel, R., Straube, E., Müller, G. and Riemschneider, M.** (2002) Effect of melt processing on crystallization behavior and rheology of poly(3-hydroxybutyrate) (PHB) and its blends. Macromol. Mat. Eng. **287**, 363-372.

**El–Shafee, E., Saad, G.R. and Fahmy, S.M.** (2001) Miscibility, crystallization and phase structure of poly(3-hydroxybutyrate)/cellulose acetate butyrate blend. Eur. Polym. J. **37**, 2091–2104.

**Erceg, M., Kovačić, T. and Klarić, I.** (2005) Thermal degradation of poly(3-hydroxybutyrate) plasticized with acetyl tributyl citrate. Polym. Degrad. Stab. **90**, 313-318.

**F**

**Feigenbaum, A.E., Ducruet, V.J., Delpal, N., Wolff, N., Gabel, J.P. and Wittmann, J.C.** (1991) Food and packaging interactions: penetration of fatty food simulants into rigid poly(vinyl chloride). J. Agrig. Food Chem. **39**, 1927-1932.

**Flynn, J.H. and Wall, L.A.** (1966) General treatment of the thermogravimetry of polymers. J. Res. Natl. Bur. Stand. **70**, 487-523.

**Frisch, K.C. and Klempner, D.** (1991) Introduction. In "Handbook of Polymeric Foams and Foam Technology" (Klempner, D. and Frisch, K.C., ed.), Oxford University Press, pp 1-4.

**Fuminobu, H., Toshio, M. and Kenichi, S.** (2007) Foamed polyhydroxyalkanoate resin particles and method of producing the foamed particles. Eur. Pat. Appl. EP 1,870,431.

**G**

**Ganjyal, G.M., Weber, R. and Hanna, M.A.** (2007) Laboratory composting of extruded starch acetate and poly lactic blended foams. Bioresource Technol. **98**, 3176-3179.

**Gibson, L.J. and Ashby, M.F.** (1997) Cellular solids, Cambridge University Press, UK.

**Grassie, N., Murray, E.J. and Holmes, P.A.** (1984a) The thermal degradation of poly(-(d)-β-hydroxybutyric acid): part 1—identification and quantitative analysis of products. Polym. Degrad. Stab. **6**, 47-61.

**Grassie, N., Murray, E.J. and Holmes, P.A.** (1984b) The thermal degradation of poly(-(d)-β-hydroxybutyric acid): part 2—changes in molecular weight. Polym. Degrad. Stab. **6**, 95-103.

**Grassie, N., Murray, E.J. and Holmes, P.A.** (1984c) The thermal degradation of poly(-(d)-β-hydroxybutyric acid): part 3—the reaction mechanism. Polym. Degrad. Stab. **6**, 127-134.

**Gross, R.A. and Bhanu, K.** (2002) Biodegradable polymers for the environment. Science. **297**, 803-807.

**Guan, J., Eskridge, K.M. and Hanna, M.A.** (2005) Acetylated starch-polylactic acid loose-fill packaging materials. Ind. Crop. Prod. **22**, 109-123.

**Gunatillake, P.A. and Adhikari, R.** (2003) Biodegradable synthetic polymers for tissue engineering. Eur. Cell. Mater. **5**, 1-16.

**H**

**Hablot, E., Perrine, B. Pollet, E. and Averous, L.** (2008) Thermal and thermo-mechanical degradation of poly(3-hydroxybutyrate)-based multiphase systems. Polym. Degrad. Stab. **93**, 413-421.

**Ham-Pichavant, F., Sebe, G., Pardon, P. and Coma, V.** (2005) Fat resistance properties of chitosan-based paper packaging for food application. Carbohyd. Polym. **61**, 259-265.

**Harding, R.H.** (1973) Effects of cell geometry on foam performance. In "Plastic Foams Part II" (Frisch, K.C. and Saunders, J.H, ed.), Marcel Dekker, pp 831-854.

**Haugaard, V.K., Udsen, A.M., Mortensen, G., Høegh, L., Petersen, K., and Monahan, F.** (2000) Food biopackaging. In "Biobased Packaging Materials for the Food Industry Status and Perspectives" (Weber, C.J., ed.), KVL Department of Dairy and Food Science, pp 45-84.

**Hayter, A.C., Smith, A.C. and Richmond, P.** (1986) The physical properties of extruded food foams. J. Mater. Sci. **21(10)**, 3729–3736.

**Holmes, P.A.** (1985) Applications of PHB - a microbially produced biodegradable thermoplastic. Phys. Technol. **16**, 32–36.

**Hutchinson, R.J., Siodlak, G.D.E. and Smith, A.C.** (1987) Influence of processing variables on the mechanical properties of extruded maize. J. Mater. Sci. **22(11)**, 3956–3962.

**I**

**Imam, S., Glenn, G., Chiou, B.S., Shey, J., Narayan, R. and Orts, W.** (2008) State-of-the-art biobased food packaging materials. In "Environmentally Compatible Food Packaging" (Chiellini, E., ed.), Woodheaded Publishing, pp 29-62.

**J**

**Janigová, I., Lacík, I. and Chodák, I.** (2002) Thermal degradation of plasticized poly(3-hydroxybutyrate) investigated by DSC. Polym. Degrad. Stab. **77**, 35-41,

**Jin, T. and Zhang, H.** (2008) Biodegradable polylactic acid polymer with nisin for use in antimicrobial food packaging. J. Food. Sci. **73**, 127-134.

**Jonas, R. and Farah, L.F.** (1998) Production and application of microbial cellulose. Polym. Degrad. Stab. **59**, 101-106.

**K**

**Kai, W., He, Y., Asakawa. N. and Inoue, Y.** (2004) Effect of lignin particles as a nucleating agent on crystallization of poly(3-hydroxybutyrate). J. Appl. Polym. Sci. **94**, 2466-2474.

**Kai, W., He, Y. and Inoue, Y.** (2005) Fast crystallization of poly(3-hydroxybutyrate) and poly(3-hydroxybutyrate-co-3-hydroxyvalerate) with talc and boron nitride as nucleating agents. Polym. Int. **54**, 780-789.

**Kaito, A.** (2006) Unique orientation textures formed in miscible blends of poly(vinylidene fluoride) and poly[(R)-3-hydroxybutyrate]. Polymer. **47**, 3548-3556.

**Kale, G., Auras, R. and Singh, S.P.** (2006) Degradation of commercial biodegradable packages under real composting and ambient exposure conditions. J. Polym. Envi. **14**, 317–334.

**Kaseem, M., Hamad, K. and Deri, F.** (2012) Thermoplastic starch blends: a review of recent works. Polym. Sci. **54**, 165–176.

**Ke, T. and Sun, X.** (2001) Effect of moisture content and heat treatment on the physical properties of starch and poly(lactic acid) blends. J. Appl. Polym. Sci. **81**, 3069–3082.

**Khardenavis, A.A., Kumar, M.S., Mudliar, S.N. and Chakrabarti, T.** (2007) Biotechnological conversion of agro-industrial wastewaters into biodegradable plastic, poly β-hydroxybutyrate. Bioresource Technol. **98**, 3579-3584.

**Kirwan, M.J. and Strawbridge, J.W.** (2003) Plastics in food packaging. In "Food Packaging Technology" (Coles, R., McDowell, D. and Kirwan, M.J., ed.), Blackwell Plublishing, pp 174-240.

**Klauss, M. and Bidlingmaier, W.** (2003) Kassel project, available at: http://www.modellprojekt-kassel.de/eng/downloads/kassel-project_brochure.pdf

**Klauss, M. and Bidlingmaier, W.** (2004) Pilot scale field test for compostable packaging materials in the city of Kassel, Germany. Waste Management. **24**, 43-51.

**Koide, S.S.** (1998) Chitin–chitosan: properties, benefits and risks. Nutri. Res. **18**, 1091–1101.

**Kong, Y. and Hay, J.N.** (2002) Miscibility and crystallisation behaviour of poly(ethylene terephthalate)/polycarbonate blends. Polymer. **43**, 1805-1811.

**Koning, G.J.M. de and Lemstra, P.J.** (1993) Crystallization phenomena in bacterial poly[(R)-3-hydroxybutyrate]: 2. Embrittlement and rejuvenation. Polymer. **34**, 4089-4094.

**Kopinke, F. D., Remmler, M. and Mackenzie, K.** (1996) Thermal decomposition of biodegradable polyesters I: poly(β-hydroxybutyric acid). Polym. Degrad. Stab. **52**, 25-38.

**Krystynowicz, A., Koziolkiewicz, M., Wiktorowska-Jezierska, A., Bielecki, S., Klemenska, E., Masny, A. and Pluciennicza k, A.** (2005) Molecular basis of cellulose biosynthesis disappearance in submerged culture of *Acetobacter xylinum*. Acta Biochimica Polonica. **52**, 691-698.

**Kunioka, M., Tamaki, A. and Doi, Y.** (1989) Crystalline and thermal properties of bacterial copolyesters: poly(3-hydroxybutyrate-co-3-hydroxyvalerate) and poly(3-hydroxybutyrate-co-4-hydroxybutyrate). Macromolecules. **22**, 694-697.

**L**

**Lacourse, N.L. and Altieri, P.A.** (1989) Biodegradable packaging material and the method of preparation. U.S. Patent No. 4,863,655.

**Landrock, A.H.** (1995) Additives, fillers and reinforcements. In. “Handbook of Plastic Foams: Types, Properties, Manufacture and Applications” (Landrock, A.H., ed.), Noyes Publications, pp 278-315.

**Lee, S.Y.** (1996) Bacterial Polyhydroxyalkanoates. Biotechnol. Bioeng. **49**, 1-14.

**Lee, S.T.** (2009) History and trends of polymeric foams: from process/product to performance/regulation. In “Polymeric Foams: Technology and Developments in Regulation, Process, and Products” (Lee, S.T. and Scholz, D.P.K, ed.), CRC press, pp 1-40.

**Lee, S.T., Park, C.B. and Ramesh, N.S.** (2007a) Introduction to polymeric foams. In "Polymeric Foams: Science and Technology" (Lee, S.T., Park, C.B., and Ramesh, N.S., ed.), CRC press, pp 1-21.

**Lee, S.T., Park, C.B. and Ramesh, N.S.** (2007b) Thermodynamics and kinetics. In "Polymeric Foams: Science and Technology" (Lee, S.T., Park, C.B., and Ramesh, N.S., ed.), CRC press, pp 23-40.

**Lee, S.T., Park, C.B. and Ramesh, N.S.** (2007c) General foam processing technologies. In "Polymeric Foams: Science and Technology" (Lee, S.T., Park, C.B., and Ramesh, N.S., ed.), CRC press, pp 73-92.

**Lee, S.T., Park, C.B. and Ramesh, N.S.** (2007d) Foaming fundamentals. In "Polymeric Foams: Science and Technology" (Lee, S.T., Park, C.B., and Ramesh, N.S., ed.), CRC press, pp 41-72.

**Lee, W.H., Loo, C.Y., Nomura, C.T. and Sudesh, K.** (2008) Biosynthesis of polyhydroxyalkanoate copolymers from mixtures of plant oils and 3-hydroxyvalerate precursors. Bioresource Technol. **99**, 6844-6851.

**Leung, S.N., Wong, A., Guo, Q., Park, C.B. and Zong, J.H.** (2009) Change in the critical nucleation radius and its impact on cell stability during polymeric foaming processes. Chem. Eng. Sci. **64**, 4899-4907.

**Liu, W.J., Yang, H.L., Wang, Z., Dong, L.S. and Liu, J.J.** (2002) Effect of nucleating agents on the crystallization of poly(3-hydroxybutyrate-co-3-hydroxyvalerate). J. Appl. Polym. Sci. **86**, 2145-2152.

**Liu, Q., Zhu, M., Wu, W. and Qin, Z.** (2009) Reducing the formation of six-membered ring ester during thermal degradation of biodegradable PHBV to enhance its thermal stability. Polym. Degrad. Stab. **94**, 18-24.

**Lorenzo, A.T., Arnal, M.L., Albuerne, J. and Muller, A.J.** (2007) DSC isothermal polymer crystallization kinetics measurements and the use of the Avrami equation to fit the data: Guidelines to avoid common problems. Polym. Test. **26**, 222-231.

**Lourdin, D., Del Valle, G. and Colonna, P.** (1995) Influence of amylose content on starch-films and foams. Carbohydr. Polym. **27**, 261–270.

**Luengo, G., Schmitt, F.J., Hill, R. and Israelachvili, J.** (1997) Thin film rheology and tribology of confined polymer melts: contrasts with bulk properties. Macromolecules. **30**, 2482-2494.

**M**

**Mackley, M.R., Moggridge, G.D. and Saquet, O.** (2000) Direct experimental evidence for flow induced fibrous polymer crystallisation occurring at a solid/melt interface. J. Mater. Sci. **35,** 5247-5253.

**Maekawa, M., Pearce, R., Marchessault, R.H., and Manley, R.S.J.** (1999) Miscibility and tensile properties of poly(*β*-hydroxybutyrate)-cellulose propionate blend. Polymer. **40**, 1501–1505.

**Matzinos, P., Bikiaris, D., Kokkou, S. and Panayiotou, C.** (2001) Processing and characterisation of LDPE/starch products. J. Appl. Polym. Sci. **79**, 2548-2557.

**Mihai, M., Huneault, M.A. and Favis, B.D.** (2010) Rheology and extrusion foaming of chain-branched poly(lactic lcid). Polym. Eng. Sci. **50**, 629-642.

**Mikos, A.G. and Temenoff, J.S.** (2000) Formation of highly porous biodegradable scaffolds for tissue engineering. J. Biotechnol. **3**, 1-6.

**Mills, N.J.** (2007) Introduction to polymer foam microstructure. In "Polymer Foams Handbook" (Mills, N.J., ed.), Elsevier, pp 1-18.

**Moore, G.F. and Saunders, S.M.** (1997) Advances in biodegradable polymers. Rapra Review Reports. **9(2)**, 1-31.

**Moosa, A.S.I. and Mills, N.J.** (1998) Analysis of bend tests on polystyrene bead foams. Polym. Test., **17**, 357-378.

**N**

**Naguib, H.E., Park, C.B., Panzer, U. and Reichelt, N.** (2002) Strategies for achieving ultra low-density polypropylene foams. Polym. Eng. Sci. **42**, 1481–1492.

**Nair, L.S. and Laurencin, C.T.** (2007) Biodegradable polymers as biomaterials. Prog. Polym. Sci. **32**, 762-798.

**Narayan, R.** (1994) Impact of governmental policies, regulations, and standards activities on an emerging biodegradable plastics industry. In "Biodegradable Plastics and Polymers" (Doi, Y. and Fukuda, K., ed.), Elsevier, pp 261-270.

**Narayan, R., and Pettigrew C.** (1999) ASTM Standardization News, December 1999.

**Nayak, P.L.** (1999) Biodegradble polymers: opportunities and challenges. Polymer Reviews. **39(3)**, 481-505.

**Neumann, P.E. and Seib, P.A.** (1993) Starch-based biodegradable packaging filler and method of preparing same. U.S. Patent No. 5,185,382.

**No, H.K., Meyers, S.P., Prinyawiwatkul, W. and Xu, Z.** (2007) Applications of chitosan for improvement of quality and shelf life of foods: a review. J. Food Sci., **72**, 87–100.

**O**

**Okamoto, K.** (2003) Microcellular Processing, Hanser, Munich, Germany.

**Organ, S.J. and Barham, P.J.** (1991) Nucleation, growth and morphology of poly(hydroxybutyrate) and its copolymers. J. Mater. Sci. **26**, 1368-1374.

**Ozawa, T.** (1965) A new method of analysing thermogravimetric data. Bull. Chem. Soc. Jpn. **38**, 1881-1889.

**P**

**Padareva, V., Djoumaliisky, S., Touleshkov, N. and Kirov, G.** (1998) Modification of blowing agent system based on sodium bicarbonate with activated natural zeolite. J. Mater. Sci. Lett. **17**, 107-109.

**Pandey, J.K., Reddy, K.R., Kumar, A.P. and Singh, R.P.** (2005) An overview on the degradability of polymer nanocomposites. Polym. Degrad. Stab. **88**, 234-250.

**Park, C.B. and Cheung, L.K.** (1997) A study of cell nucleation in the extrusion of polypropylene foams. Polym. Eng. Sci. **37**, 1-10.

**Park, C. B. and Suh, N. P.** (1996) Filamentary extrusion of microcellular polymers using a rapid decompressive element. Polym Eng. Sci. **36**, 34-48.

**Parra, D.F., Fusaro, J., Gaboardi, F. and Rosa, D.S.** (2006) Influence of poly (ethylene glycol) on the thermal, mechanical, morphological, physical–chemical and biodegradation properties of poly (3-hydroxybutyrate). Polym. Degrad. Stab. **91**, 1954-1959.

**Petersen, K., Nielsen, P.V., Bertelsen, G., Lawther, M., Olsen, M.B. and Nilssonk, N.H.** (1999) Potential of biobased materials for food packaging. Trends Food Sci. Tech. **10**, 52–68.

**Pijuan, M., Casas, C. and Baeza, J.A.** (2009) Polyhydroxyalkanoate synthesis using different carbon source by two enhanced biological phosphorus removal microbial communities. Process Biochem. **44**, 97-105.

**Pilla, S., Kramschuster, A., Gong, S., Chandra, A. and Turng, L-S.** (2007) Solid and microcellular polylactide-carbon nanotube nanocomposites. Int. Polym. Process. **XXII**, 418-428.

**PlasticEurope** (2011) Plastics - the Facts 2011- An analysis of European plastics production, demand and recovery for 2010, Brussels, Belgium. See http://www.plasticseurope.org/documents/document/20111107101127-final_pe_factsfigures_uk2011_lr_041111.pdf

**Poirier, Y., Nawrath, C. and Somerville, C.** (1995) Production of polyhydroxyalkanoates, a family of biodegradable plastics and elastomers, in bacteria and plants. Biotechnol. **13**, 142-150.

**Potente, H., Ernst, W. and Oblotzki, J.** (2006) Description of the foaming process during the extrusion of foams based on renewable resources. J. Cell. Plast. **42**, 241-253.

**Preechawong, D., Peesan, M., Supaphol, P. and Rujiravanit, R.** (2005) Preparation and characterization of starch/poly(L-lactic acid) hybrid foams. Carbohydr. Polym. **59**, 329-337.

**Project report M5**, Performance of novel packaging materials. Brunel University, Nextek, Imerys and Bangor University.

**Q**

**Qian, J., Zhu, L., Zhang, J. and Whitehouse, R.S.** (2007) Comparison of different nucleating agents on crystallization of poly(3-hydroxybutyrate-co-3-hydroxyvalerates). J. Polym. Sci. Polym. Phys. Ed. **45**, 1564-1577.

**Qiu, Z., Ikehara, T. and Nishi, T.** (2003) Poly(hydroxybutyrate)/poly(butylene succinate) blends: miscibility and nonisothermal crystallization. Polymer. **44**, 2503-2508.

**R**

**Ramsteiner, F., Fell, N. and Forster, S.** (2001) Testing the deformation behaviour of polymer foams. Polym. Test. **20**, 661-670.

**Rao, M.V.S. and Dweltz, N.E.** (1986) Influence of molecular weight on the ordered state in poly(ethylene terephthalate). J. Appl. Polym. Sci. **31**, 1239-1249.

**Ray, S.S. and Bousmina, M.** (2005) Biodegradable polymers and their layered silicate nanocomposites: In greening the 21$^{st}$ century materials world. Prog. Mater. Sci. **50**, 962-1079.

**Robertson, G.** (2008) State-of-the-art biobased food packaging materials. In "Environmentally compatible food packaging" (Chiellini, E., ed.), Woodheaded Publishing, pp 3-28.

**S**

**Sachetto, J.P., Silbiger J. and Lentz D.J.** (1991) Polymer base blend compositions containing destructurized starch. Eur. Pat. Appl. EP 409,781.

**Sakai, K., Hamada, N. and Watanabe, Y.** (1986) Degradation mechanism of poly(vinyl alcohol) by successive reactions of secondary alcohol oxidase and β-diketone hydrolase from Pseudomonas sp. Agr. Biol. Chem. Tokyo. **50**, 989-996.

**Salehizadeh, H. and Van Loosdrecht, M.C.M.** (2004) Production of polyhydroxylakanoates by mixed culture: recent trends and biotechnologicals importance. Biotechnol. Adv. **22**, 261-279.

**Sanchez-Garcia, M. D., Gimenez, E. and Lagaron, J. M.** (2008) Morphology and barrier properties of nanobiocomposites of poly(3-hydroxybutyrate) and layered silicates. J. Appl. Polym. Sci. **108**, 2787-2801.

**Sato, H., Nakamura, M., Padermshoke, A., Yamaguchi, H., Terauchi H. and Ekgasit, S.** (2004) Thermal behavior and molecular interaction of poly(3-hydroxybutyrate-co-3-hydroxyhexanoate) studied by Wide-Angle X-ray diffraction. Macromolecules. **37**, 3763-3769.

**Saunders, J.H.** (1991) Fundamentals of foam formation. In "Handbook of Polymeric Foams and Foam Technology" (Klempner, D. and Frisch, K.C., ed.), Oxford University Press, pp 5-15.

**Saunders, J.H. and Hansen, R.H.** (1972) The mechanism of foam formation. In "Plastic Foams Part I" (Frisch, K.C. and Saunders, J.H, ed.), Marcel Dekker, pp 23-108.

**Savenkova, L., Gercberga, Z., Nikolaeva, V., Dzene, A., Bibers, I. and Kalnin, M.** (2000) Mechanical properties and biodegradation characteristics of PHB-based films. Process Biochem. **35**, 573-579.

**Scandola, M., Ceccorulli, G., Pizzoli, M. and Gazzano, M.** (1992) Study of the crystal phase and crystallization rate of bacterial poly(3-hydroxybutyrate-*co*-3-hydroxyvalerate). Macromolecules. **25**, 1405-1410.

**Schneider, H.A.** (1985) The quantitative evaluation of TG-curves. Thermochim. Acta. **83**, 59-70.

**Scott, G.** (2000) Green polymers. Polym. Degrad. Stab. **68(1)**, 1-7.

**Serafim, L.S., Lemos, P.C, Torres, C., Reis, M.A.M. and Ramos, A.M.** (2008) The influence of process parameters on the characteristics of polyhydroxyalkanoates produced by mixed cultures. Macromol. Biosci. **8**, 355-366.

**Shah, A.A., Hasan, F., Hameed, A. and Ahmed, S.** (2008) Biological degradation of plastics: a comprehensive review. Biotechnol. Adv. **26**, 246-265.

**Shogren, R.** (1997) Water vapor permeability of biodegradable polymers. J. Environ. Polym. Degrad. **5**, 91-95.

**Shogren, R.L., Lawton, J.W. and Tiefenbacher, K.F.** (2002) Baked starch foams: Starch modifications and additives improve process parameters, structure and properties. Ind. Crop Prod. **16**, 69-79.

**Shutov, F.A.** (1991) Cellular structure and properties of foamed polymers. In "Handbook of Polymeric Foams and Foam Technology" (Klempner, D. and Frisch, K.C., ed.), Oxford University Press, pp 17-46.

**Simon, J., Muller, H.P., Kock, R. and Muller, V.** (1998) Thermoplastic and biodegradable polymers of cellulose. Polym. Degrad. Stab. **59**, 107-115.

**Singh, S.N.** (2004) Blowing agents. In "Handbook of Polymer Foams" (Eaves, D., ed.), Rapra Technology, pp 9-36.

**Siracusa, V.** (2012) Food packaging permeability behaviour: a report. Int. J. Polym. Sci. Article ID 302029, 11 pages.

**Siracusa, V., Rocculi, P., Romani, S. and Rosa, M.D.** (2008) Biodegradation polymer for food packaging: a review. Trends Food Sci. Technol. **19**, 634-643.

**Snell, K.D. and Peoples, O.P.** (2002) Polyhydroxyalkanoate polymers and their production in transgenic plants. Metab. Eng. **4**, 29-40.

**Song, J.H., Murphy, R.J., Narayan, R. and Davies, G.B.H.** (2009) Biodegradable and compostable alternatives to conventional plastics. Phil. Trans. R. Soc. B. **364**, 2127-2139.

**Song, J., Kay, M. and Coles, R.** (2011) Bioplastics. In "Food and Beverage Packaging Technology, Second Edition" (Coles, R. & Kirwan, M, ed.), Wiley-Blackwell, Oxford, UK, pp 295-319.

**Sorrentino, A., Gorrasi, G and Vittoria, V.** (2007) Potential perspectives of bio-nanocomposites for food packaging applications. Trends in Food Sci. Technol. **18**, 84–95.

**Sterzel, H.J.** (1995) Production of foamed polylactide injection moldings of high strength and rigidity. US Patent 5,422,053.

**Sudesh, K., Abe, H. and Doi, Y.** (2000) Synthesis, structure and properties of polyhydroxyalkanoates: biological polyester. Prog. Polym. Sci., **25**, 1503-1555.

**Sudesh, K., Loo, C.Y., Goh, L.K., Iwata, T. and Maeda, M.** (2007) The oil-absorbing property of polyhydroxyalkanoate films and its practical application: a refreshing new outlook for an old degrading material. Macromol. Biosci. **7**, 1199-1205.

**Suh, K.W. and Tusim, M.H.** (1997) Foam plastics. In "The Wiley Encyclopedia of Packaging Technology" (2nd ed.), John Wiley & Sons, pp 451-458.

**Suyatma, N.E., Copinet, A., Tighzert, L., and Coma, V.** (2004) Mechanical and barrier properties of biodegradable films made from chitosan and poly(lactic acid) blend. J. Polym. Environ. **12(1)**, 1–6.

**T**

**Tehrany, E.A., Fournier, F. and Desobry, S.** (2006) Simple method to calculate partition coefficient of migrant in food stimulant/polymer system. J. Food Eng. **77**, 135-139.

**Toshio, M., Fuminobu, H. and Kenichi, S.** (2008) Polyhydroxyalkanoate-based resin foam particle, molded article comprising the same, and process for producing the same. Eur. Pat. Appl. EP 1,873,195.

**Tripathi, S., Mehrotra, G.K. and Dutta, P.K.** (2009) Physicochemical and bioactivity of cross-linked chitosan-PVA film for food packaging applications. Biol. Macromol. **45**, 372-376.

**Tull, R.V., Fowler, P., Lawther, M. and Weber, C.J.** (2000) Properties of biobased packaging materials. In "Biobased Packaging Materials for the Food Industry Status and Perspectives" (Weber, C.J., ed.), KVL Department of Dairy and Food Science, pp 13-44.

**V**

**Vachon, C.** (2005) Research on alternative blowing agents. In "Thermoplastic Foam Processing: Principles and Development" (Gendron, R., ed.), CRC press, pp 143 -195.

**Verhoogt, H., Ramsay, B. A., Favis, B. D. and Ramsay, J. A.** (1996) The influence of thermal history on the properties of poly(3-hydroxybutyrate-*co*-12%-3-hydroxyvalerate). J. App. Polym. Sci. **61**, 87-96.

**Villalobos, M., Awojulu, A., Greeley, T., Turco, G. and Deeter, G.** (2006) Oligomeric chain extenders for economic reprocessing and recycling of condensation plastics. Energy. **31**, 3227-3234.

**Vroman, I. and Tighzert, L.** (2009) Biodegradable polymers. Materials. **2**, 307-344.

**W**

**Wang, T., Cheng, G., Ma, S., Cai, Z. and Zhang, L.** (2003) Crystallization behavior, mechanical properties, and environmental biodegradability of poly(beta-hydroxybutyrate)/cellulose acetate butyrate blends. J. Appl. Polym. Sci. **89**, 2116–2122.

**Wang, S., Song, C., Chen, G., Guo, T., Liu, J., Zhang, B. and Takeuchi, S.** (2005) Characteristics and biodegradation properties of poly(3-hydroxybutyrate-co-3-hydroxyvalerate)/organophilic montmorillonite (PHBV/OMMT) nanocomposite. Polym. Degrad. Stab. **87**, 69-76.

**Wang, S., Ma, P., Wang, R., Wang, S., Zhang, Y. and Zhang, Y.** (2008) Mechanical, thermal and degradation properties of poly(d,l-lactide)/poly(hydroxybutyrate-co-hydroxyvalerate)/poly(ethylene glycol) blend. Polym. Degrad. Stab. **93**, 1364-1369.

**Watts, F.** (1990) Materials for packaging. In "Finding Out about Packaging" (Watts, F., ed.), Hobsons Publishing, pp 16-26.

**Weber, C.J.** (2000) Introduction. In "Biobased Packaging Materials for the Food Industry Status and Perspectives" (Weber, C.J., ed.), KVL Department of Dairy and Food Science, pp 10-12.

**Wendlandt, W. W.** (1986) Thermal Analysis, John Wiley & Sons, New York, pp 19-57.

**Willett, J.L. and Shogren, R.L.** (2002) Processing and properties of extruded starch/polymer foams. Polymer. **43**, 5935–5947.

**WRAP**, (2008) Report: Domestic Mixed Plastics Packaging Waste Management Options.

**Wunderlich, B** (1976) Macromolecular Physics, Academic Press, New York.

**Wunderlich, B** (1977) Macromolecular Physics, Vol. 2, Academic Press, New York.

**X**

**Xu, X., Park, C.B., Xu D. and Pop-Ilieve, R.** (2003) Effect of die geometry on cell nucleation of PS foams blown with $CO_2$. Polym. Eng. Sci. **43**, 1378-1390.

**Xu, Y.X., Dzenis, Y. and Hanna, M.A.** (2005) Water solubility, thermal characteristics and biodegradability of extruded starch acetate foams. Ind. Crop. Prod. **21**, 361-368.

**Y**

**Yu, L., Dean, K. and Li, L.** (2006) Polymers blends and composites from renewable resources. Prog. Polym. Sci. **31**, 576-602.

**Z**

**Zhang, L., Deng, X. and Huang, Z.** (1997) Miscibility, thermal bahaviour and morphological structure of poly(3-hydroxybutyrate) and ethyl cellulose binary blends. Polymer. **38**, 5379–5387.

**Zhang, L.L., Goh, S.H., Lee, S.Y. and Hee, G.R.** (2000) Miscibility, melting and crystallization behaviour of two bacterial polyester/poly(epichlorohydrin-*co*-ethylene oxide) blend systems. Polymer. **41**, 1429-1439.

**Zhang, L., Tang, H., Hou, G., Shen, Y. and Deng, F.** (2007) The domain structure and mobility of semi-crystalline poly(3-hydroxybutyrate) and poly(3-hydroxybutyrate-co-3-hydroxyvalerate): a solid-state NMR study. Polymer. **48**, 2928-2938.

**Zhijiang, C., Chengwei, H. and Guang, Y.** (2011) Crystallization behavior, thermal property and biodegradation of poly(3-hydroxybutyrate)/poly(ethylene glycol) grafting copolymer. Polym. Degrad. Stab. **96**, 1602-1609.

**Zhong, W., Ge, J., Gu, Z., Li, W., Chen, X., Zang, Y. and Yang, Y.** (1999) Study on biodegradable polymer materials based on poly(lactic acid). I. chain extending of low molecular weight poly(lactic acid) with methylenediphenyl diisocyanate. J. Appl. Polym. Sci. **74**, 2546-2551.

**Zuchowska, D., Steller, R. and Meissner, W.** (1998) Structure and properties of degradable polyolefin-starch blends. Polym. Degrad. Stab. **60**, 471-480.

## Web References

Lotfi, Ahmad. "Plastic Recycling" available at: http://www.lotfi.net/recycle/plastic.html

# APPENDIX A

# THE EFFECT OF CHAIN EXTENDER ON POLY(3-HYDROXYBUTYRATE-*CO*-3-HYDROXYVALERATE): THERMAL DEGRADATION, CRYSTALLIZATION, AND RHEOLOGICAL BEHAVIOURS

Sitthi Duangphet, Damian Szegda, Jim Song*, Karnik Tarverdi

*Corresponding author: jim.song@brunel.ac.uk +44 (0)1895 266692

Wolfson Centre for Materials Processing, Brunel University, Uxbridge, Middlesex, UB8 3PH, UK

## Abstract

Poly(3-hydroxybutyrate-*co*-3-hydroxyvalerate) (PHBV), a semi-polycrystalline biopolymer from the polyhydroxyalkanonate (PHA) family has in recent years become a commercial bioplastic with mechanical properties comparable to isotactic polypropylene (iPP) and enhanced $O_2$, $CO_2$ and $H_2O$ barrier properties. However, its brittleness and sensitivity to thermal and hydrolysis degradations restrict its applications. To overcome the problems associated with degradation during processing blending of PHBV and an epoxy-functionalized chain extender (Joncryl® ADR-4368 S) was conducted in a twin screw extruder. The effect of concentration of the chain extender on thermal, crystallization and rheological behaviours of PHBV was investigated. Thermal gravimetric analysis (TGA) results indicated improvement in the resistance to thermal decomposition of PHBV by introducing the chain extender. This was accompanied with calculation of thermal degradation activation energy ($E_a$) using the Flyn-Walls-Ozawa method which confirmed increase of $E_a$ with the increase in content of the chain extender. The rheological behaviour and crystallization of modified PHBV was characterized by rotational rheometry and differential scanning calorimetry (DSC) techniques, respectively. The results show that addition of chain extender enhanced viscosity of PHBV and also reduce the rate of crystallization.

*Key Words*: PHBV, chain extender, thermal degradation, crystallization, rheology.

## Introduction

Poly(3-hydroxybutyrate) (PHB) and poly(3-hydroxybutyrate-co-3-hydroxyvalerate) (PHBV), are well-known bacterial polyesters from the polyhydroxyalkanoates (PHA) family.

They are synthesized by many bacteria so as to reserve carbon and energy source from various feedstocks such as sugars and plant oils under unbalanced growth conditions [1-4].

PHB presents physical and mechanical properties that are similar to those of low-density polyethylene (LDPE) and isotactic polypropylene (iPP) [5-7]. It provides better oxygen barrier than PP and PET and good resistance and barrier to moisture [8]. In addition, PHB also possesses good biocompatibility, biodegradability, and sensorial proprieties, making it a good candidate material for packaging, particularly for high barrier food packaging [9-11]. However, its inherent physical properties such as brittleness [12], and thermal instability [13] gave rise to difficulties in processing and application.

Many methods have been proposed to overcome these shortcomings, such as blending [14-16] and grafting [17, 18]. Copolymerization of PHB with other monomers is one of the most effective techniques, especially copolymerization of PHB with hydroxyvaleric acid to produce poly[(3-hydroxybutyrate)-co-(3-hydroxyvalerate)] (PHBV) resulting in a lower melting point and higher flexibility [19]. Use of chain extenders has been attempted to improve the poor thermal stability. The effect of dicumyl peroxide (DCP) on PHBV was studied by Haene et al. [20] and Fei et al. [21]. Haene et al. used low level of DCP to study branching and rheological behaviour of PHBV. The branching of PHBV was observed from the increase in strain hardening with addition of higher concentrations of DCP. Whereas Fei et al. studied the cross-linking of PHBV using high level of DCP. The cross-linked PHBV presented enhanced melt viscosity and mechanical properties without compromising the biodegradability.

An epoxy-functionalized chain extender (BASF Joncryl®) has been successfully applied to commercial petroleum-based polyesters such as poly(ethyleneterephthalate) (PET) [22, 23] and shown promising effects in biodegradable polyesters such as polylactic acid (PLA) [24-26]. The reaction between carboxylic end groups on polyesters and epoxide groups on chain extenders is the key reaction to improve molecular weight [22]. However, using of this chain extender on bacterial synthesized polyesters has been rarely studied.

In this study, an epoxy-functionalized chain extender (BASF Joncryl® ADR-4368) was employed. The reactive processing was carried out in a co-rotating twin screw extruder to investigate the effect of chain extender on crystallization, rheological and thermal degradation behaviours of PHBV.

## Experimental

### *Materials*

ENMAT™ Y1000P, a PHBV with 3 mol% hydroxyvalerate (HV) content was manufactured by Tianan Biologic Material Co. (Ningbo, P. R. China) in pellet form. The chain extender was Joncryl® ADR-4368 S, the epoxy-functionalized chain extender with high number average functionality ($f_n$ >4) and epoxy equivalent rate = 285 g/mol, obtained from BASF Germany in powder form. The general structure of the epoxy-functionalized chain extender is presented in Figure 1.

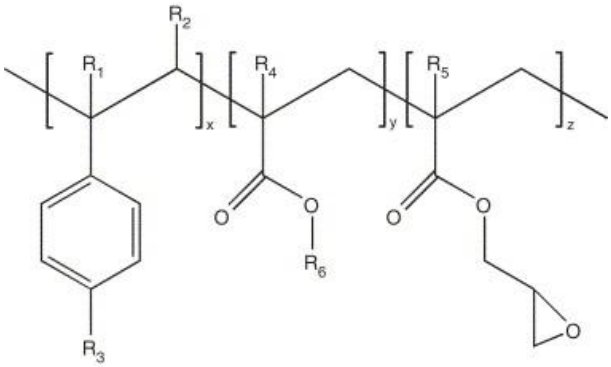


**Figure 1**. General structure of the epoxy-functionalized chain extenders. Where R1–R5 are H, CH3, a higher alkyl group, or combinations of them; R6 is an alkyl group, and x, y and z are each between 1 and 20. [25]

### *Extrusion Process*

PHBV was pre-dried in a vacuum oven for 120 min at 100 °C while the chain extender was used as received. Pellets of PHBV were tumble mixed with chain extender at various amounts up to 1.0 wt% (for cost reason and consideration of food contact safety - the US FDA Food Contact Notification 429 suggested a maximum level of 0.5 wt%) were compounded in the HAKKE Polylab twin screw extruder (Mess-Technic GmbH, Germany). The screw diameter was 24 mm and L/D ratio was 40. The extruder was fitted with a rod die with diameter of 6 mm. Temperature profile was flat 180°C across all zones. Screw speed was 100 rpm and a high mixing screw profile was used. The average residence time determined with pigment tracing was 8 min.

*Differential Scanning Calorimetry*

Differential scanning calorimetry (DSC) measurements (mass 9.5±0.5mg) were performed using a TA Instrument Q2000 DSC within nitrogen atmosphere (with a flow rate of 50 mL/min). The sample was first heated from -40 to 190 ºC and annealed for 3 min at190 ºC to erase thermal history. Then the sample was cooled to -40 ºC and kept isothermally at this temperature for 3 min. Finally the process was repeated. The ramp speed in all the heating and cooling processes was 10 ºC/min. To avoid thermal history influence, the non-isothermal thermograms of PHBV and its blends for melting process were chosen from the second cycle.

For isothermal crystallization, the sample was initially heated to 190 ºC and held for 3 min to eliminate thermal history. Then, the samples were cooled at a cooling rate of 50 ºC/min to the predetermined temperatures (120 to 140 ºC) and held at these constant temperatures until the crystallization process was complete.

*Rheological Characterization*

The extruded strands were ground using a Retsch SM 2000 cutting mill equipped with a sieve with 1.50 mm trapezoid apertures. Ground samples were dried for 120min at 100°C in a vacuum oven prior to the measurements.

A TA Instruments ARES rotational rheometer with two parallel plates (Φ = 25 mm) was used to determine the rheological properties of the samples. The measurements were conducted at 180°C. Typically 1g of sample was loaded onto the bottom plate of the instrument and allowed to melt. To maintain similar thermal history each sample was heated for 4 min in the rheometer prior to testing. The gap between the plates was set to 1.8 mm and the material was allowed to equilibrate for 2 min. To minimise the effect of thermal degradation at temperatures above the melting point, frequency sweeps were performed in the range from 1 to 512 rad/s for all tests as use of frequencies lower than 1 rad/s resulted in long exposure to heat per point which led to significant thermal degradation and considerable decrease in viscosity. The commanded strain was set to 1% for all tests.

*Thermal Gravimetric Analysis*

The thermal decomposition of the blends was investigated with a TA Instruments Q500 TGA apparatus at a nitrogen flow rate of 10 mL/min. The temperature ranged from 40

to 600 °C at various heating rates (5, 10, 20, and 40°C/min) using approximately 10 mg samples.

**Result and Discussion**

*Crystallization behaviour*

The dynamic thermal properties were investigated in order to obtain useful information in melting and crystallization characteristics in relation to processing and product application.

The DSC curves, obtained from PHBV/Joncryl blends on the first cooling scans are presented in Figure 2. The melt crystallization temperatures ($T_{mc}$) and melt crystallization enthalpies ($\Delta H_{Tmc}$) are summarized in Table I.

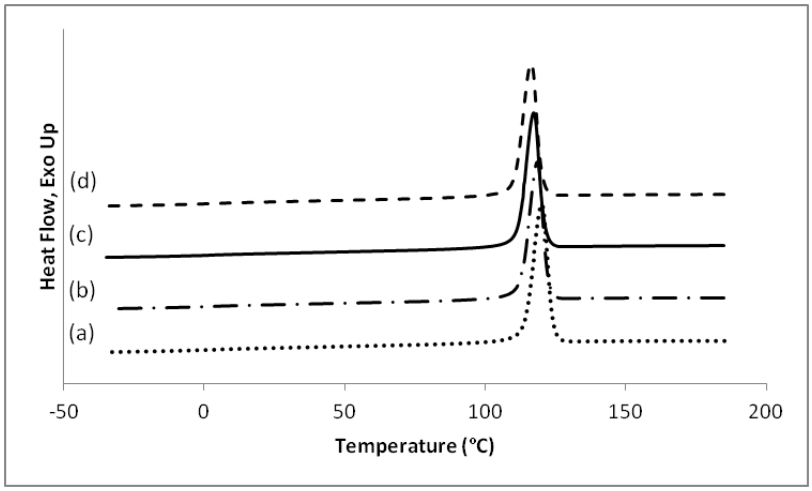


**Figure 2.** DSC first cooling curves (at a cooling rate of 10ºC/min) of the PHBV/Joncryl blends at different Joncryl concentrations:

a) 0.00 wt%; b) 0.25 wt%; c) 0.50 wt% and d) 1.00 wt%.

For all PHBV/Joncryl blends at different Joncryl concentrations, only a single crystallization peak can be observed. The melt crystallization temperature, $T_{mc}$, is an indirect indication of the crystallization rate and generally, a lower $T_{mc}$ indicates slower crystallization [27]. Figure 2 and Table I show that with increasing Joncryl content, $T_{mc}$ shifted to a lower temperature and the enthalpies of crystallization ($\Delta H_{Tmc}$) also slightly

decreased. This indicated that the chain extender resulted in a lower crystallization rate and lower percentage of crystallinity.

In addition, Figure 3 shows the non-isothermal DSC thermograms of the PHBV/Joncryl blends on the second heating scans at heating rate of 10°/min and the melting temperature ($T_m$) and the enthalpies of melting ($\Delta H_m$) are also included in Table I.

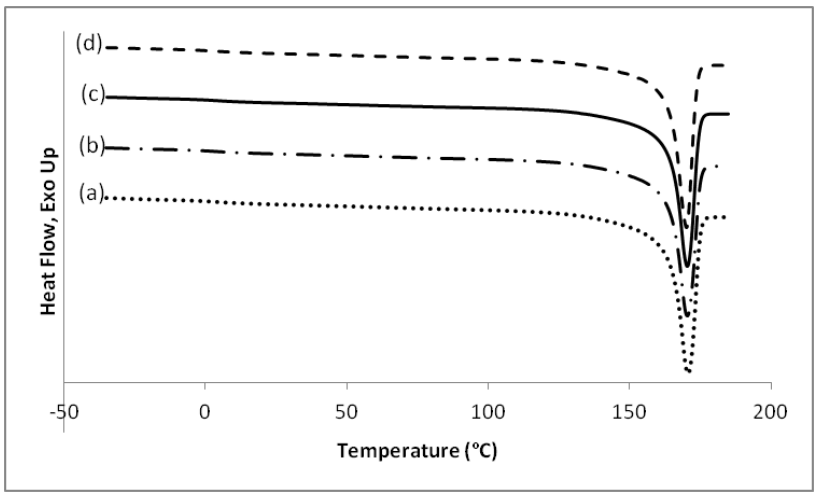


**Figure 3.** DSC second heating curves at a heating rate of 10 ºC $min^{-1}$ for PHBV/ Joncryl blends at different Joncryl contents:

a) 0.00 wt%; b) 0.25 wt%; c) 0.50 wt% and d) 1.00 wt%.

Only a single melting peak is observed for each sample. The results did not show much change in the melting temperature but the there is a decrease in enthalpies of melting with increase in the chain extender which can be attributed to the decrease in crystalinity mentioned earlier. Chain extenders are used to increase molecular weight by branching or cross-linking. This would lead to more complex molecular configuration and reduction in mobility of the polymer chains and thus to lower crystallinity and crystallinity perfection [28]. Addition of diepoxide as a chain extender to PET [29] has also shown similar effect in the decrease of crystallinity of PET.

**Table I.** Thermal characteristics of the PHBV/Joncryl blends.

| Joncryl concentration (wt%) | $T_m$ (ºC) | $\Delta H_{Tm}$ (J/g) | $T_{mc}$ (ºC) | $\Delta H_{Tmc}$ (J/g) |
|---|---|---|---|---|
| 0.00 | 170.6 | 94.8 | 120.2 | 88.0 |
| 0.25 | 170.4 | 91.8 | 118.6 | 84.5 |
| 0.50 | 170.4 | 91.2 | 117.5 | 83.8 |
| 1.00 | 170.2 | 90.6 | 116.3 | 83.4 |

The crystallization of PHBV and PHBV/Joncryl blends from molten state was also studied under isothermal conditions at various crystallization temperatures ($T_c$). Figure 4 shows the isothermal DSC curves for PHBV. With rising crystallization temperature, the crystallization rate decreases as shown by a shift of the onset of crystallization and the exothermic peak to longer time and the curves became flatter.

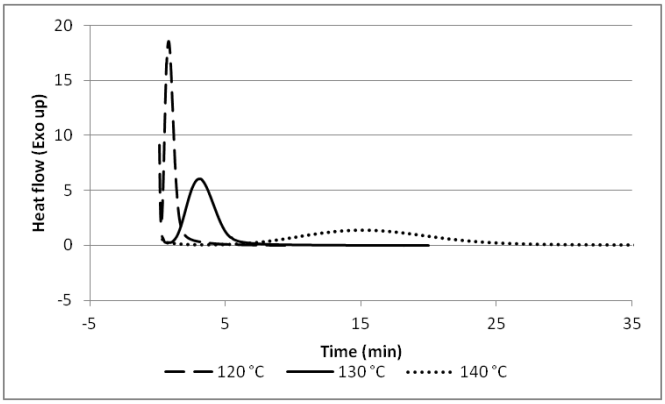


**Figure 4.** DSC isotherms crystallization thermograms of PHBV without Joncryl at different temperatures.

The kinetics of crystallization was determined from the isothermal heat flow curve of DSC measurements using Avrami equation [30-32].

$$X_{rel} = 1 - \exp(-k.t^n) \qquad (1)$$

where $X_{rel}$ refers to the relative crystallinity at time *t*, *K* is the crystallinity rate constant, and *n* is the Avrami exponent, depending on the nucleation mechanism and the dimension of crystal growth.

$X_{rel}$ could be determined from DSC thermograms in the term of:

$$X_{rel} = \frac{X_c(t)}{X_c(\infty)} = \int_0^t \frac{dH(t)}{dt} dt / \int_0^\infty \frac{dH(t)}{dt} dt \qquad (2)$$

where $X_c(t)$ and $X_c(\infty)$ refer to the degree of crystallinity at given time t and at the end of crystallization process, respectively. Equation 1 may be rewritten into the double-logarithmic form as:

$$log[-ln(1 - X_{rel})] = \log(K) + nlog(t) \quad (3)$$

Plotting $log[-ln(1 - X_{rel})]$ against $log\ (t)$ gives a straight line and two parameters ($log\ K$ and $n$) can be determined from the intercepts and slopes, respectively.

The crystallization half time $t_{1/2}$ , which is the time when half of the crystallization has been completed, $X_{rel} = 0.5$, can be obtained by the equation:

$$t_{1/2} = \left(\frac{ln2}{K}\right)^{\frac{1}{n}} \qquad (4)$$

Figure 5a presents the relative crystalinity versus time of PHBV at three different temperatures and Figure 5b shows the Avrami plots of PHBV at the same temperatures.

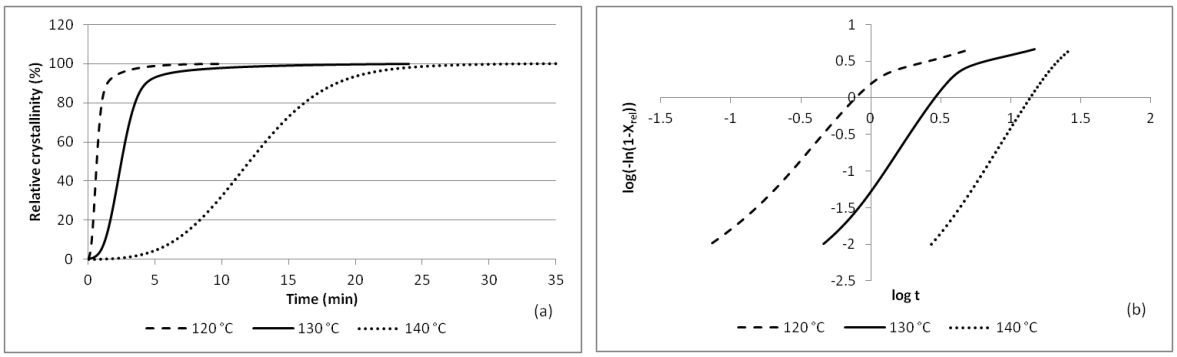


**Figure 5.** (a) Relative crystalinity as a function of time for PHBV without Joncryl and (b) the Avrami plots for PHBV at various isothermal crystallization temperatures.

Figure 5a shows that the completion time of crystallization increases with temperature, or the crystallization rate decreases with the increase of crystallization temperature.

Regarding to the Avrami plots (Figure 5b), each curve shows a linear segment during the initial stage of crystallization and bending of the curves can be attributed to the transition from primary to secondary crystallization after spherulite impingement at a later stage [33, 34] and as reported for pure PHB and PHBV [35].

Since Avrami equation (Equation 1) is based on assumptions of primary nucleation and linear crystal growth in a constant volume, it is valid at low conversions as long as the impingement is not serious [36]. Thus the values of *n* and *K* were calculated from the early linear segment in Figure 5b of the Avrami plot [27, 37-39] and the results are listed in Table II.

The *K* value for PHBV isothermal crystallization decreases with increase in temperature, resulting in longer $t_{1/2}$ value. This temperature dependence of melt crystallization is a characteristic of nucleation controlled crystallization related to degree of super cooling (i.e. the gap between the crystallization temperature and the melting temperature) [27].

The *n* value for the PHBV in this experiment ranged from 2 to 3 depending on temperature. The depression of the *n* value is probably due to the existence of athermal crystallization during the process [27] or decrease in *n* value indicate a bigger gap between melting temperature and crystallization temperature. For ideal state of nucleated crystallization, the *n* value should be exact number [31] but as the Avrami equation is derived with a number of simplifications, which do not necessarily apply to the real crystallization of macromolecules [36], the practical circumstances cannot satisfy the ideal state that the Avrami equation is supposed to match. Hence, the deviation of the *n* value from the theoretical usually occurs [27, 37, 38].

Effect of the chain extender addition on isothermal crystallization of PHBV was studied following the same procedure. The values of *n*, *K*, and $t_{1/2}$ are obtained as described earlier and summarized in Table II. Change in *n* value is predominated by the crystallization temperature (degree of super cooling) and insensitive to the Joncryl concentration. This suggests that the addition of the chain extender has not changed the mechanism of nucleation.

Change in crystallization rate is clearly demonstrated by the decrease in *K* value and increase in $t_{1/2}$ with increase in temperature and content of Joncryl. While temperature remained the dominating factor for *K* and $t_{1/2}$, addition of the chain extender can also be significant. For instance, addition of 1.0 wt% Joncryl can double the crystallization half time at 140 ºC.

This phenomenon of crystallization retardancy from chain extender might be explained by change in tacticity of the molecules. Zhong et al. [40] described the effect of chain extender on crystallization behaviour of PLA as a function of tacticity. PLA chains were branched after the chain-extending reaction and lowered the tacticity of the PLA molecule. Only the unbranched chains could crystallize at earlier stage while the branched chains could crystallize at a later period. This is consistent with the result shown here.

**Table II.** Avrami's parameters of the PHBV/Joncryl blends.

| Joncryl concentration (wt%) | $T_C$ (ºC) | *n* | *K(min-1)* | $T_{1/2}$ *(min)* |
|---|---|---|---|---|
| 0.00 | 120 | 2.17 | 1.75 | 0.65 |
| | 130 | 2.77 | $5.48 \times 10^{-2}$ | 2.50 |
| | 140 | 3.03 | $3.64 \times 10^{-4}$ | 12.05 |
| 0.25 | 120 | 2.14 | 1.66 | 0.66 |
| | 130 | 2.87 | $2.97 \times 10^{-2}$ | 3.00 |
| | 140 | 3.36 | $8.12 \times 10^{-5}$ | 14.74 |
| 0.50 | 120 | 2.64 | $6.61 \times 10^{-1}$ | 1.02 |
| | 130 | 2.76 | $1.37 \times 10^{-2}$ | 4.13 |
| | 140 | 3.14 | $5.54 \times 10^{-5}$ | 20.16 |
| 1.00 | 120 | 2.75 | $4.43 \times 10^{-1}$ | 1.18 |
| | 130 | 2.77 | $9.59 \times 10^{-3}$ | 4.68 |
| | 140 | 2.99 | $4.84 \times 10^{-5}$ | 24.60 |

*Rheological Behaviour*

The effect of chain extender on melt viscosity of the PHBV/Joncryl blends was evaluated by change in complex viscosity as a function of frequency at 180°C. As shown in

Figure 6, the blends exhibit typical shear thinning characteristic, i.e. decrease of viscosity with increase of frequency or shear rate. The PHBV blend without Joncryl used as reference showed the lowest viscosity (about 525 Pa.s at 1 rad/s). Increasing content of the chain extender resulted in consistent increase in viscosity and at 1.00 wt% level led to considerable increase to 630 Pa.s. This enhancement in shear viscosity indicated that macromolecular chain-extension had occurred during the extrusion compounding process [41]. Corre et al. [26] showed that by adding similar level of Joncryl (0.9 wt% using a 3 wt% masterbatch) to PLA resulted in a 30 times increase in the complex shear viscosity (measured at 180°C using an angular frequency of 0.1 rad/s). PLA is known to be much more resistant to thermal degradation than PHBV and it is possible that the relatively low efficiency in viscosity enhancement in the PHBV/Joncryl blends has resulted from competition of chain extension against thermal degradation of PHBV.

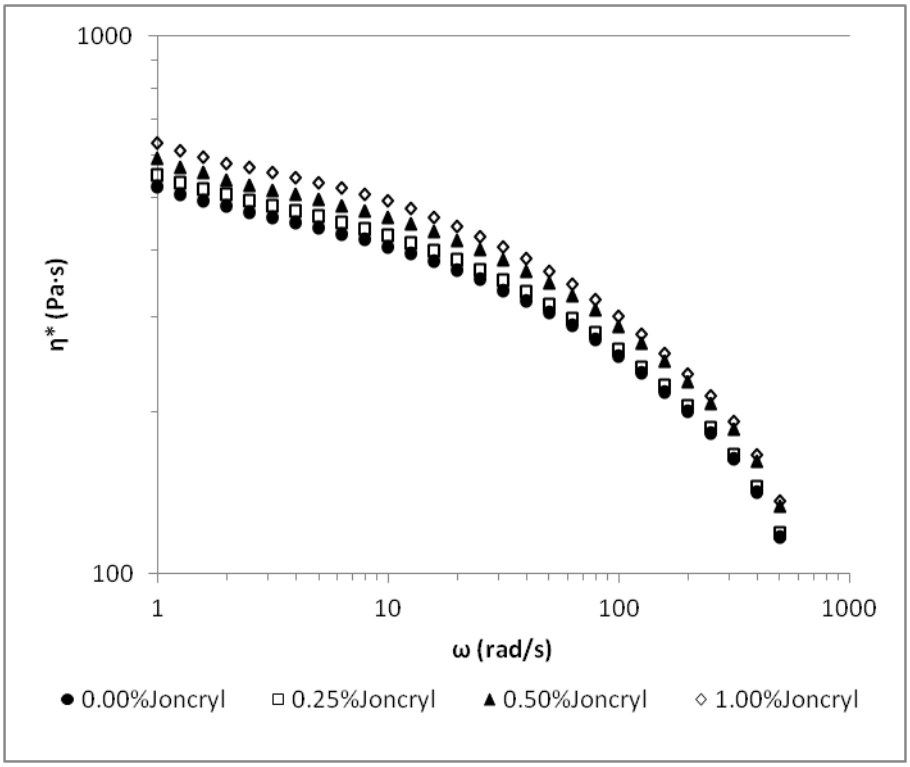


**Figure 6.** Complex viscosity of PHBV/Joncryl blends as a function of angular speed measured at180°C with 1% strain.

*Thermal Degradation Behaviour*

The effect of Joncryl on thermal degradation behaviour of PHBV was investigated using TGA. Figure 7 shows the TG and DTG curves for PHBV without Joncryl. Results for those with Joncryl additions up to 1.0 wt% level have similar feature and thus not shown here.

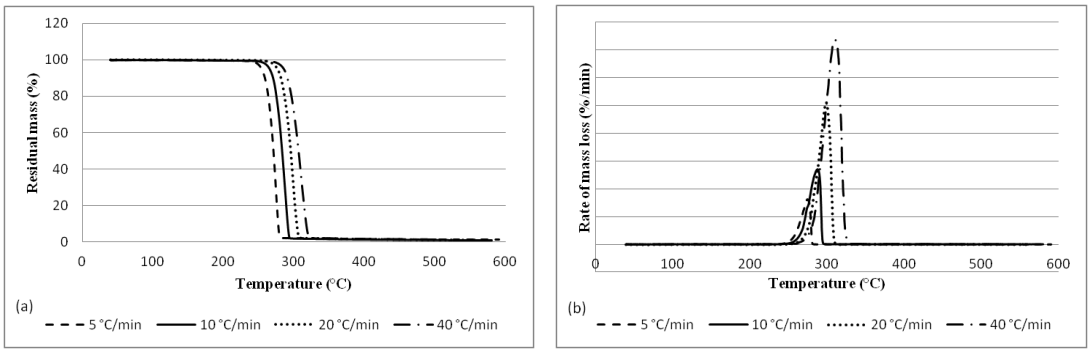


**Figure 7.** TG (a) and DTG (b) of PHBV at different heating rates.

It is noted that weight loss of PHBV and its blend with Joncryl occurs in a one-step process between 250 and 320 °C and the maximum rate of mass loss is identifiable by the single peak in DTG. Both TG and DTG are heating rate dependant: when heating rate is increased, the decomposition peak is delayed to higher temperature and the maximum decomposition rate is intensified.

The effect of chain extender to thermal stability of PHBV is studied by comparison of activation energy of thermal decomposition using the Flynn-Wall-Ozawa (FWO) method [42, 43] which is featured by its high reliability [44] and applicability to polymers which are degraded via random chain scission [44, 45]. The FWO method can be derived from an ordinary fundamental kinetic equation for heterogeneous chemical reactions. It determines activation energy directly from data between weight loss and temperature, using several different heating rates. The term of activation energy with the FWO method is defined in Equation 5.

$$E_a = -\frac{R}{b}\left(\frac{d(log\beta)}{d\left(\frac{1}{T}\right)}\right) \qquad (5)$$

where $E_a$ is the activation energy (J/mol); $R$ is the gas constant (8.314 J/mol.K); $T$ is the temperature at constant conversion amount (K); $\beta$ is the heating rate (K/min); $b$ is the constant value ($\approx$0.457 ± 0.03 for $20 < E_a/RT < 60$).

The reliance of $\log \beta$ on $1/T$ for each constant conversion corresponds to a straight line, known as isoconversional line. For every selected conversion, activation energy can be calculated from the slope of these lines. Because the activation energy from this method is the sum of activation energies of chemical reactions and physical processes in thermal decomposition, it is referred as apparent activation energy.

The values from TG curves of PHBV/Joncryl blends at different heating rates were used to calculate activation energy of thermal decomposition process by the FWO method. Typical plots obtained by the FWO method at various heating rate of are shown in Figure 8.

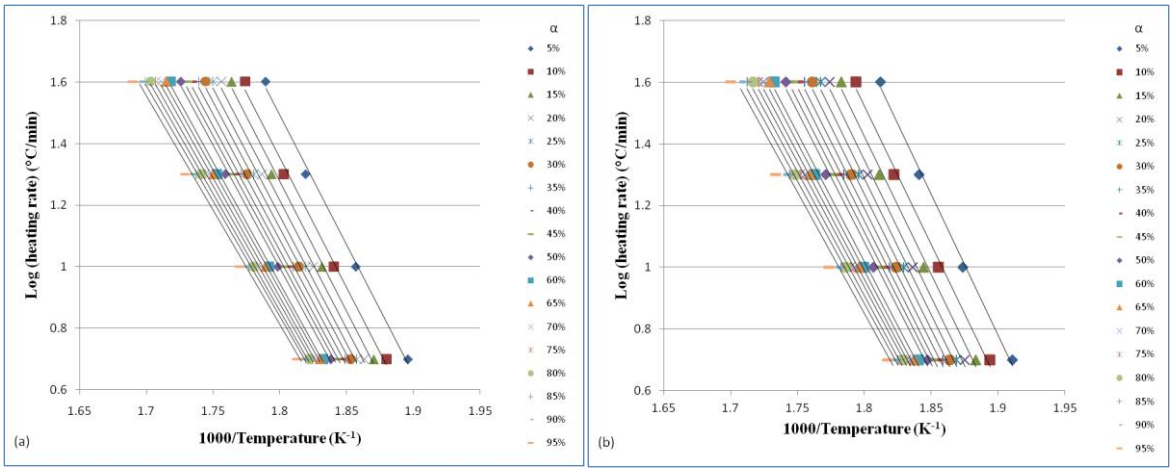


**Figure 8.** The application of Flynn-Wall-Ozawa method to calculate activation energy of thermal decomposition for PHBV/Joncryl blends at: (a) 0.00 wt% and (b) 1.00 wt% Joncryl.

The individual lines correspond to differently chosen conversion amounts (from 5 to 95%). The slope of the lines in Figure 8 can be determined as value of the derivative, d(logβ)/d(1/T), in Equation 5 and then $E_a$ can be calculated. The activation energy values of all samples of non-isothermal decomposition for each PHBV/chain extender blend are evaluated by using the data from Figure 8 in the conversion range α = 5-95% and plotted in Figure 9. The unmodified PHBV has lowest $E_a$. By introduction of Joncryl to PHBV, $E_a$ values of the blends increased with the Joncryl content at any given conversion level.

$E_a$ of PHBV and PHBV/Joncryl blends gradually declines with the increase in conversion. The reduction of $E_a$ may be described by autocatalytic reaction of thermal decomposition of PHBV. Its thermal decomposition product, for example, crotonic acid, decreases its activation energy by behaving like a catalyst in the reaction as reported by Kopinke et al. [46].

This result leads to conclusion that the introduction of Joncryl increases the apparent activation energy ($E_a$) of PHBV. Use of blends with higher $E_a$ means that they are more thermally stable during processing and thus widen the processing windows in terms of processing temperature or residence time without rapid loss of melt viscosity. The reason behind the higher thermal stability might be attributable to increasing molecular weight and chain rigidity.

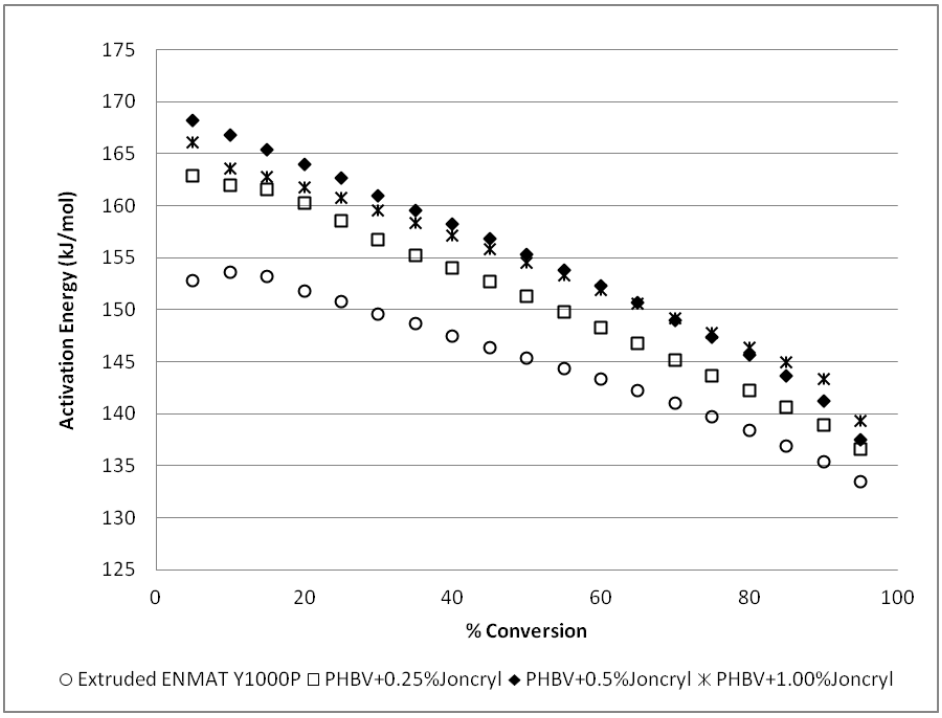


**Figure 9.** Activation energy of PHBV/Joncryl blends determined by FWO method.

## Conclusions

The effect of Joncryl chain extender on thermal degradation, crystallization and rheological behaviours of PHBV was investigated. The introduction of Joncryl improves thermal stability shown by increase in activation energy of thermal decomposition with increase in Joncryl content. This allows widening of processing window such as residence time. The chain extender also improves rheological behaviour by increasing the complex viscosity which would benefit melt processing such as sheet extrusion or foaming of the high-crystallinity polymer. The addition of Joncryl however showed marked retardancy to crystallization and hence care must be taken in solidification of the melt to avoid sagging. The addition of Joncryl in this study was kept at low levels up to 1.0 wt% for food regulation considerations and thus may be significantly increased if not restricted by such condition to enhance the benefits.

**References**


1 K. Numata, K. Yamashita, M. Fujita, T. Tsuge, K. Kasuya, and T. Iwata, Biomacromolecules. 8 (2007) 2276.

2 G.Q. Chen and Q. Wu, Biomaterials. 26(33) (2005) 6565.

3 T. Tanaka, T. Yabe, S. Teramachi and T. Iwata, Polym. Degrad. Stab. 92 (2007) 1016.

4 D.S. Sheu, W.M. Chen, J.Y. Yang and R.C. Chang, Enz. Microbial. Technol. 44 (2009) 289.

5 H. Sato, M. Nakamura, A. Padermshoke, H. Yamaguchi, H. Terauchi and S. Ekgasit, Macromolecules. 37 (2004) 3763.

6 L.S. Serafim, P.C. Lemos, C. Torres, M.A.M. Reis and A.M. Ramos, Macromol. Biosci. 8 (2008) 355.

7 K. Sudesh, C.Y. Loo, L.K. Goh, T. Iwata and M. Maeda, Macromol. Biosci. 7 (2007) 1199.

8 D.F. Parra, J. Fusaro, F. Gaboardi and D.S. Rosa, Polym. Degrad. Stab. 91 (2006) 1954.

9 D.Z. Bucci, L.B.B. Tavares and I. Sell, Polym. Test. 24 (2005) 564.

10 M.D. Sanchez-Garcia, E. Gimenez, and J.M. Lagaron, J. Appl. Polym. Sci. 108 (2008) 2787.

11 D.Z. Bucci, L.B.B. Tavares and I. Sell, Polym. Test. 26 (2007) 908.

12 G.J.M. Koning and P.J. Lemstra, Polymer. 34 (1993) 4089.

13 H. Elodie, B. Perrine, P. Eric and A. Luc, Polym. Degrad. Stab. 93 (2008) 413.

14 M.J.K. Chee, J. Ismail, C.H.W. Kummerlöwe Kammer, Polymer. 43 (2002) 1235.

15 E. Matko, K. Tonka and K. Ivka, Polym. Degrad. Stab. 90 (2005) 313.

16 K. Akira, Polymer. 47 (2006) 3548.

17 Q.S. Liu, M.F. Zhu, W.H. Wu and Z.Y. Qin, Polym. Degrad. Stab. 94 (2009) 18.

18 C. Zhijiang, H. Chengwei and Y. Guang, Polym. Degrad. Stab. 96 (2011) 1602.

19 I. Vroman and L. Tighzert, Materials. 2 (2009) 307.

20 P.D. Haene, E.E. Remsen and J. Asrar, Macromolecules. 32 (1999) 5229.

21 B. Fei, C. Chen, S. Chen, S. Peng, Y. Zhuang, Y. An and L. Dong, Polym. Int. 53 (2004) 937.

22 D.N. Bikiaris and G.P. Karayannidis, Appl. Polym. Sci. Polym. Chem. 34 (1996) 1337.

23 Y. M. Corre, J. Duchet, J. Reignier and A. Maazouz, Rheol Acta 50 (2011) 613.

24 S. Pilla, S.G. Kim, G.K. Auer, S. Gong and C.B. Park, Polym. Eng. Sci. 49 (2009) 1653.

25 M. Villalobos, A. Awojulu, T. Greeley, G. Turco and G. Deeter, Energy 31 (2006) 3227.

26 N. Najafi, M.C. Heuzey, P.J. Carreau and P. M. Wood-Adams, Polym. Degrad. Stab. 97 (2012) 554.

27 W. Kai, Y. He and Y. Inoue, Polym. Int. 54 (2005) 780.

28 M.V.S. Rao and N.E. Dweltz, J. Appl. Polym. Sci. 31 (1986) 1239.

29 D.N. Bikiaris and G.P. Karayannidis, J. Therm. Anal. 54 (1998) 721.

30 M.J. Avrami, J. Chem. Phys. 7 (1939) 1103.

31 M.J. Avrami, J. Chem. Phys. 8 (1940) 212.

32 M.J. Avrami, J. Chem. Phys. 9 (1941) 177.

33 B. Wunderlich, Macromolecular Physics Vol. 2 (Academic Press, New York, 1977).

34 J.P. Liu and Z.S. Mo, Chin. Polym. Bull. 4 (1991) 199.

35 A. Yuxian, L. Lixia, D. Lisong, M. Zhishen and F. Zhiliu, J. Polym. Sci. Polym. Phys. Ed. 37 (1999) 443.

36 B. Wunderlich, Macromolecular Physics (Academic Press, New York, 1976).

37 W.J. Liu, H.L. Yang, Z. Wang, L.S. Dong, J.J. Liu, J. Appl. Polym. Sci. 86 (2002) 2145.

38 W. Kai, Y. He, N. Asakawa and Y. Inoue, J. Appl. Polym. Sci. 94 (2004) 2466.

39 A.T. Lorenzo, M.L. Arnal, J. Albuerne, A.J. Muller, Polym. Test. 26 (2007) 222.

40 W. Zhong, J. Ge, Z. Gu, W. Li, X. Chen, Y. Zang and Y. Yang, J. Appl. Polym. Sci. 74 (1999) 2546.

41 M. Mihai, M.A. Huneault and B.D. Favis, Polym. Eng. and Sci. 50 (2010) 629.

42 J.H. Flynn and L.A. Wall, J. Res. Natl. Bur. Stand. 70A (1966) 487.

43 T. Ozawa, Bull. Chem. Soc. Jpn. 38 (1965) 1881.

44 H.A. Schneider, Thermochim. Acta. 83 (1985) 59.

45 W.W. Wendlandt, Thermal Analysis (John Wiley & Sons, New York, 1986).

46 F.D. Kopinke, M. Remmler and K. Mackenzie, Polym. Degrad. Stab. 52 (1996) 25.

# APPENDIX B

# Extrusion Foaming of PHBV

Damian Szegda, Sitthi Duangphet, Jim Song* and Karnik Tarverdi
Wolfson Centre for Materials Processing, Brunel University, Uxbridge, Middlesex, UB8 3PH, UK
*(*Corresponding author: jim.song@brunel.ac.uk)*

**ABSTRACT:** This paper reports work on extrusion foaming of poly(3-hydroxybutyrate-co-3-hydroxyvalerate) (PHBV) with a chemical blowing agent based on sodium bicarbonate and citric acid and calcium carbonate nucleation agent. It includes investigations in the effects of rheological behaviour of the polymer, blowing agent, nucleation agent and processing conditions on the foam density and morphology. PHBV is a natural biodegradable polyester with high crystallinity, low melt viscosity and slow crystallisation rate and high sensitivity to the thermal degradation at temperatures above its melting point, making it particularly difficult to control the foaming process. Use of negative gradient temperature profile was found beneficial to minimise the thermal degradation and achieve necessary melt strength to stabilise the cell structure. Solidification of the super-cooled polymer melt occurring at the die was discussed in relation to the selection of the temperature profile and rheological behaviour and solidification of the PHBV characterised by rotational rheometry. In addition to extrusion foaming conditions, effect of the blowing and nucleation agents on rheology of the polymer, the cell refinement on foam density and morphology were discussed. The PHBV was extruded with a twin screw extruder fitted with a strand die yielding up to 60% density reduction with uniform fine cell structure.

**KEY WORDS**: foams, PHBV, biodegradable, bio-plastic, extrusion foaming, rheology, crystallisation, chemical blow agent, nucleation.

## INTRODUCTION

Biopolymers can be polymers synthesised by plants and other living organisms or polymers derived from renewable resources. Their potentials as alternative to petrochemical-based materials has been recognised worldwide and many experts have predicted that the 21st century will herald the rise of the carbohydrate economy [1]. Furthermore, there is also a realistic possibility that the biopolymers could increase their market share from <1% to about 10% of global plastic consumption representing 20 million tonnes per annum. The market for

bioplastics has already grown from a small base of 262 kt in 2007 to 505 kt in 2009 and is set to reach 885 kt by 2011 [2].

PHBV, which is a biodegradable copolymer of polyhydroxy butyrate (PHB) and polyhydroxyvalerate (PHV) produced commercially using biotechnology methods [3, 4]. It possesses exceptional gas barrier properties and rigidity and hence high potentiality in advanced packaging such as modified atmosphere packaging of red meat. It has better oxygen barrier property than PET, but poorer than PP [5] and the water vapour resistance of PHBV is as good as PET and much better than other biopolymers like PLA [5, 6]. Like many biopolymers however, the material cost is typically 3 or 4 time as high as conventional plastics. Therefore, creating lightweight structures by foaming is considered to be one of the effective ways to reduce the material consumption and associated emissions.

Extrusion sheet foaming followed by thermoforming is the most common processing route for food packaging containers. Physical foaming using gas injection [7] on tandem extruders is widely used in sheet foaming. Solid state foaming where gas is saturated into the material at high pressure in an autoclave and released to create a foamed structure during a subsequent heating and forming stage has also been developed [8].

The use of chemical blowing agent on a conventional sheet extrusion line has the advantage of low capital investment and hence this work focuses on the chemical foaming method. As the applications are focused on food packaging, the choice of blowing agent must conform to the regulations for packaging in contact with foods.

PHBV foams has been studied and prepared by many researchers by using different techniques and often blended with other polymers. Richards et al. [8] used a temperature soak batch foaming technique for preparation of PLA/PHBV foams. Nascimento et al. [9] patented the preparation of Polyurethane/PHBV foamed with isocyanate, whereas the use of methyl formate to produce foamed PHBV beads was reported by Handa and Botts [10]. Extrusion foaming of starch/PHBV with water acting as a blowing agent is reported by Willett and Shogren [11]. However, the extrusion foaming of PHBV itself has not been well studied.

In this work, the extrusion foaming using food-approved chemical blowing agent is reported. This includes effect of material formulations and extrusion conditions on the rheological and foaming behaviour of PHBV and the resulting foam structures.

## EXPERIMENTAL DETAILS

### Materials

ENMAT$^{TM}$ Y1000P, a PHBV with 3 *mol%* hydroxyvalerate (HV) content was manufactured by Tianan Biologic Material Co. (Ningbo, P. R. China) in yellowish white pellet form with density of 1.24 $g/cm^3$. The melting and crystallisation temperature of PHBV was determined from DSC (model 2000, TA Insturments, USA) using a heating rate of *10°C/min* under nitrogen atmosphere. The melting peak was found at 168 *°C* and the crystallisation peak was found at 125 *°C* as shown in Figure 1.

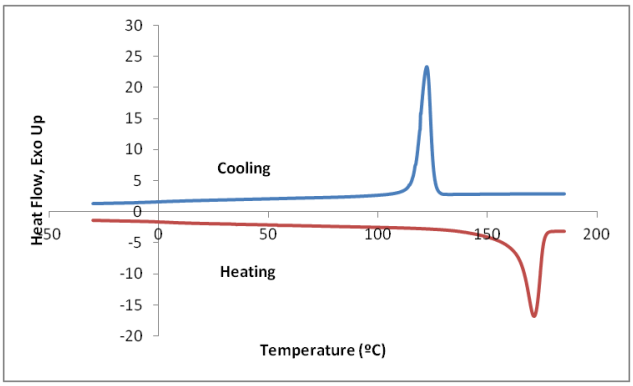


**Figure 1.** DSC curves of the PHBV during heating (red) and cooling (blue) at a rate of 10 *ºC* $min^{-1}$ under nitrogen atmosphere showing the peaks of melting and crystalisation temperatures.

The blowing agent, BA, (grade BA.F4.E MG) was supplied in white pellet form by Adeka-Palmarole (Saint Louis, France). The BA masterbatch contains 40 *wt%* active agent, a mixture of sodium bicarbonate and citric acid, in a LDPE carrier. It had an onset decomposition temperature at 150 *°C*. The calcium carbonate RLO 7999 with a density of 2.71 $g/cm^3$ was supplied by Imerys Minerals Ltd. (Par, UK) and its particle size distribution is shown in Figure 2.

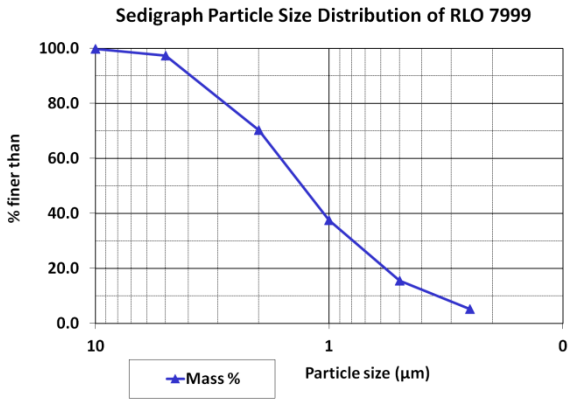


**Figure 2.** Particle size distribution of the calcium carbonate RLO 7999.

**The Extrusion Foaming Process**

Pellets of ENMAT$^{TM}$ Y1000P material were dried in an air-circulating oven at temperature of 100 °*C* for at least three hours. The dried material was then tumble-mixed with the blowing agent masterbatch and extruded with a Betol co-rotating twin screw extruder with a general metering-mixing screw profile. The screw diameter was 30 *mm* and its length to diameter ratio (L/D) was 30. The screw speed was varied between 20 to 50 *rpm* and material flow rate from 2.2 to 5.6 *kg/h*, respectively. Two die configurations were used; a sheet die with 150 *mm* width and a circular strand die with diameter of 5 and 7 *mm*. The temperatures of the five heating zones were set as shown in Table 1. This represents a negative temperature profile so that the polymer would melt in the early zones of the extruder and enters a super-cool state towards the exit. This temperature profile was designed to minimise thermal degradation and achieved the desirable high melt viscosity and melt strength at the die exit for foam stabilisation. The temperature setting was also chosen to match the decomposition temperature of the blowing agent. To study the effect of calcium carbonate on PHBV foaming behaviour, foams of PHBV filled with calcium carbonate powder were extruded with 5.0 *wt%* blowing agent masterbatch using the 5mm strand die. PHBV was firstly extrusion compounded with 5, 12 and 20 *wt%* calcium carbonate and then tumble mixed with the blowing agent masterbatch before the extrusion foaming.

**Table1.** Temperature profile along the extruder.

| **Zones** | **1** | **2** | **3** | **4** | **5** | **Die** |
|---|---|---|---|---|---|---|
| Temperature (°C) | 100 | 180 | 170 | 160 | 150 | 150 |

## Rheological Characterisation

### *Sample Preparation*

Rheological characterisation was performed on the as-received PHBV pellets and extruded foams. The extruded foam strands were first grinded by using a Retsch SM2000 cutting mill fitted with a sieve with 1.50 *mm* trapezoid apertures. Both pellets and grinded foams were dried for 2 hours at temperature of 100 *°C* in a vacuum oven prior to the measurements.

### *Complex Viscosity Measurement*

The sample polymer was then loaded onto the bottom plate of a rotational rheometer (ARES,TA Instruments, USA), to be melted and compressed by adjusting the top plate to a designated gap of 1.8 *mm*. Excess material was then removed so that the polymer could fill the volume between the plates. No air bubbles entrapment was observed. Viscosity measurements were performed at a range of temperatures from 145 to 180 *°C*. To maintain similar thermal history, each sample was molten for 4 *min* at temperature of 180 *°C* in the rheometer prior to the testing. Heating time was increase to 6 *min* for the extruded foams in order to decompose any residual blowing agent. To minimise the effect of thermal degradation at temperatures above the melting point, the angular speed sweep was conducted in the range from 1 to 512 *rad/s* for all tests, since the use of frequencies lower than 1 *rad/s* could result in much longer measurement times per point and potentially lead to thermal degradation and considerable decreased in viscosity. The commanded strain was set to 1% for all the tests.

## Foam Characterisation

A Zeiss Supra 35VP field emission scanning electron microscope (SEM) was used to observe the foam morphology. Extruded foams were quenched in liquid nitrogen and fractured. The fracture surfaces perpendicular to the direction of extrusion were used for the observations. The fracture surfaces were then sputter-coated with gold prior to the SEM

examination. The average cell size and cell population density (N) were analysed from SEM images. The cell population density was calculated using Equation 1 [7]:

$$N = \left(\frac{n}{A}\right)^{3/2} \times \frac{\rho_S}{\rho_f}, \qquad (1)$$

where $n$ is the number of cells in the defined area $A$, $\rho_s$ is the density of unfoamed material and $\rho_f$ is the density of the foam, which was measured using a density determination device AB204-S from Mettler Toledo Ltd. (Beaumont Leys Leicester, UK). Density reduction was calculated from Equation 2:

$$\Delta\rho = \frac{100(\rho_s - \rho_f)}{\rho_s}\ (\%) \qquad (2)$$

## RESULTS AND DISCUSSION

### Rheological Behaviour of the As-received PHBV

Complex viscosity as functions of shear rate at different temperatures for the as-received PHBV is shown in Figure 3. The result reveals that the PHBV exhibits shear thinning behaviour when subject to increasing shear rate (directly related to frequency or angular speed, $\omega$). The complex viscosity at 180°C and 1 *rad/s* was about 1300 *Pa.s*. This is nearly 4 times lower when compared with crystalline polylactic acid (cPLA) which has a viscosity of about 5000 *Pa.s* at the same condition [7]. Lowering the temperature led to considerable increased in viscosity and at 145 °*C* the viscosity at 1 rad/s increased to about 3000 *Pa.s*. No apparent Newtonian plateau was observed, possibly resulted from the limitation on the selected shear speed and thermal degradation during testing.

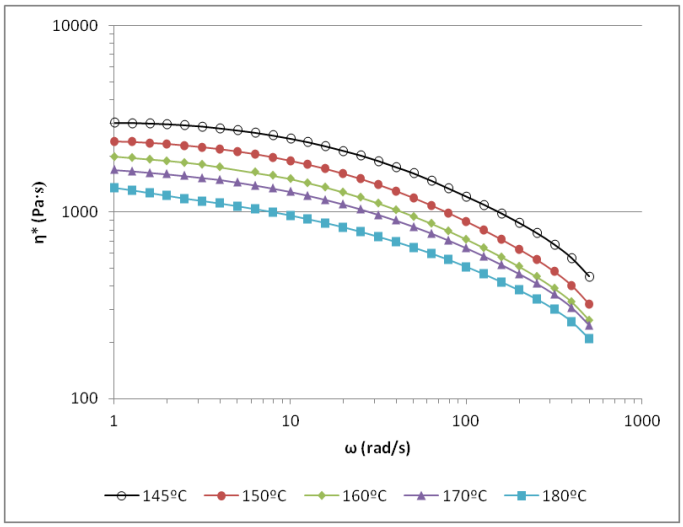


**Figure 3.** Complex viscosity of the as-received PHBV measured as a function of angular speed at different temperatures.

When tested at a fixed angular speed (at 1 *rad/s*) at different temperatures, the complex viscosity of the PHBV melt changed over time as shown in Figure 4. At temperatures above melting point (170 and 180 ℃), viscosity was continuously decreasing, indicating that the polymer was undergoing chain scission. At temperatures below melting point however, viscosity could be seen to increase over time. This can be attributed to crystallisation of the super-cooled PHBV melt. Such increase in viscosity is strongly dependant on the degree of super cooling. The lower the temperature, the faster the viscosity increase and eventually leads to solidification and slippage at the surfaces of the plates, resulting in a plateau.

Figure 5 presents time at *G'/G"* crossover for the super-cooled PHBV, where *G'* is storage modulus and *G"* is loss modulus. The crossover point is when *G'=G".* Prior to the crossover point, the molten polymer is predominantly viscous and after the crossover, the melted polymer becomes more elastic. Increase in melt elasticity over time is indicative of crystallisation which eventually results in solidification. This phenomenon was observed during extrusion foaming of PHBV and will be discussed later.

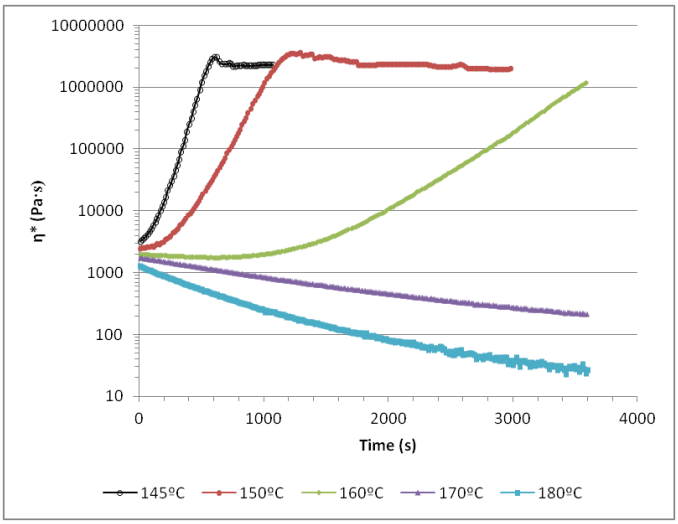


**Figure 4.** Complex viscosity of the as-received PHBV as a function of time at fixed angular speed of 1 *rad/s* and different temperatures.

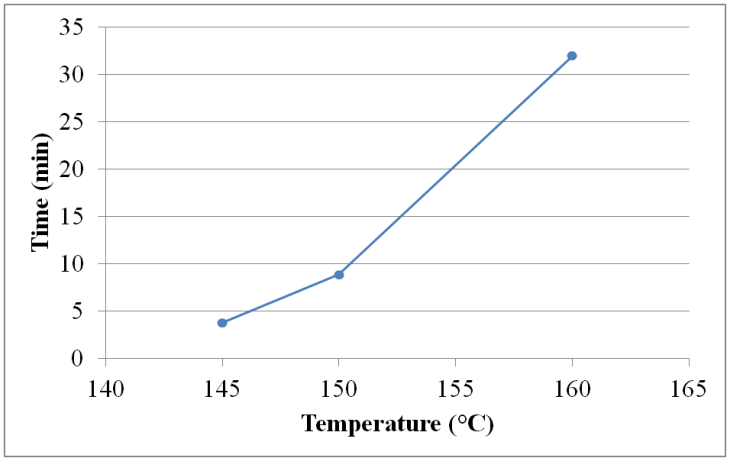


**Figure 5.** *G'/G"* crossover times for the super-cooled PHBV (as-received) melt at different temperatures.

## Rheological behaviour of post-foaming PHBV

The complex viscosity of melts from the post-foaming PHBV with different amounts of blowing agent masterbatch is shown in Figure 6. The viscosity is noticeably lower than that of the as-received PHBV (when compared with that at 180 ℃ in Figure 3), which indicates that the polymer has undergone some thermal degradation during the extrusion foaming process. Moreover, with the increase of the BA masterbatch from 2.5 to 7.5 *wt%*, further decrease in viscosity was observed. This can be attributed to the hydrolytic degradation caused by water released from the decomposed sodium bicarbonate. Since PHBV is a polyester copolymer, it is susceptible to thermal and hydrolytic degradation by water at high temperatures and pressures [12, 13]. In this regard, the use of negative temperature

profile can reduce the high temperature exposure time and minimise the thermal and hydrolytic degradation.

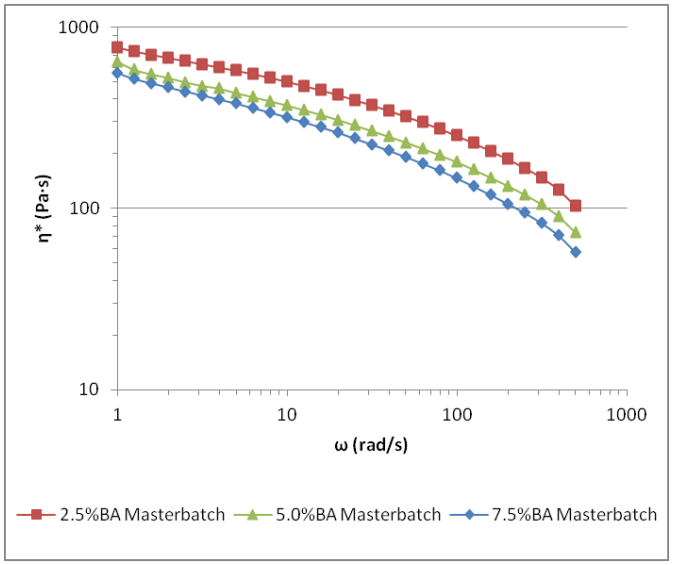


**Figure 6.** Complex viscosity the post-foaming PHBV measured at 180 °*C* showing reduction in the viscosity with increasing level of the $H_2O$ and $CO_2$ generating blowing agent.

**The PHBV Foaming Process**

Figure 7 presents the morphologies of extruded foams using the sheet die at the blowing agent masterbatch levels of 1.25, 2.50 and 3.75 *wt%*, which correspond to 0.5, 1.0 and 1.5 *wt%* active contents, respectively. The sheets were extruded with temperature profile given in Table 1 at 30 *rpm* screw speed and flow rate of 3.3 *kg/h*. The analysis in density reduction, cell size and cell population density determined from these foams were also presented in Figure 8. Sparse cell population of cells averaging 140 *μm* was observed for foams extruded with low blowing agent concentration (at 1.25 *wt%* masterbatch) and resulted in a small density reduction (14%). Increasing the masterbatch content to a medium level (2.50 *wt%*) gave rise to a high density reduction (of 32%) owing largely to the increased cell size to about 190 *μm* whereas the cell population hardly changed. At higher blowing agent concentration (3.75 *wt%*), density reduction reached 40% from considerable increasing in cell population while the cell size remained similar to that at 1.25 *wt%*. Clearly, this is attributable to more gas generated at higher blowing agent contents. One would expect the trend to continue to produce lighter foam by using higher concentrations of blowing agent. This was proved not the case as will be discussed later.

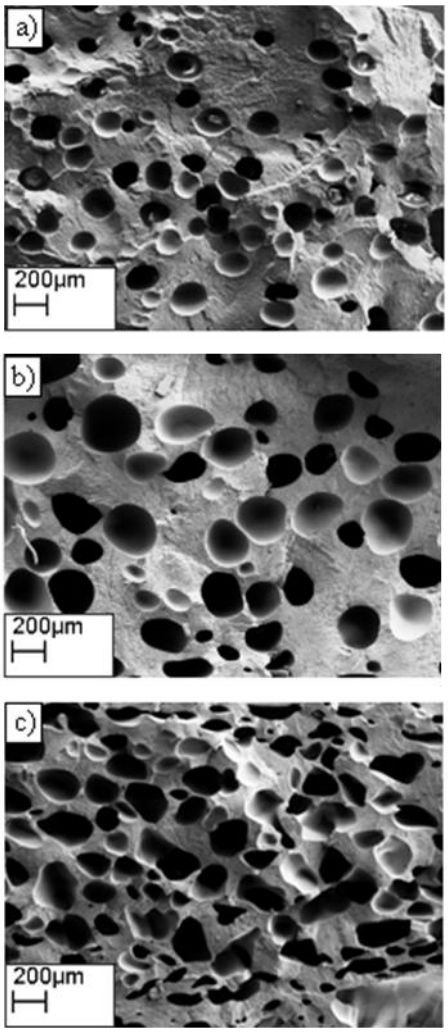


**Figure 7.** SEM images of PHBV foams extruded with the sheet die and BA masterbatch contents *(wt % )* of: (a) 1.25, (b) 2.50 and (c) 3.75 .

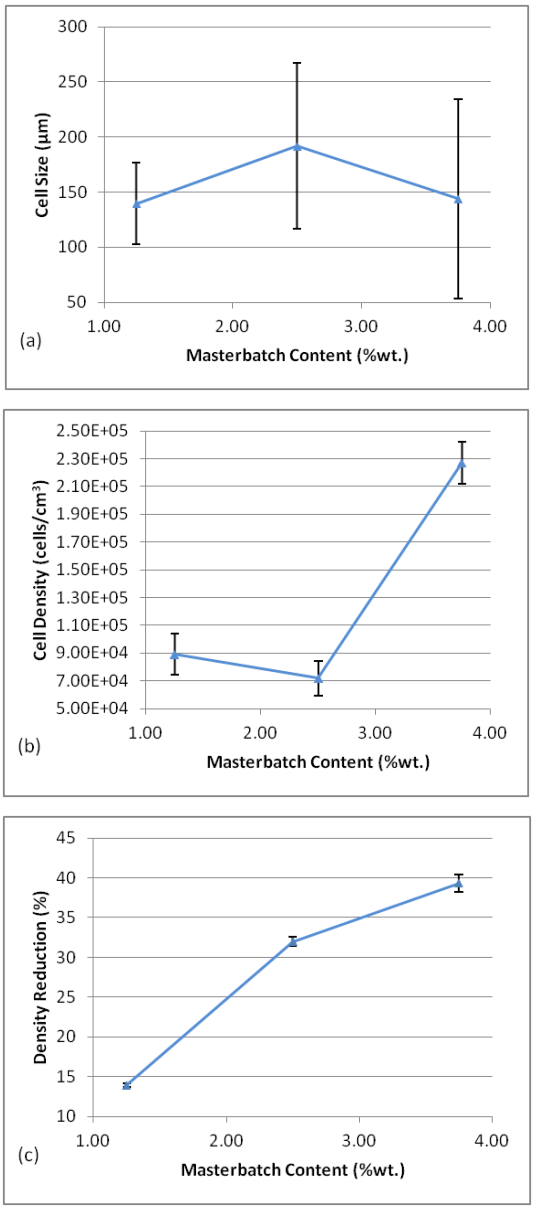


**Figure 8.** Effect of the amount of blowing agent on PHBV foam extruded with the sheet die: (a) cell size, (b) cell density population and (c) density reduction.

Figure 9 shows the influence of screw speed increase from 30 to 50 *rpm* (with corresponding feeding rate from 3.3 to 5.6 *kg/h*) without changing the other parameters. The higher screw speed resulted in lower density reductions. Higher screw speed generates higher pressure drop at the die exit which should normally enhance cell nucleation and expansion. It also reduces the residence time of the material in the barrels, particularly when use a low L/D ratio extruder. Sodium bicarbonate is an endothermic blowing agent with slow decomposition rate over wide range of temperatures [14], therefore, this result can be attributed to the shorter residence time that affected the decomposition of the blowing agent.

In addition, the shear thinning at high screw speed also reduced the melt viscosity, leading to cell rupture which was observed during the sheet foaming.

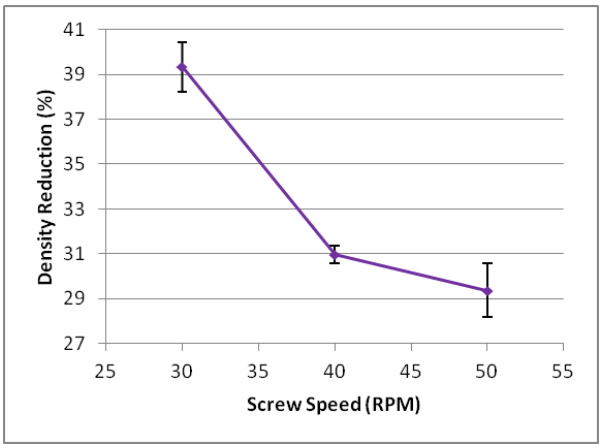


**Figure 9.** Density reduction as a function of screw speed in sheet foam extrusion at BA masterbatch content of 3.75 *wt%* .

The blowing agent masterbatch content was extended further up to 7.50 *wt%* in the extrusion process performed using the 7 *mm* circular die. The foams were extruded with screw speed of 30 *rpm* and flow rate of 3.3 *kg/h*. The morphologies of extruded foams are shown in Figure 10 whereas Figure 11 presents analysis of cell size, cell density population and density reduction of the foams. The result shows that the maximum density reduction about 57% was achieved at 5.00 *wt%* addition of the masterbatch (corresponding to 2 *wt%* active content). Use of the strand die could result in the improved pressure profile over the sheet die, where premature foaming inside the sheet die was observed. This led to significantly higher cell density population and thinner cell walls as shown in Figure 10. At 5 *wt%* masterbatch addition, a fine tuning of processing parameters by reduction of the screw speed to 20 *rpm* with feeding rate to 2.2 *kg/h* and reduction of temperate in the last zone of the extruder and the die to 140 °*C* had shown further density reduction to 61.3%.

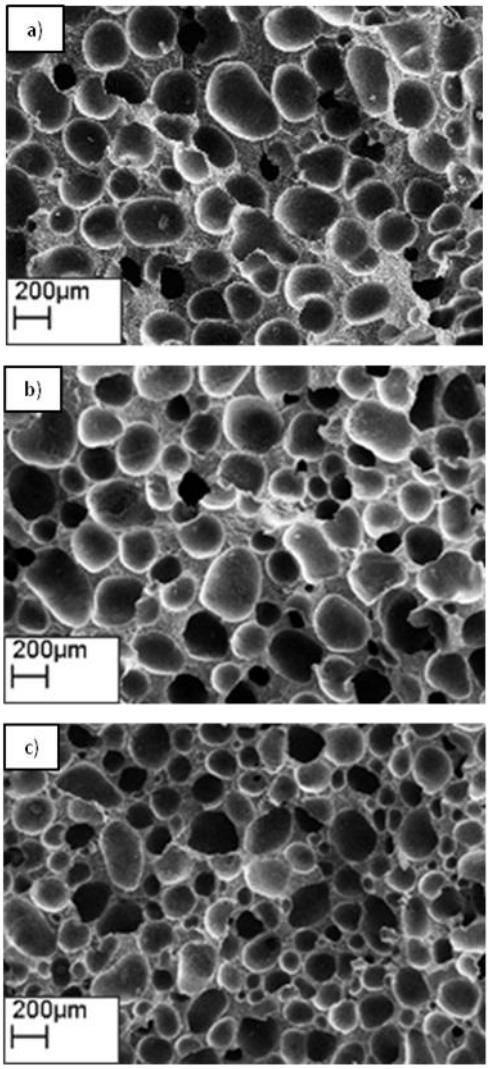


**Figure 10.** SEM images of foams extruded with the 7mm strand die at BA masterbatch contents of (a) 2.5, (b) 5 and (c) 7.5 *wt%*, respectively.

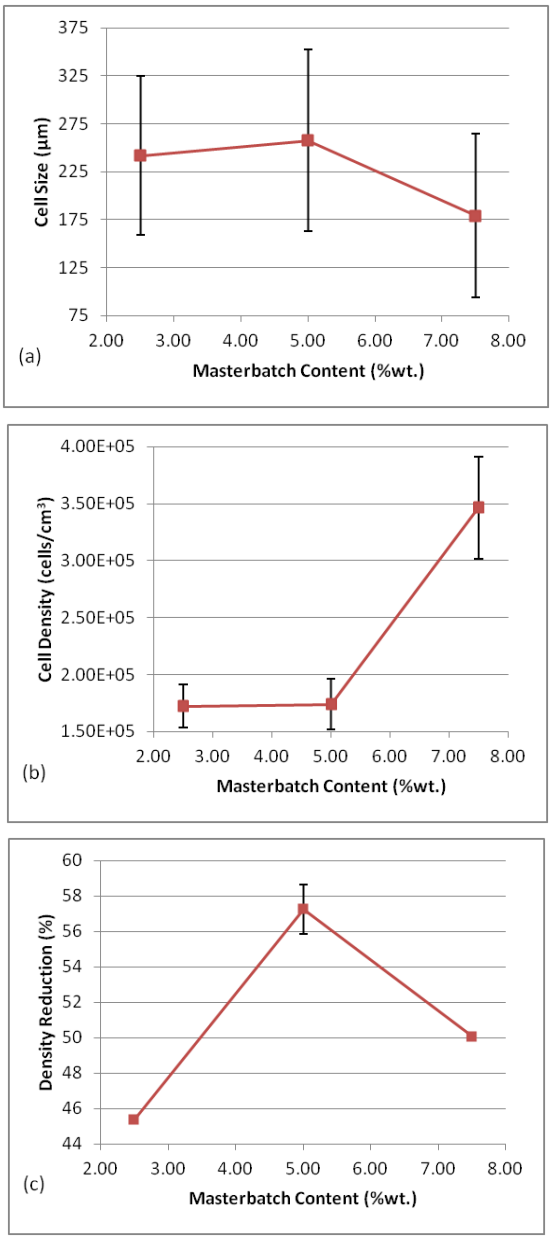


**Figure 11**. Effect of the amount of blowing agent on (a) cell size, (b) cell density population and (c) density reduction for foams extruded with the 7mm strand die.

Calcium carbonate particles were expected to act as nucleation sites and also enhance viscosity of the material for cell stabilisation. Figure 12 shows the foam morphologies corresponding to 5, 12 and 20 *wt%* calcium carbonate loading and Figure 13 presents cell size, cell density population and density reduction, respectively.

Increase in the calcium carbonate loading from 5 to 12 wt% reduced average cell size from 150 to about 100 $\mu m$ (Figure 12a & b and Figure 13a ) but no further change is observed when the loading is increased to 20 wt% (Figure 12b & c and Figure 13a). In contrast, the cell

density population increased with the loading of the calcium carbonate and reached the maximum at about 12 *wt%* and then dropped at 20 *wt%* as shown in Figure 13b. The density reductions achieved (based on densities of the $CaCO_3$ filled PHBV) similar level to the unfilled PHBV (Figure 13c) for the range of $CaCO_3$ loadings but achieved much finer cell structure (comparing Figure 12 with Figure 10 or Figure 13a with Figure 11a). The decrease of cell size and increase of cell density population could be explained by the enhancement of heterogeneous nucleation by the $CaCO_3$ particles whereas the reduction of cell density population at high loading may be attributed to insufficient dispersion of $CaCO_3$ agglomerates.

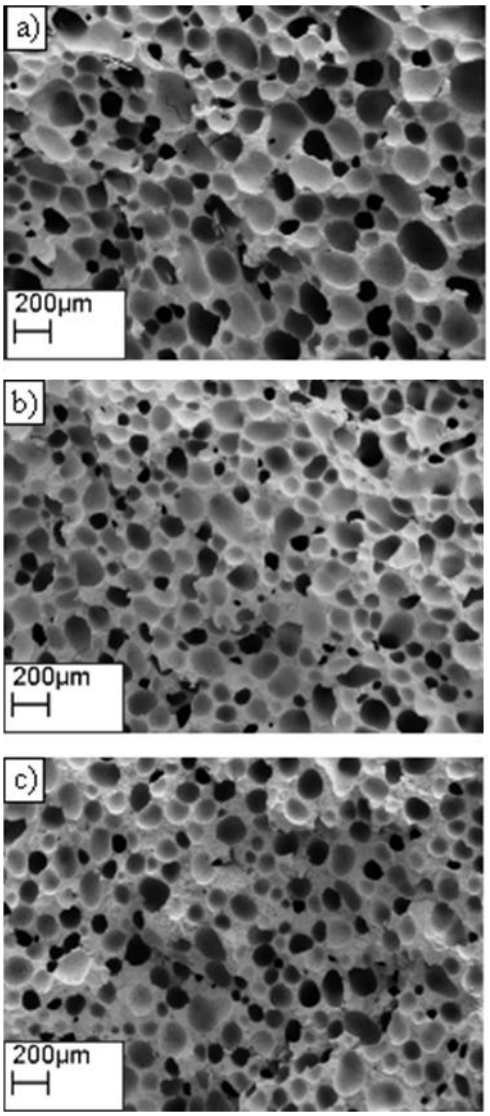


**Figure 12.** SEM images of foams extruded with the 5mm strand die using 5 wt% BA masterbatch and filled with (a) 5, (b) 12 and (c) 20 *wt%* of the calcium carbonate.

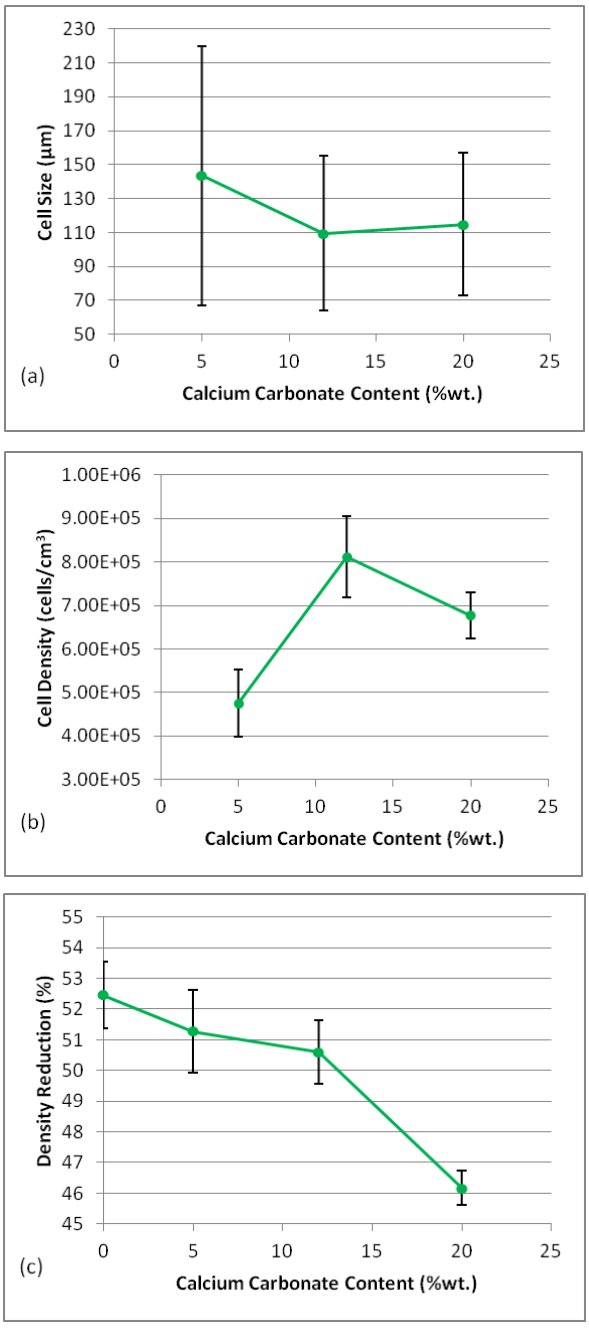


**Figure 13.** Effect of the amount of the calcium carbonate on (a) cell size, (b) cell density population and (c) density reduction for foams extruded with the 5 *mm* strand die.

Further attempts were made to increase viscosity of the PHBV in order to increase the pressure drop at the die exit and enhanced melt strength to minimise cell rapture. This was achieved using higher degree of super cooling by reduction of temperate in the last zone of the extruder and the die to 140 *°C* (below the melting point of 168 *°C*). This led to further expansion of the foams and achieved 57% density reduction using 5 *wt%* blow agent master batch and 20 *wt%* $CaCO_3$ loading. High level of super-cooling however can result in build-up

of the material in the die as shown in Figure 14. This can be correlated to solidification of the melt under super-cooling conditions as shown earlier in Figure 4. Rate of crystallisation under super-cooling conditions is dependant on temperature. Temperature drop sharply across the narrow die channel and rapid crystallisation could take place at the die surface, resulting in the build-up of a solidified polymer layer. The polymer was slowly accumulating from the wall to the centre and the rate of accumulation depended on temperature (degree of the super-cooling) and time under the super cooling conditions. The accumulation of the solid layer in the die can led to some changes in processing conditions (e.g. die pressure and flow characteristics) which led to the deterioration of foam quality and if not controlled, it was only possible to extrude quality foams for a limited time. Because this phenomenon took place at the narrow passages of the die, it seems to suggest that the stress induced crystallisation may have also played a part [15]. Further work is thus necessary to identify the extent of the limitation and optimise the processing conditions.

**Figure 14.** Die build-up associated with extrusion of the PHBV under super-cooled conditions. The outer layer is crystallised PHBV and the core is a purge polymer.

## CONCLUSIONS

Rheological behaviour of PHBV is sensitive to its thermal history and during extrusion foaming, it can experience both thermal degradation and hydrolytic degradations from a water-generating blowing agent. PHBV foams with density reduction up to about 60% were extruded using negative temperature profile to super-cooling the polymer melt using a chemical blowing agent based on a sodium bicarbonate and citric acid. The temperature profile was chosen based on rheological characteristics of PHBV and experimental

observations during extrusion foaming. The highest density reduction was obtained for extrusion with 5 *wt%* blowing agent masterbatch. Extruded foams were characterised by predominantly closed cell structure with cell sizes between about 50 to 200 $\mu m$. For the selected blowing agent and relatively low L/D ratio extruder, it was shown that lower screw speed gave necessary residence time for the decomposition of the blowing agent and resulted higher expansion of the foams. Moreover, the addition of calcium carbonate, while increasing overall density of the foams, resulted in much finer cell structure and decreased material costs. Super-cooling proved to be beneficial on two sides, viscosity increase and reduction of thermal degradation. A drawback of such processing conditions was potential build-up of solidified polymer due to the crystallised material in the narrow channel of the die. Further refinement of processing conditions is necessary so as to remove premature crystallisation and improve quality of the foams.

## REFRENCES


1. Song, J., Kay, M. and Coles, R. (2011). Bioplastics, In: Coles, R. et al. (ed.), *Food Packaging Technology 2nd Ed*, Ch. 11, Blackwell Publishing, Oxford.
2. EU Bioplastics (2011) www.european-bioplastics.org
3. Biopol® (Metabolix USA, www.metabolix.com)
4. www.tianan-enmat.com
5. Cava, D., Gimenez, E., Gavara, R. and Lagaron, J.M. (2006). Comparative Performance and Barrier Properties of Biodegradable Thermoplastics and Nanobiocomposites versus PET for Food Packaging Applications, *J. Plast. Film Sheet*, **22**: 265-274.
6. Shogren, R. (1997). Water Vapor Permeability of Biodegradable Polymers, *J. Environ. Polym. Degrad.*, **5**: 91-95.
7. Mihai, M., Huneault, M.A. and Favis B.D. (2010). Rheology and Extrusion Foaming of Chain-Branched Poly(Lactic Acid), *Polym. Eng. Sci.*, **50**: 629-642.
8. Richards, E., Rizvi, R., Chow, A. and Naguib, H. (2008). Biodegradable Composite Foams of PLA and PHBV Using Subcritical $CO_2$, *J. Polym. Envi.*, **16**: 258-266.
9. Nascimento, J.F., Pachekoski, W.M. and De Lello Vicino, J.R. (2007). *Composition for Preparing a Biodegradable Polyurethane-based Foam and a Biodegradable Polyurethane foam*, US Patent Publications 2009/0253816.

10. Handa, Y.P. (2008). *Expanded and Extruded Biodegradable and Reduced Emission Foams Made with Methyl Formate-Based Blowing Agents*, US Patent Publications 2008/0146686.
11. Willett, J.L. and Shogren, R.L. (2002). Processing and properties of extruded starch/polymer foams, *Polymer,* **43**: 5935-5947.
12. Verhoogt, H., Ramsay, B.A., Favis, B.D. and Ramsay, J.A. (1996). The influence of thermal history on the properties of poly(3-hydroxybutyrate-co-12%-3-hydroxyvalerate), *J. Appl. Polym. Sci.*, **61**: 87-96.
13. Cabedo, L., Plackett, D., Gimenez, E. and Lagaron, J.M. (2009). Studying the degradation of polyhydroxybutyrate-co-valerate during processing with clay-based nanofillers, *J. Appl. Polym. Sci.*, **112**: 3669-3676.
14. Padareva, V., Djoumaliisky, S., Touleshkov, N. and Kirov, G. (1998). Modification of blowing agent system based on sodium bicarbonate with activated natural zeolite, *J. Mater. Sci. Lett.*, **17**: 107-109.
15. Mackley, M.R., Moggridge, G.D. and Saquet, O. (2000). Direct experimental evidence for flow induced fibrous polymer crystallisation occurring at a solid/melt interface, *J. Mater. Sci.*, **35**: 5247-5253.

## ACKNOWLEDGEMENTS

The authors wish to acknowledge the collaboration from the research team in this project and the financial support from the Technology Strategy Board (TSB) of the UK government. The research consortium incorporates the following industrial and academic partners: Sainsburys Supermarkets Ltd., Nextek Ltd., Sharp Interpack Ltd., Imerys Minerals Ltd., Wells Plastics Ltd., Bangor University and Imperial Collage London. TSB is a business-led executive non-departmental public body, established by the government. Its mission is to promote and support research into, and development and exploitation of, technology and innovation for the benefit of UK business, in order to increase economic growth and improve the quality of life. It is sponsored by the Department for Innovation, Universities and Skills (DIUS).